FINAL REPORT

Application of Landscape Mosaic Technology to Complement Coral Reef Resource Mapping and Monitoring

SERDP Project RC-1333

OCTOBER 2010

R. Pamela Reid
D. Lirman
N. Gracias
S. Negahdaripour
A. Gleason
B. Gintert
University of Miami

This document has been cleared for public release

SERDP
DOD ▪ EPA ▪ DOE

Report Documentation Page

Form Approved
OMB No. 0704-0188

Public reporting burden for the collection of information is estimated to average 1 hour per response, including the time for reviewing instructions, searching existing data sources, gathering and maintaining the data needed, and completing and reviewing the collection of information. Send comments regarding this burden estimate or any other aspect of this collection of information, including suggestions for reducing this burden, to Washington Headquarters Services, Directorate for Information Operations and Reports, 1215 Jefferson Davis Highway, Suite 1204, Arlington VA 22202-4302. Respondents should be aware that notwithstanding any other provision of law, no person shall be subject to a penalty for failing to comply with a collection of information if it does not display a currently valid OMB control number.

1. REPORT DATE	2. REPORT TYPE	3. DATES COVERED
OCT 2010	**N/A**	**-**

4. TITLE AND SUBTITLE	5a. CONTRACT NUMBER
Application of Landscape Mosaic Technology to Complement Coral Reef Resource Mapping and Monitoring SERDP Project RC-1333	5b. GRANT NUMBER
	5c. PROGRAM ELEMENT NUMBER
6. AUTHOR(S)	5d. PROJECT NUMBER
	5e. TASK NUMBER
	5f. WORK UNIT NUMBER
7. PERFORMING ORGANIZATION NAME(S) AND ADDRESS(ES) **Strategic Environmental Research and Development Program (SERDP)**	8. PERFORMING ORGANIZATION REPORT NUMBER
9. SPONSORING/MONITORING AGENCY NAME(S) AND ADDRESS(ES)	10. SPONSOR/MONITOR'S ACRONYM(S)
	11. SPONSOR/MONITOR'S REPORT NUMBER(S)

12. DISTRIBUTION/AVAILABILITY STATEMENT
Approved for public release, distribution unlimited

13. SUPPLEMENTARY NOTES
The original document contains color images.

14. ABSTRACT

The primary objective of SI 1333 was to develop innovative technology to increase the speed and repeatability with which reef plots can be mapped and inventoried. Specifically, we used underwater images to create landscape (2D) mosaics of reef plots in a highly automated way. The innovative aspect of the mosaicing technology is that the images provide both landscapelevel (meter-scale) maps and high-resolution (sub-millimeter) images of individual coral colonies. Users can collect imagery for areas of several hundred square meters in under an hour of in-water dive time to create mosaics that provide information on coral colony health and small-scale competitive interactions. The mosaic products are useful for extracting ecological indicators of reef health and for damage assessment; they also have excellent archive potential and are superior tools for tracking changes over time.

15. SUBJECT TERMS

16. SECURITY CLASSIFICATION OF:			17. LIMITATION OF ABSTRACT	18. NUMBER OF PAGES	19a. NAME OF RESPONSIBLE PERSON
a. REPORT	b. ABSTRACT	c. THIS PAGE			
unclassified	**unclassified**	**unclassified**	**SAR**	**188**	

Table of Contents

TABLE OF FIGURES VI

TABLE OF TABLES X

KEYWORDS XI

LIST OF ACRONYMS XI

ACKNOWLEDGEMENTS XII

ABSTRACT 1

OBJECTIVES 1

BACKGROUND 2

SECTION A: LANDSCAPE MOSAICS 7

A1. METHODS 7

A2. RESULTS AND DISCUSSION 8

A2.1 Mosaic algorithm development 8
A2.1.1 Initial mosaicing capability 8
A2.1.2 Refined algorithm 11
A2.1.3Enhancements to the 2D Mosaicing Algorithm 13
A2.1.3.1 Topography: Combining Different Altitude Sequences 13
A2.1.3.2 Efficient Image Blending 14
A2.1.3.3 Removal of Sunflickering interference 18
A2.1.3.4 Profiling and identification of bottlenecks 23
A2.1.3.5 Memory Enhancements 25
A2.1.3.6 Speed Enhancements 25
A2.1.4 Second-generation landscape mosaics 26
A2.1.4.1 Integrating high resolution stills with video image acquisition 30
A2.1.4.2 Integration of heading information in 2D mosaic processing 31
A2.1.5 Collaborative work on further algorithm development 39
A2.1.5.1 Selection of best candidates for image matching 39
A2.1.5.2 Automated change detection 40
A2.1.5.3 Extension of the graph-cut blending to 3D surfaces 40

A2.2 Mosaic Products 41

A2.3 Analysis of mosaics 41
A2.3.1 Geometric analysis of landscape mosaics 42
A2.3.2 Ecological analysis of landscape mosaics 44
A2.3.2.1 Mosaic Selection 44
A2.3.2.2 Spatial Accuracy 48
A2.3.2.3 Percent Cover 48
A2.3.2.4 Colony Size 50
A2.3.2.5 Change Detection 51
A2.3.3 Benefits of second-generation mosaic technology to ecological analysis 53
A2.3.4 Recommendations for Field Implementation 57

A2.4 Applications of coral reef monitoring and mapping using landscape mosaic technology 69
A2.4.1 Ship Grounding 69
A2.4.1.1 Status and Trends of the Benthic Community 72
A2.4.1.2 Comments and Recommendations 75
A2.4.2 Spatio-temporal analysis of coral communities 75
A2.4.3 Monitoring and Assessment of Mesophotic coral communities 80
A2.4.4 Using Landscape Mosaics to Assess the Impacts of Hurricane Damage on Acropora palmata populations 84
A2.4.5 Use of 2D Video Mosaics for Assessing the Impacts of Mass-Bleaching Events on Coral Communities 87

A2.5 Users/Partners 89
A2.5.1 SERDP Coral Reef Monitoring and Assessment Workshop 89
A2.5.2 The National Park Service: Surveys of the threatened coral Acropora palmata 91
A2.5.3 University of Puerto Rico 91
A2.5.4 The US Navy's Coral Reef Monitoring Program at AUTEC 92
A2.5.5 The Nature Conservancy 93
A2.5.6 Rutgers University 98
A2.5.7 NOAA Restoration Group 101
A2.5.8 NOAA Marine Heritage 103
A2.5.9 Florida Fish and Wildlife Conservation Commission 105
A2.5.10 Potential Department of Defense Collaborations/Users 106
A2.5.11 Landscape Mosaics website 109

A2.6 Software deliverables 110
A2.6.1 Landscape (2D) Mosaic Software 110
A2.6.1.1 Frame Extraction 111
A2.6.1.2 Sunflickering Removal 112
A2.6.1.3 Global Matching 112
A2.6.1.4 Video and Still Registration 113
A2.6.1.5 Global Match Inspection 114
A2.6.1.6 Mosaic Rendering with Improved Blending 115
A2.6.1.7 Heading Integration Module 115
A2.6.1.8 Additional Features 116
A2.6.2 Ecological Analysis Module 118

A2.6.3 External viewer.....*121*

A3. CONCLUSIONS AND IMPLICATIONS FOR FUTURE RESEARCH/IMPLEMENTATION:..... **123**

A4. ACTION ITEM **128**

SECTION B: SINGLE OBJECT 3D RECONSTRUCTION **133**

B1. MATERIALS AND METHODS **133**

B2. RESULTS AND DISCUSSION..... **135**

B3. CONCLUSIONS AND IMPLICATIONS FOR FUTURE RESEARCH/IMPLEMENTATION..... **142**

SECTION C: MULTISPECTRAL IMAGING..... **144**

C1. MATERIALS AND METHODS **144**
C1.1 System Development, Data Acquisition, and Preliminary Processing *144*
C1.2 Experiments with Filter Set 1.....*146*
C1.3 Experiments with Filter Set 2.....*147*
C1.4 Experiments with Combined Spectral / Texture Classification.....*147*

C2. RESULTS AND DISCUSSION..... **149**
C2.1 System Development.....*149*
C2.2 Experiments with Filter Set 1.....*150*
C2.3 Experiments with Filter Set 2.....*151*
C2.4 Experiments with Combined Spectral / Texture Classification.....*152*

C3. CONCLUSIONS AND IMPLICATIONS FOR FUTURE RESEARCH/IMPLEMENTATION..... **153**

LITERATURE CITED..... **155**

APPENDIX 1. PUBLICATIONS AND PRESENTATIONS ACKNOWLEDGING SERDP SUPPORT..... **162**

APPENDIX 2. SUPPORTING DATA: LANDSCAPE MOSAICS **167**

APPENDIX 3. SUPPORTING DATA: LANDSCAPE MOSAIC CREATION MANUAL..... **167**

APPENDIX 4. SUPPORTING DATA: LANDSCAPE MOSAIC CREATION SOFTWARE..... 167

APPENDIX 5. SUPPORTING DATA: 3D MOSAICING..... 167

APPENDIX 6. SUPPORTING DATA: MULTISPECTRAL DATA..... 167

APPENDIX 7. SUPPORTING DATA: LANDSCAPE MOSAIC SURVEYING TECHNOLOGY REQUIREMENTS..... 168

Software Requirements.....168

Software Installation.....169

Acquisition Hardware.....169

Computing hardware and typical disk and CPU usage.....170

Guidelines for handheld image acquisition.....171

APPENDIX 8. SUPPORTING DATA: ACTION ITEMS..... 176

APPENDIX9. OTHER MATERIALS (AWARDS)..... 176

Table of Figures

Figure A1. Early mosaicing results. 9
Figure A2. Mosaics of the 4 tracks of Andros data 10
Figure A3. Mosaic creation example using Andros data. 12
Figure A4. Left: Mosaic created using the global mosaicing approach on a low altitude sequence alone. 14
Figure A5. Mosaic rendering. 15
Figure A6. Example of the watershed/graph-cut method. 16
Figure A7. Example of frame selection, used before the watershed/graph-cut blending method 17
Figure A8. Comparison of blending methods. 18
Figure A9. Example of application of the motion compensated filtering algorithm 20
Figure A10. Original frames of a shallow water sequence 21
Figure A11. Sections of the same shallow water survey under strong refracted sunlight 21
Figure A12. Performance of sunflicker removal methods under poor registration 23
Figure A13. Completed enhanced imaging system. 27
Figure A14. Plot of the Measured Voltage Transfer Function 28
Figure A15. Plot of the Angular transfer Function. 29
Figure A16. Heading Calibration Setup 29
Figure A17. Table representing matches between video images and photo stills. 31
Figure A18. Examples of audio samples 32
Figure A19. Examples of audio samples and corresponding power spectral density 33
Figure A20. Illustration of the large settling time for a 360 to 0 degree transition. 34
Figure A21. Rotation angles obtained 35
Figure A22. Calibration of the heading sensor. 36
Figure A23. Example of a globally aligned mosaic with geometric distortions. 37
Figure A24. Example of the use of heading on a globally aligned mosaic.. 38
Figure A25. Example of use of heading in the estimation of the initial trajectory. 39
FigureA26. Comparison of blending over a 3D surface, obtained using a simple geometric criterion. 41
Figure A27. Mosaic image from the Key Biscayne site with selected marker positions. 43
Figure A28. Histogram of the error components, with superimposed normal distribution fit. 43

Figure A29. Video mosaic created from hand held video images taken at the Brooke's Reef site in June 2004. 45

Figure A30. ROV Video Mosaic created from a high altitude. 46

Figure A31. ROV based video mosaic created from a low altitude pass. 47

Figure A32. Abundance, spatial distribution, and sizes of stony corals obtained from a low-altitude. 50

Figure A33. Example of co-registered mosaic sub-sections or tiles. 52

Figure A34. A second-generation video mosaic from Brooke's Reef, FL. 54

Figure A35. of change detection potential using second-generation imagery. 56

Figure A36. Environmental data from Media Luna Integrated Coral Observing Network (ICON) station. 60

Figure A37. Image of benthos from ~2m at Media Luna Reef. 61

Figure A38. Mosaic of Media Luna Reef video data from December 12th, 2007. 62

Figure A39. Maximum allowed speed of translation for the camera as a function of the shutter speed for different altitudes. 63

Figure A40. Effect of light variations on image products. 64

Figure A41. Example of a area coverage pattern comprising two lawnmower's patterns rotated 90 degrees. 65

Figure A42. Benefits of image pre-processing. 66

Figure A43. A) Superficial damage to a coral colony caused by a small ship grounding. 70

Figure A44. Flow-charts depicting the differences between the Image-only method (A) and the Image-Plus GCP method (B). 72

Figure A45. Landscape video mosaic surveys of the ship-grounding damage caused by the Evening Star in 2005 and 2006. 73

Figure A46. Encroachment of seagrass into the affected area. 74

Figure A47. Example of digitized hand-drawn species distribution map of a 10x10m reef patch. 76

Figure A48. Partially digitized high resolution video mosaic of the 10x10m plot located at site S1-10. 77

Figure A49. A) The 1972 (purple) and 2008 (orange) distributions of live coral cover at the study site. 78

Figure A50. A). Shows the 1972 and 2008 distributions of live coral cover within the study area. 78

Figure A51. The 1972 (blue) and 2008(purple) distributions of the coral species *Porites porites* overlaid on top of a depth map of the study area. 79

Figure A52. Site one from Sherwood Forest Reef, Dry Tortugas, Florida. 82

Figure A53. Site two, a coral hillock from St. Thomas USVI. 83

Figure A54. Video mosaics from a study plot at Molasses Reef in the Florida Reef Tract 84

Figure A55. a) Photograph of the reef section dislodged during Hurricane Rita. 86

Figure A56. Landscape video mosaics of site S1-10 located offshore of Andros Island, Bahamas. 88

Figure A57. 2D video mosaics of *Acropora palmata* reefs at Buck Island National Monument, St. Croix, USVI. 91

Figure A58. Example of coral reef monitoring at Andros Island, Bahamas.....92

Figure A59. Location of the permanent sites established as part of the bleaching-mosaic assessment of the Biscayne Subregion of the Florida Reef Tract in the summer of 2008.93

Figure A60. Landscape video mosaic of a permanent plot established within an Offshore Patch Reef habitat as part of the Florida Reef Resilience Program in the summer of 2008.94

Figure A61. Landscape video mosaic of a permanent plot established within a Mid-Channel Patch Reef habitat as part of the Florida Reef Resilience Program in the summer of 2008. 95

Figure A62. Landscape video mosaic of a permanent plot established within an Inshore Patch Reef habitat as part of the Florida Reef Resilience Program in the summer of 2008.96

Figure A63. Landscape video mosaic of a permanent plot established within a Fore-Reef habitat as part of the Florida Reef Resilience Program in the summer of 2008. 97

Figure A64. Landscape mosaic of a Fore-Reef habitat showing the location of bleached colonies of *Siderastrea siderea*. 98

Figure A65. Combined mosaic/FIRe product. Locations of individual organisms examined with the underwater FIRe instrument are demarcated by the triangles (above).100

Figure A66. Future of integrated mosaic/FIRe survey technology.....101

Figure A67. South Carysfort Reef, Florida Keys. 102

Figure A68. Horseshoe Reef, Florida Keys. 103

Figure A69. Landscape mosaics of the Kyle Spangler. 105

Figure A70. Video mosaic of 2mx20mtransect at Sombrero Reef, Florida Keys. 106

Figure A71. Screen-capture of landscape mosaic website homepage. 110

Figure A72. Main Mosiacing Program GUI. 111

Figure A73. A screen capture of the video frame extraction GUI. 111

Figure A74. Graphic user interface for the sunflicker removal module. 112

Figure A75. The global matching interface. 113

Figure A76. The video frame and still image registration interface. 114

Figure A77. The match inspector GUI. 114

Figure A78. Mosaic Rendering GUI.....115

Figure A79. Heading integration module. 116

Figure A80. Basic point click GUI. 116

Figure A81. Basic Point Click GUI showing a selected video frame.....117

Figure A82. Mosaic Info GUI.....117

Figure A83. A mosaic with distance markers created by the mosaic_info GUI.....118

Figure A84. Screen-capture of a mosaic image being used with CPCe point count program. 120

Figure A85. Extracted still image of point I. 121

Figure A86. Screenshot of GUI that creates the file used for the external point and click viewer.....122

Figure A87. External point click viewer interface. 122

Figure A88. Result of clicking on mosaic on interface. 123

Figure B1. A sample stereo pair, shown in (a) and (b), are processed by our method to generate the 3D map. 136

Figure B2. Sample stereo pair with matching features. 137

Figure B3. Sample left view of a stereo pair, showing the corals that have been processed for 3D reconstruction. 138

Figure B4. Scan lines from the 3D reconstruction of corals in figure B3. 139

Figure B5. Height measurements for various corals or reef rubble imaged by the stereo camera system. 140

Figure B6. Control points for 3D point and click calibration. 141

Figure B7. Independent measurements of the same coral colony or reef rubble by the 3D point and click system (3 different stereo pairs) and 2 diver measurements. 142

Figure C1. Proposed spectral bands for coral reef mapping. 145

Figure C2. (Left) Interior of multi-spectral camera. 149

Figure C3. System rolloff factor as a function of angle from the center pixel. 150

Figure C4. False color 600, 589, 568 nm RGB image of the 150

Figure C5. False color 600, 589, 568 nm RGB image of the 151

Figure C6. Discriminant functions one (DF1) and two (DF2) computed from our full-spectrum data base (left), from our partial-spectrum data base (center), and from Hochberg and Atkinson's (2003) database for their hypothetical CRESPO sensor.....151

Figure C7. Four MSCAM scenes acquired with filter set two. 152

Figure C8. Summary of results for combined spectral / texture classification. 153

Table of Tables

Table A1. Table showing areas where speed and memory efficiency could be improved in existing mosaic creation modules. 24

Table A2. Table showing areas where of speed and memory efficiency could be improved in enhanced mosaic capabilities. 24

Table A3. Measured Transfer Function. 27

Table A4. Description of the three mosaics used in the monitoring assessment. 44

Table A5. Mean cover (± S.E.M.) of the different benthic categories surveyed by divers and measured from video mosaics from a reef site in the northern Florida Reef Tract (depth = 7-10 m). 49

Table A6. Comparison of coral size measurements between: (1) two divers measuring the same colonies; and (2) between diver measurements and measurements of the same colonies obtained directly from the video mosaics. 50

Table A7. Biological and Environmental characteristics of Brooke's Reef and Grecian Patch permanent monitoring sites. 58

Table A8. Environmental observations on dates in which permanent monitoring sites were sampled. 58

Table A9. Image quality characteristics for mosaic datasets. 66

Table A10. Image quality information for mosaic data acquired at permanent monitoring sites Brooke's Reef and Grecian Rocks. 67

Table A11. Average standard deviations for mosaics that could not be created (..... 68

Table A12. Technology overlay and potential collaborations resulting from SERDP coral reef monitoring and assessment workshop. 90

Table A13. Military Facilities with Adjacent Coral Reef Resources. 108

Table A14. Summary of advancements to the state-of-the-art in coral reef monitoring techniques. 124

Table A15. Methods comparison. 129

Table A16 Cost estimates of coral reef monitoring techniques. 132

Table C1. Images for Experiments with Filter Set 1. 146

Table C2. Images for Experiments with Filter Set 2. 147

Table C3. Thresholds Used For Each Algorithm and Dataset. 148

Table C4. Images for Experiments with Spectral / Texture Classification. 149

Table C5. Image-Wide Accuracy. 152

Table C6. Point-Based Overall Accuracy. 152

Keywords

Video mosaics; benthic surveys; image motion; reef condition; ROV; video surveys; benthic mapping; survey methods; second-generation landscape mosaics; improved monitoring methods; archive; benthic assessment; coral monitoring; rapid field assessment; sunlight flickering; image filtering; mesophotic coral reef; image blending; *Acropora palmata;* hurricane damage; ship grounding; reef framework damage; watershed segmentation; 3D texture blending; image mosaicing; graph cuts; reef groundings; damage assessment; Florida; global alignment; optical flow;3D mapping; color imagery; underwater image model; mixed adjustment model; stereovision; automated classification; multispectral imagery;

List of acronyms

AE – Absolute Error
AFB – Air Force Base
AGRRA – Atlantic and Gulf Rapid Reef Assessment
ANOVA – Analysis of Variance statistical tests
AUTEC – Atlantic Undersea Test and Evaluation Center
AUV - Autonomous Underwater Vehicle
CCA – Crustose Coralline Algae
C-MAN - Coastal-Marine Automated Network
CPCe - Coral Point Count with Extensions
CPU- Central Processing Unit
CREMP – Coral Reef Evaluation and Monitoring Program
DF – Discriminant Function
DoD – Department of Defense
EIMS - Environmental Information Management System
EGTTR - Eglin Gulf Test and Training Range
EPA – Environmental Protection Agency
ESA – Endangered Species Act
ESTCP - Environmental Security Technology Certification Program
FFT - fast Fourier transform
FIRe – Fluorescence Induction and Relaxation System
GB - Gigabyte
GCP – Ground Control Point
GIS- Geographic Information Systems
GPS - Global Positioning System
GUI – Graphical User Interface
HDV – High-definition Video
ICON – Integrated Coral Observing Network
IEEE - Institute of Electrical and Electronics Engineers
IFFT- Inverse fast Fourier transform
LCD - Liquid Crystal Display
GHz - Gigahertz

KHz – Kilohertz
MCD – Marine Conservation District
MP – Mega-pixel
MSCAM – Multi-Spectral Camera
NAVFAC – Naval Facilities Engineering Command
NEPA - National Environmental Policy Act
NMS – National Marine Sanctuaries
NOAA - National Oceanic and Atmospheric Administration
NRDA - Natural Resource Damage Assessment
PC – Personal Computer
PNG – Portable Network Graphic
RAE – Relative Absolute Error
PVC - Polyvinyl chloride
RAM- Random-access memory
RGB – Red, Green, & Blue
ROV – Remotely Operated Vehicle
RSMAS – Rosenstiel School of Marine and Atmospheric Science
SCUBA - Self Contained Underwater Breathing Apparatus
SD – Standard Deviation
SDS – Scientific Diving Service
SERDP – Strategic Environmental Research and Development Program
SI – Sustainable Infrastructure
SIFT - Scale-invariant feature transform
SLR - single-lens reflex
SPAWARSYSCEN-PAC – Space and Naval Warfare Systems Center Pacific
SWaPS – Shallow Water Positioning System
SON – Statement of Need
UPRM – University of Puerto Rico Mayaguez
US – United States
USVI – U.S. Virgin Islands
UVI – University of the Virgin Islands
VCO – Voltage Controlled Oscillator

Acknowledgements

Funding for this project was provided by the Strategic Environmental Research and Development Program (SERDP), Award CS1333 to Reid *et al*. Logistical support for field work at the Atlantic Undersea Test and Evaluation Center (AUTEC) was provided by Mr. Tom Szlyk and Mr. Marc Ciminello. Dr. Humberto Guarin assisted with hardware development. Laboratory and field assistance were provided by M. Gonzalez, E. Martinez, R. Freedman, K. Cantwell, and P. Matich. We would also like to thank our numerous collaborators for their support and continued interest in developing the underwater mosaicing technology.

Abstract

The primary objective of SI 1333 was to develop innovative technology to increase the speed and repeatability with which reef plots can be mapped and inventoried. Specifically, we used underwater images to create landscape (2D) mosaics of reef plots in a highly automated way. The innovative aspect of the mosaicing technology is that the images provide both landscape-level (meter-scale) maps and high-resolution (sub-millimeter) images of individual coral colonies. Users can collect imagery for areas of several hundred square meters in under an hour of in-water dive time to create mosaics that provide information on coral colony health and small-scale competitive interactions. The mosaic products are useful for extracting ecological indicators of reef health and for damage assessment; they also have excellent archive potential and are superior tools for tracking changes over time.

As secondary goals, SI 1333 explored two techniques to assist or automate classification of underwater imagery: (i) 3D reconstruction of specific reef features and (ii) high resolution multispectral imaging. A 3D tool was developed that allows users to visualize and measure topographic structure and heights of single objects, such as coral colonies, from landscape mosaics created using stereo imagery. In addition, an automated seabed classification algorithm based on texture analysis of narrow spectral band images was identified that can reliably segment corals, algae and the non-photosynthetic background. These results suggest that high spectral resolution combined with texture-based image segmentation may be an optimal methodology for automated classification of underwater coral reef imagery.

Objectives

The development of underwater landscape mosaicing capability addresses an emerging need to augment diver surveys in an effort to efficiently inventory and monitor large areas of DoD-held coral reef resources. Mapping is a crucial component of establishing baseline environmental data and a primary goal of SON CSSON-03-02. For coral reefs, successful and legally defensible monitoring of reef condition requires estimates of basic ecological parameters, such as live coral cover, species diversity, and mortality/recruitment rates. Presently, such parameters are typically measured during field surveys using trained divers. Airborne or satellite-based remotely sensed data are not currently able to reliably quantify coral condition at the required level of detail (Mumby et al. 1998). The most appropriate strategy for reef monitoring is detailed analysis of meter-scale plots at high spatial resolution.

The aim of Project SI 1333 was to develop technology that will increase the speed and repeatability with which reef plots can be mapped and inventoried. Specifically, we are using underwater video to create landscape mosaics of reef plots in a highly automated way. Our objective was is to construct spatially accurate landscape (2D) video mosaics of reef plots and to extract meaningful ecological indices of reef condition from these mosaics. This landscape mosaicing technology offers numerous advantages over traditional, diver-based video transects (1D) for coral reef mapping and monitoring. Landscape mosaics produce single, spatially accurate, plot-scale, high-resolution images that can be georeferenced.

As an extension to our original funded proposal we expanded our primary objective to include expanded mosaicing capabilities and streamlined processing. The specific goals of this project extension were to 1) reduce the impact of sunflickering interference on mosaic processing, 2) improve image blending to create seamless mosaics, 3) integrate a heading sensor for use in high relief settings and 4) integrate a still camera for increased benthic resolution of landscape mosaics. The resulting landscape mosaics allow users to extract increased reef health information in complex reef habitats and provide a better overall product with increased value to coral reef monitoring users for change detection analyses. These are essential capabilities for the legally mandated environmental documentation necessary for conducting military operations and could provide decision-makers with crucial information necessary to maintain compliance with relevant statutes, regulations, and executive orders.

In addition to the *primary goal* of developing an underwater landscape mosaicing capability for use in coral reef monitoring and mapping applications, we have explored two techniques as *secondary project goals* to assist or automate classification of underwater imagery: (i) 3D reconstruction of specific reef features and (ii) underwater multispectral imaging.

The objective of the 3D effort was to develop a 3D reconstruction tool that allows a user to visualize and measure topographic structure and heights of single objects, such as coral colonies, from 2D mosaics created from stereo imagery. Our work on 3D reconstruction of reef features investigated two types of approaches: 1) an optical flow-based method applied to monocular video sequence for the dense estimation of a 3D map, and 2) a feature-based technique allowing 3D reconstruction of single objects from stereo imagery. We determined that the second approach was more suitable for developing a tool for non-expert use in coral reef monitoring applications. The materials and methods as well as results of this secondary goal are presented in Section B of this report and can be read as a standalone report.

The objectives of the multispectral imaging effort were to build and deploy an underwater multispectral camera to test whether the spectral bands suggested in the literature (Holden and LeDrew 1998; Holden and LeDrew 1999; Clark et al. 2000; Hochberg and Atkinson 2000; Holden and LeDrew 2001; Holden and LeDrew 2002; Hochberg and Atkinson 2003; Hochberg et al. 2003) could be used to automate the classification of underwater imagery from coral reef environments. A further objective, which developed during the course of the research, was to test whether simple texture metrics in combination with narrow-band spectral imagery could automatically classify basic bottom cover types associated with coral reefs, such as coral, algae, and sand. The materials and methods as well as results of this secondary goal are presented in Section C of this report and can be read as a standalone report.

Background

Recent declines in coral reefs across the globe underscore the need for new scientific tools to better understand ecological patterns and rates of change. Of immediate interest to the Dept. of Defense are mesoscale measurements that detect changes within reef systems by monitoring meter-scale plots.

The state-of-the-art in mesoscale coral reef assessment consists of a combination of diver-based and image-based measurements. The "gold standard" of reef monitoring, in terms of obtaining maximum level of detail, is assessment by expert scientific divers. Diver-based assessments are, however, often time consuming in the water, require a high level of individual training, and provide a limited permanent record of the state-of-the-reef at the time of the survey. Technological aids, in the form of image-based techniques such as photo quadrats and 1D strip mosaics, have been adopted to complement diver-based assessments. Digital photographs or video images of small plots (< $1m^2$) are commonly used to measure benthic cover, species diversity, and coral condition within reef habitats. Similarly, photographs of permanent plots and coral colonies marked with metal stakes or nails are used to track changes over time. Video surveys of the reef benthos can be analyzed by extracting individual frames, which are then treated as photo-quadrats or by stitching the frames together into a 1-dimensional 'strip' mosaic, which provides a limited landscape view of the bottom.

At least one coral reef monitoring program, the Coral Reef Monitoring Program of the Florida Keys National Marine Sanctuary, is using strip-mosaic software (*RavenView* by Observera) to provide expanded views of the bottom and extract ecological information (Jaap et al., 2002). In this program, divers collect video and the imagery is stitched together to provide a strip mosaic of 22 m x 40 cm. The video mosaics are then analyzed to extract information on the benthic cover of reef organisms. Because these images are collected at a short distance from the bottom (generally 40 cm) and only partial views of larger organisms are obtained, size-estimation is limited to the smallest coral colonies that are completely imaged within a frame or a transect. Moreover, the lack of image registration limits spatial accuracy and precludes the estimation of spatial patterns within plots.

Although photo-quadrats and video surveys improve the efficiency of diver-based surveys by shifting expert analysis and species identifications from the field to the lab, these image based monitoring tools have many limitations. In particular, photo-quadrats and 1D strip mosaics have limited footprints, thereby restricting the assessment area and often requiring placement of numerous markers and tags for repeated surveys of the plots or colonies of interest.

Work in terrestrial systems has successfully implemented image-based mosaicing covering large areas. State-of-the-art aerial photogrammetric mapping methods using digital technology are highly automated and efficient. These techniques are, however, not applicable to underwater imaging because they rely on input from Global Positioning Systems (GPS), which do not operate underwater. Aerial imaging algorithms can be modified for underwater mosaicing through use of acoustic networks to provide navigation information. This approach has been used for well-funded deep-sea projects (e.g. archaeology with the WHOI Jason submersible; Foley and Mindell, 2002); it is, however, not suitable for routine reef monitoring because of the expense of the equipment and the time required to install a sonar network, combined with the number of sites that are normally surveyed in a routine monitoring program.

Image panorama software that blends components of several images taken from a stationary point (such as *PTgui* by NHIS, *Panorama Composer* by FirmTool or *Cool360* by ULead) is universally unsuited to coral reef mapping applications because the algorithms cannot handle movement of the camera over an area of interest. Algorithms designed for this type of

application assume all images are acquired from the same point, with camera *rotation* being the variable between images. Due to the attenuation of light by water, underwater mapping images must be acquired by moving the camera between images. The resulting images vary not only in rotation but also significantly in *translation*. Algorithms that assume no translation fail with this type of data input.

Many manual photogrammetric systems that allow users to define common points between images are available, and some have been used for underwater 2-D and even 3-D applications (Gifford, 1997; Courtney et al., 2006). These systems produce good results, but require intensive user input and are not practical for producing mosaics comprised of several hundred to over a thousand images on a routine basis.

2D landscape mosaic technology, as developed during this project, presents significant advances in state-of-the-art capabilities for reef mapping and monitoring. The most significant advances result from the fact that large areas can now be imaged at high spatial resolution (on the order of 400 m^2 at 1-2 mm/pixel), resulting in spatially accurate, landscape views of the bottom that were previously unobtainable. These landscape mosaics will be useful for DoD reef monitoring requirements and open doors for new applications in reef mapping and change detection.

Project SI 1333 is based on the premise that the use of large-scale, 2D mosaic images of reef plots can circumvent the limitations of diver transects, photo-quadrats, and 1D strip mosaics, while simultaneously maintaining the strengths of the diver approach for the purposes of coral reef monitoring by the Navy.

Secondary goal: 3D reconstructions

One of the defining and most important attributes of coral reef communities is the 3D structure provided by stony corals. Within coral reefs, the topographical complexity created by corals provides essential habitat for the multitude of organisms that form part of one of the most diverse and productive ecosystems in the planet. In addition to supporting these diverse communities, the structures created by corals provide shoreline protection that prevents storm damage and coastal erosion.

Because of the key role of habitat complexity in reef health, monitoring tools able to document 3D topography can provide valuable information on reef structure and function. These parameters are not commonly obtained by standard monitoring methodologies, which measure coral cover as the proportion of the bottom occupied by corals in a planar view.

Previous research has demonstrated that a 3D approach provides a more realistic quantification of coral structure available as essential habitat and, when combined with estimates of living coral tissue, quantifies the amount of live coral tissue available (Fisher et al. 2007). In colonial organisms like corals, most physiological processes, such as calcification, growth, mortality, and fecundity, are directly linked to the surface area of coral colonies. Accordingly, the estimation of colony size based on single planar dimensions (e.g., maximum diameter, projected surface area) commonly underestimates the amount of coral tissue.

Although 2D video mosaics are effective tools to measure the size of coral colonies based on maximum diameter, the added capability of extracting colony height measurements from stereo views can provide all of the information needed to calculate both the volume and the surface area of coral colonies. Most coral colonies approximate hemispherical shapes and, therefore, by measuring colony diameter and colony height and incorporating these measurements into standard geometric formulae, both the volume of the skeletal structures and the surface area of live tissue available can be easily calculated (Fisher et al. 2007).

Secondary goal: Multispectral Imaging

Underwater video and still imagery are useful tools for coral reef monitoring programs because they speed up the data acquisition process, allowing more sites to be visited for a given allotment of field time and because imagery can be acquired by divers with minimal biological training. The disadvantage of an image-based approach is the time required to extract useful ecological information from the underwater imagery. Current state-of-the-art techniques require identifying organisms and substrate through the use of either random points placed on each image (point counting) or tracing individual objects. Such manual processing of each video/still frame is not only labor intensive, but also requires an analyst able to identify coral reef organisms.

Extracting data from underwater imagery is thus a major portion of the budget for coral reef monitoring programs. Any procedure that automates or streamlines part of the image analysis process could, therefore, reduce costs associated with monitoring reef resources. Increasing the efficiency of information extraction from underwater imagery is the DoD regulatory problem that this technology addresses. Several software packages designed to streamline the point counting process have been released in the past decade[1] (Kohler and Gill 2006). These packages do not actually automate the extraction of data; however, they simply facilitate manual data entry and storage.

Color matching, laser line scan imagery, and texture segmentation are three approaches that have been explored previously in attempts to automate the classification of underwater imagery. Classification using color segmentation of standard broad-band imagery has not been successful (Bernhardt and Griffing 2001). Interactive classification using color matching was more successful (Bernhardt and Griffing 2001), but very time consuming. Underwater laser line scan imagery showed potential for automatically classifying the seabed in coral reef environments (Mazel et al. 2003), but laser line scan instruments are currently far too expensive for routine coral reef monitoring projects. Recently, several groups have initiated efforts to automate classification of underwater imagery using image texture in combination with neural network (Konotchick et al. 2006; Pizarro et al. 2006) or support vector machine (Mehta et al. 2007) classifiers. Such an approach may prove fruitful, but requires many training images (or portions of images) and significant computing resources.

Several studies have shown that, at least in principle, the hyperspectral reflectance of coral reef organisms can be used to discriminate functional groups (e.g. corals, algae, and sediment) (Hochberg and Atkinson 2000; Hochberg and Atkinson 2003; Hochberg et al. 2003), identify the "health" of coral tissue (live, dead, bleached) (Holden and LeDrew 1998; Holden and LeDrew

[1] For example PointCount99 (http://www.cofc.edu/~coral/pc99/pc99.htm) and Vidana (http://www.projects.ex.ac.uk/msel/vidana/)

1999; Clark et al. 2000; Holden and LeDrew 2001; Holden and LeDrew 2002), and map coral reef communities (Louchard et al. 2003; Mobley et al. 2004). The major contribution of these efforts has been to suggest spectral bands that might be optimum for mapping and monitoring coral reefs from satellite or airborne imagery.

A first step in our effort in multispectral imaging was to test whether the spectral bands suggested in (Holden and LeDrew 1998; Holden and LeDrew 1999; Clark et al. 2000; Hochberg and Atkinson 2000; Holden and LeDrew 2001; Holden and LeDrew 2002; Hochberg and Atkinson 2003; Hochberg et al. 2003) could be used to automate the classification of underwater imagery (Figure C1). A computer-controlled underwater camera with a filter wheel that holds six narrow-band (10 nm) interference filters was used to acquire multispectral images both in salt-water tanks at the University of Miami and on coral reefs in the Bahamas and Florida Keys.

Attempts to classify the multispectral images using the algorithms suggested by (Holden and LeDrew 1998; Holden and LeDrew 1999; Clark et al. 2000; Hochberg and Atkinson 2000; Holden and LeDrew 2001; Holden and LeDrew 2002; Hochberg and Atkinson 2003; Hochberg et al. 2003) were not successful. As a byproduct of those experiments, however, it was noted that spectral bands near 545 and 570 nm were repeatedly identified as significant in discriminating live coral from other spectra. A ratio of the two bands chosen in that spectral range (546 and 568 nm) was able to segment coral and algae, together, from other objects but was not able to separate coral from algae.

Since segmenting coral and algae, together as one class, is not especially useful for ecological purposes, image texture analysis methods were investigated to determine if a simple spatial technique could assist the spectral processing by separating coral and algae into two distinct classes.

A second step, we then investigated whether simple texture metrics in combination with narrow-band spectral imagery could automatically classify basic bottom cover types associated with coral reefs, specifically: coral, algae, and "other". The general approach was first to segment coral and algae from the background using the normalized difference ratio of images at 546 and 568 nm, then to segment coral from algae using texture metrics computed from grey level co-occurrence matrices.

Methods, Results, and Conclusions

Methods, results and conclusions pertaining to the primary and secondary goals of project SI 1333 are presented in three independent sections. Section A presents information relevant to the primary goal: creation and analysis of landscape (2D) mosaics for coral reef mapping and monitoring. Sections B and C summarize research associated with the secondary goals, namely single object 3D reconstruction (Section B) and underwater multispectral imaging (Section C) as tools to assist mosaic classification and analysis.

Section A: Landscape Mosaics

Our research on landscape (2D) mosaics is based on the premise that use of large-scale, 2D images of reef plots can circumvent the limitations of current state-of-the-art methods in coral reef monitoring (i.e. diver transects, photo-quadrats, strip mosaics), while simultaneously maintaining the strengths of a diver-based approach. We have developed techniques to construct spatially accurate mosaics ~ 20 m x 20 m in extent with millimeter-scale resolution.

Our mosaic algorithm involves three major steps (1) estimating image motion by matching sequential video frames, (2) global alignment to match non-sequential frames, and (3) blending to render the mosaic image. The first generation mosaics provided centimeter-scale resolution, but lacked sufficient detail needed for species-level identification of benthic organisms. In 2007 the mosaicing system was upgraded by integrating a high-resolution still camera with the video acquisition system. This 'second generation' mosaicing system produces mosaics with mm-scale resolution.

The resulting mosaics excel in several areas limited by poor performance using traditional, state of-the-art, reef monitoring techniques:

- Mosaics provide a landscape view of coral reefs that has previously been unobtainable.
- Mosaics are superior tools to track patterns of change over time.
- Mosaics have a spatial accuracy on the order of centimeters to millimeters.

As a consequence of the capabilities above, mosaics are superior tools for monitoring disease, bleaching, and partial mortality--all important indicators of reef health.

A1. Methods

The basic algorithm used in this project for creating underwater mosaics stems from work by Gracias and Santos-Victor (2000; 2001). The basic algorithm involves three main steps. The first step computes the sequential estimation of image motion, using a subset of the images captured by the video camera. The set of resulting consecutive homographies (i.e., coordinate mapping between two image projections of the same 3D plane) is cascaded to infer the approximate trajectory of the camera. The trajectory information is then used to predict the areas where there will be image overlap from non-consecutive images (i.e., neighboring video strips). To reduce the algorithmic complexity and memory requirements, a set of key frames are selected based on an image superposition criterion (typically 65%-80%). Only such key frames are used in the following optimization steps.

In the second step, a global alignment is performed where the overall camera trajectory is refined by performing the following: (1) point correspondences are established between non-adjacent pairs of images that present enough overlap; and (2) the trajectory is updated by searching for the set of trajectory parameters that minimizes the overall sum of distances in the point matches. A least squares criterion is minimized using a non-linear optimization algorithm.

The final step of the mosaicing process consists of blending the images (i.e., choosing representative pixels from the spatially registered images to render the mosaic image). The mosaic is created by choosing the contributing pixels that are closest to the center of their frames. This method preserves the texture of the seafloor and reduces artifacts due to registration misalignments of 3D structure.

The method for mosaic creation was initially tailored for processing video acquired by a single camera, either deployed by a diver or by an underwater vehicle. The method was further extended to deal with a two-camera configuration, comprising a video and a high-resolution still camera. The extended method performs the registration of stills against the video frames in order to find the adequate placement of the stills in the mosaic. Upgrades and extensions to the original algorithm are described in Section A2

A2. Results and Discussion

Major accomplishments for project SI 1333, as summarized by year, include the following: Year 1 (June-Dec 2003) focused on system development (camera resolution improvement and better positioning capability) and collection of initial data sets at Florida and Andros sites. Year 2 (2004), was devoted to creating 2D mosaics of reef plots, assessing the geometric accuracy of the mosaics and performing ecological analysis of the plots. Accomplishments in Year 3 (2005) focused on exploratory enhancements of the 2D mosaicing algorithm, groundtruthing ecological analyses from mosaic products, and applying mosaics to non-traditional reef monitoring applications. In Year 4 (2006), 2D video mosaic technology was applied to different reef monitoring needs such as hurricane damage assessment, grounding and coral bleaching recovery. Year 5 (2007) focused on upgrading the mosaicing imaging platform and integrating new features into the 2D mosaicing software; the new platform with enhanced capability is referred to as a 'second generation' system, which produces 'high resolution' mosaics. In addition, user-friendly software for 2D mosaic creation and extraction of ecological indices was developed in Year 5. Work during Year 6 (2008) focused on continued development and utilization of the second-generation mosaic technology for coral reef monitoring applications, development and integration of enhanced capabilities in the mosaicing software deliverable, and continuing collaborations with other government and scientific users. Year 7 (2009) has focused on continued research with governmental and educational collaborators as well as a finalization of the mosaic module deliverable and manual. Below is a summary of major accomplishments throughout the project. These accomplishments are subdivided with respect to 1) mosaic algorithm development, 2) mosaic products, 3) analysis of mosaic products, 4) applications of landscape mosaic technology to reef monitoring and mapping, 5) collaborations with governmental and educational users, and 6) project deliverables.

A2.1 Mosaic algorithm development

A2.1.1 Initial mosaicing capability

The first mosaics constructed in project SI 1333 were based on techniques outlined by Negahdaripour et al (1998). A low-resolution, real-time algorithm was used to estimate the image motion and to create a live preview of small areas of the benthos (in the order of tens of

square meters). This algorithm was built for fast operation, and was targeted at real-time image motion estimation for ROV position control and station-keeping.

The initial mosaicing capability was restricted to low-resolution black and white images of short duration such as those shown in Figure A1. Although this was a necessary first step in creating useful mosaics for reef resource mapping and monitoring, black and white video images did not provide the benthic detail necessary for ecological analysis. Therefore, our cameras were upgraded to color video cameras with single mega-pixel frames (~1000x800), rather than the standard 640x480 interlaced video. The difference in benthic identification ability is shown in figure A1. Objects that were unidentifiable, such as the brick in the top portion of the image, are became clear using megapixel color imagery.

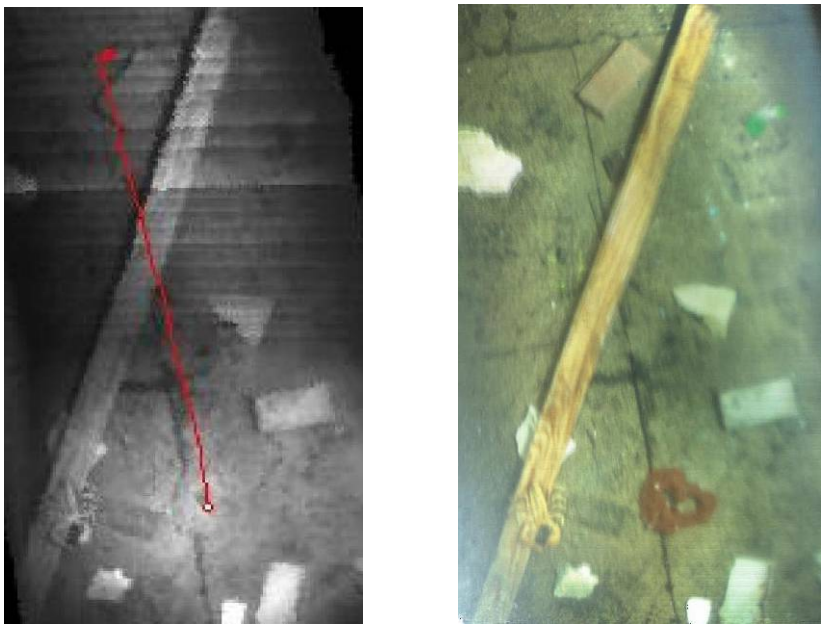


Figure A1. Early mosaicing results. Low-resolution mosaic (a) constructed with the real-time vision system of our ROV in comparison with a high-resolution color mosaic generated offline (b). The red line in (a) shows the trajectory.

The Negahdaripour et al (1998) algorithm had difficulty creating a 2D "landscape" view over complex seabeds, so the first mosaics for this project had to be assembled as a series of strips covering the area of interest (Figure A2).

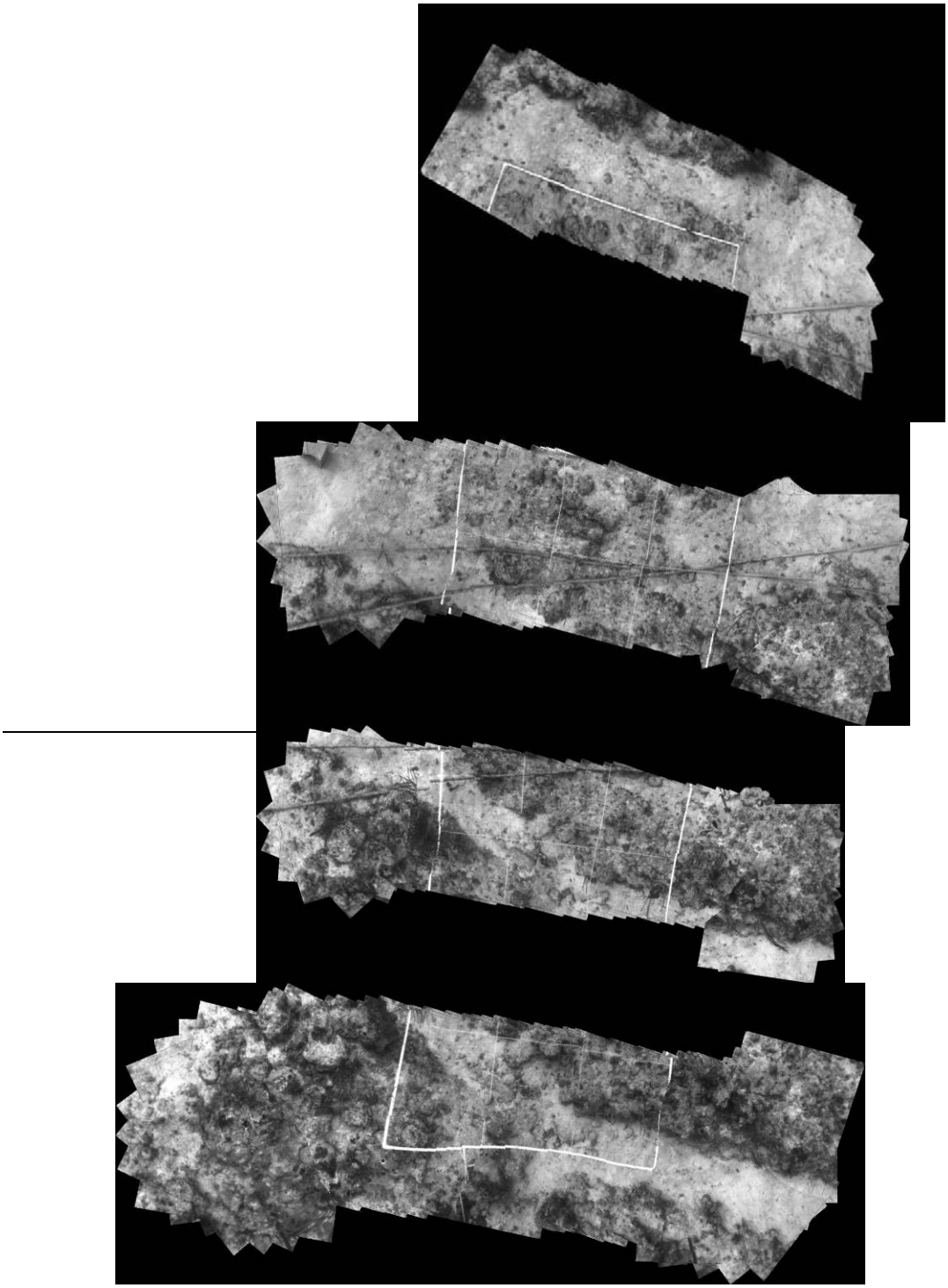


Figure A2 . Mosaics of the 4 tracks of Andros data, collected over a 3mx3m grid. Misalignments in certain parts of each view are directly tied to the 3D nature of the terrain, as current mosaicing algorithms assume a flat terrain model.

Image motion estimation in the early mosaics was based in optical-flow techniques, which are not able to deal with departures from the underlying assumption of a flat sea floor. Using this technique, image motion estimation and mosaic previews were being made concurrently. The motion estimation used the mosaic as a reference map. As a result, any misalignments created by improper image motion estimation were immediately incorporated into the resulting mosaic, which would further hinder the motion estimation. This process, although fast, did not produce the geometrically accurate results needed for repeated mosaic surveys of the same area. This in combination with the of low resolution of the real-time image processing made the approach unsuited for mosaicing areas larger than tens of square meters.

A2.1.2 Refined algorithm

In 2004, we implemented a new technique for off-line creation of 2D mosaics, which enabled creation of mosaics with extended area coverage. This capability was developed by building on the Ph.D. work of project member Nuno Gracias (Gracias et al 2003). The technique involves three processing phases, as follows:

i. Sequential Estimation. In this step, image motion between time consecutive video frames is estimated by finding corresponding image points across pairs of images. This results in a set of ordered image-to-image mappings. The correspondences are found using a mixture of Scale Invariant Feature Transform (SIFT) (Lowe, 2004) and the Harris corner detector (Harris and Stephens, 1988) with normalized cross-correlation. Robust estimation techniques are used to filter out wrongly matched pairs of points, which may appear due to strong 3D or to moving algae or fish. These techniques make the newer mosaicing capability much more resilient to a non-flat benthos. The mappings are cascaded in order to infer the approximate camera trajectory. The accuracy of this step is limited because small unavoidable errors in motion estimation lead to growth of errors in camera trajectory. This feature-based approach to estimating image motion replaced the flow-based motion estimation technique described in our original proposal.

ii. Alignment. In this step, an estimate of the camera trajectory is used to predict areas of image overlap resulting from loops. When such regions are found, additional constraints on the camera trajectory can be imposed, thereby improving the spatial correctness of the final mosaic. The algorithm performs a batch optimization on the global set of motion constraints. (Gracias et al 2003, Lirman et al 2007).

iii. Rendering. The final mosaic image is created by warping and blending the original video frames, using the optimization result of the previous step (Gracias et al 2006, Gracias et al 2009).

Figure A3 shows results using the Gracias et al 2003 mosaicing algorithm. To illustrate the need for the global estimation phase, the upper image was rendered using only sequential estimation (first phase only), while the lower one was created with the full algorithm. The error accumulation is visible on the repetitive pattern (marked by the dotted lines), which corresponds to the same area of the seabed: a single cross over point of two cables.

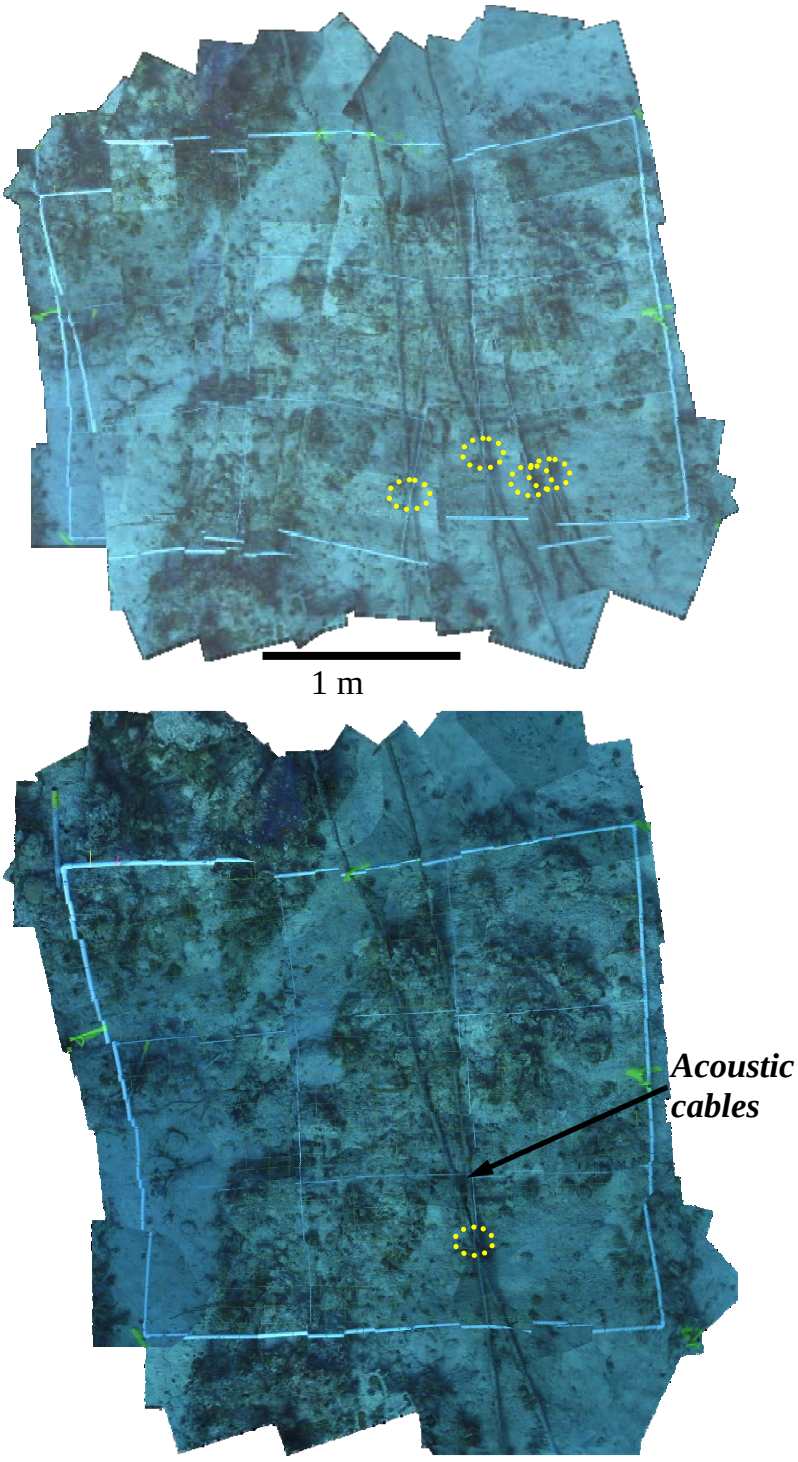


Figure A3. Mosaic creation example using Andros data. Top: Mosaic created using only sequential motion estimation. Bottom: Mosaic incorporating global alignment. The circled areas designate a single cross-over point of two cables. Note that this single point is repeated several times in the top, unaligned mosaic due to accumulated error.

The implementation of the revised mosaicing approach allowed for mosaic creation of color imagery in a single landscape image that was previously unattainable.

A2.1.3Enhancements to the 2D Mosaicing Algorithm

Considerable effort from 2004-2009 was devoted to enhancing the Gracias et al 2003 2D mosaicing algorithm. An important limitation to this algorithm is an underlying assumption that the area being imaged is dominantly flat. We were able to mosaic the sea floor for moderate departures of this assumption such as areas where the height of the benthic structures is roughly less than ¼ of the distance to the sea floor. However 3D content can lead to registration inaccuracies that degrade the appearance of the resulting mosaics and hinder analysis. To better deal with topography, improve the quality of the mosaic products and increase processing speed, a variety of enhancements to the 2D mosaicing technique were developed, as described below.

A2.1.3.1 Topography: Combining Different Altitude Sequences

In order to make more accurate mosaics of areas with topographic relief, we devised and tested two different methods. One method creates a higher altitude mosaic against which lower altitude images are directly registered. When using 2D registration methods, higher altitude images are more reliably registered. This is due to the smaller topography variations, scaled by the distance to the scene. Conversely, lower altitude images provide higher resolution views, but are more difficult to register. Combining both can significantly increase the robustness and efficiency of the mosaicing process, since higher altitude sequences can be used to guide the registration of the lower ones.

The second method for dealing with topography uses the displacement of the images on a common spatial reference frame. The images of the lower altitude sequences are matched directly against the higher altitude ones. For both methods the resulting set of geometric constraints is used in a bundle adjustment step, which promotes the final geometric accuracy. The methods were evaluated in terms of accuracy and computational efficiency. We found the first method to be significantly faster while marginally less precise.

When compared to the case of single altitude sequences, we show that by combining geometric information from different sequences, we are able to successfully estimate the topology of much lower altitude sequences. This allows for creating benthic views with higher resolution and geometric accuracy.

An illustrative result is presented with a low altitude sequence, captured at approx. 1.4 m above sea floor. It contains benthic structures with distinct 3D content, such as colonies that protrude 50-70 cm above the floor. When using this sequence alone, the 3D content and the low overlap among strips leads to inaccurate mapping (Figure A4 Left). By combining with a second sequence captured at approx. 2.5 m, we are able to create a mosaic of much higher geometric accuracy (Figure A4 Right).

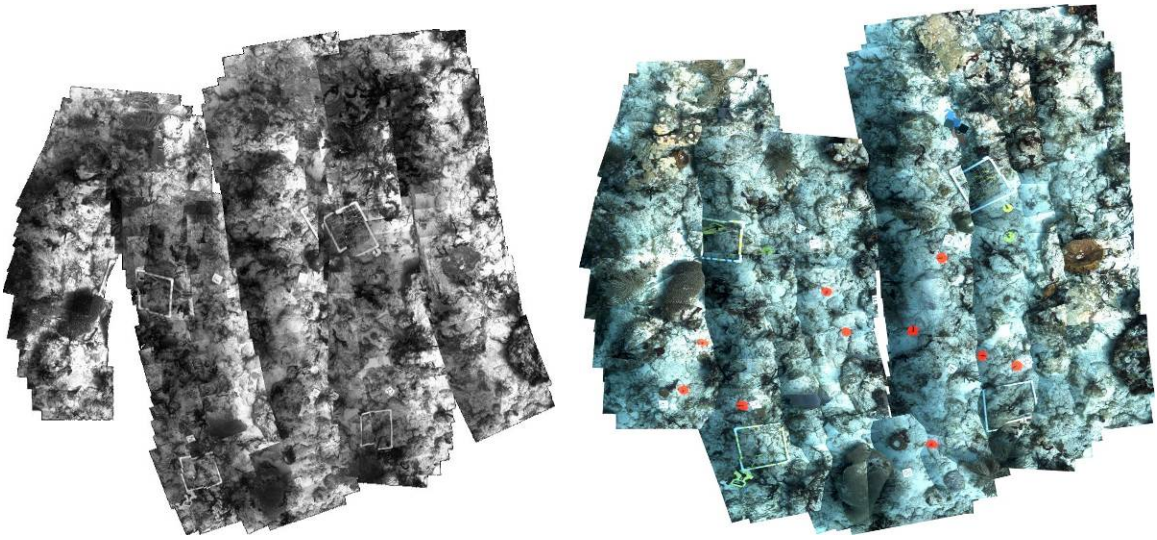


Figure A4. – Left: Mosaic created using the global mosaicing approach on a low altitude sequence alone. The low overlap between strips leads to large registration errors which are clearly visible. The first two strips on the left hand side should be overlapping. Note the broken image of the quadrat, made of white PVC tubing. Right: The improved low altitude mosaic resulting created using geometric information from both the low and high altitude sequences. Improvements are easily visualized when comparing the shapes of the 4 PVC quadrats in the two examples.

This work resulted was presented orally at the IEEE conference on Ocean Engineering in Washington DC in 2005 and was published in the following journal:

Gracias, N. and Negahdaripour, S. (2005) Underwater Mosaic Creation Using Video Sequences from Different Altitudes. Proc. IEEE/MTS Oceans'05, Washington, DC.

A2.1.3.2 Efficient Image Blending

Image blending is an integral final step in mosaic processing in which information from the hundreds or thousands of component frames used in the image matching steps are combined to create a single large image. The most straightforward method for assembling a single mosaic from multiple registered images is to simply fill the mosaic with the portion of each single image closest to its center. This approach was implemented in the basic mosaicing package, but it often left visible seams in the mosaic at the sudden transitions between component images. These visible seams from blending are distracting to the user and can interfere with interpretation of the mosaic (Figure A5).

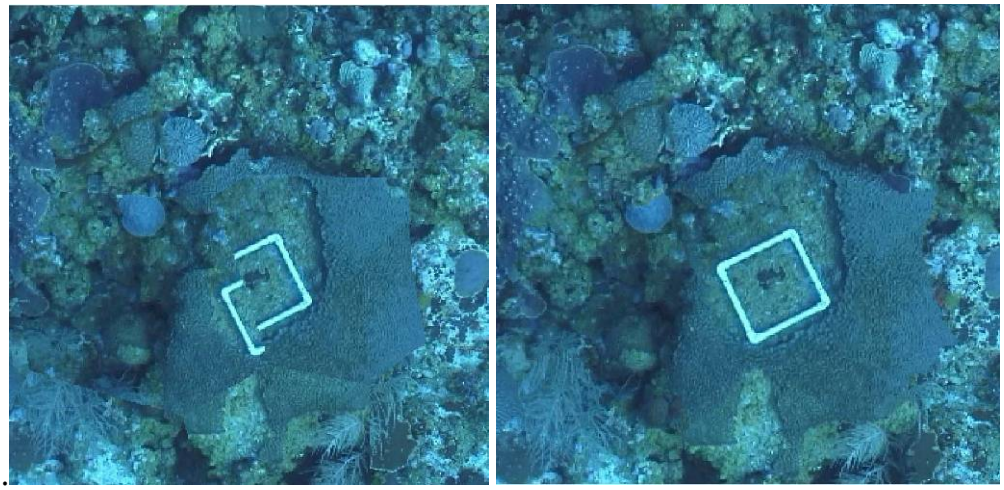


Figure A5. Mosaic rendering. Left: Area detail illustrating a mosaic rendered using a purely geometric method – closest distance to each image center. Right: Result using our improved blending approach; this method uses geometric and photometric information, to compute image boundaries that avoid cutting benthic structures.

During 2006 and 2007, a new approach was devised to blend images using watershed segmentation and graphcut optimization (Figure A6.). Watershed segmentation allows for grouping sets of neighboring pixels into clusters which are then treated as indivisible units in the blending process. This leads to substantial time saving since the number of clusters is much smaller than the number of pixels. Graphcut optimization is a recent energy minimization method that is particularly well adapted to image segmentation applications. Our improved blending method presents important advantages for underwater mosaics over existing state-of-the-art approaches. It combines geometric and photometric criteria to effectively erase seams between images. The algorithm stores data in an efficient way, thereby reducing memory requirements, and is suited to parallel implementation. It allows the efficient blending of large mosaics, with no user intervention. The method, referred to as watershed/graph-cut blending, has been presented at an international conference (Gracias et al. 2006) and later published in the following journal publication:

Gracias, N., M. Mahoor, S. Negahdaripour, and A. Gleason. (2009) Fast Image Blending using Watersheds and Graph Cuts, Image and Vision Computing, 27(5): 597-607.

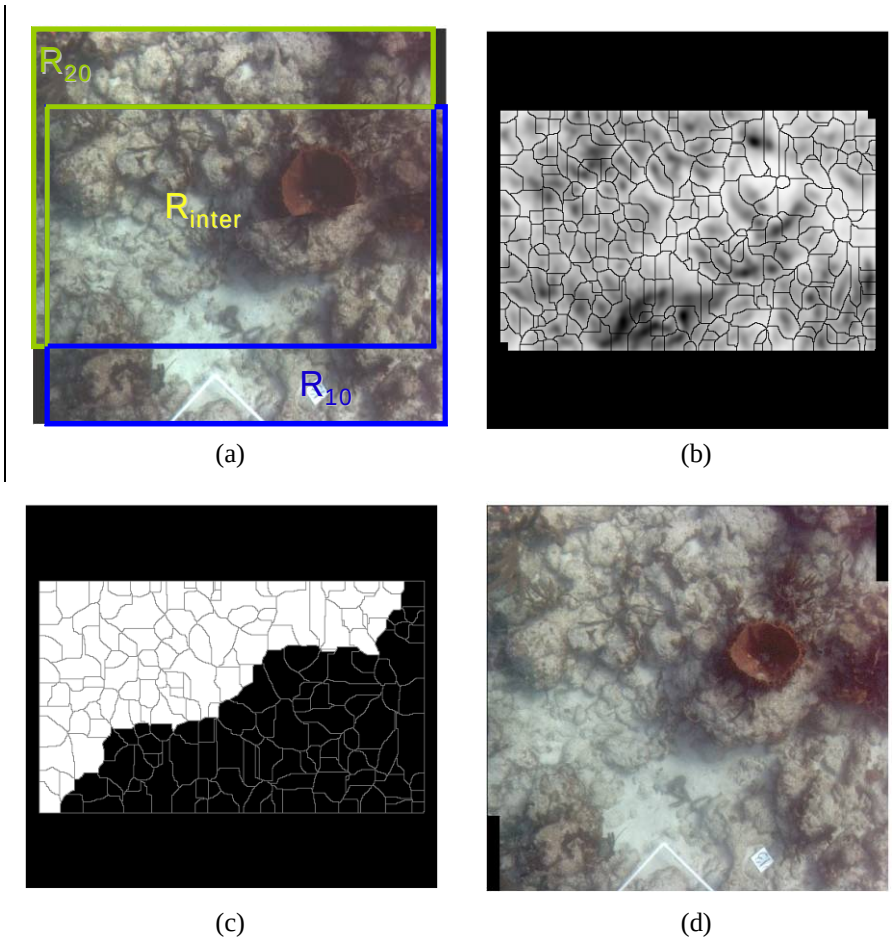


Figure A6. Example of the watershed/graph-cut method. The region of intersection of the two images (marked as R_{inter} in (a)) is divided into small segments using watershed segmentation (b). The white regions in (b) represent the areas where the two images are most similar in terms of color and intensity. These are the areas where the seams should be placed. The graph-cut optimization is used to assign each segment to each image in order to reduce the overall visibility of the seam (c). The resulting blended image is shown in (d).

Two additional improvements to the blending procedures have been incorporated into the mosaic deliverable:

i. A new selection scheme to reduce the number of images to be blended. The mosaicing of large areas may involve the registration and joint optimization of several thousand images. This number can be particularly high under difficult mosaicing conditions, namely in the presence of high topography, moving algae and reduced visibility, where the amount of overlap between images needs to be high to insure proper registration. Blending many images with high overlap often leads to each image having a small contribution on the final mosaic and to a large number of seams among neighboring images. To address this issue, an image selection scheme was devised to find a much smaller sub-set of images to be blended. The selection insures that the area

covered by the mosaic remains the same, and leads to substantial time savings on the subsequent blending. An example is given in figure A7.

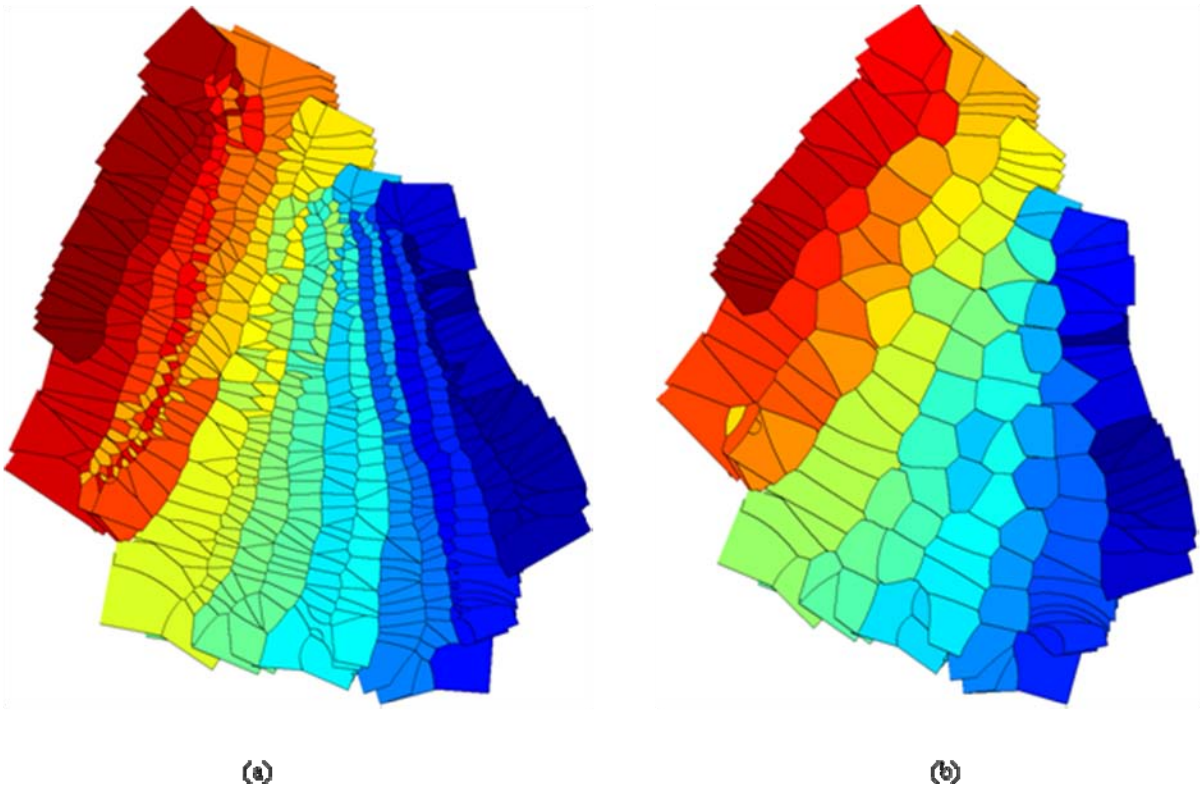


Figure A7. Example of frame selection, used before the watershed/graph-cut blending method. The original set of 691 images (a) is reduced to 145 images (b). The frame selection method rejects images with small footprints while ensuring enough overlap among neighboring images required by the watershed/graph-cut blending method. The total area of the mosaic is not affected.

ii. A new complementary blending method using image gradients. A new method was developed to improve the final rendering of the mosaics. It uses the derivatives of the pixel values to impose smooth transitions between neighboring images. This method complements the existing watershed/graph-cut blending module. The purpose of the watershed/graph-cut blending method is to place the seams (i.e. the common border among pairs of neighboring images) where these seams are the least visible. This means that the seams are placed in the areas where the neighboring images have similar pixel color and intensity. However, in the cases where the neighboring images have very different intensities (for example due to uncorrected refracted sunlight); the watershed/graph-cut method is not able to totally eliminate the visibility of the seams. Conversely, the purpose of this new gradient blending module is to smooth the transition of pixel color and intensity over the pre-established seam. The smoothing is done by (1) computing the horizontal and vertical derivatives of the mosaic, (2) imposing zero derivatives along the seams, and (3) integrating the derivative field to obtain a smoothed mosaic. The last step involves performing an approximation, since the derivatives

modified in (2) cannot be directly integrated. This approximation is done by solving a Poisson equation using Fourier analysis. An example of the result of the new gradient blending module is given in Figure A8.

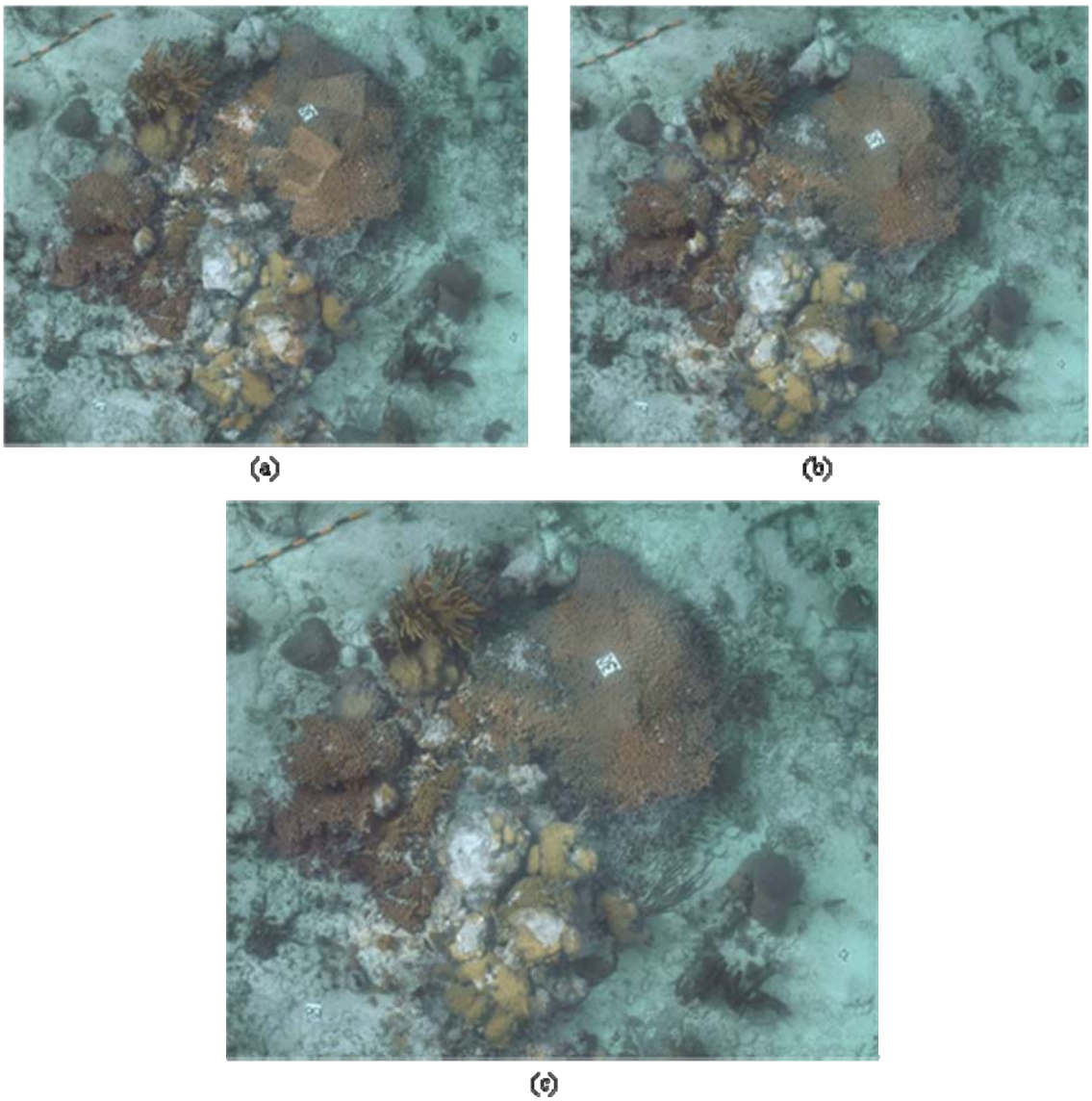


Figure A8. Comparison of blending methods. Fig (a) was obtained with the standard blending using all images. For each point in the mosaic, the standard method selects the contribution from the closest image, which results in a large number of visible seams. Fig (b) presents the result of the watershed/graph-cut method after selecting a subset of representative images (see text). The watershed/graph-cut method places the seams over the areas where they are the least visible. However seams are still visible between images captured under different illumination. Fig (c) show the result of the new gradient blending module applied to the result of (b). The image transitions are smoothed out, thus making the seams practically invisible.

A2.1.3.3 Removal of Sunflickering interference

A common problem in video surveys in very shallow waters is the presence of strong light fluctuations, due to sunlight refraction. Refracted sunlight casts fast moving patterns, which can significantly degrade the quality of the acquired data.

A new module for the removal of refracted sunlight from shallow water video was created. This module is based on a method developed earlier at a proof-of-concept level.

The method of sunflickering removal exploits the fact that video sequences allow several observations of the same area of the sea floor, over time. The image difference between a given reference frame and the temporal median of a registered set of neighboring images is computed and used to correct the original image frame. A key observation is that this difference will have two components with separable spectral content. One is related to the illumination field (lower spatial frequencies) and the other to the registration error (higher frequencies). The illumination field, recovered by lowpass filtering, is used to correct the reference image. In addition to removing the sunflickering patterns, an important advantage of our approach is the ability to preserve the sharpness in the flicker-free image, even in the presence of registration inaccuracies.

The intermediate results of the method are illustrated in figure A9. This example was constructed from stack of nine registered frames over a relatively flat area. A low resolution median was constructed, and then subtracted from the original image. The two components of the difference image are easily seen. They can be effectively separated into the low frequency illumination field and the high frequency residues (resulting from imprecise registration and the low resolution median).

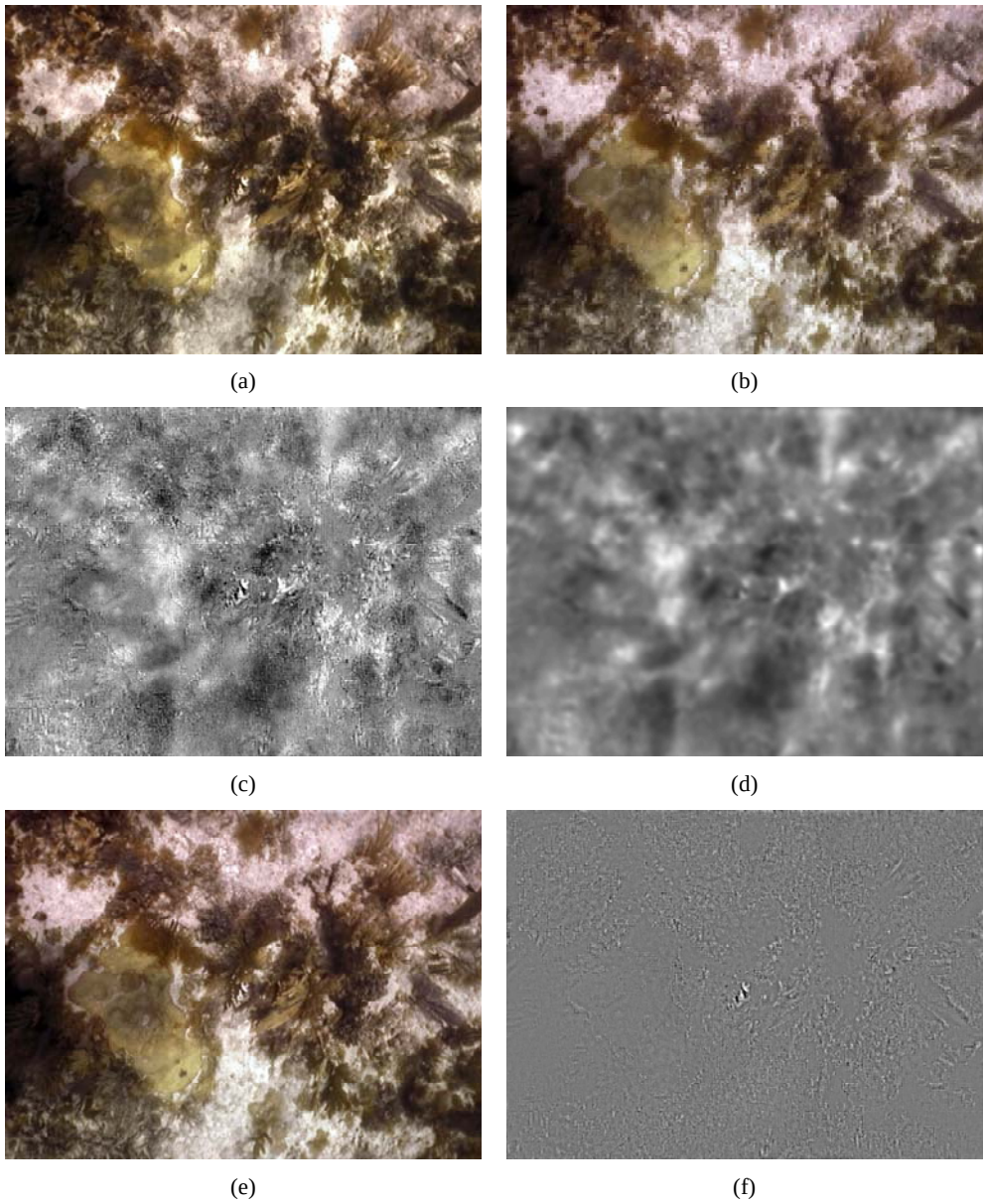


Figure A9. Example of application of the motion compensated filtering algorithm -Original (reference) frame (a), sub--sampled temporal median of the registered stack after projection into the reference frame (b), image difference between the median image and the original for one of the color channels(c), low--pass filtered version of the difference (d), result of the illumination correction to the original image (e), and difference between the corrected image and the median (f). The values of images (c), (d) and (f) have been stretched to improve visualization.

The method was tested on several underwater video sequences. Figure A10 provides an example of the input and output of the method on a shallow water sequence (2.5 meter depth), where the camera was close to the surface and moving at approximately 0.5 m/s. The method is able to remove the sunlight patterns without degrading image detail. Figure A11 illustrates the impact of refracted sunlight and the benefit of its removal, on a mosaic section of a shallow water survey.

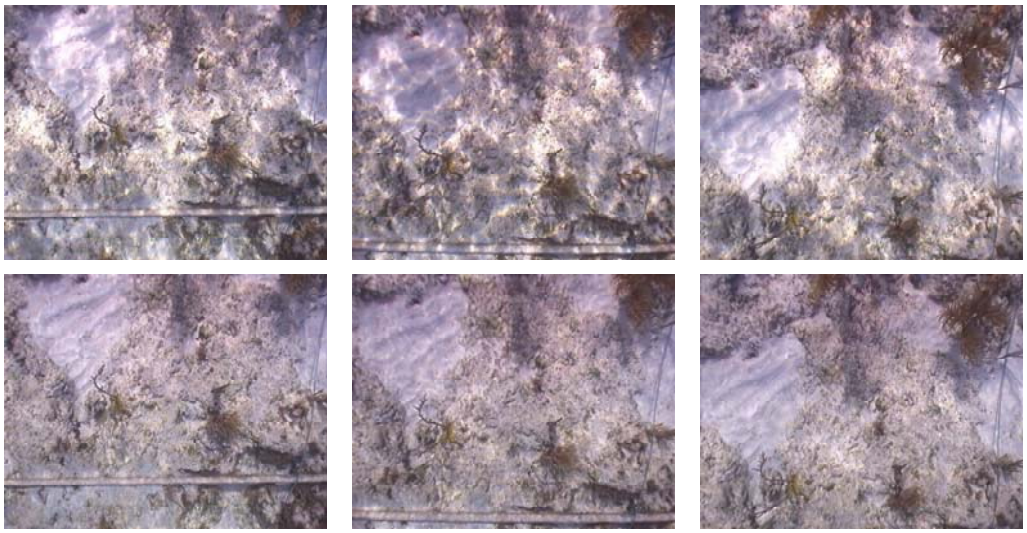
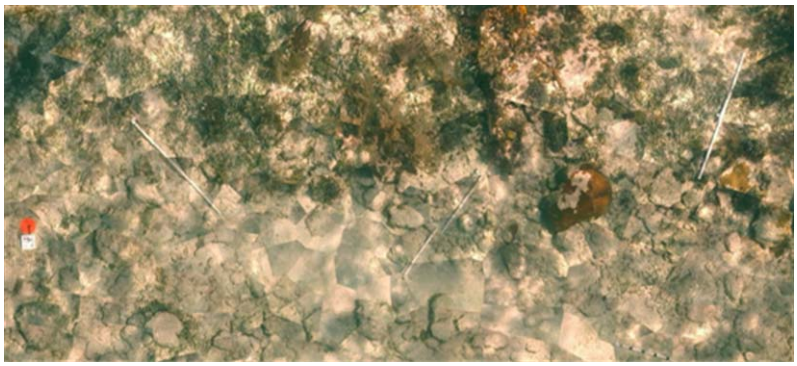
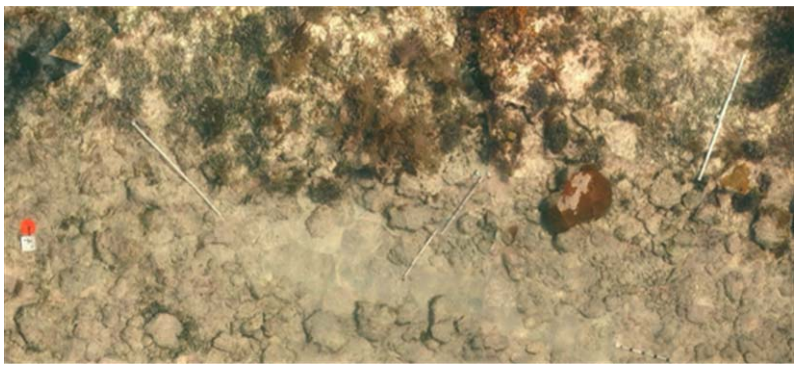


Figure A10. Original frames of a shallow water sequence (2–3 meter) with refracted sunlight (upper row) and resulting frames after applying our filtering technique (lower row).



(a)



(b)

Figure A11. Sections of the same shallow water survey under strong refracted sunlight, using the original images (a) and the output images of our algorithm for sun-flickering removal. For both cases the same blending method was used.

The motivation behind the sunflickering work was mainly practical, due to the large number of shallow water surveys carried out on sunny days. Unexpectedly only one previous work, by Schechner and Karpel (2004), exists on the topic of multi-image sunflicker removal. Their method is based on the median of gradients and is inspired by effective methods for removing shadows in open-air scenes (Weiss 2001). This approach is based on the observation that the spatial intensity gradients of the caustics tend to be sparse (*i.e.* affect small areas of the image). Therefore, by performing the temporal median over the gradients of a small number of images, it is possible to obtain a gradient field where the effects of the varying illumination are eliminated or at least greatly reduced. The flicker-free image is obtained by integrating the median gradient field. As the gradient field is likely to be inconsistent, a least squares approximation is performed using reversed derivative kernels. This approach does not attempt to estimate any particular time instance of the refracted sunlight illumination field. Rather, the flicker-free image is reconstructed using contributions from all images, as determined by the temporal median. Therefore this method can lead to blurry results under camera motion, since small registration errors are practically unavoidable.

In order to compare performance we implemented the median of gradients method, closely following the algorithm provided in (Schechner and Karpel 2004). Figure A12 provides an example using 5 registered images where the 3D content of the scene is clearly not well represented by planar image motion. The method based on the median of gradients, lead to blurry results due to the local misalignments from the 3D content, whereas our method is able to produce a sharp flicker-free image.

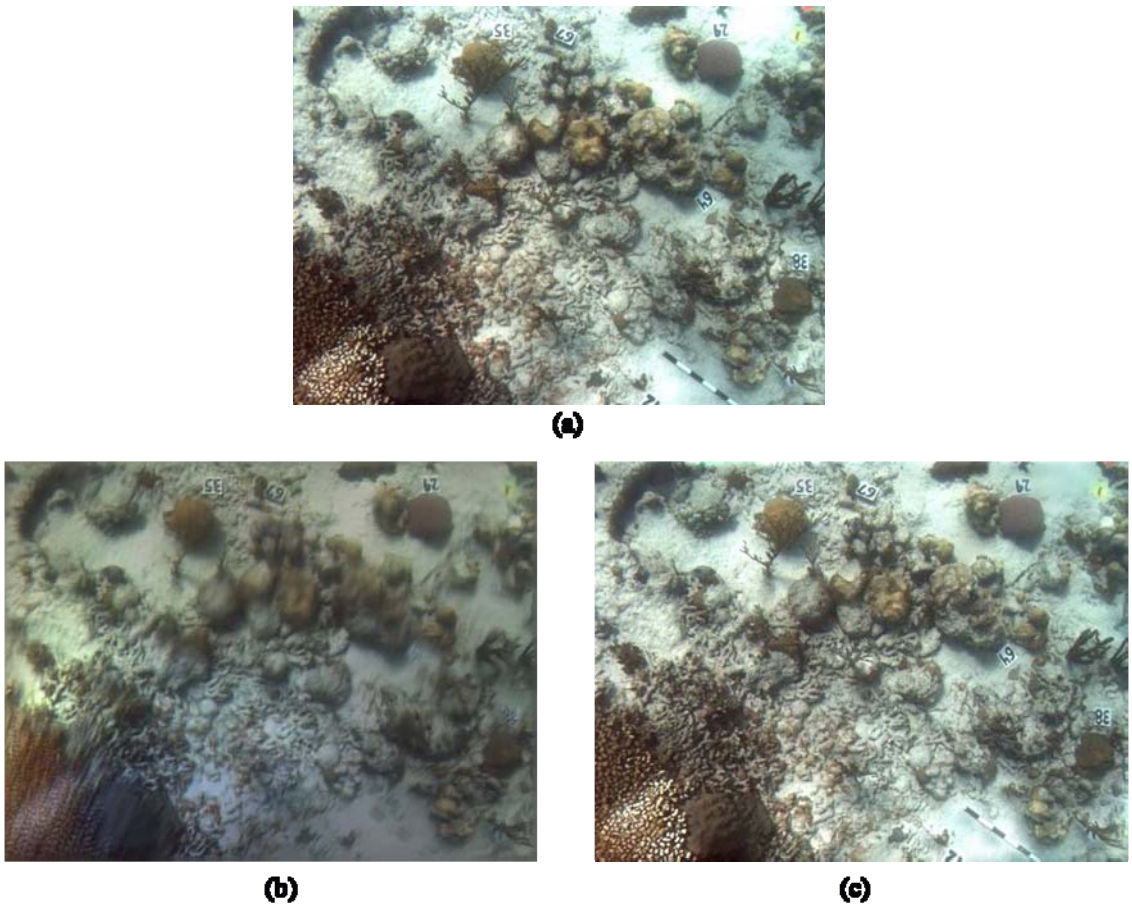


Figure A12. Performance of sunflicker removal methods under poor registration — Original frame from a sequence of 5 images registered under the assumption of flat seafloor (a), result of the median of gradients method (Schechner and Karpel 2004) showing blurring and color bleeding (b), and result of our method which is capable of removing the illumination artifacts without degrading the image quality (c).

Our work on sunflickering resulted in a research paper (Gracias *et al*., 2008) that was submitted, accepted and presented orally at the IEEE conference on Ocean Engineering in Quebec City, Canada in September 2008. Details on the method and a formal description of the approach are given in the paper. An extended version is in preparation for journal submission.

The initial research code (used for producing the paper results) was streamlined into an easy-to-use software module that is part of the project deliverable. The streamlining was done at two levels: (1) several input parameters now have data-driven values that are automatically adjusted from analysis of the images, thus releasing the user from that requirement, and (2) a graphical user interface was created for the complete process.

A2.1.3.4 Profiling and identification of bottlenecks

As part of improving the overall efficiency of mosaic creation, a profiling of processing bottlenecks was conducted. The purpose was to evaluate the entire mosaic production pipeline and identify the areas that need improvement. This effort lead to improvements conducted in

2008 and 2009, which involved recoding some parts of the software with gains at two levels – execution speed and memory limits.

The execution speed and memory limitations were addressed in two ways, and are detailed in sections A5.1.3.5 and A5.1.3.6. The following tables (Table A1 and Table) summarize the processing steps and indicate the level of improvement expected after re-coding. The first table refers to the existing mosaic creation modules and the second to the newer added capabilities.

Table A1. Table showing areas where speed and memory efficiency could be improved in existing mosaic creation modules.

Task	Subtask	Time presently required, and % of total (small size mosaic)	Suitability for Parallel Implementation	Impact of Parallel Implem.	Convertible to C / Mex	Impact of conversion to C / Mex
Image extraction	Image extraction	660 sec (1.8%)	Low	Low	No	Very low
Global Matching	Computing SIFTs	608 sec (1.6%)	High	Medium	No	Low
Global Matching	Image Matching	34600 sec (95%)	High	Very High	Low	Low
Global Matching	Optimization	70 sec (0.2%)	None	None	No	None
Blending	Image mapping	80 sec (0.2%)	Low	Low	Yes	Medium
Blending	Image Warping	300 sec (0.8%)	Low	Low	No	None

Table A2. Table showing areas where of speed and memory efficiency could be improved in enhanced mosaic capabilities.

Added Capability	Suitability for Parallel Implementation	Impact of Parallel Implem.	Convertible to C / Mex	Impact of conversion to C / Mex
Reduction of Sun flickering	Low	Low	Partially	Low
Use of Heading Sensor	None	None	No	Low
Graphcut Blending	High	Low	Partially	Medium
Integration of Stills and Video	High	High	No	None

The following routines were identified as key candidates that would benefit from recoding:

Image mapping in Blending, and Graphcut Blending – These steps contain very repetitive low-level operations which can be suitably implemented in C/C++.

Computing SIFTs, Image matching, and Integration of video and stills – A substantial part of these routines operate on pairs of images. The processing of each pair is totally independent of any other pair. Thus there is a potential for large speed increase after parallelization.

The memory limitations affect mostly the global optimization and the blending part of the mosaic creation. The limitations were imposed by the Matlab version 6.5, now outdated, for which the code was developed.

A2.1.3.5 Memory Enhancements

Memory limitations of the original mosaic deliverable product stemmed from problems inherent in running the mosaicing algorithm in an outdated version of Matlab. Although version 6.5 of Matlab was the programming environment in which the mosaicing processing algorithms were created, this version is bound to 32bits architectures with a maximum size for a single data structure of 1GByte. As an example, this environment precludes the rendering of mosaics larger than 50 Mpixel thereby limiting the size and resolution of all mosaic products produced in this format. Conversion and adaptation of the code to the newer version of Matlab and to a 64 bit version of the operation system raised this limit considerably.

All components of the mosaic creation code were successfully converted from Matlab version 6.5 (released in 2002) to version 2007b/64 bit (released in late 2007). Among other advantages, the newer 64 bit version allows for significantly larger data structures, thus releasing the existing memory limitation. With this conversion, the processing is only limited by the amount of physical memory in the computer. In a PC with 8GB RAM, the mosaic software in now able to produce mosaics in excess of 300 Mpixel, which are six times larger than previously possible. This allows us to not only process larger datasets but to incorporate higher resolution imagery into our mosaic processing systems. Both changes have resulted in improved products for coral reef monitoring.

Apart from the conversion to the 64 bits platform, several improvements were made on the data structures to promote a lower use of memory. Among these was a new tiling scheme for the gradient blending method**.** The new gradient blending module requires the use of the 2D Fast Fourier Transform algorithm (FFT) and its inverse (IFFT). The FFT and IFFT are applied to matrices that are as large as the final mosaic size. For very large mosaics (of more than hundred Mpixels) this requires enormous amounts of memory which are not available in standard or high-end PCs. In order to address this issue, we have created a scheme to divide the mosaic space into smaller tiles. Each tile is processed individually, taking into account the tile border conditions (to avoid creating seams along these borders). This scheme allow for running the gradient blending method for very large mosaics in PCs with standard memory capacity (3GByte). Furthermore the processing of all the tiles is significantly faster than a single run on the whole mosaic.

A2.1.3.6 Speed Enhancements

Parallelization

A central limitation of our previous mosaic processing capability was the single thread processing of many key routines. As such we have recoded many of these routines into C language, using multithreaded programming. Multithread programming allows for low-level parallelization in processors with several cores. For example the lower-level blending routines

operate at pixel-level, and perform a very large number of independent operations which can be executed in parallel. The recoding into multi-threaded C language resulted in an eight-fold increase of speed in our dual quad core PC.

Improvement in the linear optimization module - Implementation of a rigid sub-mosaic approach
A central component in the mosaic creation process is the so-called *global optimization* where the relative displacements of all images are computed. This process is carried out in two stages: (1) linear optimization to provide a fast, approximate solution and (2) non-linear optimization to improve on that solution. The linear optimization module requires the inversion of very large matrices, and sets the limit on the number of images that can be simultaneously mosaiced. Due to the memory limitations of version 6.5 of Matlab, the matrix inversion could not be performed for mosaics of more than 2000 images. This became a limiting factor for mosaicing larger areas. The conversion to Matlab version 2007b/64bit allowed for inverting matrices of much larger sizes. However the execution time for matrix inversion grows cubically with the size of the matrix. When doubling the number of images the processing time increases 8-fold.

To address this issue, a new linear optimization module was created in which the number of variables is reduced by considering several small rigid sub-mosaics. Using sub-mosaics of 5 to 10 images each, the linear solution is 125 to 1000 times faster, without adverse effects to the non-linear optimization stage. With the new module, more than 7000 images can be processed efficiently.

Improvement in the non-linear optimization module - Computation of analytic derivatives instead of numerical approximations
The non-linear optimization stage searches for the best displacement of images in the mosaic, by minimizing a given cost function. It requires the repeated computation of the derivatives of the cost function with respect to the parameters being minimized. On our initial implementation, this computation took most of the processing time, since it was done by numerical approximations. The non-linear optimization module was re-coded to use sparse matrix structures and to compute the derivative from symbolic formulas, instead numerical approximations. As a result, the execution time was cut by a factor of 3 for the typical number of images in our mosaics (about 800 to 1200). For larger sets, the speed increase is even larger.

A2.1.4 Second-generation landscape mosaics

The second-generation system was designed and built to incorporate high resolution still imagery and real time heading information into a standardized video acquisition system that would be easily deployed and utilized by a single research diver. The purpose of this upgraded system was to increase benthic resolution of the standard 2D video mosaic products (as developed during this project) and incorporate real world heading information into the video acquisition process to assist mosaic processing for high relief reef areas (See Section A2.1.4.2).

The upgraded mosaicing system was created using commercially available imaging components including: a Nikon D200 10MP Digital SLR camera and Ikelite underwater housing, Sony HDV video camera and Amphibico housing, fluxgate compass, and 3.5” LCD external color video monitor (Figure A13). All components of the enhanced mosaicing system were mounted in an

aluminum/stainless steel frame.

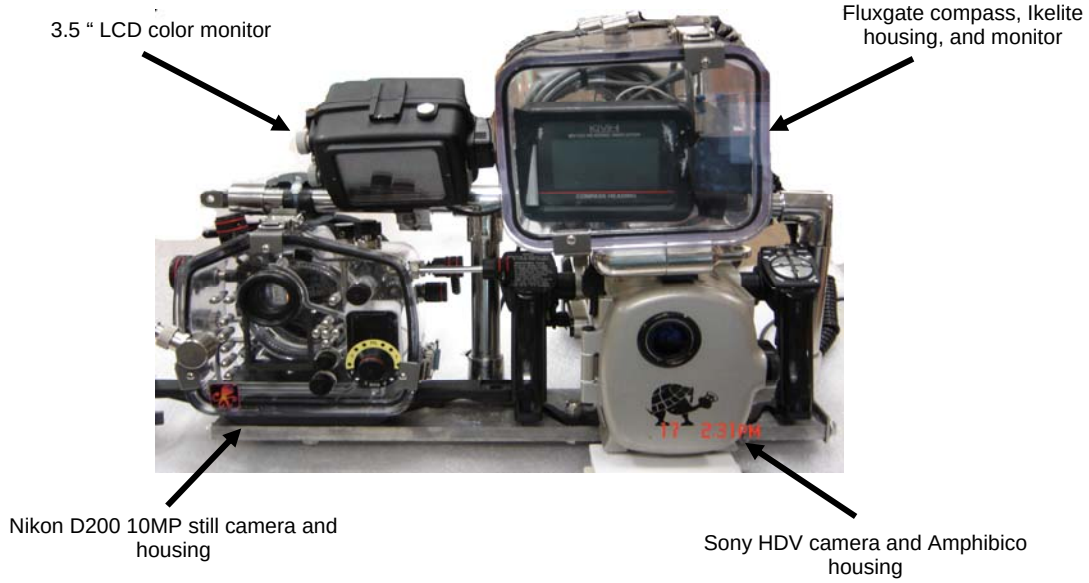


Figure A13. Completed enhanced imaging system.

Synchronization of the digital still frames with the video was achieved by installing an audio microphone inside the still digital camera housing to detect the click noise produced when the camera shutter is activated when a still picture is taken. This audio signal is routed to one of the audio channels of the video camera using a bulkhead waterproof connector.

To integrate heading information, a compass interface electronic circuit was designed, tested and calibrated. The heading information is provided by a KVH fluxgate electronic compass that measures the Earth's magnetic field and produces an analog voltage output proportional to the compass heading. This voltage is converted to a frequency in the audio range and stored in the audio channel #1 of the high definition video camera. The transfer function of the electronic circuit was measured on the bench obtaining the values shown in Table A3 and plotted as Figures A14and Figure A15.

Table A3. Measured Transfer Function

Degrees	Vin (Volts)	Fout (Hertz)
0	0.1	236
21.4	0.207	485
43.2	0.316	737
60.6	0.403	940
81.4	0.507	1185
101	0.605	1410
123	0.715	1660
140	0.8	1860
163.6	0.918	2140
193.4	1.067	2480
224	1.22	2840
241.6	1.308	3040
260.6	1.403	3260
281.2	1.506	3500
300.4	1.602	3730
323	1.715	4000
341.2	1.806	4200
359	1.895	4400

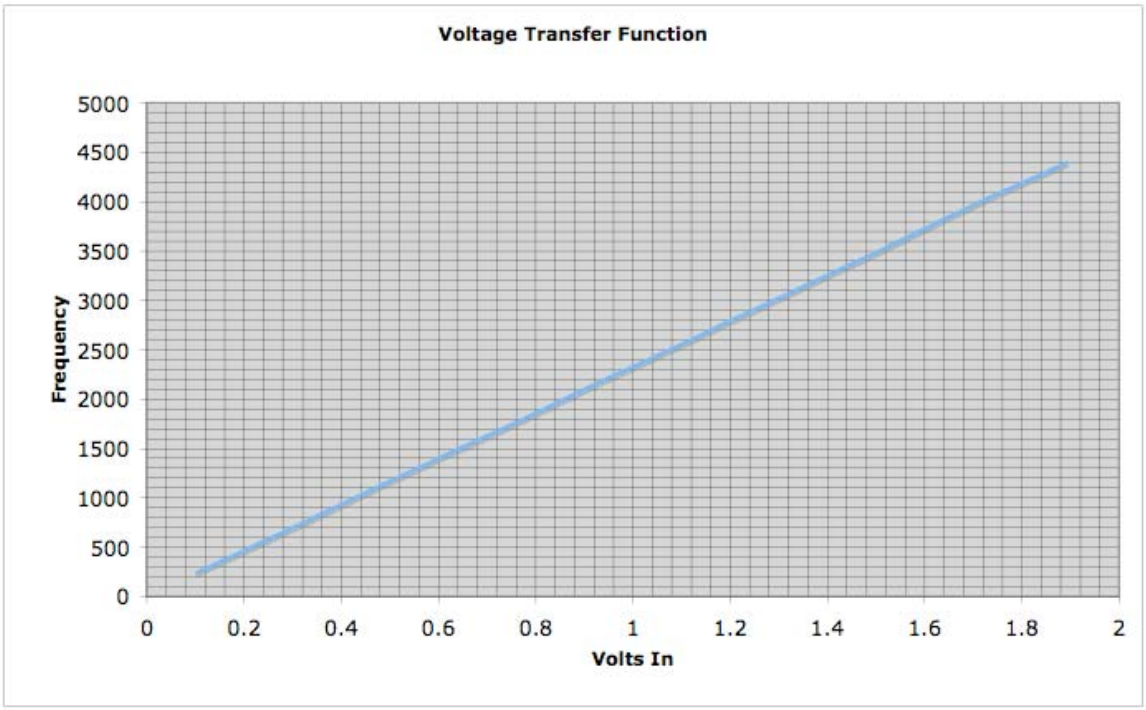


Figure A14. Plot of the Measured Voltage Transfer Function

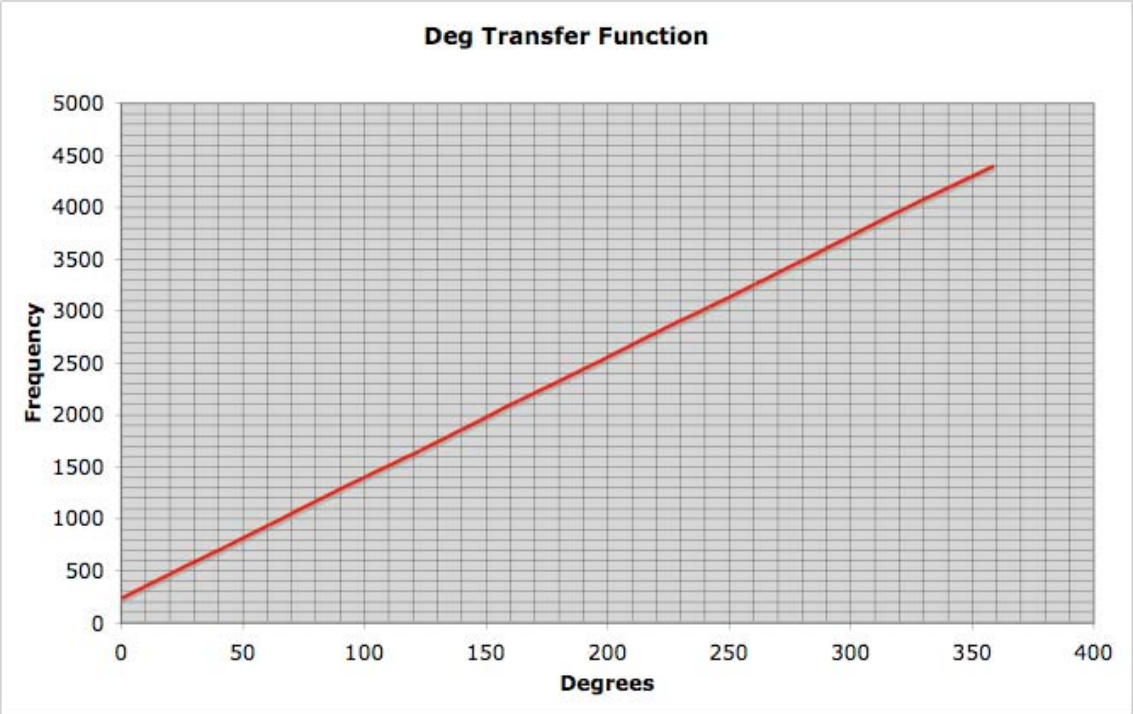


Figure A15. Plot of the Angular transfer Function.

To calibrate the compass, the system was mounted on a rotating table with the real time LCD compass display mounted in front of the cameras enabling the video camera to record the displayed compass heading while recording in one of its audio channels the tone corresponding to this particular heading and also recording in the second audio channel the instant that a still picture was taken with the Nikon camera. The system was rotated following a pre-established protocol while the video camera was recording the heading and a still was taken every two seconds. Figure A16 illustrates the calibration setup.



Figure A16. Heading Calibration Setup

The upgraded mosaic imaging system was designed for deployment by a single research diver, and is neutrally buoyant in saltwater. The imaging system is designed to record up to an hour of video per tape and up to 1300 10MP still images before downloading. The interval timer mode of the Nikon D200 allows users to change the rate of image acquisition depending on survey requirements. Field testing of the enhanced mosaic imaging system has shown that surveys performed with still images taken once every 2 seconds provided sufficient overlap to cover a 10x10m area.

A2.1.4.1 Integrating high resolution stills with video image acquisition

The objective of this effort was to increase the resolution of the mosaics by combining images from two coupled optic sensors (i.e. cameras) with different resolutions and frame-capture rates. The mosaic algorithm requires a high overlap between sequential images to accurately estimate camera motion. In the field, high overlap between images is achieved by using video cameras with a high rate of frame capture. In addition, the ability to detect and identify small organisms (< 10 cm) from the mosaic requires a high image resolution. Current camera technology does not provide a system that can simultaneously capture frames at a high rate with high image resolution.

The proposed solution was to combine information from two cameras: (1) a high-definition video camera capable of high frame-capture rates (30 fps) with lower image resolution (< 1Mpixel); and (2) a digital still camera capable of acquiring very high-resolution images (> 10 Mpixel) at low capture rates (one image every sec).

The enhanced acquisition hardware allows for the simultaneously collecting video and photographic stills using two independent cameras mounted on the same frame. The video sensor can provide images of 0.7 Mpixel at 30 frames per second, while the still camera provides 10 Mpixel images at 1 frame per second. The sensors are not synchronized, so the correspondence between the video and the still frames is not known during acquisition. However, the sound of the shutter release of the still camera is recorded in one of the audio channels of the video camera. The approach for combining video and stills comprises the following three steps:
1 – Find correspondences between individual video frames and stills.
2 – Create a mosaic from the video images.
3 – Relate the stills with the mosaic.

Step 1 deals with determining which video frame most closely relates to each photo still. Two approaches were tested:

1 - Detecting the audio signatures of the shutter release.
2 – Using image matching between video and stills.

The first method requires the user to establish the first corresponding pair of video and still. It assumes that all subsequent shutter releases are successfully detected. The second method uses the image matching tools already developed for the mosaic creation. It does not require user intervention, is significantly more robust in finding the correct correspondences, and provides the

geometric displacement between images. Albeit slower (taking a few hours ***instead*** of few minutes), it was the method of choice.

Step 2 is the standard mosaic creation procedure. In a final step the information of the first two steps is combined to establish the position of each still in the mosaic frame.

Results of the joint processing of video images and photo stills were obtained using data collected in Andros, Bahamas in October 2007. Figure A17 illustrates the results of matching pairs of images from the two different sensors. For each video frame, this matching allowed establishing the closest corresponding still, by choosing the largest overlap between frames.

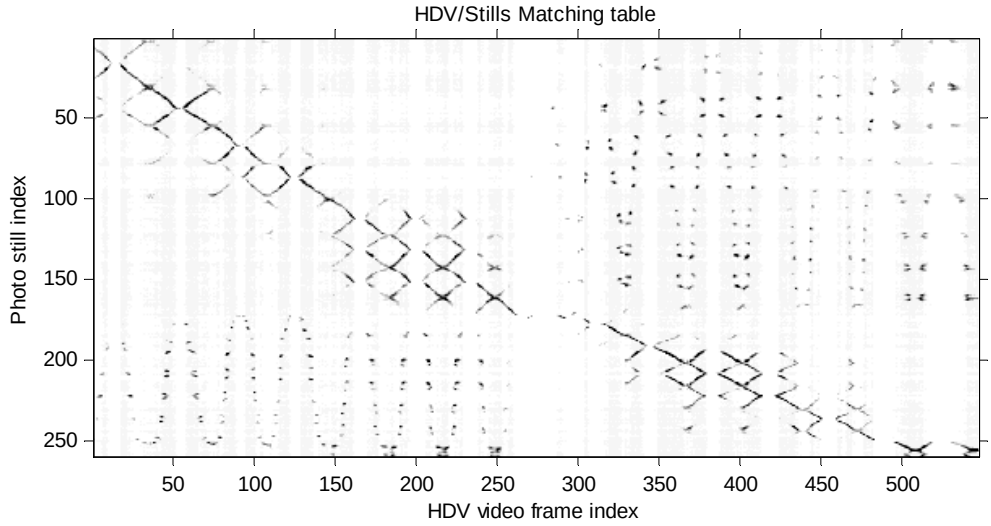


Figure A17. Table representing matches between video images and photo stills. Successful matches are represented by dark dots.

A simple point and click tool was created to illustrate the usefulness of combining video and stills. The tool allows for retrieving the video image and the still photo that are closest to a point of interest in the mosaic, defined by the user. Figure A17 illustrates the concept.

This tool was further developed into a stand-alone Windows application. It provides the same point and click functionality to retrieve and inspect individual video and still images. Since it does not require the presence of the Matlab environment in the computer. It can easily be distributed and used in any windows machine. The application is described in Section A2.6.3

A2.1.4.2 Integration of heading information in 2D mosaic processing

In a further attempt to improve mosaicing in areas of high topographic relief, we investigated integration of heading information to help track the trajectory of the video cameras. The detection of camera trajectory is a crucial step needed to obtain high quality mosaics with low geometric distortions. The proposed solution was to integrate a heading sensor with the video

camera, in order to provide absolute orientation of each image frame with respect to North. The heading sensor allows all frames to be oriented, thus increasing the chances of tracking the correct camera trajectory.

Integration of a heading sensor for improved mosaicing in high relief areas involved two steps:
i – Develop algorithms to *decode the compass output information.* This information is recorded in one of the audio channels of the High Definition Video (HDV) camera.
ii– Develop a *calibration procedure* to obtain a relationship between the output of the compass and the heading values and to assess the sensor accuracy.

i. Decoding the heading
The flux gate compass outputs a voltage proportional to the heading angle. This voltage is converted into a squared wave of varying frequency using a Voltage Controlled Oscillator (VCO). The frequency ranges from 250Hz to 4400Hz, approximately corresponding to heading angles of 0 to 360 degrees. The camera is set to record at 48 KHz thus being able to reproduce signals of frequencies up to its Nyquist cut-off frequency of 24 KHz. Thus the frequencies of the heading signal are well within the range adequately recorded in the audio channel of the camera without aliasing.

Each cycle of a squared wave comprises a high value output and a low value output. The duty cycle is defined as the ratio of the duration of the high value output with the duration of the complete cycle. The squared wave produced by the VCO has a duty cycle that varies with the frequency. Figure A18 illustrates audio samples for a low frequency and a high frequency case.

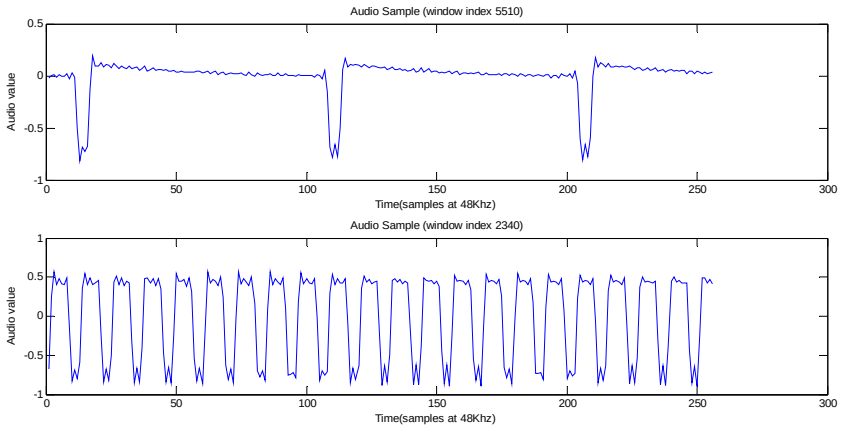


Figure A18. Examples of audio samples for a low frequency case (top, 250Hz corresponding to heading of approximately 0 deg) and high frequency case (bottom, 4400Hz corresponding to approximately 360 deg).

Our goal was to determine the base frequency of the square wave (first harmonic). The fact that the duty cycle is not constant results in distinct spectral content for wave of different base frequencies. To determine the base frequency, the audio signal is divided into non-overlapping segments of 1600 samples. Each segment has the duration of one frame of the original HD video, at 30 frames per second (fps), and is processed independently.

To analyze the frequency content of each segment, three approaches were considered. These are based on computing the values of: 1 – the power spectral density, 2 – the temporal autocorrelation and 3 – the magnitude of the Fast Fourier Transform. A representation of these computations is given in Figure A19 for low frequency and high frequency examples.

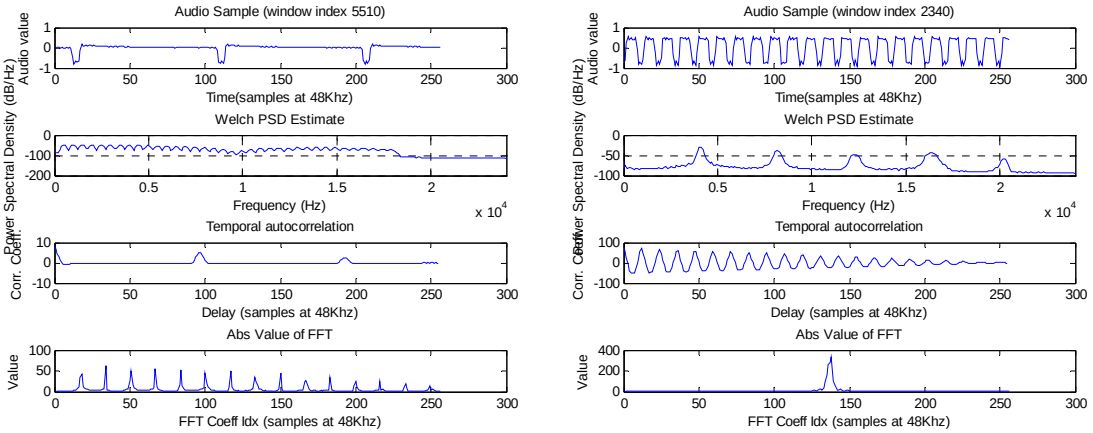


Figure A19. Examples of audio samples (first row), and corresponding power spectral density (second row), temporal autocorrelation (third row) and magnitude of the FFT (forth row), for the low frequency case (left column) and the high frequency case (right column).

All three approaches can be used to determine the base frequency, by localizing the first peak. However the best results were obtained by the magnitude of the FFT. This approach is the most robust to artifacts caused by changes of base frequency within the segment. Changes in frequency occur when the sensor outputs a new heading value.

An unexpected issue occurs when the heading sensor crosses the 0 to 360 degree boundary. The heading sensor has relatively large settling time and thus outputs intermediate values over an interval of approximately one second. These intermediate values need to be filtered out, since they will lead to largely inconsistent heading readings. In addition, the sensor has gaps in the output when it changes its output values. These gaps last for approximately 50 msec, during which the frequency is close to zero, and can corrupt the segments to the point of resulting in wrong base frequency estimation.

The issues of the large settling times and the output gaps were solved by (1) performing a filtering of the estimated base frequency using the median over a temporal sliding window, and (2) explicitly detecting the north crossing transitions and removing intermediate outputs during the settling time. An illustration of this process is given in Figure A20.

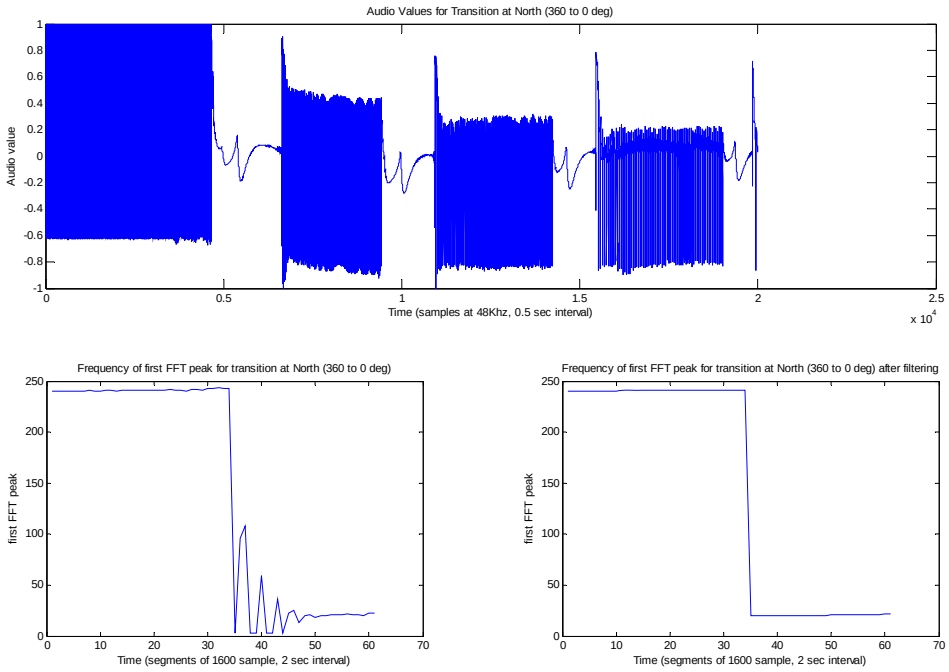


Figure A20. Illustration of the large settling time for a 360 to 0 degree transition. The top figure contains an audio sample for an interval of approximately one second. The lower left figure shows the raw value of the decoded heading signal, which is proportional to the audio frequency. The gaps and the multiple intermediate frequencies are visible in the several peaks. The lower right figure shows the raw decoded heading after filtering, with these artifacts removed.

ii. Heading sensor calibration

The purpose of the sensor calibration is twofold: (1) to obtain a way to convert the frequency output values into heading angles, and (2) check for systematic errors caused by the magnetic interference of the hardware surrounding the compass, and estimate sensor accuracy.

A calibration procedure was devised. It comprises the following steps:

1. Acquire video under pure vertical rotation – The acquisition is done with the complete setup, in the water, with the camera roughly pointing towards the same area in the bottom.
2. Use image registration to obtain rotation angles between images – This involves performing the global matching step of the 2D mosaic creation software. Since all images look at the same area of the bottom, it is possible to perform the image registration between any pair of images. Therefore, there we can estimate the rotation angle of each image with respect to the first image (considered the reference frame) without accumulating errors. This measurement is taken as ground-truth and compared against the compass measurements.
3. Fit a curve to the pairs of compass reading and image rotation angles.
4. Characterize distribution of residues, to check for systematic errors and obtain a sensor accuracy estimate.

The image rotation angles measured from the calibration sequence and the sensor readings are plotted in Figure A21.

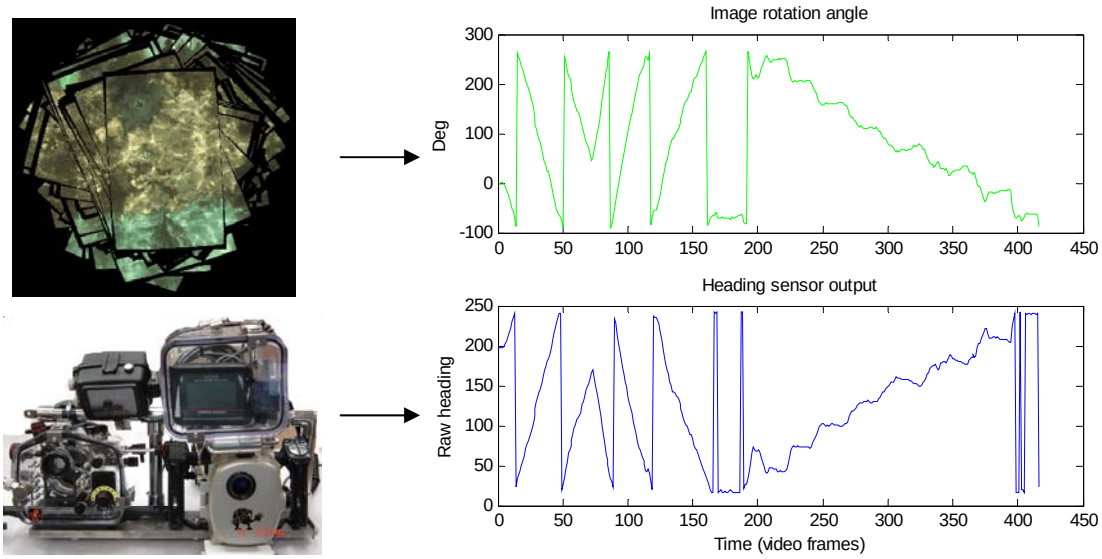


Figure A21. Rotation angles obtained from the calibration sequence using image registration (upper row) and raw sensor readings decoded from the compass audio recording (lower row).

Figure A22 (left) shows that the pairs of compass readings and image angle measurements have a close linear relationship. Additionally, no large deviation from this line is observed, which indicates the absence of large systematic errors. As such, there was no need to correct for these errors.

The uncertainty of the heading sensor was estimated by checking the distribution of residues of the linear fit. The histogram is presented in Figure A22 (right), and approximately follows a Normal distribution with standard deviation of 2.2 degrees. This value is consistent with the rated precision reported by the manufacturer, and is well suited for our needs.

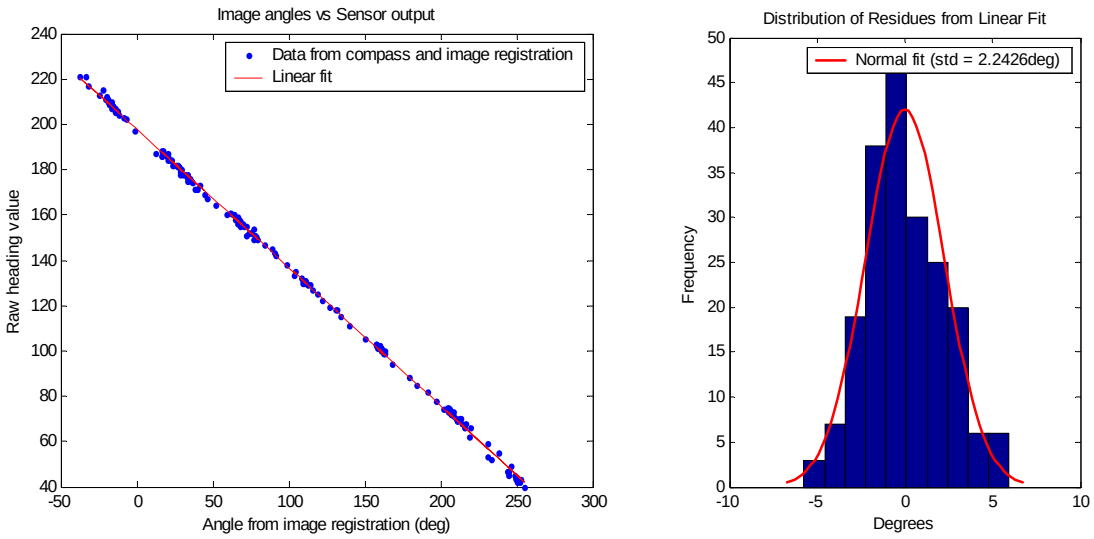


Figure A22. Calibration of the heading sensor – The left figure shows pairs of compass readings and image angle measurements (blue dots) with a linear fit (red line). The right figure presents the histogram of residues from the linear fit. The red line is a Normal distribution with the same zero mean and the same standard deviation of 2.24 degrees as the residues.

To investigate the usefulness of the heading information, we performed two experiments. The experiments differ regarding the stage of the mosaic creation process where the heading information was used.

The current implementation of the 2D mosaicing algorithm assumes that a set of images have been extracted from a video sequence. In the first step, called *initial trajectory estimation*, the images are matched consecutively in pairs along time. The purpose of this step is to remove images that have high overlap with the previous ones, thus reducing the number of total images to be mosaiced. In the second step, called *global matching*, the selected images are matched against the others in order to establish as many *links* as possible. These links are geometric constraints among images that result from a successful image matching. In the third step, called *global alignment*, all the image links are taken into account to establish the best geometric arrangement for all images.

The first result is an *a posteriori* application of the heading information to a globally aligned mosaic that was created using information from the image matching alone. We selected an example where the presence of high topography prevented the mosaicing algorithm from producing geometrically accurate results (Figure A23). The survey pattern consists of horizontal strips. The two central strips have very low overlap. A close inspection of the right hand side of the mosaic reveals that the mosaic section above and below the wedge-shaped dent should be slightly overlapping. Due to the low superposition of these images and high topography area in the middle, the mosaic algorithm did not join these sections.

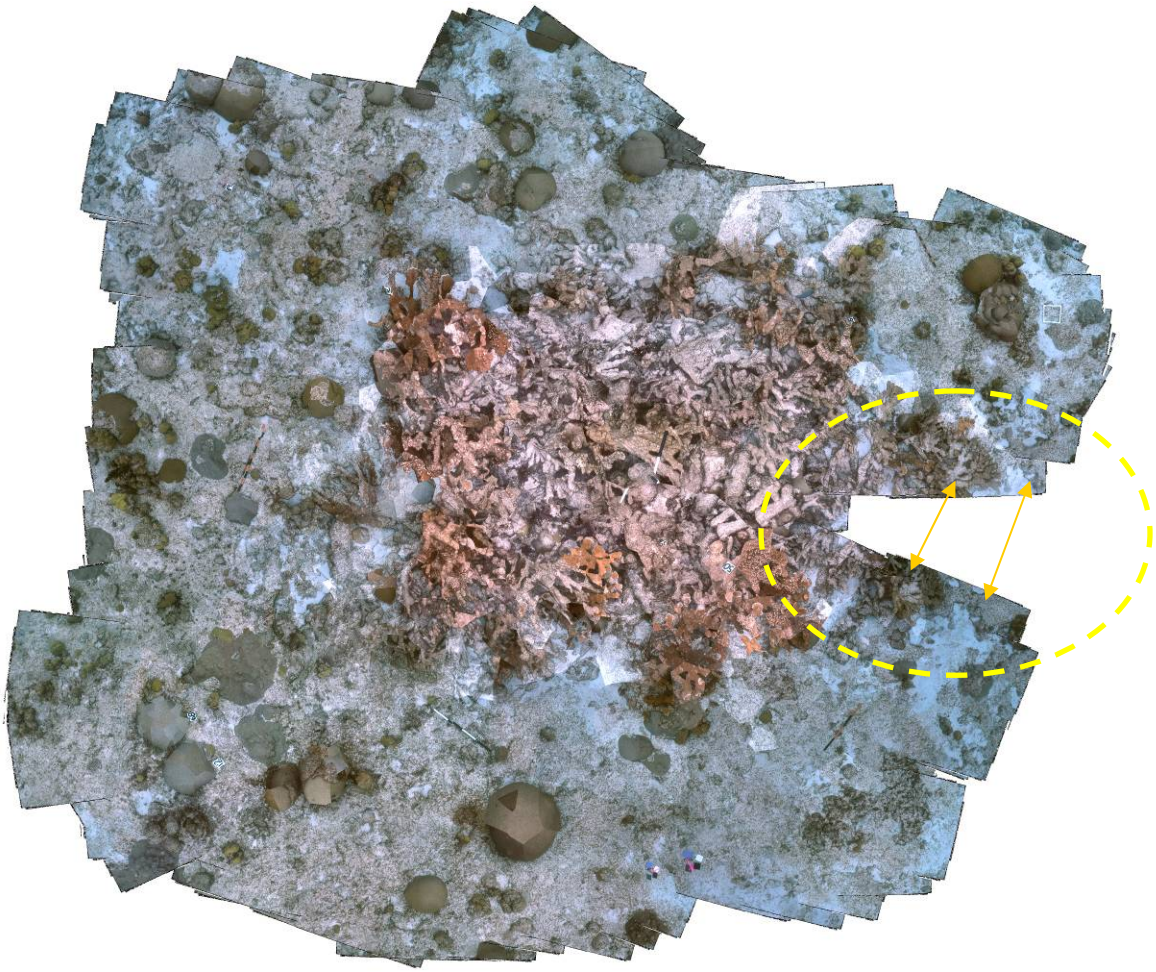


Figure A23. Example of a globally aligned mosaic with geometric distortions. The gap inside the area marked in yellow should not exist since the upper and lower portions of mosaic overlap. The arrows mark the same benthic structures. The distortions are due to high relief (in the central area of the mosaic) and low overlap among the images inside the marked region.

The heading information is used by replacing the orientation of the images usually obtained by the global alignment, with the compass readings. The relative translation among neighboring images along the trajectory was kept intact. This process changes both the position and the orientation of each image, and has the effect of restoring the parallelism among the horizontal strips that form the survey pattern.

A schematic of the image displacement before and after the use of heading is given in Figure A24. The use of heading leads to a small improvement, since the two sides of the gap are closer. However it is not sufficient to remove the gap and join the overlapping areas.

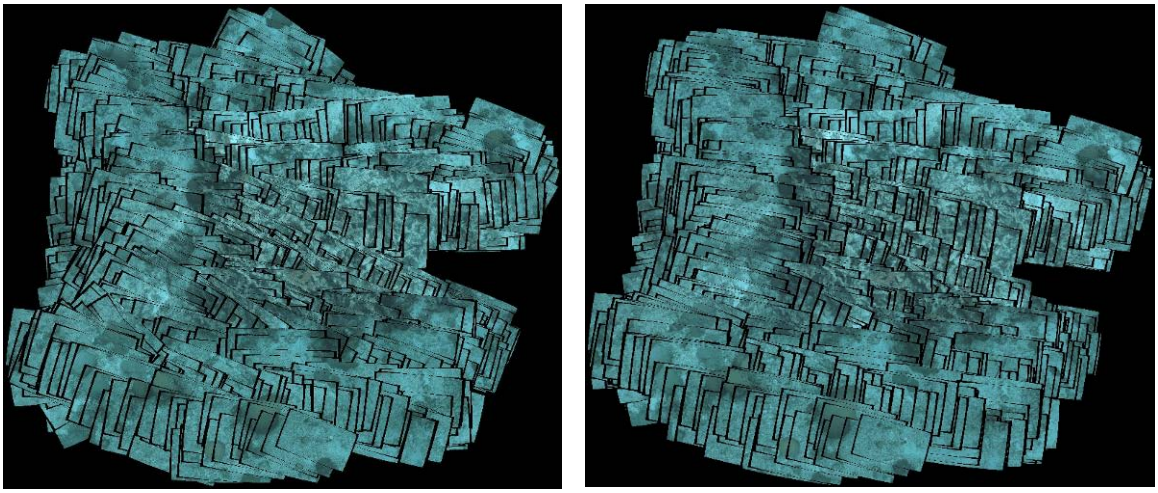


Figure A24. Example of the use of heading on a globally aligned mosaic. The mosaic on the left was obtained from image matching alone and is the same in Figure A23. The mosaic on the right was created by combining the heading information from the compass with the image translation provided by the image matching. The heading improved the results but not enough to avoid the gap on the right. These mosaics were rendered with visible image frames to emphasize differences in orientation.

The second example illustrates a potential benefit of using heading during the step of initial trajectory estimation. Figure A25 shows an example from a short video sequence where the camera moved sideways while keeping roughly the same heading. The survey pattern consisted of 4 parallel strips. Without heading information the initial trajectory rapidly accumulates errors (namely in the orientation of the images), which leads to large displacements in the trajectory. Using the heading information the error growth is much smaller, resulting in a trajectory closer to what is obtained after the complete mosaicing process.

As mentioned previously, in the current implementation of the mosaicing algorithm, the initial trajectory estimation step is only used to check the superposition among time-consecutive images, and to discard redundant images. However, if the trajectory is accurate enough, it can be used to predict areas of possible image overlap. The global matching step (that follows) can concentrate on attempting to match images in these areas, where successful matches are more likely to be found. This will potentially have a large impact in reducing the amount of processing time required for the global matching step.

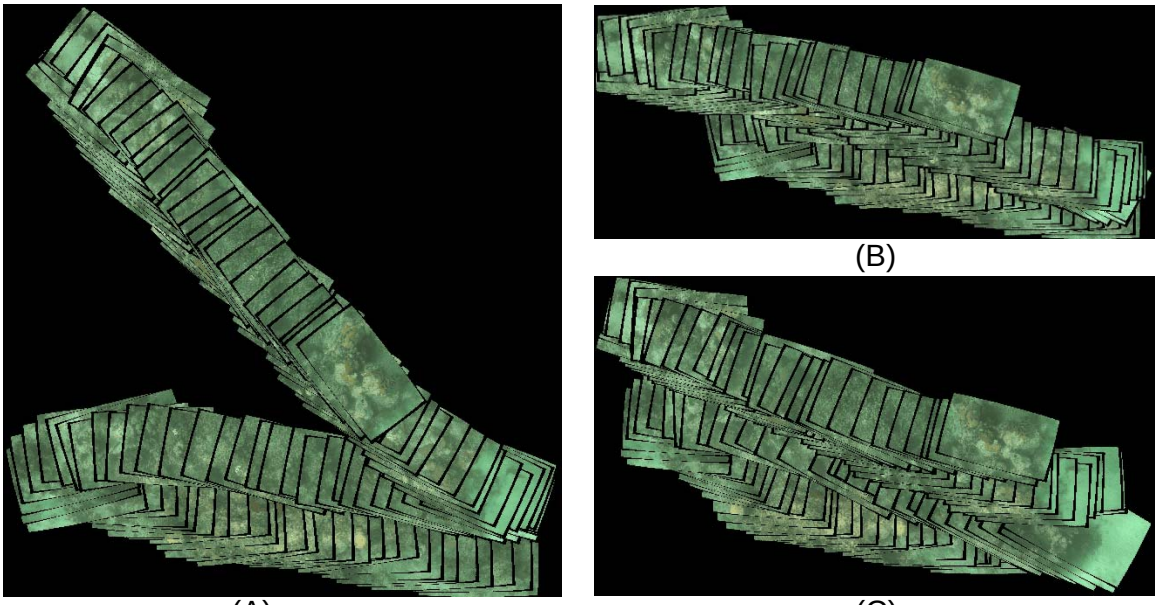


Figure A25. Example of use of heading in the estimation of the initial trajectory. In this short video, the camera moved sideways, keeping roughly the same heading. The survey pattern consists of 4 strips, which are approximately parallel. (A) is the initial trajectory estimate without heading information. The motion estimation errors accumulate rapidly resulting in non-parallel strips. (B) is the initial trajectory where the heading was obtained from the compass and the translation from the image matching. The error accumulation is smaller since the strips remain parallel. (C) is the result of the complete mosaicing process using global matching and global estimation, and serves here as ground-truth. The heading information leads to a trajectory (B) closer to (C), than (A) is.

A2.1.5 Collaborative work on further algorithm development

Motivated by the scope of our SERDP project, exploratory work on image processing algorithms was carried in collaboration with the University of Girona, in Spain. Several publications acknowledging SERDP resulted from this effort. Given the exploratory nature of this research, the outcomes were not intended to be incorporated into the software deliverables. Nonetheless it resulted in several algorithmic improvements that benefitted the final software deliverables.

The exploratory work focused on three topics: 1) Selection of best candidates for image matching, 2) Automatic change detection and 3) Extension of the graph-cut blending to 3D surfaces.

A2.1.5.1 Selection of best candidates for image matching

Recent advances in image matching methods, such as the SIFT, allow for registering pairs of images in the absence of prior information on orientation, scale or overlap between images. Evaluating the benefit of potential matches between images before the actual matching operation is an important issue that has not yet been fully addressed in the literature and which can have a large impact in the computational efficiency of batch mosaic algorithms. A new approach for solving this issue was investigated using the Observation Mutual Information as a criterion to evaluate the benefit. This allows for ranking and ordering a list of potential matches in order to make the loop-closing process more efficient. The criterion was compared against other

proposed strategies and results are presented using underwater imagery. This work was presented at a conference and published as the following paper:

Elibol, A., N. Gracias and R. Garcia (2009) Match Selection in Batch Mosaicing using Mutual Information. *Proc. of the 4th Iberian Conference on Pattern Recognition and Image Analysis* (IbPRIA2009), Povoa do Varzim, Portugal, June 2009

An outcome of this work was the development of a fast method to find the most similar image pairs, using SIFT descriptors (Lowe 2004). The most similar image pairs are matched first. Since the image matching step is the most time consuming part of all the mosaicing process, the use of this similarity criterion results in a significant saving in computation time. The method was implemented in multithreaded C and incorporated in the project deliverables.

A2.1.5.2 Automated change detection

The automated detection of changes between images of the same area of the benthos is of great interest for improving the speed of environmental monitoring. However, the existing algorithms for change detection were developed mainly for aerial surveying and require highly accurate registration in 3D. This requirement has precluded their use in underwater imagery.

To deal with this problem, a new approach was developed, based on the creation of 3D models of small areas. Using image-to-3D-model registration and local photometric adjustment, it attained the required levels for accuracy in geometric and photometric registration. This work is the first successful attempt to detect changes in underwater image sets, of small coral reef patches. It was published and presented at the leading conference in ocean engineering and published in the following paper:

Delaunoy, O, N. Gracias, R. Garcia, (2008) Towards detecting changes in underwater image sequences, Proceedings of the IEEE / MTS Oceans 2008 conference. Kobe, Japan, April 2008.

A2.1.5.3 Extension of the graph-cut blending to 3D surfaces

The method for efficient image blending (Gracias et al, 2009), described above as part of the enhancement of the 2d mosaicing algorithm, was extended for blending multiple images over a 3D surface for creating ortho-mosaics. As before, the objective was to produce seamless image blending that preserves the clarity of object textures, even in the presence of illumination changes and image misalignments.

The blending is performed by optimizing two distinct geometric and photometric criteria. A meaningful geometric criterion was considered to select the images where the camera position and orientation are the best to provide texture to each triangle in the 3D model. This criterion provides a balance between choosing nearby cameras and reducing perspective distortions induced by the slanting. The photometric criterion minimizes the visibility of the seams that occur at the boundaries of neighboring image contributions. The balance between these independent and conflicting criteria is obtained by graphcut optimization.

Figure A26 provides an example of the blending over a 3D surface for creating an ortho-mosaic. This extended blending method was published in the Journal of Field Robotics (Nicosevici et al 2009).

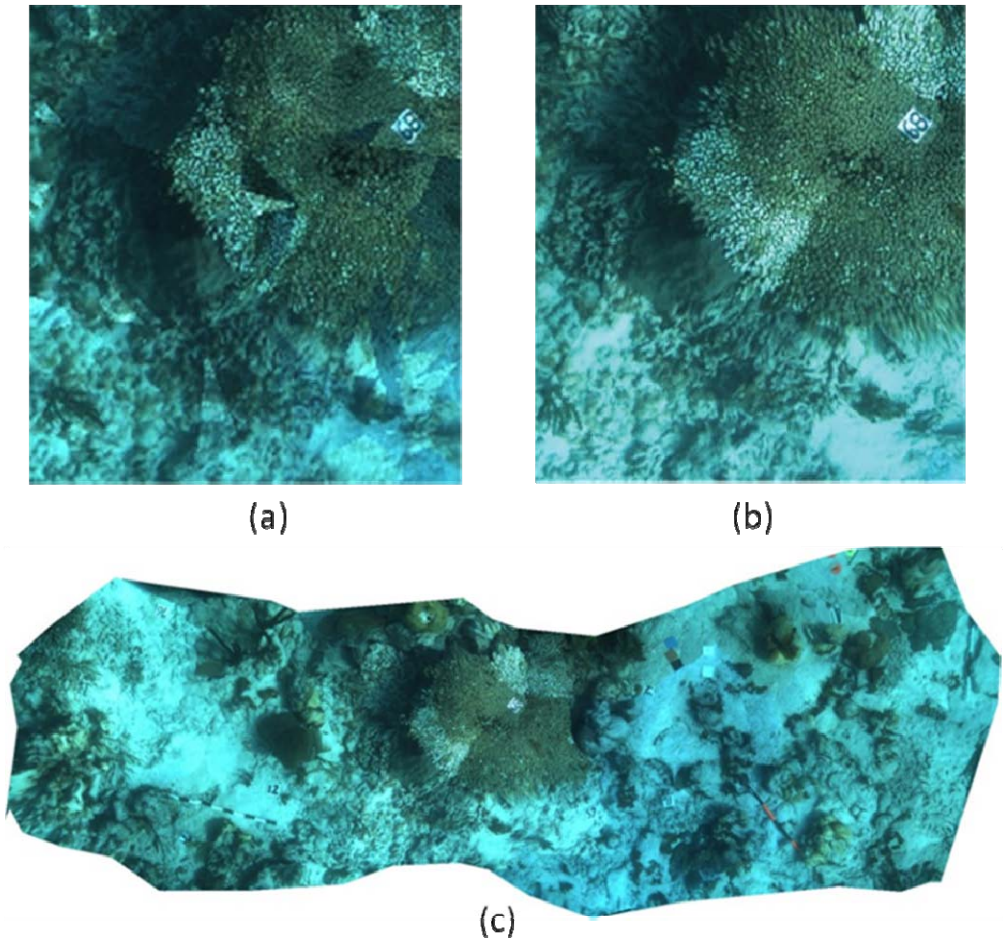


Figure A26. Comparison of blending over a 3D surface, obtained using a simple geometric criterion (a) and the improved graph-cut blending method extended to 3D, which combines geometric and photometric criteria (b). The seams visible in the middle and bottom of (a) are eliminated in (b). An orthomosaic using the improved method is presented in (c).

A2.2 Mosaic Products

Between 2003 and 2009, numerous reef sites were imaged with our 2D mosaicing technology. These surveys resulted in the production of 93 mosaic images for use in traditional and non-traditional monitoring applications. These mosaics are presented in Appendix 2, with information on ground resolution (pixel size) and total benthic area.

A2.3 Analysis of mosaics

A2.3.1 Geometric analysis of landscape mosaics

An important aspect in evaluating the utility of the 2D mosaics is to determine their geometric accuracy. To some extent, our current mosaicing algorithm can successfully cope with violations of the assumption that the bottom is static and flat. However, significant topography can contribute to geometric distortions. The amount of distortion needs to be quantified for ecological analysis involving spatial measurements. In order to assess geometric accuracy, we have established a method and performed the analysis over our two test sites.

The method involves two steps.

1. In the first step, divers establish the metric positions (XY coordinates) of a set of markers placed on the sea floor. Once established, the location of these markers is considered ground-truth. Since it is difficult to directly measure the XY coordinates of points underwater, the creation of the ground-truth data is done indirectly using a network of distance measurements between points. Field data for measuring these distances were collected by divers.
2. In the second step, the locations of the markers as measured from the mosaic are compared with diver ground truth. To do this, the mosaic image has to be georeferenced. The georeferencing is done by computing the coordinate mapping between the mosaic image and the world metric frame, using a subset (or all) of the ground-truth. After this, the image locations of the markers are projected onto the world coordinate frame. An error vector is defined as the XY differences of the projections with the ground-truth. As measures of accuracy, we consider (1) the standard deviation of the error components, and (2) the maximum error magnitude.

An initial accuracy assessment was performed on a mosaic from the Key Biscayne site using video data acquired in June 2004. A ground-truth set of 24 positions was estimated. The residuals approximate a Normal distribution with 2 cm standard deviation, which is consistent with the measurement noise. A subset of 20 marker points, visible on the mosaic (Figure A27), was used both for georeferencing and error measurements. The error vector presents a standard deviation of 5.1 cm. The maximum error magnitude is 14.2 cm. The histogram of the error vector is shown in Figure A28.

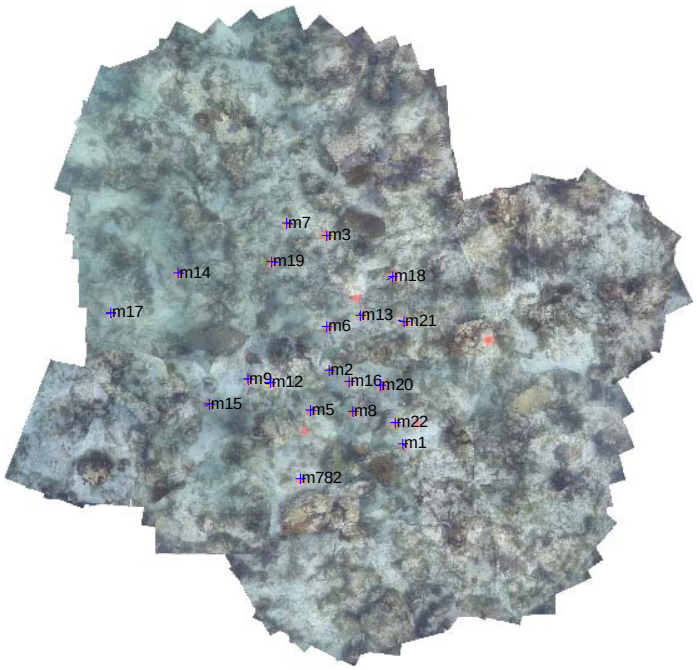


Figure A27. Mosaic image from the Key Biscayne site with selected marker positions.

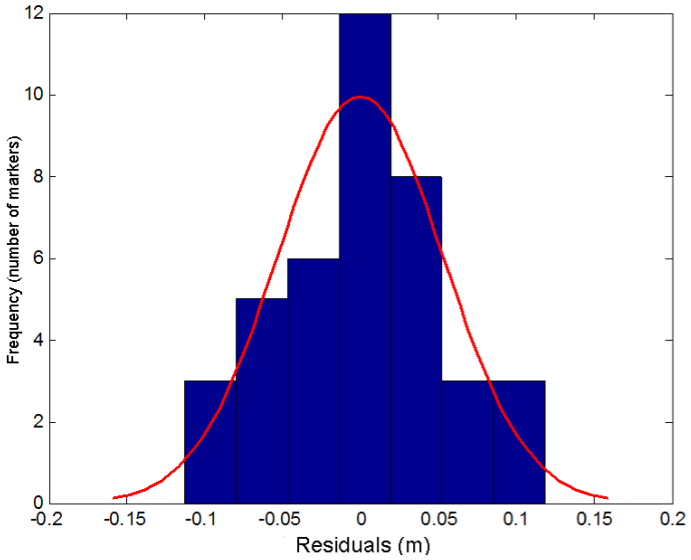


Figure A28. Histogram of the error components, with superimposed normal distribution fit.

Geometric accuracy analysis of the Key Largo site used 22 visible ground truth points and produced comparable results. The error standard deviation is 7.7 cm and the maximum error magnitude is 18 cm.

Two factors influence the accuracy and applicability of this analysis. One is the fact that the ground-truth positions are obtained in 2D, thus assuming constant elevation. Although care was taken in choosing locations for the markers that were approximately on the main plane of the terrain, there are always elevation differences that are not accounted for. The other is the number of markers and the area covered. Current results correspond to around 20 markers over 5x5 meter areas.

A2.3.2 Ecological analysis of landscape mosaics

A subset of our existing mosaics was selected to evaluate the utility of the mosaicing technique in coral reef monitoring applications. The performance of the mosaics was assessed in terms of the ability to 1) produce spatially accurate coral reef scenes, 2) extract percent cover measurements of major benthic categories, 3) accurately measure colony size from video mosaics, and 4) detect changes in benthic composition over time. These measures of reef condition were measured by divers and then compared directly to the same indicators obtained from mosaics created with video sequences collected at the same time. The indicators measured by a single diver (D. Lirman) were used as the standard against which all other measurements were compared.

A2.3.2.1 Mosaic Selection

Three mosaics were used in the monitoring assessment. The three mosaics are of the same reef plot; they were collected using different survey platforms and represent a range of altitudes and ground resolution (Table A4).

Table A4. Description of the three mosaics used in the monitoring assessment. Each of the mosaics was created from video taken at the Brooke's Reef site in the northern Florida Reef Tract (depth = 7-10 m).

Survey	Date	Survey Platform (Camera Resolution)	Altitude	Area Covered	Ground Resolution
1	June 04	Diver (720 x 530 pixels)	2 m	53 m^2	3.0 mm/pixel
2	April 05	ROV (1024 x 768 pixels)	2.5 m	400 m^2	2.5-3.0 mm/pixel
3	April 05	ROV (1024 x 768 pixels)	1.5 m	45 m^2	1.4 mm/pixel

For the first mosaic (Figure A29), video footage was acquired in June 2004 using a Sony TVR 900 DV camcorder in an underwater camera housing. This first survey is included to illustrate that the mosaicing algorithm can produce geometrically accurate mosaics from a standard, low-

cost, handheld camera. The mosaic was created from 365 key-frames selected using a criterion of 75% overlap between consecutive images. Frame resolution is 720 x 530 pixels.
.

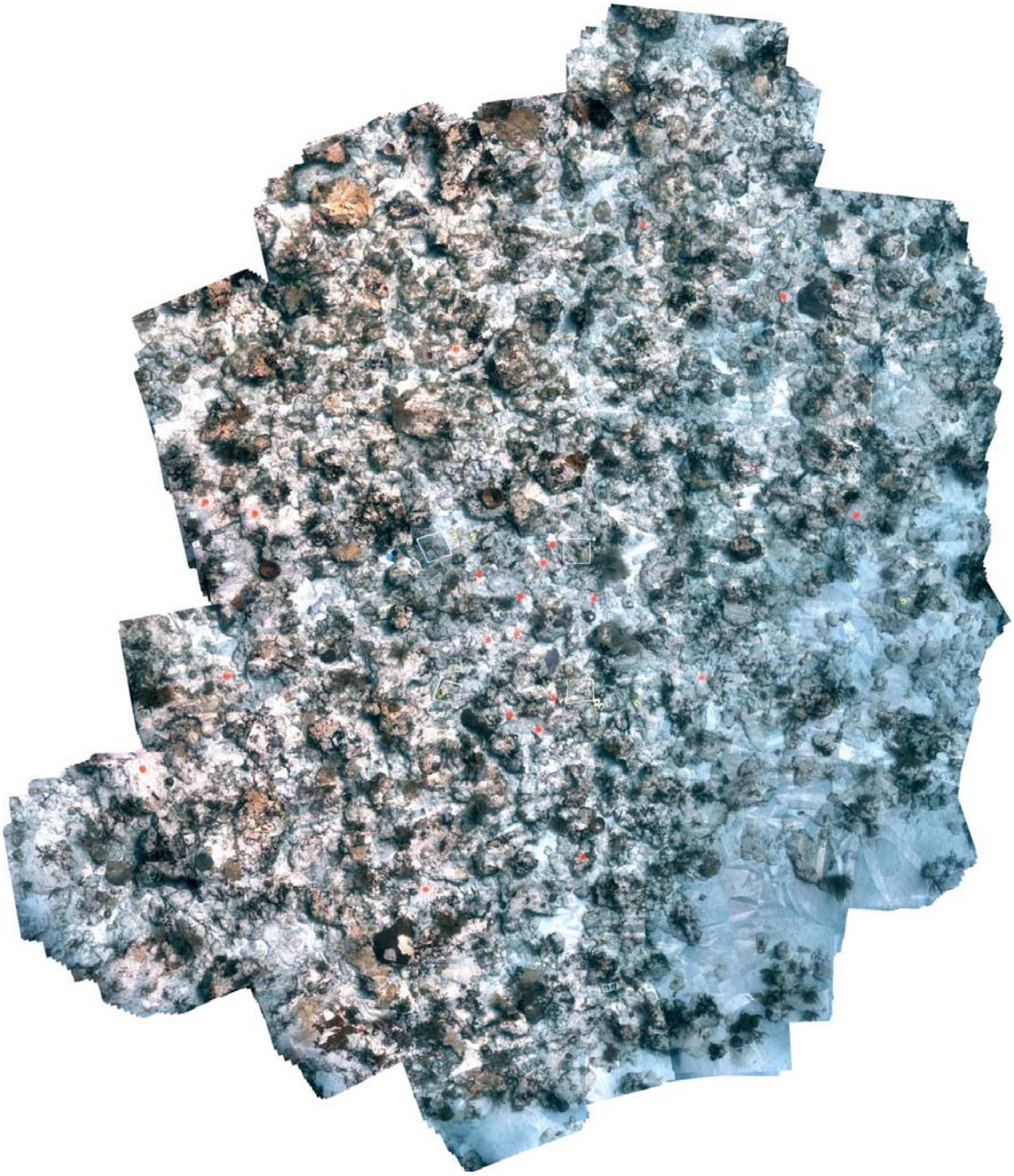


Figure A29. Video mosaic created from hand held video images taken at the Brooke's Reef site in June 2004.

For all mosaics, the camera followed a "lawnmower pattern" of side-by-side strips, complemented by the same pattern rotated 90° to ensure full coverage of the area and high superposition among the strips. The colors on all mosaics were adjusted by manually selecting both a white and a black reference and linearly interpolating the red, green, and blue intensities.

The algorithms were coded in Matlab 6.2, and the overall processing took between 6-12 hours per mosaic using a 3.0GHz PC.

For the second and third mosaics (Figures A30 and A31), video was collected using a Pt Grey Flea camera mounted on a Phantom remotely operated vehicle (ROV) (Xu, 2000) in April 2005. Both high and low altitude datasets were used for assessing ecological indices. The cameras were internally calibrated to reduce image distortion from the lens and housing (Bouguet, 2002). Frame resolution is 1024 x 768 pixels.

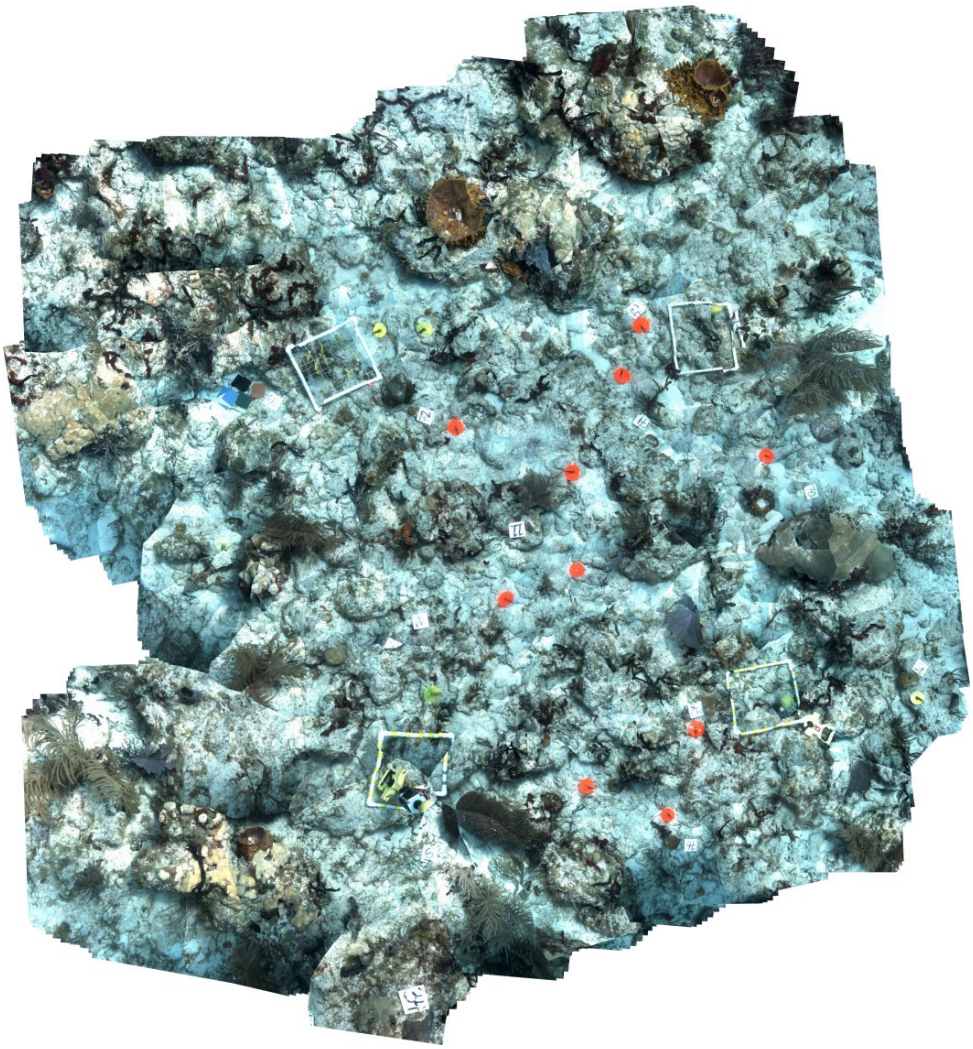


Figure A30. ROV Video Mosaic created from a high altitude (2.5m) pass of the Brooke's Reef site in April 2005.

For the second mosaic (Figure A30), 496 key frames were selected out of the complete set of 5061 images, using 72% overlap. The registration parameters for the non key-frames were obtained by linear adjustment of the sequential matching, constrained by the registration

parameters of the two closest key-frames. For the third mosaic (Figure A31), 872 key frames were selected from a set of 3439 images with a 75% overlap criterion.



Figure A31. ROV based video mosaic created from a low altitude pass (1.5m) of the Brooke's Reef site in April 2005.

A2.3.2.2 Spatial Accuracy

The geometric accuracy of three of the 2D mosaics was analyzed by comparing the locations of points measured from the mosaics with diver measurements of the locations of the same points. Distortion indicators showed an improvement in spatial accuracy (i.e., decreases in the standard deviations of the residuals and maximum distance errors) going from video collected by a diver holding a digital camcorder (first mosaic) to video collected by a high-resolution camera mounted on the ROV (second mosaic). Distortion indicators did not improve with increased image resolution (i.e. a smaller pixel size), however, because to obtain smaller pixel size requires image acquisition closer to the bottom, thereby increasing the distortions due to 3D structure of the scene. Standard deviations of the residuals were 5.1, 3.9, and 5.5 cm, while maximum distance errors were 12.9, 10.7, and 13.5 for the first, second, and third mosaics respectively.

The ability to extract accurate distance measurements from the mosaics was evidenced by the low values calculated for the distortion indicators. Moreover, the spatial accuracy of the video mosaics presented here was similar or lower than the measurement uncertainty of diver measurements, which typically exhibits a standard deviation of 5 cm (Holt, 2000). While an improvement in camera resolution resulted in a reduction in spatial distortion, the higher distortion of the low-altitude mosaic highlighted a present limitation of the mosaic algorithm. The sources that contribute to spatial distortions in mosaics include: (1) departures from the model assumption of a flat environment; (2) amount of superposition among strips during the acquisition; (3) limited visibility underwater; (4) limited resolution of the imaging sensors; and (5) limited accuracy of the image matching algorithm. The higher distortion recorded for the third mosaic, collected closest to the bottom, can be likely attributed to the fact that the planarity assumptions were clearly violated at the low altitude at which the video sequence was collected.

A2.3.2.3 Percent Cover

The percent cover of the dominant benthic organisms measured by trained divers *in situ* compared favorably with those measured directly from the video mosaics. Five out of the eight categories chosen (hard corals, octocorals, *Palythoa*, sponges, and sand) showed no significant differences between diver based surveys and high and low altitude video mosaics in terms of percent cover (Table **A5**, $p > 0.05$). The remaining three categories, all corresponding to functional forms of reef macroalgae (erect macroalgae, turf, and crustose coralline algae) did show significant differences among survey methodologies ($p < 0.05$). However, when these categories are grouped together into a single macroalgae group, no significant differences were found among survey methodologies ($p > 0.05$).

Table A5. Mean cover (± S.E.M.) of the different benthic categories surveyed by divers and measured from video mosaics from a reef site in the northern Florida Reef Tract (depth = 7-10 m). Divers surveyed twenty-five 0.25 m^2 quadrats. For comparison, a subset of twenty-five quadrats (0.25 m^2) was sampled at random from the video mosaics collected at 2 different resolutions. High-resolution mosaics were collected at a distance of 1.5 m to the bottom (2.5-3.0 mm/pixel). Low-resolution mosaics were collected at a distance of 2.5 m to the bottom (1.4 mm/pixel). CCA = Crustose Coralline Algae. p-values from a Kruskal-Wallis test.

Benthic Categories	Diver	Mosaic - High Resolution	Mosaic - Low Resolution	p
Stony Corals	1.4 (0.5)	2.0 (0.7)	1.8 (1.0)	0.6
Octocorals	7.5 (2.6)	6.2 (1.6)	4.7 (1.6)	0.6
Macroalgae	38.1 (3.4)	31.7 (3.0)	21.2 (3.1)	< 0.01
CCA	1.1 (0.4)	0.3 (0.2)	0	0.02
Sponges	3.4 (1.2)	12.9 (1.9)	13.6 (1.9)	< 0.01
Palythoa	4.2 (2.6)	1.2 (0.5)	2.7 (1.7)	0.3
Sand	5.8 (2.0)	9.2 (2.0)	7.5 (1.7)	0.6
Turf	38.9 (2.9)	36.5 (3.0)	41.6 (3.9)	0.3

As an additional measurement of coral cover, the boundaries of all stony corals found within the area imaged by the low-altitude mosaic were digitized and analyzed using the "particle analysis" feature in the ImageJ software that calculates the total area of polygon features within an area of interest. The coral cover value obtained by digitizing the boundaries of all of the coral colonies within the area imaged by the high-resolution mosaic (2.8 %) was within the 95% confidence intervals of the values obtained by divers (1.4%) and from video mosaics (2.0 and 1.8%) using the point-count method (Table **A5**).

Finally, the abundance of juvenile corals (< 4 cm in diameter) measured by divers within benthic quadrats was compared to the abundance of juvenile corals measured from the mosaic tiles. While the mean abundance of juvenile corals (< 4 cm in diameter) documented by divers during visual surveys were 1.1 and 1.4 juveniles m^{-2}, no juvenile corals were detected from the mosaics. We conclude that a major limitation of video-mosaic surveys is the ability to detect and identify juvenile corals (< 4 cm in diameter). This limitation of video mosaic surveys is usually due to the fact that these small corals are often found on cryptic habitats and can only be seen in visual surveys where the observer can shift the angle of view. Future improvements in camera resolution should enhance the ability to detect juvenile corals from 2D mosaics and facilitate the classification of additional benthic categories. These issues have been mostly addressed with the implementation of the second-generation mosaicing system and its benefits are discussed in section A2.3.3.

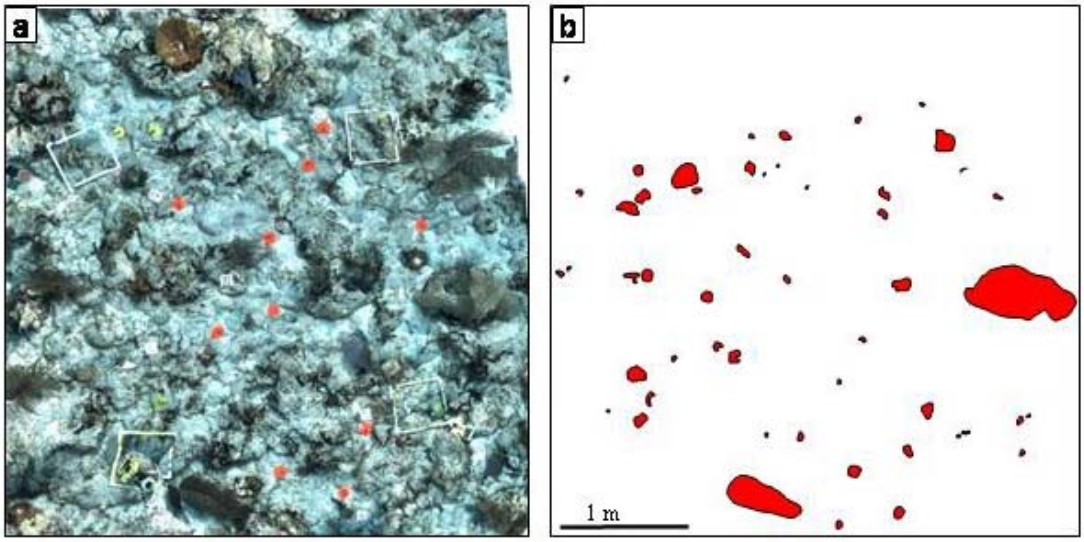


Figure A32. Abundance, spatial distribution, and sizes of stony corals obtained from a low-altitude (1.5 m from the bottom) high-resolution (1.4 mm/pixel) video mosaic (a). The boundaries of each coral colony (b) were digitized and the benthic coverage of stony corals was measured using the ImageJ software. The coral cover obtained by this method (2.8 %) was within the 95% confidence intervals of the values obtained by divers (1.4%) and from video mosaics (2.0 and 1.8%) using the point-count method.

A2.3.2.4 Colony Size

To determine the accuracy of diver surveys and video mosaics to estimate coral colony size, the differences between the values obtained by Lirman and those obtained by a second diver (B. Gintert), or directly from the video mosaics were measured. Accuracy of the size measurements was ascertained by calculating two measurements of error as described by Harvey et al. (2000):

Absolute Error = AE = (| Diver 1 - Diver 2|) and (| Diver 1 - Mosaic|)
Relative Absolute Error = RAE = [(| Diver 1 - Diver 2|) / Diver 1]
and [(| Diver 1 - Mosaic|) / Diver 1]

To compare the size data collected by divers and mosaics, an ANOVA with two factors, survey method and coral size category, was performed using the AE values. When the accuracy of the two methods was compared using the AE, significant differences were found among the size categories, with AE increasing with colony size and height (ANOVA, $p < 0.01$) (Table A5). However, no significant differences were documented based on survey method (ANOVA, $p > 0.05$). The mosaic-diver deviations were generally higher for the diver-mosaic comparisons for small colonies (< 20 cm) but higher for diver-diver comparisons for larger colonies (Table A5).

Table A6. Comparison of coral size measurements between: (1) two divers measuring the same colonies; and (2) between diver measurements and measurements of the same colonies obtained directly from the video mosaics. AE_1 = Absolute Error = (| Diver 1 - Diver 2|), RAE_1 = Relative Absolute Error = [(| Diver 1 - Diver

2|) / Diver 1]. AE_2 = Absolute Error = (| Diver 1 - Mosaic|), RAE_2 = Relative Absolute Error = [(| Diver 1 - Mosaic|) / Diver 1]. Measurements taken by Diver 1 (Lirman) were considered here as the standard against which all other measurements were compared. Values reported are means (± S.D.).

Coral Sizes (cm)	Diver-Diver Comparison$_1$			Diver-Mosaic Comparison$_2$		
	AE_1	RAE_1	N	AE_2	RAE_2	N
<10	0.7 (0.3)	8.9	9	1.6 (0.4)	21.0	22
10-20	1.9 (0.7)	10.6	15	2.5 (0.4)	16.5	45
>20-30	4.8 (1.2)	17.7	7	3.4 (0.8)	14.2	19
>30-80	5.4 (2.7)	11.1	7	5.6 (1.4)	13.1	20

The capability of identifying individual coral colonies and measuring their size directly from each mosaic is one of the most important benefits of 2D video mosaics. While the accuracy of the mosaic measurements relative to the diver-based measurements was influenced by colony size, these patterns result from the difficulty that divers commonly encounter while trying to measure coral colonies in the field. Colony boundaries are easily distinguished in small (< 20 cm) colonies that commonly exhibit circular shapes, but larger colonies with irregular shapes pose a challenge for divers trying to delimit live tissue boundaries. Future improvements in the 3D representation of benthic mosaics, such as the work presented in Section B (Negahdaripour and Madjidi, 2003; Negahdaripour et al., 2005), are expected to substantially improve the accuracy of colony size measured from mosaics, particularly for larger colonies with more complex topographies. The analysis of mosaics constructed over two spatial dimensions has highlighted several advantages over strip mosaics constructed along a single spatial dimension. For example, the sizes of coral colonies were accurately measured from two-dimensional mosaics, even though they are typically hard to acquire from one-dimensional mosaics where only the smallest coral colonies are completely imaged along a single transect.

A2.3.2.5 Change Detection

An additional benefit of using spatially accurate mosaics is our ability to easily return to a fixed point within the resulting image, making it easy to follow single colonies over time. This ability to track changes in single colonies may help to identify the effects of disease or bleaching more quickly and precisely than if using percent cover alone. The removal of coral colonies or other benthic organisms and changes in the composition of the substrate can be easily discerned by looking at the same section of the reef in a time series of video mosaics (Figure A33).

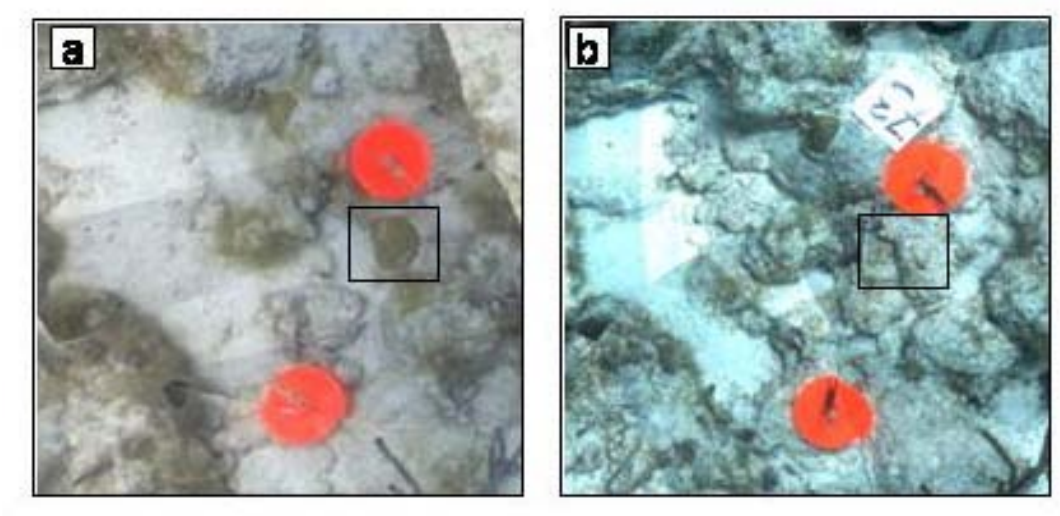


Figure A33. Example of co-registered mosaic sub-sections or tiles (1 m x 1 m) used to assess patterns of change in the abundance and distribution of benthic organisms between 2004 (a) and 2005 (b). The box highlights the removal or mortality of a small (< 10 cm in diameter) coral colony between surveys.

Using this method, the mortality or removal of four coral colonies (out of 50 colonies) was documented between 2004-2005 (Mosaics 1 and 3) from an area of approximately 16 m^2 (Figure A33). Moreover, two-dimensional imagery from repeated surveys was accurately referenced to assist with change-detection, unlike linear transects that are exceedingly difficult to duplicate precisely over time.

Previous research on the design of field programs aimed at documenting patterns of change in benthic resources over time has highlighted the increased statistical power gained by surveying precise specific locations repeatedly compared to the survey of random locations (Van de Meer, 1997; Ryan and Heyward, 2003). The demarcation of permanent plots on hard benthic substrate is commonly achieved by attaching pipes or nails on the bottom, and the number of markers needed to mark multiple colonies, quadrats, or transects at a given site can be quite large. Video mosaics provide an alternative to these labor-intensive methods. By placing a limited number of permanent markers to provide a reference frame within each video mosaic (only four permanent markers were used in this study to accurately survey an area of 400 m^2), the technique described in this study can reduce significantly the bottom-time needed to collect ecological information in the field. Moreover, by providing the ability to survey specific sub-plots repeatedly within a larger area of the benthos, video mosaics provide increased statistical power to detect small changes in abundance, cover, and size of benthic organisms. However, a trade-off exists between within-site precision and the ability to survey large areas, making the video mosaic technique an ideal method to survey areas < 500 m^2 but impractical for documenting changes in the extent and condition of benthic resources at larger spatial scales within a single image. Of course multiple mosaics can be used to statistically sample larger areas. It is expected that further improvements in the mosaicing algorithms combined with the use of improved positioning systems (e.g., acoustic transponder networks) will make construction of even larger 2-D mosaics practical at in the near future.

A2.3.3 Benefits of second-generation mosaic technology to ecological analysis

First-generation video mosaics were an innovative reef survey technology that provided large-scale (up to 400 m^2), spatially accurate, high-resolution images of the reef benthos without extensive survey times or a need for scientific divers. Despite these advances, first-generation mosaic products were insufficient for species-level identification of many benthic taxa, thereby limiting the monitoring potential of the technique. The second-generation mosaic survey technology that was developed in 2007 integrates high-resolution still-image acquisition with high-definition video surveys of the reef benthos (see section A2.1.4 for methods).

The first-generation landscape mosaics were created from video taken with either a Sony TRV 900 DV camera hand-held by a diver, or a Point Grey Research Flea camera mounted on a Remotely Operated Vehicle. These two camera systems provided spatial resolution ranging from one to four mm/pixel, which was sufficient to identify taxonomic groups, such as stony corals, sponges, gorgonians, macroalgae and sand, but was not fine enough to allow species-level identification in most cases (Lirman et al. 2007). Organisms smaller than 5 cm in diameter were typically not detectable using first-generation mosaic products (Lirman et al. 2007).

To overcome the resolution limits of the first-generation mosaic survey technology while maintaining the high frame rate and altitude requirements of the mosaic processing algorithms, a two-camera system was adopted. This second-generation mosaic imaging system combines information from (1) a high-definition video (HDV) camera capable of full video frame rate (30 fps) and (2) a digital still camera capable of acquiring very high-resolution images (10 MP) at low capture rates (1 fps).

In the field, the second-generation imaging system is deployed with both cameras in a down-looking position. Cameras are swum by a single diver 2 m above the reef area-of-interest in a double lawn-mower pattern as described previously (Lirman et al. 2007).

Data processing of the second-generation mosaic data is described previously (section A2.1.4.1). Display software was developed that allows users to select any point within the landscape mosaic produced by the second-generation imaging technology and retrieve the corresponding 10 MP still image and corresponding video frame of the area surrounding that point (Reid et al, 2007).

Testing of the second-generation mosaicing system continued in 2008, with the mapping of a portion of Brooke's Reef, FL (25^o 40.508'N, 80^o 5.908'W) in June. The landscape mosaic generated from the high-definition video of the second-generation system covered 156 m^2 (Figure A34A). The first-generation landscape mosaic of Brooke's Reef taken in June 2004 has a spatial resolution of 3 mm/pixel (Figure A34B), whereas the second generation version has a spatial resolution of 2 mm/pixel (Figure A34C). The second-generation still camera images were acquired at a frame rate of 1 fps, resulting in approximately 1,800 10 MP images of the reef benthos. The 1,800 still images were then matched to key video frames. The average spatial resolution of the still images from the second-generation system was 0.4 mm/pixel, almost an order of magnitude improvement over the video of the first generation system (Figure A34D, E).

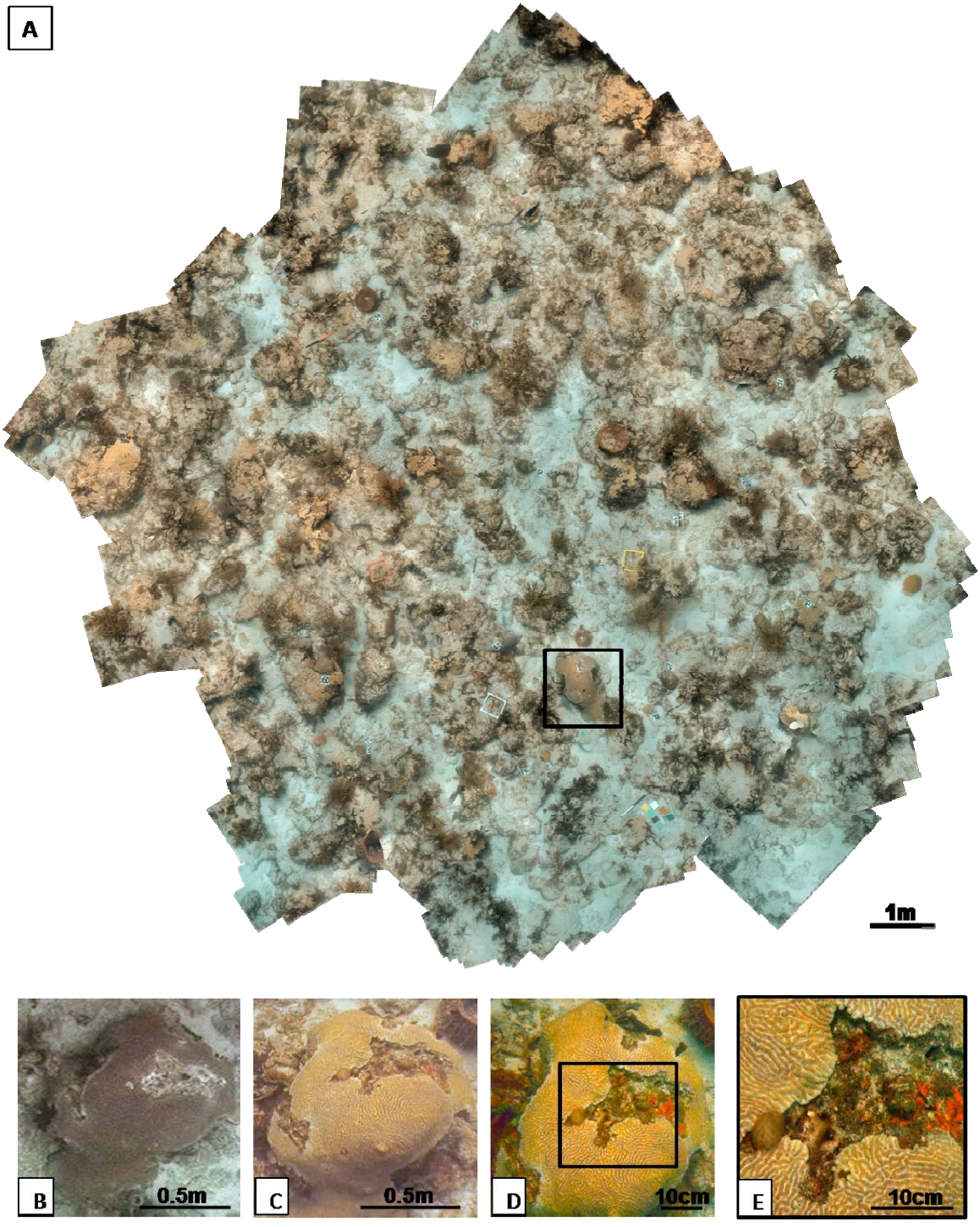


Figure A34. (A) A second-generation video mosaic from Brooke's Reef, FL taken in June 2008. Images of a Meandrina meandrites colony (shown in A) selected from mosaic surveys created using: (B) a Sony DV camcorder in June 2004, (C) high definition Sony camcorder from June 2008, and (D-E) 10 MP Nikon D200 still camera. All images were acquired at a distance of 2 m from the benthos. The combination of high resolution still images with video acquisition provides increased reef health information such as (D) tissue partial mortality and (E) cyanobacterial, macroalgal, and sponge interactions.

The 2 mm/pixel spatial resolution of the second- generation landscape mosaic, produced from the high-definition video, enabled improved analysis of the mosaic. Boundaries between sponges, corals and gorgonians were clearer and large colony identification (> 25 cm) was possible for most Caribbean species (Figure A34C).

Analysis of the 10 MP still images from the second-generation system provided high taxonomic resolution. The sub-millimeter resolution of the still images allowed for species-level identification of colonies as small as 3 cm in diameter. In addition, macroalgal groups were identifiable to genus with species level identification possible for macroalgae with obvious defining characteristics such as *Halimeda tuna* and *H. opuntia*. Coral colony health information such as partial mortality boundaries and evidence of bleaching and disease were all recognizable using the still images. Small-scale indicators of reef health such as cyanobacteria, macroalgal, and sponge competition were also visible using high-resolution still data (Figure A34D, E).

The first-generation video mosaics demonstrated that mosaic-based monitoring could be accomplished without trained, expert scientific divers, long dive times, or extensive tagging of coral colonies. This technique also allowed users to assess basic reef health indices and monitor coral colonies using a large-scale image-based approach that limited the need for extensive dive-time and provided long lasting visual information on the state-of the reef at the time of the survey (Lirman et al. 2007).

Second-generation mosaics retain these monitoring strengths while providing increased benthic resolution over the entire survey area; enabling species level information for most coral colonies. This allows greater taxonomic information with respect to percent cover and diversity indices than was available from first-generation mosaics. In addition, change detection analysis using second-generation mosaic products provides information on conspicuous indices of reef health (such as bleaching and tissue loss) while also allowing users to monitor fine scale stressors such as macroalgal and cyanobacterial interactions and predation events (Figure A35). This represents a significant monitoring improvement over first-generation products that could only discern dramatic indicators of colony health such as bleaching, and significant tissue loss (Gleason et al. 2007).

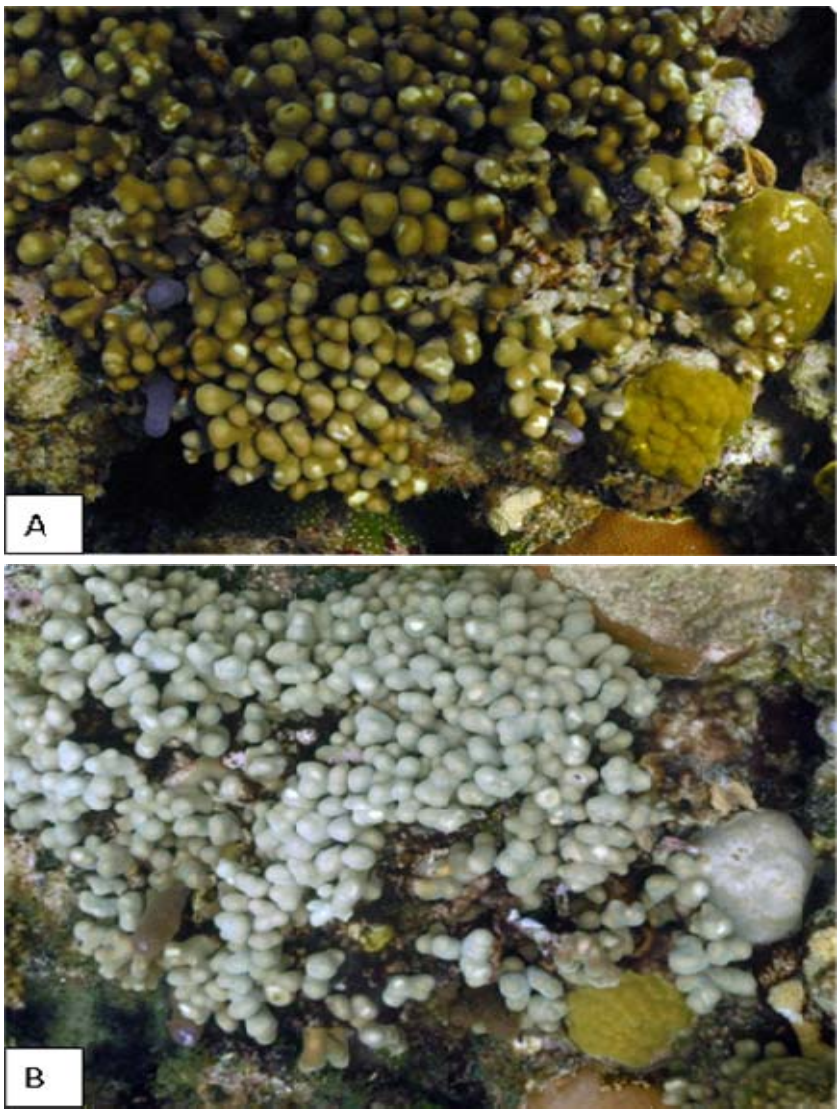


Figure A35. Example of change detection potential using second-generation imagery. High resolution still images were acquired from approximately 2 m water depth during video mosaic surveys. Images were automatically matched to their geographic locations within the survey area for change detection analyses. Between February 2008 (A) and September 2008 (B) the Porites porites (center) and Stephanocoenia intersepta (right) colonies shown above have undergone considerable paling. Evidence of partial mortality and an increase of cyanobacteria within the P. porites colony are also identifiable by comparing the survey images. Small indicators of coral health such as fish bite predation are also clearly present on both the P. porites and the S. intersepta in February 2008 and can be followed through time to monitor long-term impacts (A).

Although many monitoring programs take pictures of the reef for analysis and documentation purposes, the extensive cataloging and database management required in the laboratory often limits the amount of photographic data acquired during a survey. The automated matching of high resolution still images to their geographic location within a second-generation mosaic removes the need for user-intensive laboratory cataloging and allows the archiving of several thousand high resolution images of a reef area with minimal user input.

Image-based techniques for reef monitoring have an excellent archive potential that is vastly superior to written notes by divers. The second-generation mosaic survey technology described here provides both landscape level and colony level (as small as 3 cm) permanent records of the state-of-the-reef at the time of the survey without increasing the dive-time of first-generation mosaic products. The simultaneous capture of both of these scales of information allows users to monitor large-scale changes in reef communities such as hurricane or ship grounding damage, as well as small scale interactions such as sponge and macroalgal competition using the same survey design and the same raw data set.

The incorporation of high-resolution still imagery into the second-generation imaging equipment and mosaic processing resolved the species identification limitations of the first-generation system. The ability to capture high resolution images over 100's of square meters and georeference these images within video mosaics without user input is a major advantage of the landscape mosaic technology. The combination of large-scale image maps and high-resolution benthic information provides a unique tool that maintains the strengths of most traditional monitoring methods, such as the ability to extract indices of reef health (percent cover, coral colony sizes, and diversity indices), while also providing a rapid method to document and assess changes at both large and small scales in coral communities without extensive tagging. This combined with the extensive archive potential inherent to this technology provides a significant advancement in coral reef community monitoring technology

The above information is presented in the following paper:
Gintert, B., Gracias, N., Gleason, A.C.R., Lirman, D., Dick, M., Kramer, P., Reid, R.P. (2008) Second-Generation Landscape Mosaics of Coral Reefs. Proceedings of the 11th International Coral Reef Symposium. Fort Lauderdale, FL, July 7-11, 2008. (In-press)

A2.3.4 Recommendations for Field Implementation

The collection, processing, and analysis of landscape video mosaics may be affected by water quality parameters at the time of collection. In addition, because of the mosaic algorithm that calculates camera trajectory based on pixel location within sequential images, camera motion and movement of objects on the bottom are issues of concern.

Over the past six years, video footage has been collected for mosaic development under a wide variety of environmental conditions. The range of conditions and the quality of the resulting mosaics have allowed us to develop a set of guidelines or best practices for the collection of field data that can be use to determine under which conditions the likelihood
of creating a good mosaic can be maximized and, more importantly, which conditions to avoid if possible.

These guidelines are as follows:

1. Environmental conditions: At the inception of project SI1333 two fixed monitoring sites were established in Florida at Brooke's Reef and Grecian Patch. These two sites were

characterized by both their environmental and biological characteristics in an attempt to parameterize successful data collection of the prototype system (Table A7).

Table A7. Biological and Environmental characteristics of Brooke's Reef and Grecian Patch permanent monitoring sites.

	BROOKE'S REEF	GRECIAN PATCH
REGION	KEY BISCAYNE	KEY LARGO
HABITAT TYPE	PATCH REEF	PATCH REEF
LOCATION	25 40.508 N, 80 5.908 W	25 6.362 N, 80 19.086 W
DEPTH (m)	7-10	4-6
EXPOSURE	HIGH	LOW
SEDIMENTATION (g/day)	0.81 (1.13)	0.03 (0.01)
HARD CORALS (%)	5.4 (1.60)	9.4 (2.1)
SOFT CORALS (%)	4.1 (0.9)	11.4 (2.6)
SPONGES (%)	10.1 (1.1)	7.1 (1.5)
PALYTHOA (%)	4.9 (1.9)	4.4 (1.7)
MACROALGAE (%)	32.8 (2.3)	25.3 (2.5)
TURF ALGAE (%)	18.2 (2.3)	24.1 (3.3)
CRUSTOSE ALGAE (%)	8.8 (1.1)	6.2 (1.7)
SAND (%)	15.7 (2.2)	12.2 (2.4)
JUVENILE CORALS (n/m^2)	1.3 (0.6)	1.6 (0.9)
N OF *DIADEMA*	0	0
TOPOGRAPHY (cm)	108 (41)	57 (5)

Visibility and water clarity were different at the two sites. The large tidal influence and proximity to Biscayne Bay at Brooke's Reef caused visibility to be generally lower and mean sedimentation to be more than 20 times higher than at the Grecian Patch site (Table A7). Visibility at the Grecian Patch site is usually excellent and only after severe storms does sediment resuspension result in reduced water clarity. Despite the disparity in environmental characteristics of these two sites, the in-water conditions were never severe enough to prevent mosaic creation at these fixed sites. Table A8 gives a summary of environmental conditions on days in which permanent monitoring sites were sampled.

Table A8. Environmental observations on dates in which permanent monitoring sites were sampled.

Date	Air Temp (^{O}C)	Avg wind speed (knots)	Barometric pressure (mb)	Practical Salinity
3/30/2004	21.3	11.4	1018.3	24.2
4/1/2004	22.2	17.3	1014.4	24.5
4/6/2004	21.5	8.6	1017.4	24.1
10/20/2004	27.7	7.8	1015.1	28.1
3/5/2005	19.7	10.2	1019.5	23.0
4/1/2005	24.3	14.2	1016.1	24.2
5/9/2005	23.4	10.7	1018.3	25.2
12/9/2005	25.3	14.3	1020.8	24.4
5/9/2006	26.1	12.3	1014.1	26.4
3/2/2007	25.0	12.4	1012.2	24.3
6/16/2008	28.5	8.6	1014.7	28.2
8/7/2008	30.0	5.0	1016.1	30.2
8/11/2008	28.5	9.7	1014.9	29.3
9/15/2009	28.5	9.3	1013.7	29.7

In general, successful mosaic sampling occurred when average wind speeds were below 15knots. The one exception to this trend occurred on 4/1/2004 in which the Brooke's Reef site was successfully sampled on a day with an average wind speed of 17.3 knots. The success of this mosaicing is attributed to the greater water depth and decreased dependence on surface wave conditions for water clarity at this site.

In addition to the permanent monitoring sites established in Florida, nearly 40 other sites were sampled during the term of the SI 1333 project. Although environmental data were not collected for each of these additional sites due to heavy processing costs and limitations of collaborative projects, some important environmental observations were extracted from non-permanent sites to establish optimal working conditions for the prototype system. Of the data collected, conditions were suitable for creating mosaics in all but one set of field collections. During a collaborative effort with the University of Puerto Rico, in-water properties were encountered that prevented mosaic creation. In association with NOAA, environmental parameters for the study area near Media Luna Reef, Puerto Rico were obtained and analyzed to provide optimum environmental parameters for mosaic acquisition.

On December 11, 2007 an out of season tropical storm (Tropical Storm Olga) passed over the island of Puerto Rico. Due to inflexible travel constraints mosaic data was collected on December 12th 13th at 4 reef sites near the Media Luna Reef Integrated Coral Observation Network (ICON) station in Puerto Rico.

Due to the passage of the storm the previous day, water clarity (as measured by the diffuse light attenuation coefficient K_d) was very low. K_d varied between 0.3 and 0.34 both during the tropical storm and the two sampling days that followed (Figure A36). In clear tropical waters K_d is typically 0.05, indicating that the waters in Puerto Rico were substantially more

turbid than normal during the entire study period and for several days afterwards. Additionally, wind speed was near the upper end of operational limits experienced at the Florida fixed sites during mosaic sampling (average wind speed was between 14-15knots)(Figure A36). While these wind speeds are not out of range of those successfully surveyed in Florida (Table A8), wind gusts during the study period were above 25 knots and during the previous day were near 50 knots. At the Media Luna site the cumulative effect of multiple high wind days caused decreased visibility to persist even after average wind speeds fell back within operational ranges (Figure A36 see K_d data).

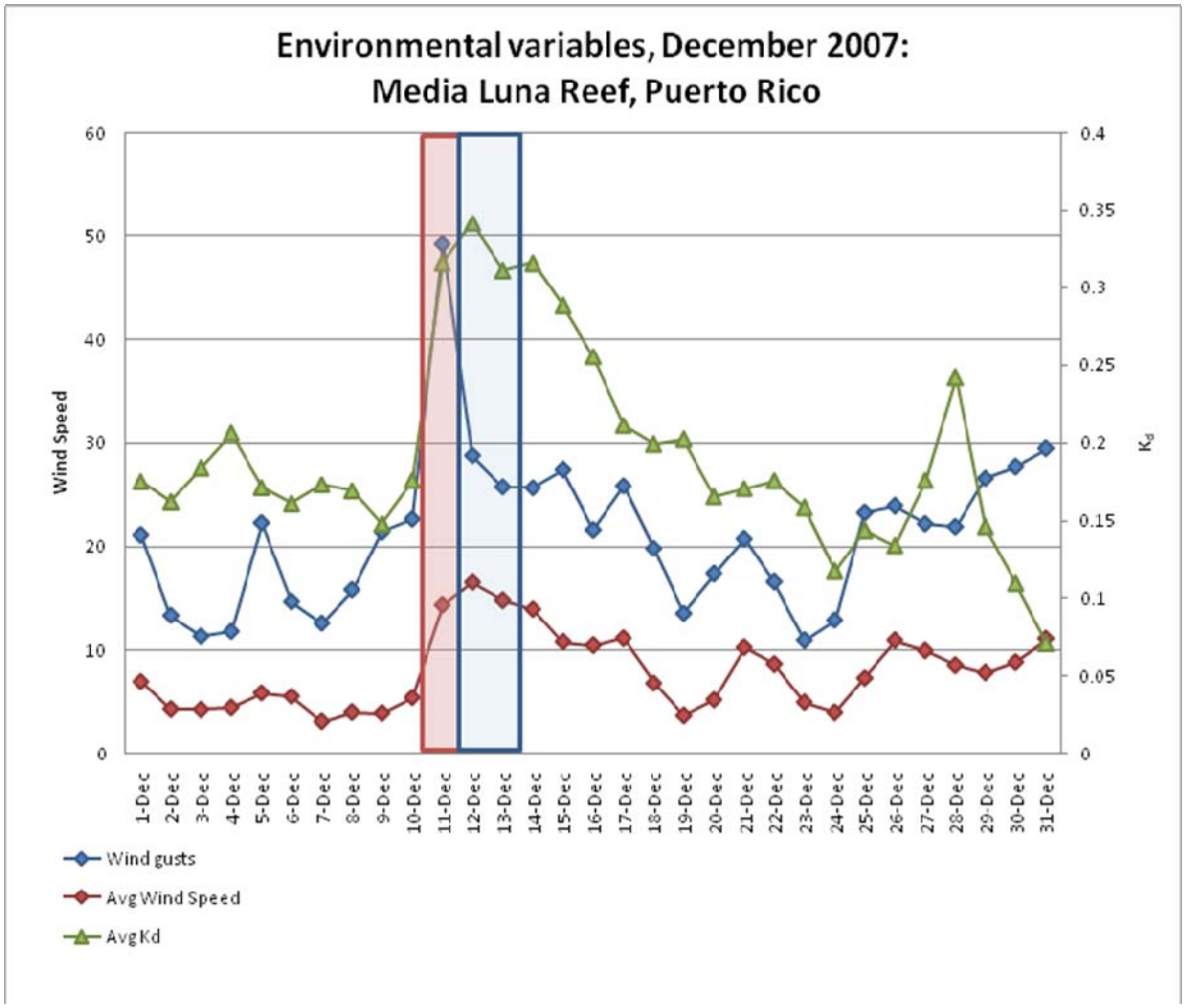


Figure A36. Environmental data from Media Luna Integrated Coral Observing Network (ICON) station for the month of December 2007). Average and Maximum wind speeds are shown in knots while visibility is given by the light attenuation coefficient K_d. December 11th, the date in which Tropical Storm Olga passed over Puerto Rico is highlighted in Red; survey dates are highlighted in blue.

The result was decreased underwater visibility and consequently decreased contrast in the acquired images. An example image from Media Luna Reef collected on December 12th, 2007 is shown below (Figure A37).

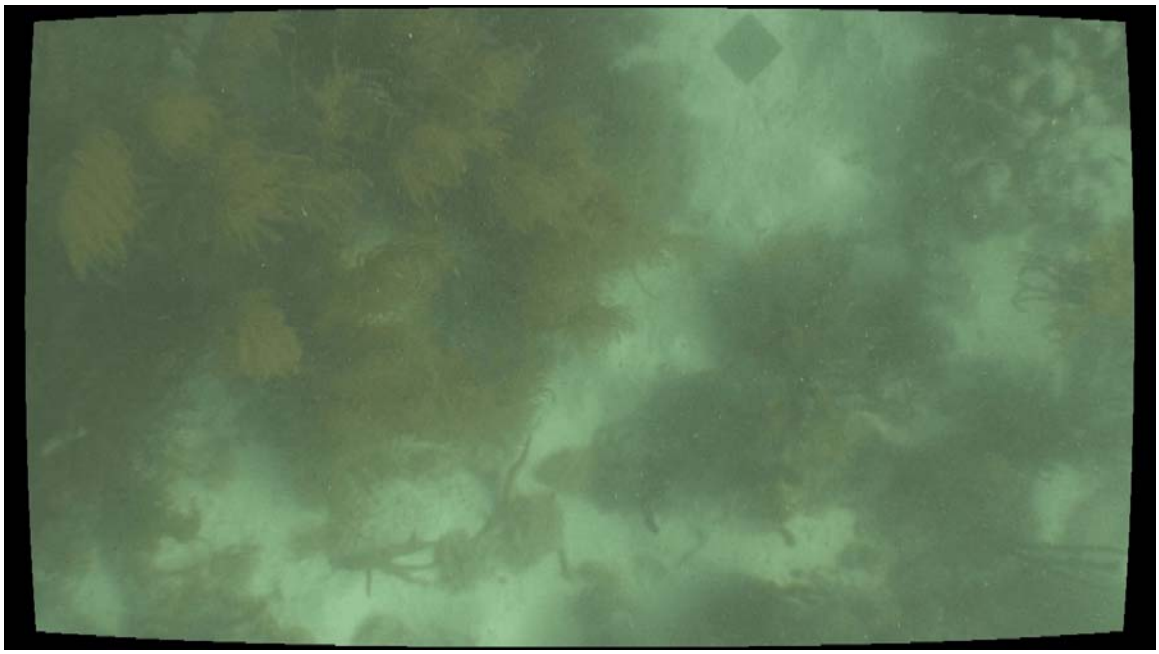


Figure A37. Image of benthos from ~2m at Media Luna Reef on December 12th, 2007.

The high degree of sediment suspended in the water column created a very low-contrast dataset for the mosaic creation algorithms. As such, only small portions of high contrast images from the study sites were successfully matched and assembled into a composite mosaic image. It should also be noted that these limited results were only available after considerable color and contrast adjustments to the original video frames (Figure A38).

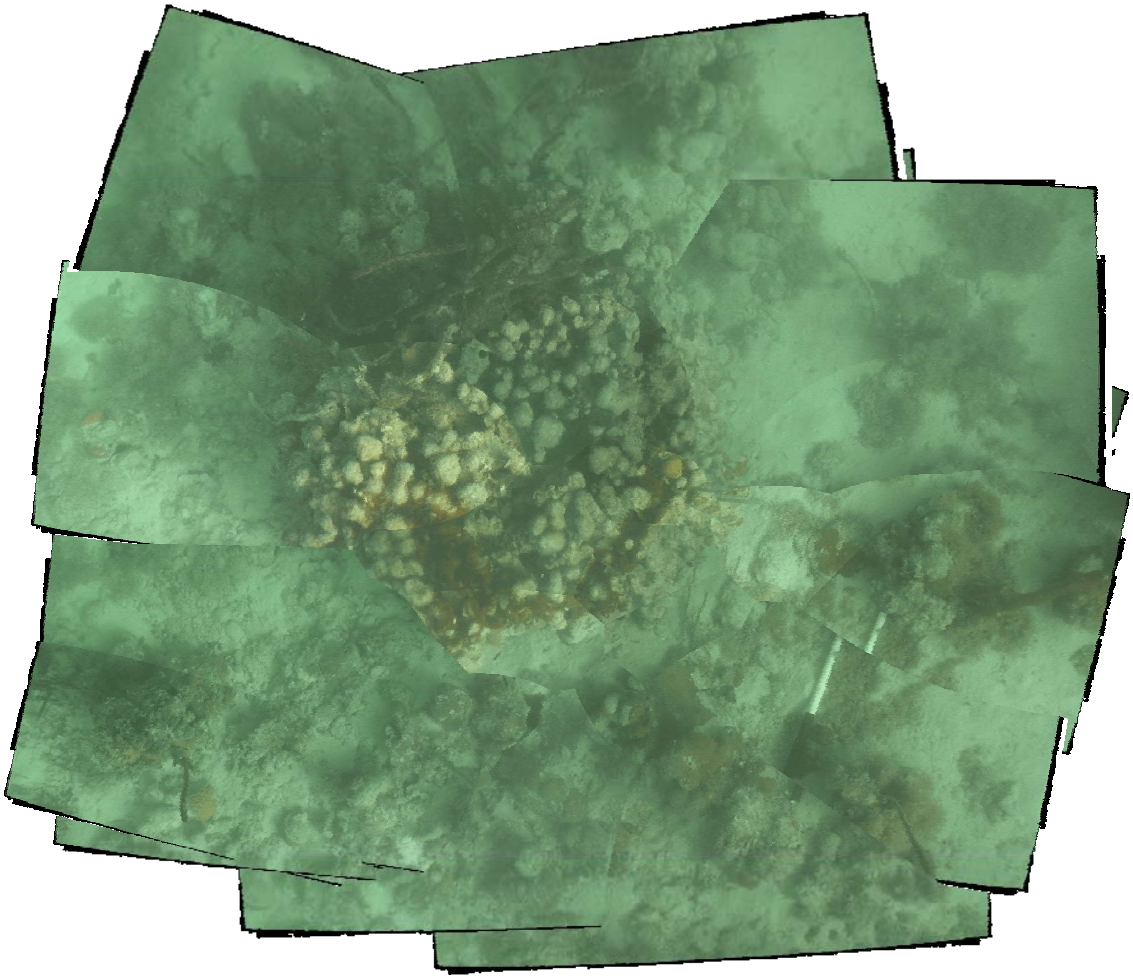


Figure A38. Mosaic of Media Luna Reef video data from December 12th, 2007. Only a handful of frames containing high contrast objects (such as the large *Montastrea* colony above) were successfully matched using this dataset.

The low-contrast of the majority of the dataset prevented an entire landscape video mosaic to be created with this dataset. As a result it is recommended that video mosaic data only be acquired when average wind speeds are less than 15 knots and that sufficient time be given after multiple high wind days to allow for sediment settlement before mosaic acquisition is attempted.

Finally it is recommended that while it is possible to successfully mosaic video imagery acquired under a range of environmental conditions, the best products with the highest benthic resolution are acquired under the best visibility conditions.

2. Camera motion: Guidelines for collecting good video for mosaic creation are no different than those required for collecting good photographs underwater. Blurry images with a lot of motion will impede the mosaic algorithm. Camera motion can be controlled conducting surveys at low speed (this applies to divers, ROVs, and AUVs) and avoiding conditions in which high surge or currents cause rapid shifts in position along the survey track.

The blur caused by camera motion can be quantified by the length (in pixels) that a given image point moves during the image exposure interval. For our image processing algorithms it is not advisable to have motion blur more than 4 pixels, since it reduces significantly the ability to properly register the images. To have a guideline on the maximum speed allowed we consider our typical case where the camera is straight looking down at the bottom at a height of h meters and translating at a speed of v meters per second. The camera lenses provide a horizontal field of view of a degrees and the image sensor has r pixels along the horizontal. The shutter speed is s second^{-1}. With these parameters the motion blur b is approximated by $b = \frac{v}{\sin(a/r)\cdot h \cdot s}$. By imposing that the blur should be smaller than b_0=4 pixels, we can establish a condition for the maximum allowed translation speed for a given shutter speed: $v < \sin(a/r)\cdot h \cdot b_0 \cdot s$. In practical conditions the shutter speed should be set to the highest possible value that does not produce a noticeable darkening of the image. Therefore it should be adjusted in the field to match the particular illumination conditions of that day. Figure A39 presents the plots for a high definition video camera with 60 deg field of view, for different heights above the sea floor.

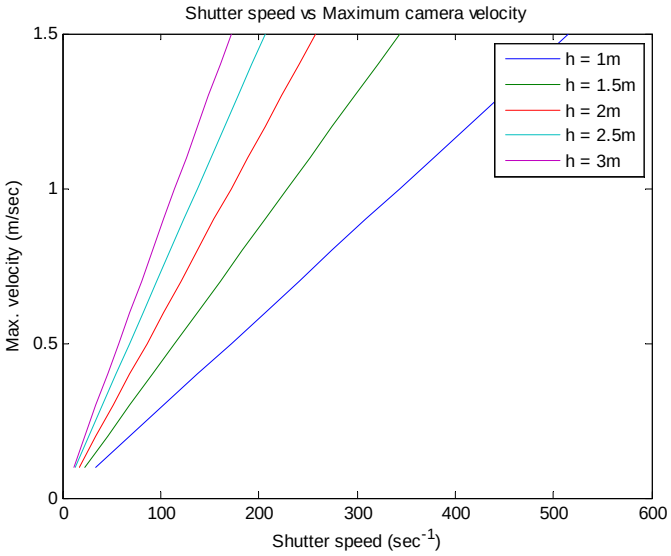


Figure A39 –Maximum allowed speed of translation for the camera as a function of the shutter speed for different altitudes. The plots were computed for a high definition video camera with 60 deg horizontal field of view, and motion blur under 4 pixels.

In addition, camera motion should be minimized by not making any sudden turns or movements with the video camera during acquisition. This is accomplished by the diver moving around the camera to push it in a new direction while swimming the lawn-mower pattern over the area of interest while keeping the camera in the same orientation throughout the survey.

3. Motion of organisms on the bottom: The same issues that apply to camera motion apply to the motion of organisms like fish, macroalgal fronds, and soft corals that can translate into blurry images that can cause problems for the mosaicing algorithm. To minimize these

impacts, surveys should be conducted at times where the motion of organisms on the bottom caused by surge and currents is minimized. Due to the natural surge of areas of interest, the mosaicing algorithms are designed to find matches between two images that follow the same motion pattern. This eliminates some of the problems with small movements of individual soft corals or fish within the field of view as the matching algorithms are designed to follow the features of the more static benthos. However, this feature of the matching algorithm will not work if the moving object fills the entire field of view. Therefore, it is beneficial to avoid large areas of swaying soft corals or swimming divers while acquiring mosaic data. Soft corals in particular will also often block the view of other benthic organisms and hinder the analysis of benthic features. Thus areas of high density of swaying soft corals should be avoided. In addition, the deployment of flexible tapes that demark areas of interest can sway with the currents and cause problems during processing. Markers used to identify areas or organisms of interest should be weighted and stationary to provide minimal artifacts during processing. Numbered ceramic tiles are heavy enough that they do not move in normal surge and present a large surface area for numbers to be read from video, making them ideal markers for mosaic acquisition.

4. Lighting: Imaging of benthic features is best completed under moderate sunlight conditions. While light is needed for imaging any set of benthic data, high sunlight can often cause artifacts during mosaic processing. Even lighting has been found to create the best mosaic products, as shown in Figure A40. In this figure we have compared two sites of similar depth (~2.5m) under different light conditions. The site on the left was taken under overcast conditions with no direct sunlight reaching the benthos, while the example on the right was taken on a sparsely cloudy day with ample direct sunlight. While sunflickering effects (as seen in the right image) can be removed using the module developed in this project (See section A2.1.3.3), it is still recommended that video footage (if possible) be collected at times or conditions when lighting of the benthos is even. This is usually best accomplished on overcast days. Deeper sites often limit light penetration and thus lighting and image quality are less variable during the day. At deeper sites color loss is often more important, and if possible, images should be taken with a red filter at depths deeper than 10m.

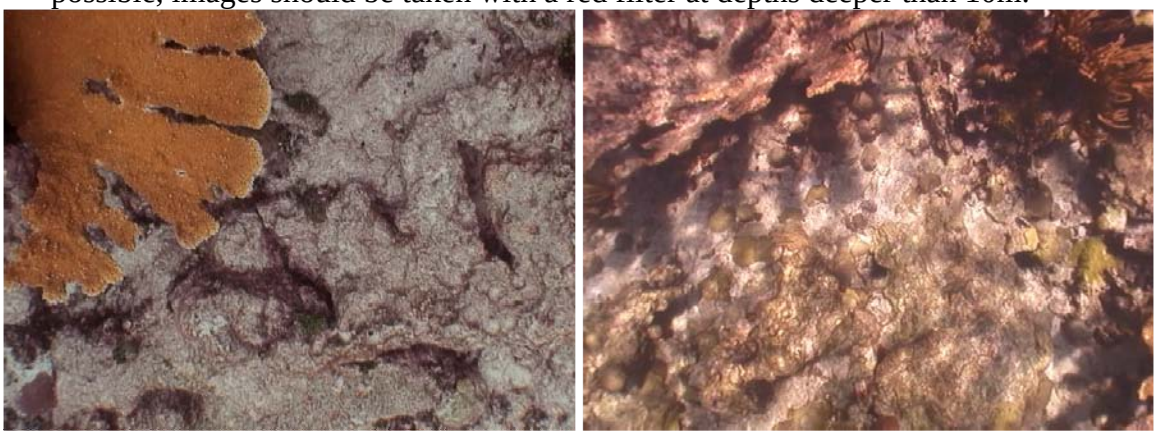


Figure A40. Effect of light variations on image products. Still camera image from Carysfort reef (~2.5m deep) on an overcast day (Left). Video image from shallow (~2.5m) Acropora palmata site in St. Croix on a sunny day (Right). Light refraction against the bottom is clearly seen at the St. Croix site.

5. Image overlap: The mosaicing algorithm depends on a minimum of 60% overlap between images to process effectively. A lack of sufficient image overlap may lead to failure of image registration which results in parts of the survey being rejected during processing, or in visible artifacts in the mosaic (such as the same benthic objects appearing repeated in different locations). Most of these failures can be compensated by manually performing the image matching. However this is a tedious process requiring user intervention.

   To adequately cover the area of interest it is suggested that surveyors use a double lawnmower's pattern. This pattern comprises two simple lawnmower's patterns rotated 90 degrees between each other. Figure A41 illustrates this pattern. The double lawnmower pattern provides extensive overlap among perpendicular strips. To increase the ability of the diver to follow the intended coverage pattern, it is recommended that markers are deployed on the bottom to delimit the boundaries of the area and that these landmarks are used to ensure that each survey track provides adequate overlap.

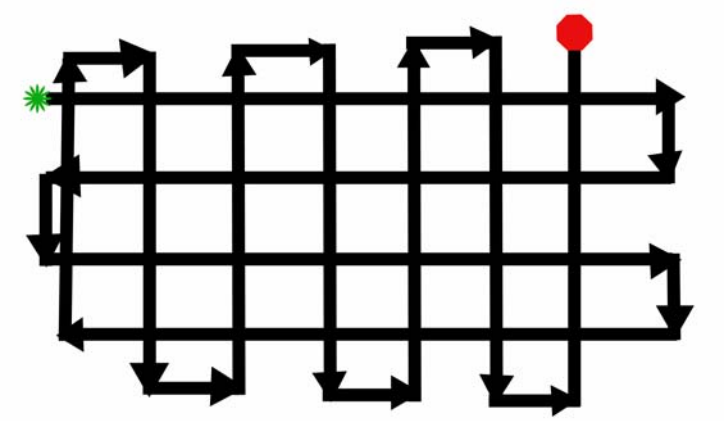


Figure A41 - Example of a area coverage pattern comprising two lawnmower's patterns rotated 90 degrees.

6. Image processing: As discussed above, low visibility is the primary limiting factor for the collection of good video footage to be used for mosaics. As a rule of thumb, mosaic surveys should be avoided when sedimentation or water color impedes a clear view of the bottom (See part 1 of this section). In cases where sediment re-suspension is high, the video camera and the mosaic algorithm may focus on the moving sediment particles and impede processing. Due to the fact that field data is often expensive to collect, many datasets have been collected and successfully mosaiced under less-than optimal conditions. As such a number of steps have been put in place to deal with less than ideal conditions of water clarity. In particular pre-processing of video data using standard color and contrast correction often provides much clearer images than were possible to extract in the field on the day of collection. Several sub-routines have been developed in Matlab to do batch processing of the large sets of video data, but image manipulation software such as Photoshop are also capable of the same results. Below is an example of mosaicing results before and after color and brightness correction (Figure A42). In this example, raw video, taken in the field, was degraded by the presence of sediment suspended in the water column, decreasing visibility. When attempting to mosaic this dataset without pre-processing only 10 frames were able to be matched (Figure A42.A). After pre-processing the extracted frames using color and

contrast correction the entire set of images was able to be assembled into a single mosaic image (Figure A42.B). In this case, the sediment and decreased water clarity prevented enough benthic texture for the successful use of the landscape mosaic feature matching algorithms in the original video frames. However, simple procedures for increasing the benthic clarity were able to overcome these limitations and allow the creation of a mosaic image of higher clarity than the original video frames (Figure A42). This ability to pre-process extracted video frames has allowed the landscape mosaicing software to be used in a more robust set of working environments including areas where the visibility was less than 20 feet. However it must be noted that optimum sampling will occur with high water clarity and visibility.

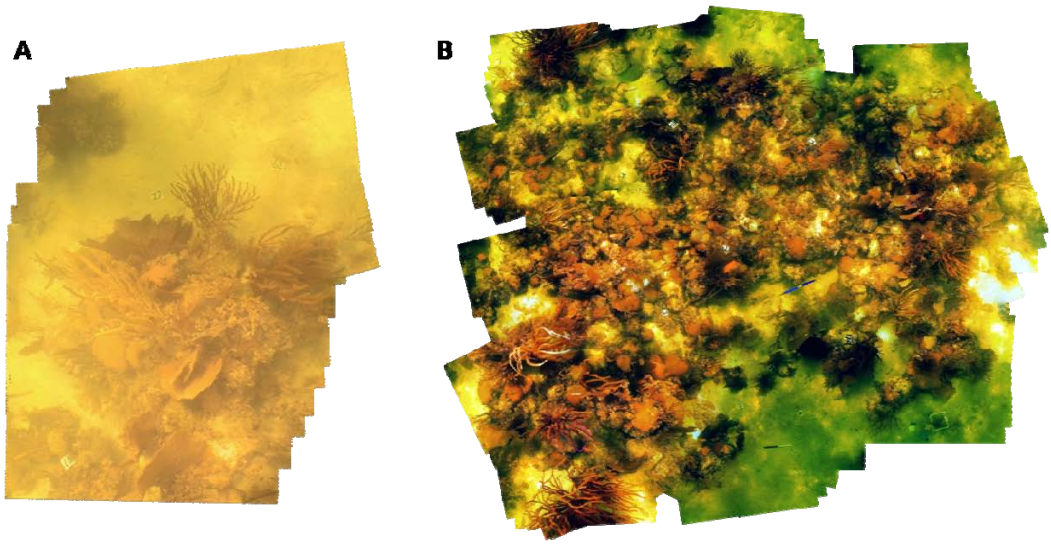


Figure A42. Benefits of image pre-processing. Video data from a shallow patch reef in the Florida Keys was hampered by low visibility and suspended sediments in the water column during data collection. Unprocessed video frames only produced matches between 10 video frames from the dataset (A) while color and contrast corrections allowed the entire dataset to be used and mosaiced despite poor initial conditions (B).

7. Image quality. As discussed above, many factors can influence the successful mosaicing of an image dataset. In an attempt to define parameters for the successful use of the landscape mosaicing algorithms we compared the image quality of several datasets collected during the course of this project. The results of this comparison are shown in Table A9 and Table A10.

Table A9. Image quality characteristics for mosaic datasets.

	Dataset	Avg red	std dev	Avg green	std dev	Avg blue	std dev	Histogram	Example Frame
Poor Mosaic Data (no mosaic produced)	E:\serdp\data\PuertoRico2007\20071213_ICON\DV	128.08	21.37	147.01	19.71	146.14	19.48		
	E:\serdp\data\Florida 2008\20080811_marker14\test\nocorrection	217.82	24.12	168.71	23.38	63.15	7.90		
Color Skewed	E:\serdp\data\Florida2005\20050517_tortugas	49.86	22.36	106.56	39.73	130.30	40.66		
Excellent Mosaic Data	E:\serdp\data\Florida2009\20090602_Carysfort\set2	116.09	38.56	103.65	43.18	100.57	40.66		
	E:\serdp\data\Florida2009\20090915_Brookes\set2	152.66	31.31	162.00	35.01	115.67	28.48		
	E:\Stills\Florida2009\20090915_Coopers\resize	90.28	43.07	83.61	40.47	69.55	37.03		
Effects of Color Correction	E:\Stills\Florida2009\20090624_Horseshoe\PartII\142ND200	96.38	28.91	101.83	26.31	40.02	17.62		
	E:\Stills\Florida2009\20090624_Horseshoe\colorII	110.79	39.26	87.60	32.39	81.05	28.18		
	S:\raw_Stills\Andros2009\20090314_Q6-3\127ND200	94.02	37.14	118.81	39.02	77.30	28.76		
	E:\Stills\Andros2009\20090315_Q6-3\color	111.64	49.99	113.52	54.74	108.62	57.31		

In this analysis, the average and standard deviation of the digital numbers of the red, green, and blue channels were calculated for a subset of images extracted from each dataset. In addition, the average histograms and example images are shown. This comparison allows us to determine the range of image quality conditions with which the landscape mosaic algorithms are capable of handling. In general, the two datasets that did not allow for mosaic creation (in their original form) were characterized by relatively narrow sharp peaks (Table A9 grey shaded rows). The low standard deviation of digital numbers observed in each color channel of these datasets indicates very low-contrast images. The position of the sharp peaks to the left of the image also indicates a preponderance of shadows in the dataset. The presence of a single narrow peak can indicate the preponderance of a single color in the dataset (Table A9 blue shaded row). While this can create a skewed result, the presence of a single narrow peak may not preclude successful mosaic creation and maybe corrected using color and contrast adjustments. The presence of sharp narrow bands were absent in the datasets that were considered excellent for mosaic creation (Table A9 orange shaded rows). These datasets are characterized by very wide peaks across all color bands, indicating high contrast color images. These results produced the best mosaic images for ecological analysis. It should also be noted that the use of color and contrast correction in general created images that had wider histogram bands after processing (Table A9; the green shaded rows show the pre-processed and processed data). Finally, an examination of the datasets collected from the permanent sites Brooke's Reef and Grecian Rocks showed a wide variety of image quality examples that were successfully matched using the landscape mosaic algorithms (Table A10).

Table A10. Image quality information for mosaic data acquired at permanent monitoring sites Brooke's Reef and Grecian Rocks.

	Dataset	Avg red	std dev	Avg green	std dev	Avg blue	std dev	Histogram	Example Frame
Acceptable Mosaic Data (taken at permanent sites Brooke's reef and Grecian Rocks)	E:\serdp\data\Florida 2008\20080617_Bleaching1_stills_nocommon	93.27	35.76	94.60	38.74	73.29	36.91		
	E:\serdp\data\Florida 2008\20080617_Bleaching1_noborder	147.28	59.60	139.10	50.21	131.07	44.46		
	E:\serdp\data\Florida 2008\20080807_Bleaching1	182.49	58.69	149.39	51.14	104.72	35.44		
	E:\serdp\data\Florida2004\20041020_keylargo\rcsq	142.63	41.01	146.09	40.36	146.33	36.82		
	E:\serdp\data\Florida2007\20070302_kl\sfish\movie_8	29.31	10.53	119.16	45.64	96.45	38.47		
	E:\serdp\data\Florida2004\20040330_keybiscayne\dv2	77.96	21.19	111.59	26.69	100.52	22.63		
	E:\serdp\data\Florida2004\20040408_keybiscayne\3.2mega.pics\3.2.pics	17.90	18.59	146.97	46.92	115.45	35.40		
	E:\serdp\data\Florida2005\20050305_kb\seq1lowres	78.73	39.86	77.50	42.36	73.20	38.53		
	E:\serdp\data\Florida2005\20050401_kb\seq1corr	106.32	57.73	137.71	65.71	138.30	65.49		
	E:\serdp\data\Florida2005\20050509_kb\high1lowres	127.07	56.74	140.05	58.96	156.51	60.88		
	E:\serdp\data\Florida 2008\20080616_BrookesReef	148.87	46.73	159.93	52.23	117.35	40.48		
	E:\serdp\data\Florida 2008\20080616_BrookesReef\subset_Nuno	145.87	47.44	144.44	47.57	123.53	48.04		
	E:\serdp\data\Florida 2008\20080807_BrookesReef	171.38	55.44	152.91	52.01	66.07	23.63		
	E:\serdp\data\Florida2009\20090915_Brookes\set2	152.50	31.13	162.68	35.23	116.91	28.83		

While these datasets were mosaiced under a wide range of image quality conditions, in general bands were wide and shallow. This range of successful processing parameters indicates that it is the presence of sharp narrow peaks among multiple channels that prohibits successful mosaicing (Table A10). The average standard deviation in each band of the mosaics that were not successfully processed was between 13.7 and 22.5, whereas the average standard deviation of the mosaics that were either assessed as excellent or acceptable ranged from 35.4 to 46.7. The color-skewed mosaic from the deep site in the Dry Tortugas had one channel (red) with low contrast (S.D. = 24.1) but two channels with high contrast (green and blue with S.D. = 39.7 and 40.7, respectively). From these data, we can suggest a rule of thumb that images with standard deviations in all bands less than about 20 digital numbers will not produce acceptable mosaics (Table A11).

Table A11: Average standard deviations for mosaics that could not be created ("poor mosaics") compared with mosaics that were successfully created (the other rows). Data taken from Tables A9 and A10.

Dataset	Standard deviation in red band	Standard deviation in green band	Standard deviation in blue band
Poor mosaics	22.5	21.6	13.7
Color skewed	24.1	39.7	40.7
Excellent mosaics	37.7	39.6	35.4
Mosiacs from FL	41.5	46.7	39.7

A2.4 Applications of coral reef monitoring and mapping using landscape mosaic technology

A2.4.1 Ship Grounding

Vessel groundings are a major source of disturbance to coral reefs worldwide. Documenting the extent of damage caused by groundings is a crucial first step in the reef restoration process. Video mosaics, created by merging thousands of video frames, combine quantitative and qualitative aspects of damage assessment and provide a geo-referenced, landscape, high-resolution, spatially accurate permanent record of an injury.

The active rehabilitation and restoration of damaged reef habitats in the US relies largely on the ability of authorities with jurisdiction over the resources to prosecute the parties responsible for the damage and retain monetary recoveries that can be used directly for restoration (Precht and Robbart 2006; Shutler et al. 2006). To determine the proper amount of restoration required, a two-stage Natural Resource Damage Assessment (NRDA) is conducted to determine: (1) the "primary" actions needed to return the habitat to its original baseline structure and function; and (2) the "compensatory" actions needed to compensate the public for the loss of resources and services until primary restoration is completed (Symons et al. 2006). Central to the NRDA process is the accurate and comprehensive quantification of the damage caused by a vessel on a benthic community. In this study, we describe the application of a novel methodology, landscape video mosaics that are ideally suited for the quantification of damage caused by vessel groundings on coral reefs as well as subsequent recovery patterns. This methodology can, with limited time in the field, satisfy the crucial initial damage assessment needs that are required for the subsequent recovery of funds from responsible parties as well as establish a visual baseline of the damage against which future recovery can be ascertained.

On 5 December 2002, the 49-foot vessel "Evening Star" ran aground on a hardbottom community dominated by stony and soft corals within the waters of Biscayne National Park, Florida (25º 23.332' N, 80º 09.874' W, 3 m of depth). On May 23, 2005 and again on July 19, 2006, video data of the damaged and surrounding areas was collected using a Sony TRV900 DV camcorder placed in an underwater housing following the methods described by Lirman et al. (2007). The camera operator swam a lawnmower's pattern of side-by-side strips followed by a similar pattern rotated 90º. A bubble level taped to the back of the camera housing helped the diver keep the camera pointed in a nominally nadir angle. The camera operator used a digital depth gauge to keep a consistent depth during the surveys. The time required for a single diver to collect the video used for mosaic creation was less than one hour in both years.

During the 2006 survey, positional (GPS) information was obtained for the outline of the injury as well as 25 ground-control points (GCPs) along the periphery of the scar using the diver platform of the Shallow Water Positioning System (SWaPS) (Figure A43.D). The GPS tracks recorded by the diver were used to demark the perimeter of the scar, and the area of the scar was

then computed from the polygon delimited by the scar perimeter using linear distances between GCPs. Positions of the 25 GCPs, identified using numbered ceramic tiles and painted disks easily visible in the video (Figure A43.C), were captured by the SWaPS platform and used for mosaic creation. The deployment of the tiles used to establish the position of the GCPs as well as the SWaPS survey took a single operator less than one hour.

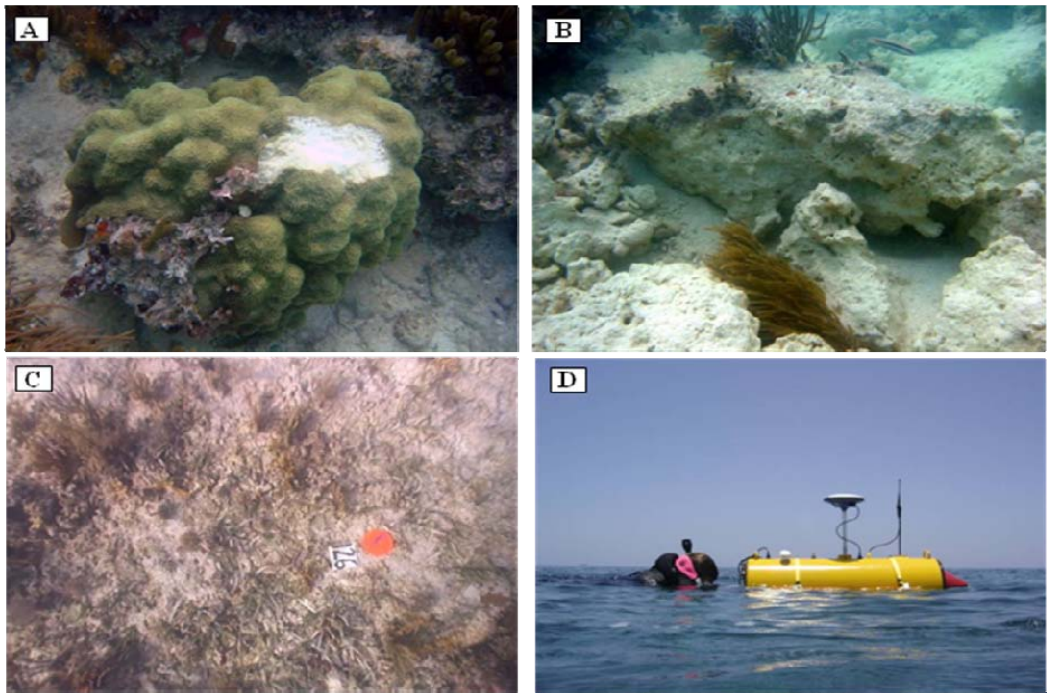


Figure A43. A) Superficial damage to a coral colony caused by a small ship grounding. B) Severe reef framework damage caused by a large vessel grounding. C) Numbered tiles and painted disks used as Ground Control Points (GCPs) for mosaic creation. D) Diver version of the Shallow Water Positioning System (SWaPS) used to determine the location of GCPs along the scar boundary. The unit integrates a GPS unit and a video camera to provide get-tagged frames of the bottom.

The scar, imaged in 2005 and 2006 in a Florida reef impacted by a 49-foot vessel, covered an area of 150 m^2 (total imaged area was > 600 m^2). The impacted coral community showed limited signs of coral recovery more than three years after the initial impact; the cover of corals was still significantly higher in the undamaged areas compared to the scar. However, seagrass colonization of the scar was observed.

Accurately documenting patterns of physical damage (and subsequent recovery patterns) to benthic habitats can be especially challenging when the spatial extent of injuries exceeds tens of square meters. These large injuries are often too difficult to measure *in situ* by divers and too small or costly to be quantified effectively using aerial and satellite remote sensing tools. Moreover, in cases where immediate action is required to initiate recovery efforts and avoid secondary damage to the resources, damage assessment activities need to be conducted quickly. Landscape mosaics capture data at a scale between diver observations and aerial imagery, thereby providing an ideal approach to assess grounding injuries because: (1) the images are recorded close to the seabed (< 2 m from the bottom) thus capturing detailed visual information,

(2) the resulting mosaics cover large areas of the bottom at scales commensurate with the damage caused by large vessel groundings; and (3) the imagery needed to document patterns can be collected quickly with an underwater video camera and, optionally, a surface GPS. Using this mosaic-based (or image-based) methodology, the dimensions of the injury caused by the 49-foot cabin cruiser “Evening Star” in December 2002 in the waters of Biscayne National Park, Florida, as well as the condition of the affected benthic community were documented in 2005.

In addition to providing a method for measuring the extent of injuries, landscape mosaics create a spatially accurate map of the distribution and condition of benthic organisms so that patterns of recovery (or further damage) can be more easily assessed than by diver-based methods alone. Repeat mosaics taken over time at the same location can be used to measure changes to a study site without requiring extensive tagging of individual organisms. In the present study, a second mosaic of the same grounding scar was constructed in 2006 to assess patterns of community succession and further damage caused by the passage of four hurricanes (Dennis, Katrina, Rita, and Wilma) during the summer of 2005 (Manzello et al. 2007).

The image-plus-GCP mosaicing method differs from the image-only method in the global optimization step (Figure A44). Under the image-only method, the cost function that is minimized uses only the image-to-image registration points (Gracias et al. 2003). In contrast, under the image-plus-GCP method, the cost function to be minimized uses terms for both the image-to-image registration points and the image-to-GPS registration points (Farrer et al. 2007). In both the image-only and image-plus-GCP algorithms, the image registration process estimates the 3D position and orientation of the camera for each image thus accommodating for changes in altitude and pitch and roll. In addition, the image-plus-GCP algorithm georeferences the mosaic to a world coordinate system (Universal Transverse Mercator Zone 17N in this case). Therefore, following the blending step, the mosaics created with GPS input are directly exportable to GIS software or Google Earth (Geotiff® and KMZ formats).

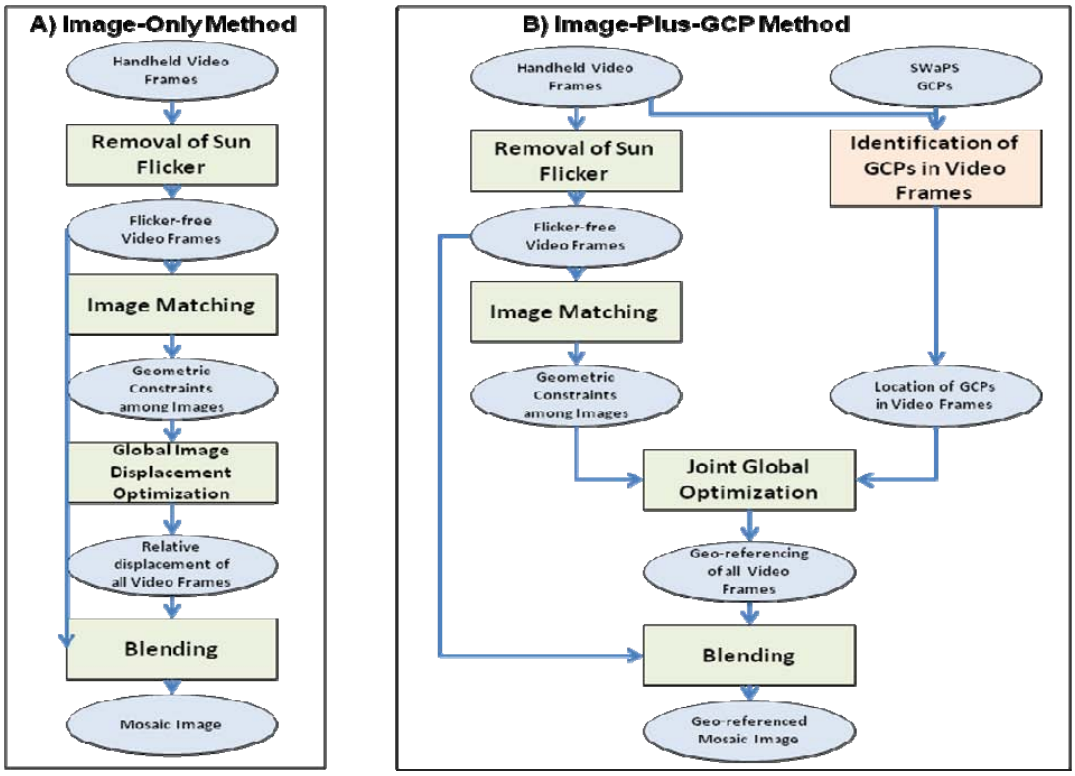


Figure A44. Flow-charts depicting the differences between the Image-only method (A) and the Image-Plus GCP method (B).

The use of mosaics to survey the damage caused by groundings shifts the bulk of time needed to complete a diver-based classic damage assessment from the field to the lab. The time required to collect both the video (< 1 hour) and the GCPs (< 1 hour) in the field was minimal and was easily achieved with one pair of divers. The processing time for the completion of the landscape mosaics ranged from 5-10 days. However, it is important to note that most of the processing steps are automated and therefore require only minimal operator input, so the actual operator time required was only a few hours for each mosaic. More importantly, significant improvements to the mosaic algorithms have been made over the past three years, and total processing times for mosaics similar to those presented here are now 1-2 days. The processing time is roughly divided into the following portions: sunflickering removal (33 % of the time), global matching (64 %), optimization (1%), blending (2%). For the 2006 mosaic, documenting the position of the GCPs from the geo-tagged video took approximately 3 hours.

A2.4.1.1 Status and Trends of the Benthic Community

The mosaics of the grounding site created in 2005 and 2006 were analyzed to assess the percent cover of benthic organisms in both the grounding scar and adjacent, undamaged areas as well as the patterns of permanence and removal of stony corals between 2005 and 2006.

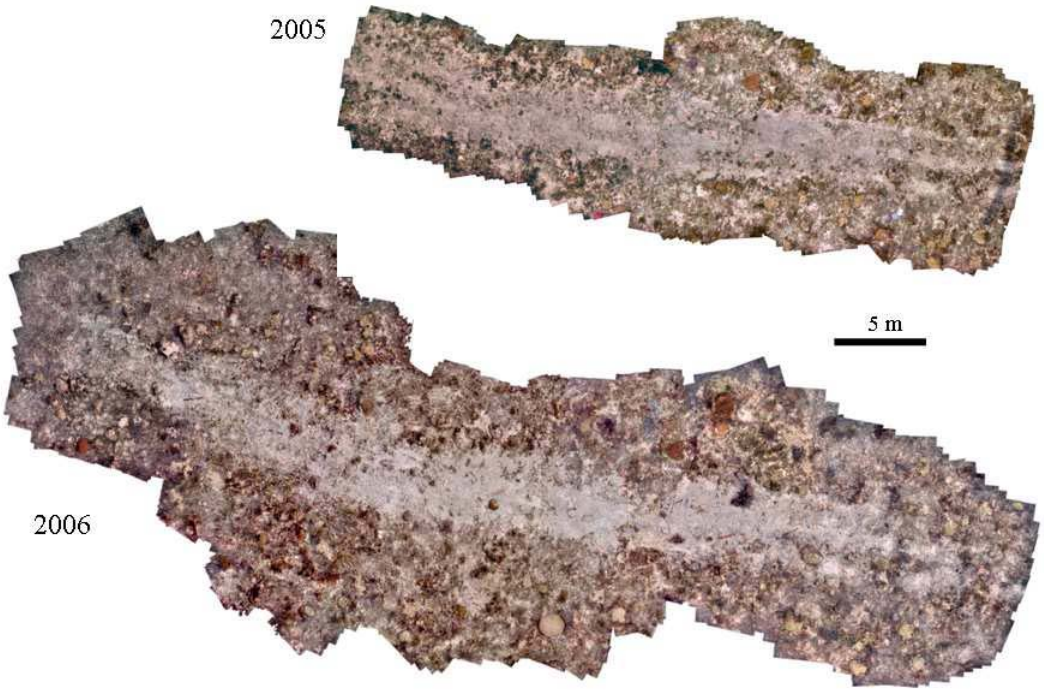


Figure A45. Landscape video mosaic surveys of the ship-grounding damage caused by the Evening Star in 2005 and 2006.

All information on the percent cover of the dominant benthic taxa (i.e., stony corals, soft corals, sponges, seagrass) was measured using the point-intercept method within replicate 1 m x 1 m sections of the mosaics (Lirman et al. 2007). For this assessment, a set of random points was superimposed onto each mosaic using the image analysis software CPCe (Kohler and Gill 2006). The random points were used as the central locations of simulated 1 m x 1 m quadrats used as sampling units. Once the quadrats had been positioned within each mosaic, a set of 25 quadrats within the grounding scar and 25 quadrats from the adjacent, undamaged areas were selected (the first 25 random points were selected for each habitat type). Each individual quadrat was then analyzed by superimposing 25 random points within its boundary using CPCe (Kohler and Gill 2006). The identity of the organism or bottom type immediately under each point was determined and the percent cover of each category was calculated as the proportion of the points occupied by a given taxon over the total number of points (i.e., 25 points per quadrat) as described by Lirman et al. (2007). The percent cover data were analyzed in a 2-way ANOVA with time (2005, 2006) and habitat type (scar, undamaged area) as factors. Finally, a subset of organisms (corals, sponges) visible in the 2005 mosaic were identified and relocated in the 2006 mosaic to determine permanence or removal/mortality between surveys. Because mosaics of the same area collected over time are easily referenced to each other, it is possible to determine the location of organisms or features in different surveys without the need to deploy markers. Thus, removal of organisms can be easily determined by locating their initial position in a prior survey.

In the area of overlap between the 2005 and 2006 mosaics, a total of 69 coral colonies were identified in 2005. Of the 69 colonies identified in 2005, 62 (90%) were relocated in the 2006 mosaic showing that limited physical damage was experienced by this site due to the 2005

hurricanes (or any other potential source of physical damage like swells or additional groundings). A total of seven colonies were removed or died completely between surveys (10 %). Lastly, two surviving colonies, both within the scar, appeared to have become dislodged and moved from their original location between surveys.

Three years after the initial vessel impact, the benthic communities in damaged and undamaged areas were still significantly different in the percent cover of the dominant taxa. The cover of stony corals and soft corals was significantly higher in the undamaged areas, while no significant differences in the cover of sponges between habitats were detected. No significant differences in the cover of corals and sponges were documented between 2005 and 2006. The most striking feature of the inter-annual comparison was the evident encroachment of seagrass (*Thalassia testudinum*) into the scar from the surrounding, unaffected habitat (Figure A46). The cover of seagrass within the scar increased significantly between 2005 (3.7 %, S.D. = 4.4) and 2006 (8.2 %, S.D. = 8.5).

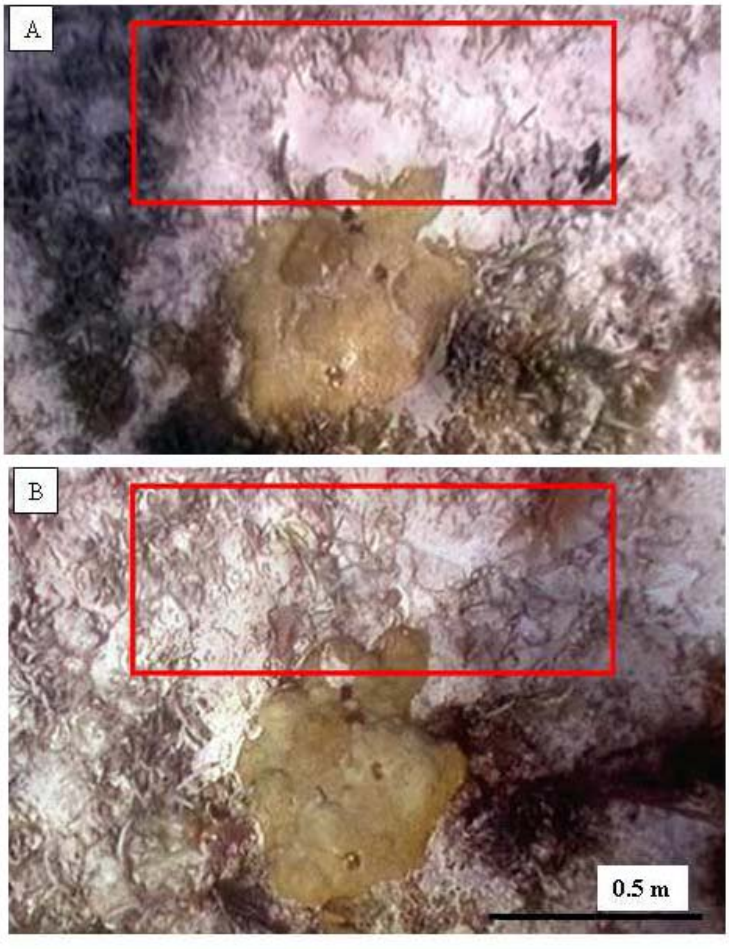


Figure A46. Encroachment of seagrass into the affected area between the 2005 survey (A) and the 2006 survey (B) as assessed through repeat video-mosaics.

A2.4.1.2 Comments and Recommendations

Providing a rapid and accurate assessment of the damage caused by vessel groundings on coral reef habitats is a crucial first step in the reef restoration process. This new application of underwater mosaics covered a larger area (> 600 m^2) than previous surveys with this technology and demonstrated the potential to incorporate external navigation into the mosaic processing, thereby enhancing the spatial accuracy of the resulting landscape map. The video mosaics provided a means to accurately and efficiently collect information on the size of the damage area as well as the status and trends of the impacted biological communities, thereby expanding the quality and diversity of information that can be collected during field surveys. The damaged portion of the reef surveyed in Florida covered an area of 150 m^2 and the impacted coral reef community showed limited convergence to the undisturbed community in the same habitat more than three years after the initial impact.

For a complete assessment of the use of landscape mosaic technology for the documentation and monitoring of ship-grounding disturbance on coral reefs please see:

Lirman, D., N. Gracias, B. Gintert, A. C. R. Gleason, G. Deangelo, M. Gonzalez, E. Martinez, R. P. Reid (in press): Damage and Recovery Assessment of Vessel Grounding Injuries on Coral Reef Habitats Using Georeferenced Landscape Video Mosaics. Limnology and Oceanography: Methods.

A2.4.2 Spatio-temporal analysis of coral communities

As part of an ongoing collaboration with the coral reef monitoring program at the Atlantic Undersea Test and Evaluation Center (AUTEC) changes in the abundance and spatial arrangement of benthic organisms of an inshore patch reef at Andros Island, Bahamas were examined over a 35-year time period.

Recent decades have been marked by extreme changes in coral reef communities both in terms of abundance and community composition. Despite extensive research into the causes and effects of recent changes in coral communities, little is known about how the spatial distributions of benthic organisms within reefs have changed over recent decades. In association with the coral reef monitoring program at the U.S. Navy's Atlantic Undersea Test and Evaluation Center (AUTEC) at Andros Island, Bahamas, the spatial arrangement of benthic organisms within a 10x10-m reef plot has been mapped over a 35 year period, providing a unique historical dataset to evaluate long-term changes in abundance and spatial distribution of reef organisms.

The hand drawn coral species distribution map used in this collaboration consists of a 10m x10m area of an inshore patch reef just offshore of the Atlantic and Undersea Test and Evaluation Center (AUTEC) (Figure A47). This 10x10m reef plot was installed in the late 1960's for use in a Navy coral reef monitoring program. Within the 10x10m reef plot all sessile benthic invertebrates were surveyed and mapped to species level for corals and genus for sponges, gorgonians and zoanthids.

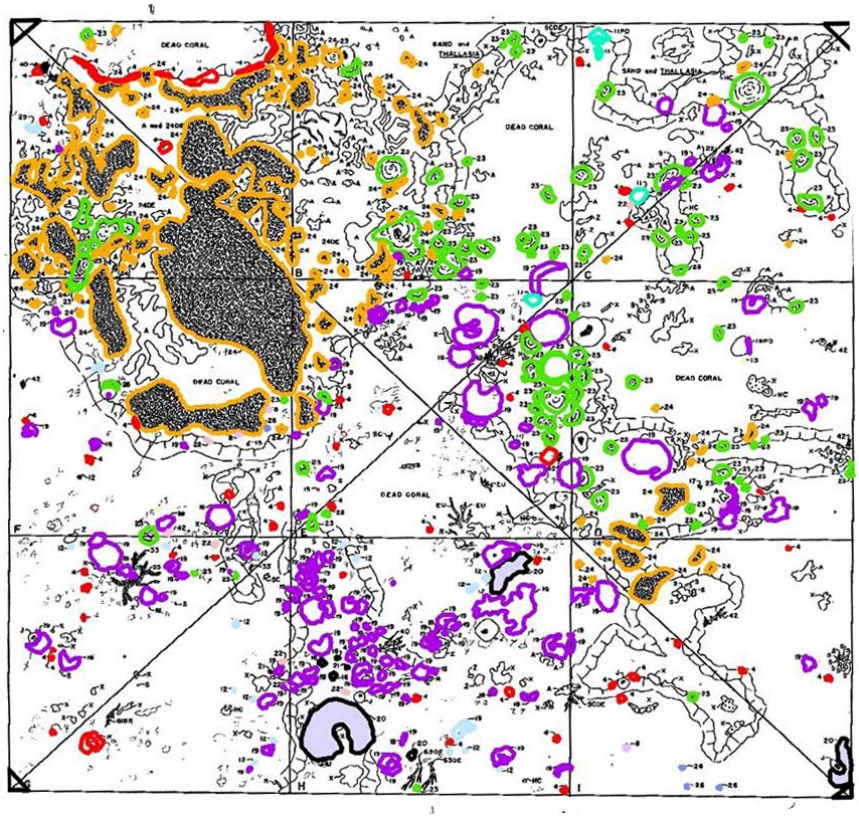


Figure A47. Example of digitized hand-drawn species distribution map of a 10x10m reef patch. The area has been digitized by coral species with the following color codes: orange (Porites porites), purple (Montastrea annularis complex), gray (Montastrea cavernosa), red (Agaricia agaricites), green (Porites astreoides).

A second survey of the inshore patch reef site was made in February 2008 using second-generation mosaic survey technology (Figure A48). The resulting video mosaic was used to document the location and areal extent of coral species within the study area.

Both the hand drawn and mosaic derived species distribution maps were georeferenced using ArcGISv9.0. The boundaries of individual coral colonies were digitized by hand and categorized by species. Analysis of spatial distribution patterns of individual species was accomplished by examining the nearest neighbor statistics, spatial means and standard deviational ellipses, and a test for local spatial autocorrelation (the Getis-Ord G_i*).

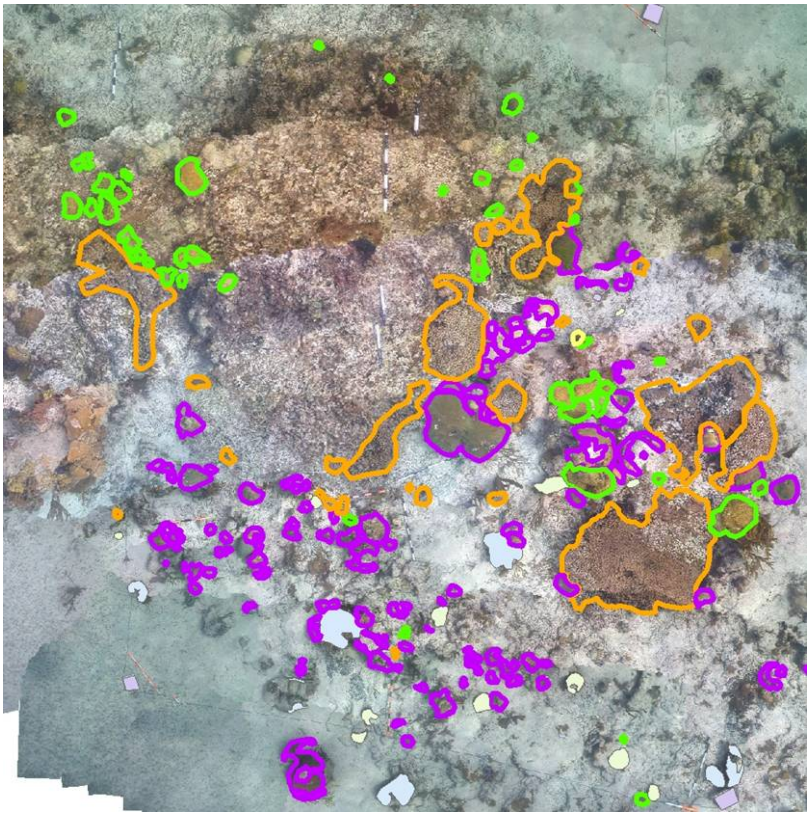


Figure A48. Partially digitized high resolution video mosaic of the 10x10m plot located at site S1-10. Coral species are coded by color: Orange (Porites porites), Purple (Montastrea annularis complex), Green (Porites astreoides), and Light Blue (Montastrea cavernosa).

Live coral cover within the 10mx10m study plot showed a slight increase over the 35 year time period (14.0%-15.7%). Despite this increase the number of colonies found in the study plot declined significantly (from 350 to 260) while the average colony size was found to increase over the time period (from 3.8cm^2 to 6.0cm^2). These changes indicate not only a loss of small colonies but also significant growth of large colonies resulting in the slightly higher coral cover.

Examination of the spatial distribution maps of the two time periods (Figure A49.A) indicates significant changes in the arrangement of coral colonies within the site despite the similar levels of abundance at the two time periods. For comparison purposes the digitized area coverages of the two distributions were gridded and the 1972 distribution was subtracted from the 2008 areal distribution map. Changes in coral cover are shown in figure A49.B. Areas of high mortality are shown in red and areas of growth are depicted in dark blue.

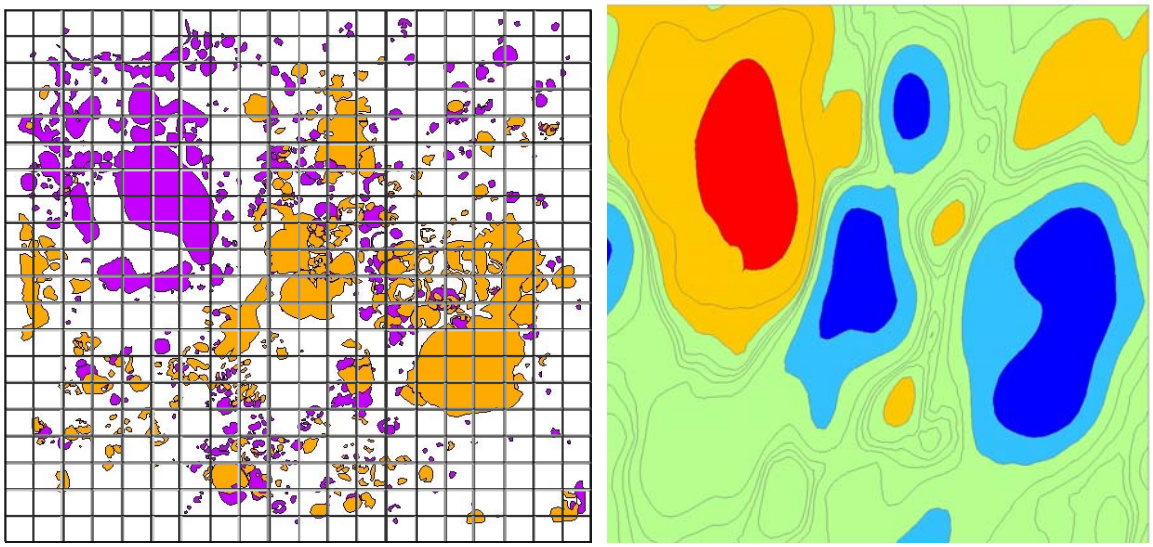


Figure A49. A) The 1972 (purple) and 2008 (orange) distributions of live coral cover at the study site. The grid shows the ½ m grid cells used to create the change in area map (B). B) An interpolated area map based on the change in live coral cover values from 1972-2008. Areas in red represent areas of high coral cover loss within grid cells (-2500 cm2- -1000 cm2) orange represents moderate loss (-1000 cm2 -230 cm2) green is little to no loss (-230 cm2 -350 cm2) light blue is moderate growth (350 cm2 -1000 cm2) and dark blue is high growth (1000 cm2 -2500 cm2).

In order to determine if local areas within the 10x10m plot were prone to coral mortality or growth (as opposed to a random pattern) a clustering analysis was performed on the change in area information. The results were mapped over the original area (Figure A50.B)

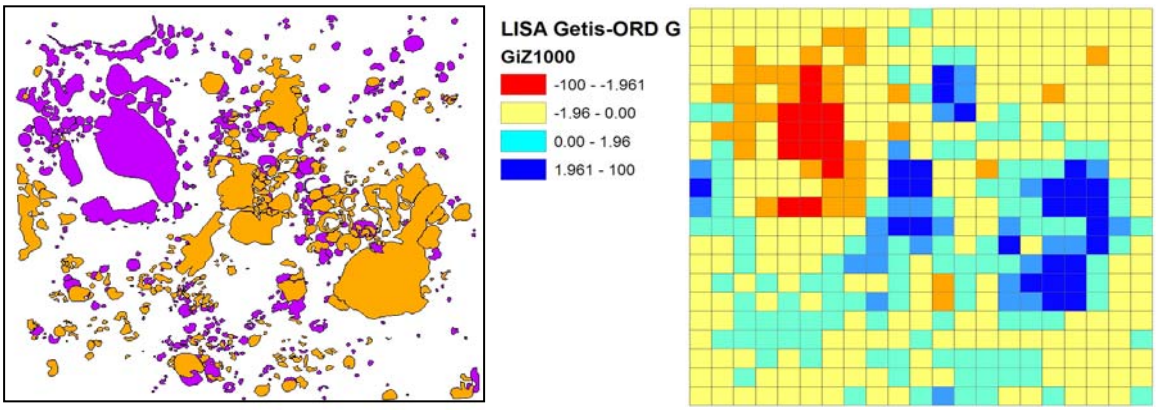


Figure A50. A). Shows the 1972 and 2008 distributions of live coral cover within the study area. B) Depicts the results of the local indicators of spatial autocorrelation Getis-ORD G test over the same study area as seen in (A). Significant negative changes in area (high mortality) are shown in red. Significant areas of high positive changes in area (high growth) are shown in dark blue.

The local indicators of spatial autocorrelation test (Getis-Ord G_i^*) indicate that neither mortality nor growth during the 35 year time period occurred in a random pattern. The top left of the quadrat seems to have undergone significant mortality while growth was localized in the lower right portion of the study area.

One of the most promising features of the spatial analysis of coral communities is that by mapping clusters of high mortality and high growth characteristics over time we may be able to identify local environmental or habitat characteristics that maybe influential in the persistence of coral communities in these locations. From the present study we found that the finger coral *Porites porites* had the highest change in spatial distribution over time at the study site. These analyses also showed distinct regions of high growth and mortality characteristics for this species over the 35-year time period. As an initial attempt to understand these patterns we overlaid the two distributions over a depth map of the area (Figure A51).

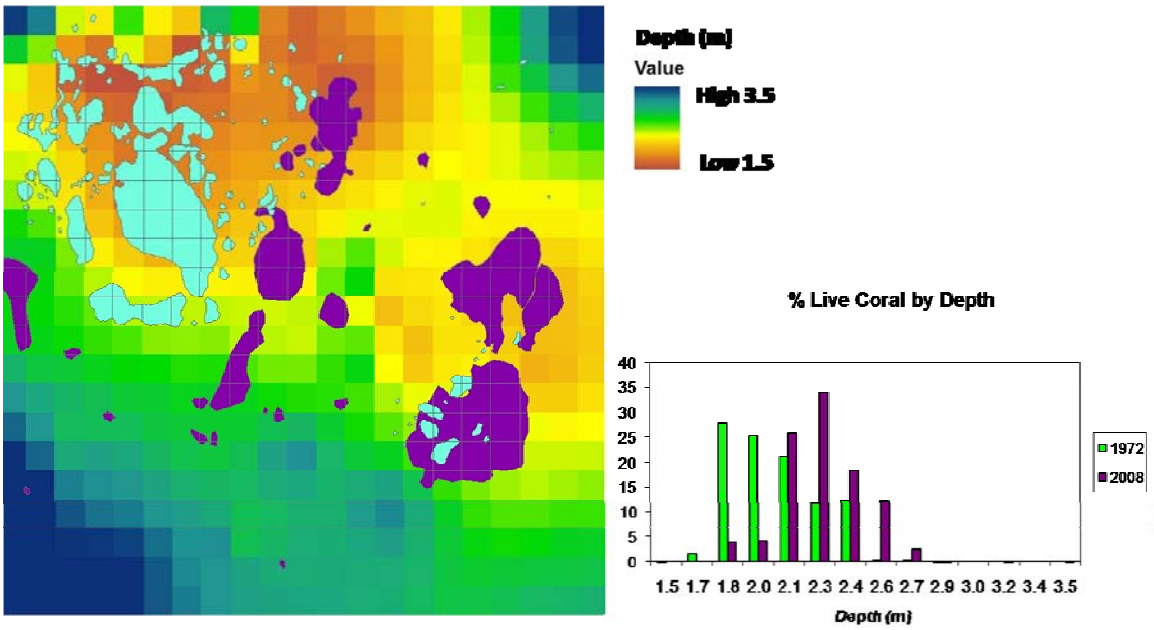


Figure A51. The 1972 (blue) and 2008(purple) distributions of the coral species *Porites porites* overlaid on top of a depth map of the study area. Graph shows the % live coral cover of P. porites by depth for 1972 (green) and 2008(purple).

From this it was apparent that the majority of the 2008 distribution was found in deeper water than the 1972 distribution. In addition the only areas of overlap between the two distributions (found in the lower right portion of the study area) are again located in slightly deeper waters than the majority of the 1972 distribution. The smaller colonies located in 2008 (and those most likely newest) are located in deeper portions of the reef than the rest of the 2008 distribution. Although not conclusive these findings suggest that depth, or other environmental variables related to depth (light intensity, temperature etc) may have played a role in the survivorship and persistence of *Porites porites* over the last 35 years at this site.

The results of the spatial analysis represent some of the first analyses of changes in spatial distributions over time for coral species. Although limited in its spatial extent these results show

that despite being long-lived species, corals do show changes in their distributions over time. Additionally the use of local cluster analyses such as the Getis-ORD G_i^* have provided coral ecologists with a new tool in which to view and map local areas of mortality and growth that can provide more information on coral community dynamics than changes in abundance alone. This is especially apparent at the study site discussed here in which measures of abundance stayed relatively constant over the 35 year time span while the distributions of corals within this area changed significantly. In addition the ability to create local maps of high mortality and high growth characteristics may allow researchers to identify local environmental or habitat characteristics that maybe beneficial to the persistence of coral reef communities into the future.

A2.4.3 Monitoring and Assessment of Mesophotic coral communities

Landscape mosaic products provide an excellent record of the state-of–the-reef at the time of a survey and can be used over time to monitor changes in reef communities. Because of the short dive times required for acquisition, these tools are uniquely suited for use in reef environments that are not easily accessible. As such we have collaborated with other researchers at the University of Miami and at the University of the Virgin Islands to survey and create baseline data for mesophotic reef communities.

Well-developed coral communities in mesophotic habitats have been historically under-represented in regional reef monitoring programs due to difficulties associated with access of trained observers to deep areas. Mesophotic coral reef communities may play a significant role as essential habitat for associated reef organisms and as potential refugia (Riegl and Piller 2003) from which shallow-water coral ecosystems might recover from disturbance events that have decimated shallow-water counterparts (Gardner et al. 2003). In this study, we describe landscape video mosaics, which have several advantages for monitoring the status and trends of mesophotic reef habitats. Landscape mosaics can help circumvent the limitations to diver-based monitoring imposed by limited bottom time at mesophotic depths because they consist of high-resolution, spatially accurate imagery that can be analyzed to extract key metrics of coral community condition such as cover, prevalence of disease and bleaching, and colony sizes.

The effectiveness of using landscape mosaics for mapping and monitoring shallow reefs, suggests that landscape mosaics may also prove useful for mosaicing mesophotic coral ecosystems. The goals for this study were to mosaic video data from two regions containing extensive coral ecosystems at mesophotic depths (the US Virgin Islands and the Dry Tortugas, USA), analyze the mosaics to measure the cover of dominant benthic taxa, and determine if cover from mosaics was comparable to diver-based measurements for the same areas.

As part of the collaborative effort between the University of Miami and UVI, two mesophotic reef sites were surveyed and analyzed. Site one (24° 42.295’ N, 83° 2.622’ W, 23 m depth) in the Sherwood Forest region of the Dry Tortugas, FL was surveyed on 17 May 2005. This general area has been described by Miller et al. (2001). Video data were acquired with a Sony TRV900 digital video camera in an Aquavideo housing using ambient lighting. The corners of an approximately 7 x 7 m survey plot were marked with inflatable diver signaling devices to help

guide the diver while swimming, and three 25 x 25 cm PVC quadrats were placed within the survey plot for scale.

Site two (18° 11.8083' N, 65° 04.7451' W, 38.5 m depth) in the Hind Bank Marine Conservation District (MCD), US Virgin Islands (USVI) was surveyed on 4 December 2007. This area has been described by Smith et al. (2009). Video data were acquired with a Sony TRV900 digital video camera in a Light and Motion Stingray II housing. A Halcyon Apollo light system with dual 50 W HID lamps was used to provide supplementary artificial illumination. The corners of an approximately 5 x 5 m survey plot were marked with Styrofoam floats and a single 25 x 25 cm PVC quadrat was placed within the survey plot for scale.

At both sites, a single diver swam transects over the survey plot while holding the video camera as vertical as possible. One set of parallel transects was completed with high (at least 50%) overlap between the swaths and then a second set of transects with little overlap between the swaths was acquired perpendicular to the first set.

Landscape mosaics of both sites were created using the procedure described by Lirman et al. (2007). The cover and composition of the coral communities on the two survey plots were assessed directly from each mosaic using the point-intercept method (Lirman et al. 2007). Four hundred random points were superimposed onto each image using the CPCe software (Kohler and Gill 2006) and the identity of the organisms or bottom type found directly under each point was determined.

In the Dry Tortugas, in addition to collecting the video for the construction of the landscape mosaics, divers estimated the percent cover of stony corals along four 10 m line-intercept transects following the Atlantic and Gulf Rapid Reef Assessment (AGRRA) protocol (Kramer and Lang 2003). One of these four transects was at the site of the mosaic, the other three were within 500 m of the mosaic. Additional data at the USVI site included habitat type, benthic composition, and coral health (Smith et al. 2009). Benthic cover was extracted from four 20 - 30 m video transects, producing 63 to 87 non-overlapping frames. Percent cover of benthic categories was determined under 10 randomly placed points per frame (Smith et al. 2008). One of these four transects was at the site of the mosaic, other three were within 1 km of the mosaic.

The Dry Tortugas mosaic (Figure A52) covered 52 m^2 with an approximate spatial resolution of 2.3 mm/pixel. The USVI mosaic (Figure A53) covered 31 m^2 with an approximate spatial resolution of 1.8 mm/pixel. Cover of stony coral was high at both sites but coral cover at the USVI plot (42.5%) was higher than the coral cover at the Dry Tortugas plot (23.1%). Plating or encrusting forms of colonies of the genus *Montastraea* dominated both communities. The mean relative cover of this genus was 85% at the USVI and 54% at the Dry Tortugas. Other coral genera found at lower abundances in both plots included *Agaricia, Colpophyllia, Helioseris*, *Mycetophyllia*, and *Porites*. The dominant macroalgae was *Lobophora variegata*, seen growing on dead coral skeletons at both locations. The cover of both soft corals and sponges was low at both sites (< 2 %). Measurements of coral cover derived from the mosaics are within one standard deviation of diver line-intercept transects at and within 500 m of the Dry Tortugas site (25.4 %, ± 8.1 S.D.) and diver video transects at and within 1 km of the USVI site (41.0 %, ± 1.9 S.D.).

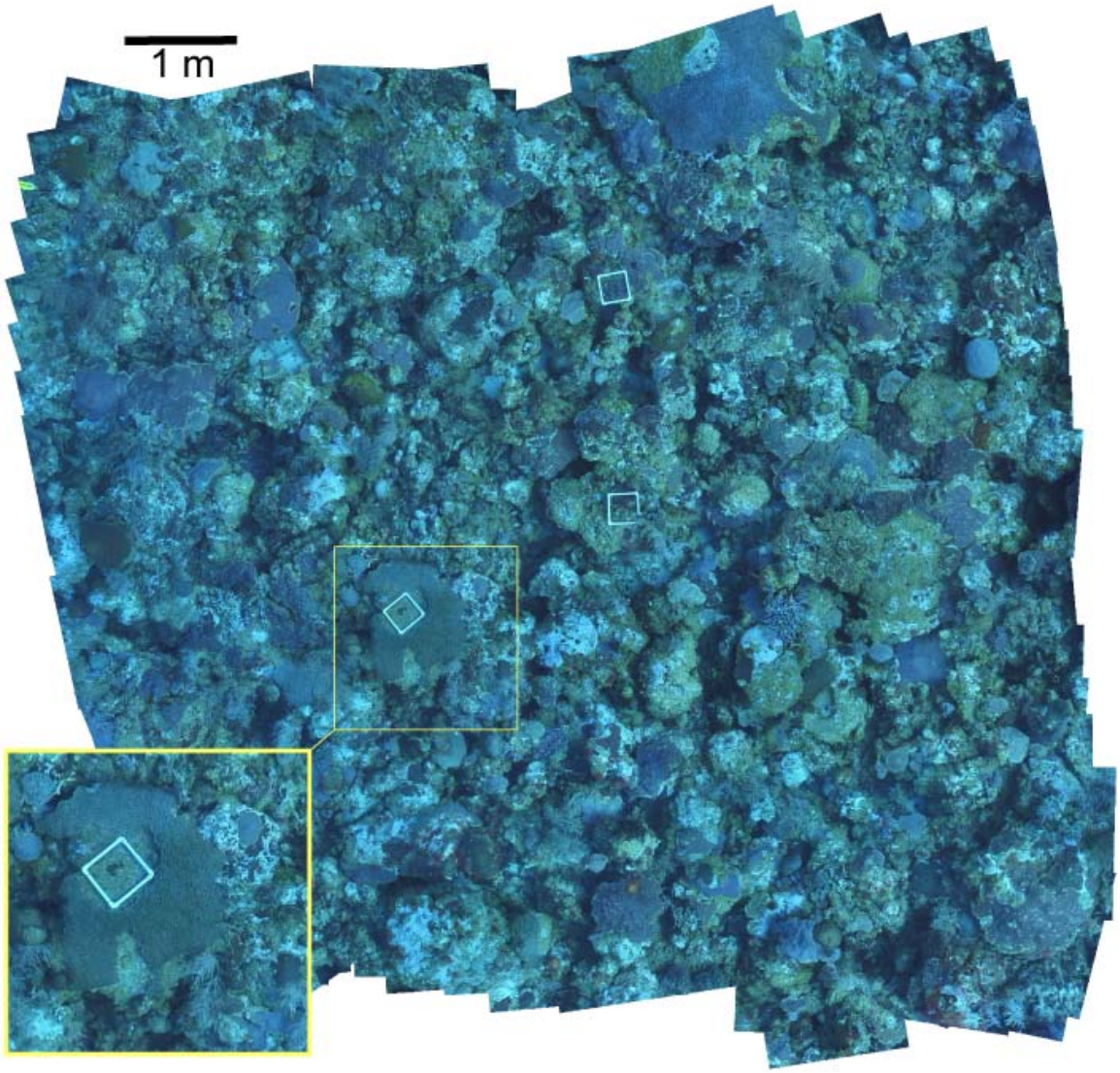


Figure A52. Site one from Sherwood Forest Reef, Dry Tortugas, Florida (23m water depth).

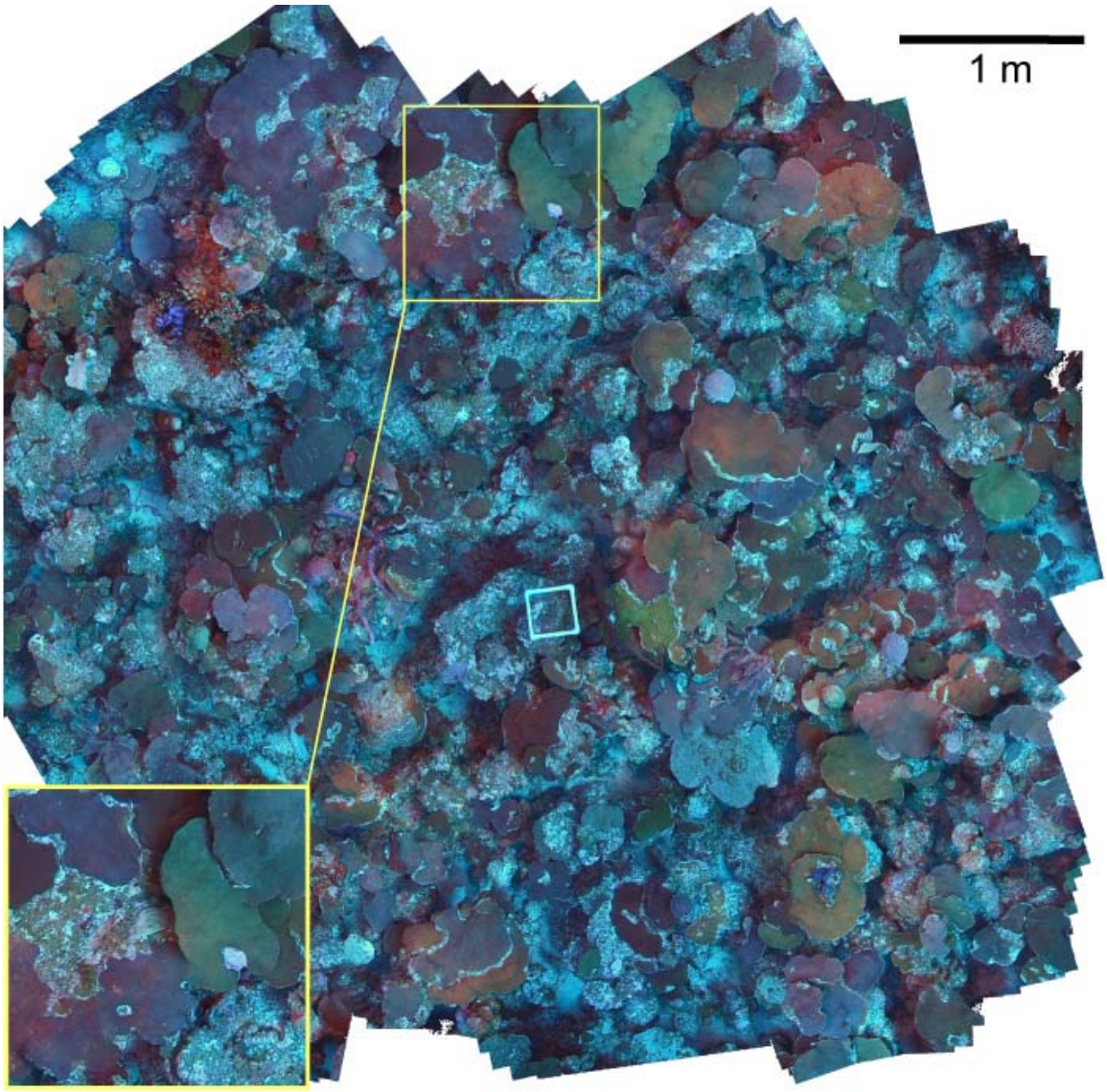


Figure A53. Site two, a coral hillock from St. Thomas USVI (38.5m water depth).

In this study, the software previously used to create landscape mosaics for shallow coral reefs was applied to mesophotic coral reef ecosystems. Landscape mosaics are well suited to this environment, in part due to the plating and encrusting growth forms of coral colonies at mesophotic depths that lend themselves to down-looking image-based monitoring.

One benefit of landscape mosaics is that they capture a permanent record from which percent cover, size, diversity indices, and the status of hundreds of individual colonies may be extracted as needed. A second benefit of landscape mosaics, like other image-based survey methods, is that shifting analysis to the lab saves dive time, which is critical at the depths of mesophotic reef ecosystems. Dive time and diver training were not obstacles to video acquisition for landscape mosaics, which in each case took 25 minutes. Different divers acquired the footage for each mosaic. Although both were experienced science divers, the diver for the Dry Tortugas survey had never acquired footage for video mosaics before, and the diver for the USVI survey had

made just one practice survey. The ease of data acquisition, in combination with the ability to use off-the-shelf hardware that most coral reef ecologists probably have already (i.e. a video camera and possibly lights), suggests that landscape mosaics could be applied widely for inexpensive surveys of mesophotic coral ecosystems.

A portion of the above work was presented in the following paper:
Gleason, A. C. R., N. Gracias, D. Lirman, B. E. Gintert, T. B. Smith, M. C. Dick, R. P. Reid (2009). Landscape video mosaic from a mesophotic coral reef, Coral Reefs, doi: 10.1007/s00338-009-0544-2.

A2.4.4 Using Landscape Mosaics to Assess the Impacts of Hurricane Damage on Acropora palmata populations

To document the impacts of storm damage on populations of *Acropora palmata* we used video-mosaic technology to document a population of the branching coral *Acropora palmata* at Molasses Reef (25º 0.609, N 80º 22.397 W, depth = 3.5-4.5 m) both before and after the 2005 hurricane season.

Mosaics of the study plot (approximately 10 m x 10 m) were constructed from underwater video collected before and after the 2005 hurricane season (Figure A54).

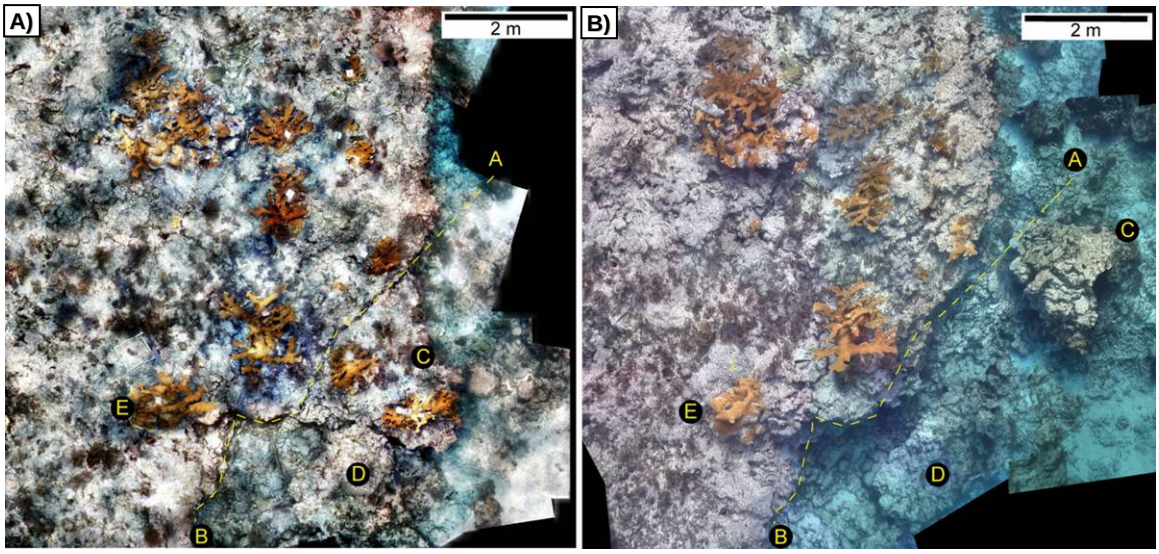


Figure A54. Video mosaics from a study plot at Molasses Reef in the Florida Reef Tract (depth= 3.5 – 4.5 m). A) Mosaic from May 2005, prior to the start of the 2005 hurricane season. B) Mosaic from February 2006 following the passage of Hurricanes Dennis (July 9-10), Katrina (August 25-26), Rita (September 19-20), and Wilma (October 24-25). The yellow line A-B shows where the reef framework was dislodged during hurricane Rita causing sections of the reef marked C and D to collapse. The section labeled C also appears in the figure bellow.

Video data were collected at Molasses Reef in May 2005 and in February 2006 after the passage of Hurricanes Dennis (dates of influence over the Florida Keys = July 9-10, peak wind gusts at Molasses Reef (C-MAN station) = 90 kph), Katrina (August 25-26, 116 kph), Rita (September 19-20, 100 kph) and Wilma (October 24-25, 147kph).

The video-mosaics produced in this study have high spatial accuracy and thereby provide the capability to measure distances and sizes directly from the images once a scale has been established (Lirman et al. 2006). The scale in these mosaics is provided by PVC segments and ceramic tiles scattered throughout the images. The size of the *A. palmata* colonies found within each mosaic was measured as: (1) the maximum colony diameter; and (2) the projected surface area of live tissue using the image-analysis software Image-J.

The direct physical damage caused by hurricanes and tropical storms can vary significantly across multiple spatial scales, ranging from minimal to severe (Harmeline-Vivien 1997). Whereas changes in coral cover, abundance, and condition can be easily discerned from traditional before-and after surveys, changes to the structure of reefs are harder to quantify. The video mosaics created in this study provide a unique view of the reef benthos that facilitates the documentation of colony-level impacts as well as large-scale structural changes to the reef framework.

If only colony-based information such as coral cover, abundance, and size-structure had been collected prior to the onset of the 2005 hurricane season, the damage report for the *A. palmata* population at Molasses Reef would have revealed limited damage. A total of 19 *A. palmata* colonies were identified from the video mosaics from May 2005, prior to the onset of the 2005 hurricane season, and 17 of these colonies remained (in the same location) in the study plot in February 2006 (Figure A54). The two colonies that were removed from the plot were located on the sections of the reef framework that was dislodged during Hurricane Rita (Figure A55.a). These two colonies remained attached to the dislodged reef section but ended up in contact with bottom sediments and died shortly after the storm (Figure A55.b). The tissue on these large colonies (110 and 115cm in maximum diameter) represented 14% of the total live *Acropora* tissue on the plot prior to the storms. For those colonies that remained, the net tissue losses between surveys were only 10%. Fifty-two percent of colonies lost live tissue; the maximum tissue loss for an individual colony was 46%, and the maximum tissue gain was 47% of the original tissue area. The mean diameter of colonies decreased slightly from 88.4cm (SD ±70.1) to 79.6 (±63.3) cm. Tissue losses were mainly attributed to the removal of branches (Figure A55.c, d).

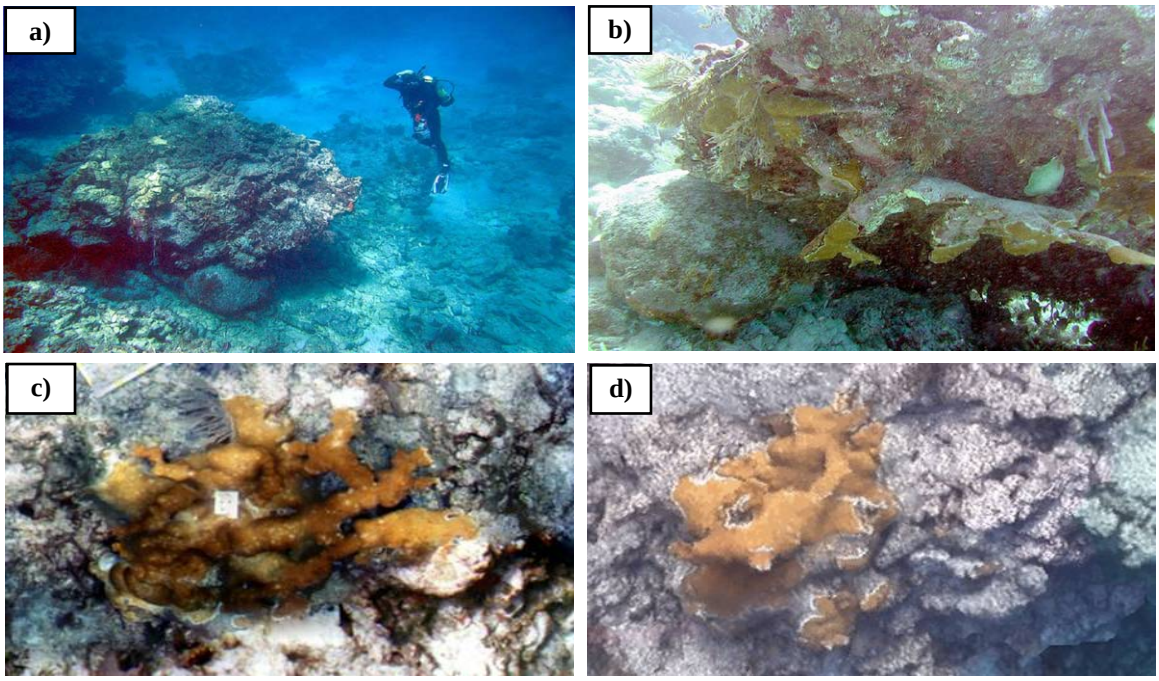


Figure A55. a) Photograph of the reef section dislodged during Hurricane Rita. b) Photograph of two *A. palmata* colonies attached to the dislodged reef section. These colonies ended up facing the sediments and died shortly after the storm. Sections of video mosaics from May 2005 (c) and Feb 2006 (d) showing an *A. palmata* colony (labeled E in the figure above) that experienced fragmentation and tissue mortality due to the 2005 hurricanes.

Previous studies have documented an increase in the abundance of *A. palmata* colonies through fragment formation and reattachment after storms (Fong and Lirman 1995). This was not observed within the 2005-2006 study plot at Molasses Reef. Fragment reattachment requires time (Lirman 2000) and the succession of storms during the summer of 2005 may have impeded this process.

Although there was limited impact from the 2005 storms on individual coral colonies, large changes to the reef framework were documented at this site. Within the study plot, a large section of the reef (surface area = 12.7 m^2, diameter = 6m) was dislodged and deposited on the sand at the bottom of the reef spur (Figure A54, A55a). The shift in orientation of these sections resulted in the smothering and burial of coral colonies and the exposure of reef framework, which may be further weakened by the future activities of bioeroders (Glynn 1988). The precise documentation of such large-scale modifications to the structure of the reef would not have been possible without the availability of the landscape view provided by the video-mosaics.

The methods used to assess damage and recovery patterns of reef communities commonly entail the construction of underwater maps of the benthos based on diver-collected distance measurements and drawings, and the deployment of survey markers and permanent tags for coral colonies within plots. Assessing the impacts of severe physical disturbance on coral reefs can be especially challenging when large-scale modifications to the reef structure takes place and both coral colonies and survey markers are removed (Hudson and Diaz 1988; Jaap 2000). The data

presented in this study show that landscape video-mosaics provide the tools needed to accurately assess reef damage and recovery patterns at multiple scales and represent a significant improvement over existing survey techniques, which require extensive bottom time and the use of trained research divers.

The above research was included in the following publication:
Gleason, A.C., Lirman, D., Williams, D., Gracias, N.R., Gintert, B.E., Madjidi, H., Reid, R.P., Boynton, G.C., Negahdaripour, S., Miller, M. and Kramer, P. (2007) Documenting hurricane impacts on coral reefs using two-dimensional video-mosaic technology. Marine Ecology 28:1-5.

A2.4.5 Use of 2D Video Mosaics for Assessing the Impacts of Mass-Bleaching Events on Coral Communities

Our efforts in 2006 showed the benefits of mosaics in assessing the impact of mass bleaching events on coral communities. In 2005, Caribbean reefs experienced a major bleaching event that resulted in significant coral mortality throughout the region. The magnitude of the 2005 bleaching event has prompted a federal response by the US Coral Reef Task Force to initiate large scale assessments of short and long term impacts of this event on Caribbean coral communities.

During December 2005, we surveyed a shallow patch reef offshore of the AUTEC naval base on Andros Island, Bahamas. Although our survey was not conducted at the peak of the bleaching event (August-October), bleached colonies were still observed at this site. 2D video mosaics were made from video footage acquired in December of 2005 and again in October 2006.

By rectifying the resulting mosaics, pale or bleached colonies identified in the 2005 mosaic were relocated in the October 2006 mosaic to document patterns of coral mortality and/or recovery (Figure A56.a). The analysis of these mosaics indicates that bleaching status in 2005 was not a good predictor of mortality as examples of both partial mortality and colony recovery occurred within the site (Figure A56.b & c). Several of the coral colonies that were completely bleached in December 2005, had recovered their pigmentation by October 2006 (Figure A56.c), while other colonies that showed only slight paling in December 2005 showed significant partial mortality 8 months later (Figure A56.c).

The inability to use bleaching severity as a predictor of coral recovery potential highlights the appeal of using landscape video mosaics that capture the health of all colonies >5 cm within a given area to follow changes over time. This feature allows users to follow individual colonies through time with limited field effort. Although standard tagging based approaches that randomly tag large numbers of colonies will yield similar information on the health of bleached and non-bleached colonies over time, these approaches are time consuming underwater and are often plagued by tag loss that can cause coral health information to be lost.

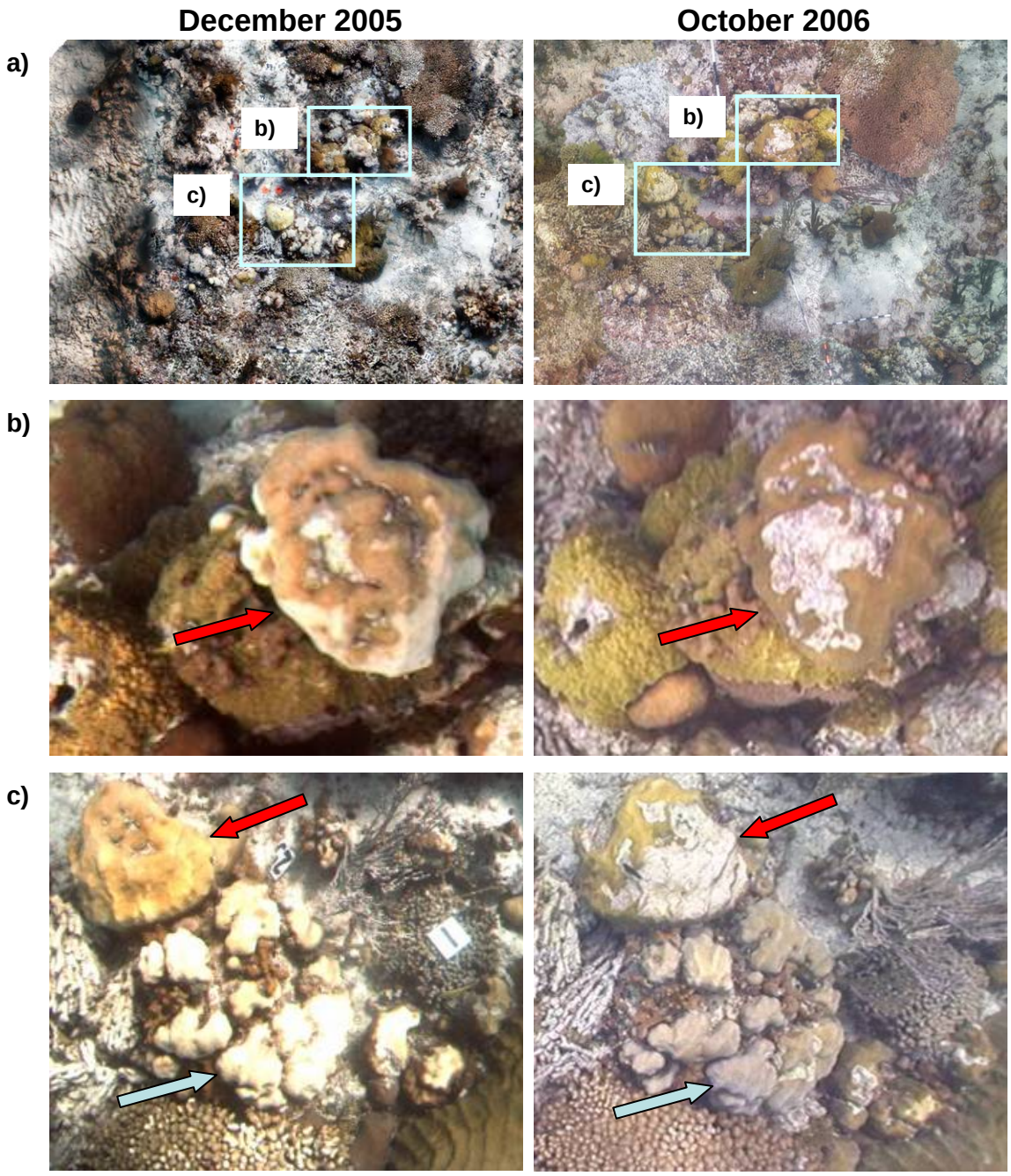


Figure A56. (a) Landscape video mosaics of site S1-10 located offshore of Andros Island, Bahamas in December 2005 (left column) and October 2006 (right column). Affected colonies were identified using the 2D video mosaics shown in (a). Red arrows indicate colonies that underwent partial mortality between December 2005 and October 2006. Blue arrows indicate colony recovery during the same time period.

The application of our 2D mosaic products to the assessment of mass bleaching events indicates that this technology provides a large scale permanent record of colony location, and health that can be followed over time to assess coral colony mortality and recovery without extensive field efforts.

A2.5 Users/Partners

Throughout the term of this project our group has developed several collaborations with both government and scientific users of landscape video mosaics. The results of these collaborations are outlined below:

A2.5.1 SERDP Coral Reef Monitoring and Assessment Workshop

A SERDP-sponsored workshop was held at the Rosenstiel School of Marine and Atmospheric Science, University of Miami Nov 18-19, 2008. The primary focus for the workshop was to: (1) understand the DoD client perspective on assessment and monitoring needs; (2) understand other potential user perspectives (i.e., in addition to DoD) regarding their coral reef monitoring and assessment needs and how the two SERDP-developed technologies (landscape mosaics and FIRe) may help address those needs; and (3) identify how the two approaches/technologies are complementary to each other and how they might be integrated to meet end-user needs.

Presentations by DoD personnel, representatives from key governmental and non-governmental organizations/offices actively involved in coral reef management and research, and the research teams from the University of Miami and Rutgers were interspersed with active discussion. Results from the workshop are summarized in a comprehensive report (SPAWARSYSCEN PAC. 2008). Key findings include the following:

1) Federal policy mandates that DoD characterize, assess, and monitor underwater benthic communities at Air Force, Army, and Navy bases in order to document compliance with national policy and to ensure that DoD operations do not lead to natural resource degradation, particularly with respect to coral reefs. DoD is looking for technologies and methodologies that will enable the collection of the data with less dive time, reproduce data collection transects reliably year after year, and retain flexibility to be modified based on expert evaluation of site conditions at the time of the survey. DoD is also interested in exploring how emerging technologies may foster new opportunities to develop productive partnerships between the NAVY and other organizations.

2) Workshop participants were in agreement that current monitoring and assessment strategies conducted by the agencies are, in general, adequate to meet present mandates, but there was broad interest from all agencies in developing methodologies that reduce dive time and cost efficiency. Specific challenges and needs to expand present methodologies include capabilities for detailed mapping with improved accuracy compared to currently used strip (1D) mosaics, monitoring deep reefs, studies of infection patterns of coral disease, and non destructive methods for determining coral physiology.

3) There was consensus regarding the usefulness of landscapes mosaics and FIRe technologies for advancing coral reef monitoring and assessment practices. Individually

or combined, these techniques offer potential for more efficient methods of monitoring coral cover, colony size, mortality, bleaching and disease prevalence, coral population structure, extent of injury and recovery patterns. There was also agreement that the transition of both technologies to the end-user community would be valuable.

The potential for the two SERDP technologies to augment and enhance the specific reef monitoring and assessment activities of the participating agencies is summarized in Table A12. Column 1 of Table A12 lists the governmental and non-governmental agencies represented by workshop presenters and other participants. Columns 2, 3 and 4 are color coded to indicate potential contributions of mosaics (green), FIRe (yellow) or both technologies (purple) to augment or enhance monitoring of present metrics (Column 2), enable new desired capabilities (Column 3), or provide new opportunities for partnerships (Column 4). Text in Column 2 identifies indices of reef health presently monitored by each agency that could benefit from the use of mosaics and/or FIRe. Text in Column 3 identifies desired enhanced monitoring capabilities that could be accomplished using mosaics and/or FIRe. Column 4 summarizes potential collaborations using mosaics and/or FIRe.

Table A12. Technology overlay and potential collaborations resulting from SERDP coral reef monitoring and assessment workshop.

Potential roles for: Mosaics FIRe Mosaics & FIRe

Agency	Current Metrics / Indicators	Desired Capabilities	Collaborations
Presentors			
US Navy	coral cover, colony size, disease & bleaching, mortality	increased sampling efficiency; multi-tier approach; safe, efficient, cost effective; digital technology;	
MMS	coral cover, diversity, coral growth		reef condition & coral growth, Flower Gardens
NPS	coral cover, disease & bleaching	detailed mapping; disease causes and infection research	coral monitoring program, Biscayne National Park
FWS	coral cover, diversity, disease & bleaching	improved monitoring techniques and technologies	monitoring at remote refuges, e.g. Palmyra Island
EPA	coral cover (2D & 3D), colony size, disease & bleaching, mortality, population structure	expand surveys to include additional benthic organisms and determine links to stressors	investigate sampling efficiency in different environments (mosaics); assess coral viability, identify stressors, and collect database of FIRe signatures
NOAA Fisheries	coral cover, colony size, disease & bleaching, mortality	reduce dive time and expand surveys to deep reefs (e.g., *Oculina* banks)	survey deep coral communities (i.e., *Oculina* banks) and thickets of thretened corals (i.e., *Acropora*)
NOAA Coastal Monitoring and Assessement	biomarkers, coral diseases	rapid, effective, non-destructive methods to evaluate coral physiological condition	use in-situ FIRe in combination with chemical, microbiological & biomarker sampling to assess coral response to mixed stressors.
NOAA Sanctuaries	injury & % cover at damaged and reference sites, recovery patterns	increase survey spped; reduce need for trained divers; improvements relative to strip mosaics	groundings assessment, FKNMS
NOAA Restoration	coral colony size, partial mortality, disease & bleaching % cover, urchin abundance	survey deep reefs (> 30 m)	survey coral reef and seagrass sites to compare survey methods, products, & cost effectiveness
TNC	coral cover, disease & bleaching, colony size, mortality	identify causes of changes in coral condition and demographics occurring between annual sampling events	continue ongoing collaboration with the Florida Reef Resilence Program
Other participants			
US Navy AUTEC			continue ongoing collaboration mosaicing permanent monitoring sites
NCRI			address pixel mixing problem in airborne remote sensing images
Florida Sea Grant			surveys at CREWS/ICON stations

Following the SERDP coral reef monitoring and assessment workshop several collaborations with reef monitoring user groups were created and/or extended. Overviews of our collaborative efforts are described in the following sections.

A2.5.2 The National Park Service: Surveys of the threatened coral Acropora palmata

In conjunction with the National Park Service in St. Croix, USVI, mosaic surveys were completed at four sites within the Buck Island Reef National Monument. Sites were chosen to document the current state of the threatened coral species *Acropora palmata* at Buck Island reefs and provide baseline data from which impacts of future hurricanes, bleaching, and disease events could be assessed. These sites at Buck Island are known to be some of the best remaining *Acropora palmata* reefs in the Caribbean. The four reefs surveyed varied in terms of exposure and depth providing a comprehensive survey of the types of *Acropora palmata* reefs present at Buck Island.

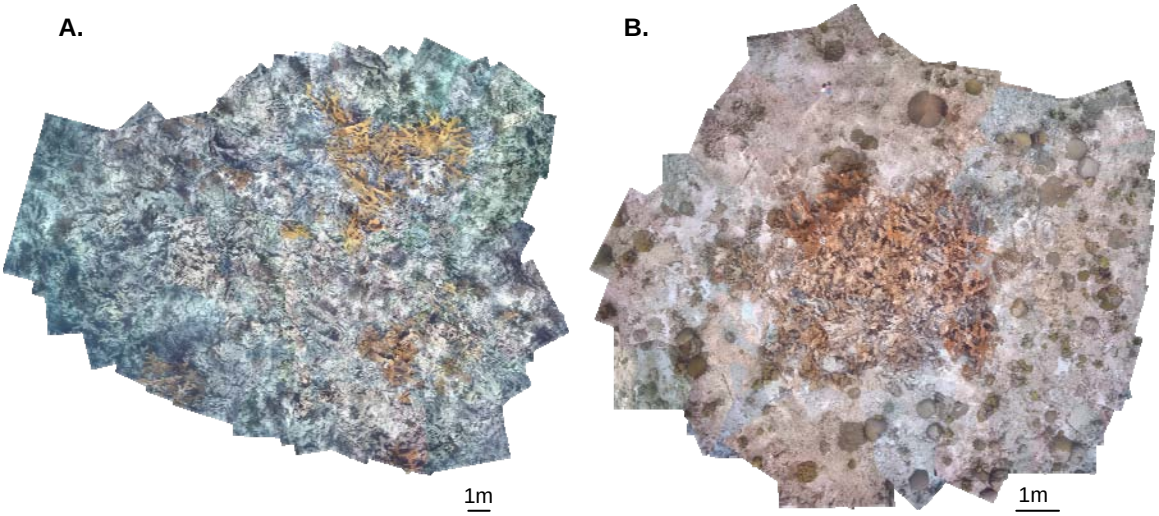


Figure A57. 2D video mosaics of *Acropora palmata* reefs at Buck Island National Monument, St. Croix, USVI. The reef in (A) is a deep patch reef consisting of very large individual colonies of *Acropora palmata*. B) Is a shallow inshore patch reef site.

A2.5.3 University of Puerto Rico

In December 2007 we were invited to participate in a large multi-organizational hyperspectral mission headed by the University of Puerto Rico at Mayagüez (UPRM). As part of this mission, different resolution airborne hyperspectral imagery was acquired over designated reef science areas. During the mission 2D video mosaics were acquired in four different reef environments to provide spatially explicit groundtruth information for the hyperspectral images. Additional spectral data and precision gps information was taken during mosaic acquisition. The image based groundtruthing will allow for an in-laboratory assessment of the accuracy of hyperspectral image classification at various resolutions. This is the first attempt at using 2D video mosaicing technology to groundtruth hyperspectral imagery.

A2.5.4 The US Navy's Coral Reef Monitoring Program at AUTEC

In association with the US Navy's coral reef monitoring program at the Atlantic Undersea Test and Evaluation Center (AUTEC) we have begun using 2D video mosaics to monitor a number of their 10x10m permanent reef monitoring sites. Installed in the late 1960's these sites provide a long history of reef health information. 2D video mosaics have been acquired repeatedly at a number of these sites between 2005 and 2009.

As a result of this monitoring effort we have been able to monitor Andros Island coral populations following the 2005 Caribbean-wide mass bleaching event, the 2009 region-wide bleaching and disease event, and assess the spatio-temporal dynamics of Andros Island coral communities over the last 40 years (See sections A5.4.2 and A5.4.5).

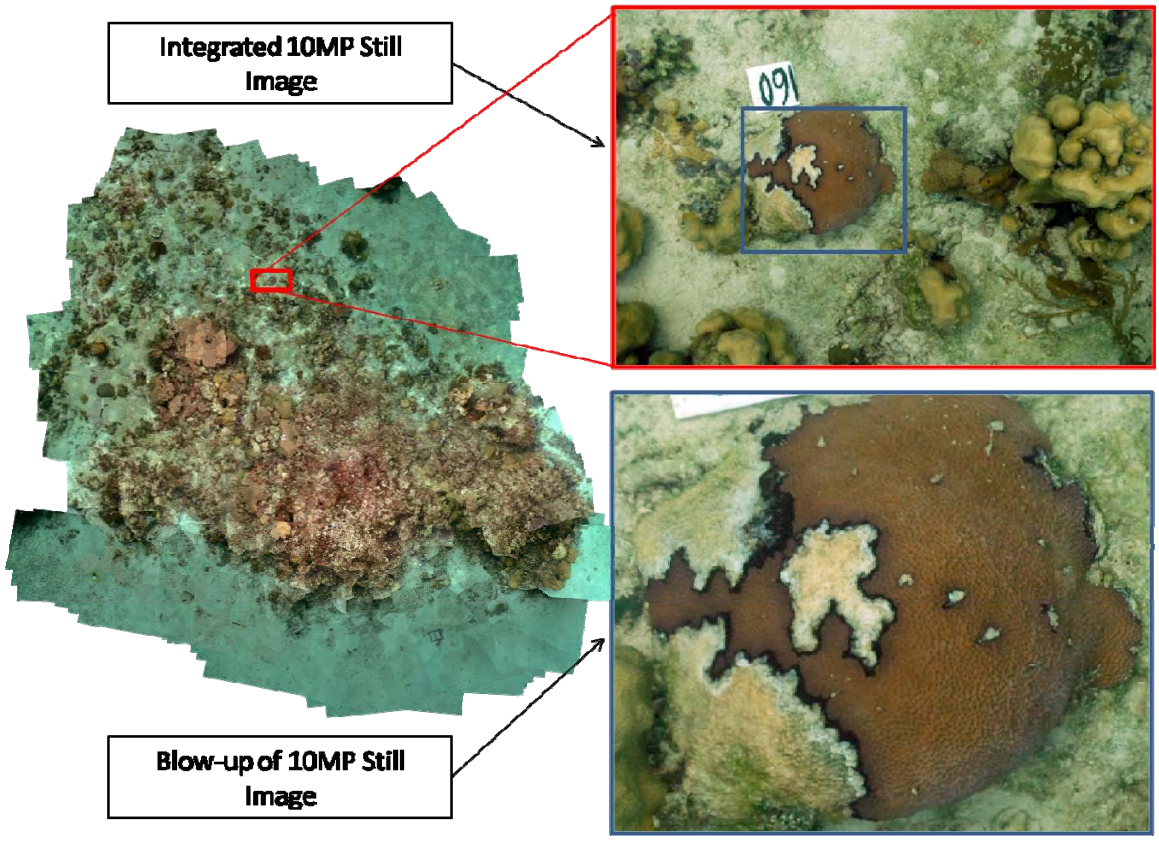


Figure A58. Example of coral reef monitoring at Andros Island, Bahamas. In the images above all coral colonies within a 10x10m permanent reef plot were surveyed and monitored during the 2009 bleaching and disease event using second-generation video mosaicing technology. This high resolution imagery allowed for the identification of diseased coral colonies (such as the one shown above) without the use of tagging. Colonies at this site have been continuously monitored for changes since the inception of the collaboration in 2005.

A2.5.5 The Nature Conservancy

In collaboration with the Florida Reef Resilience Program we proposed to construct video mosaics of reef plots (5 x 5 m) within four reef habitats (i.e., inshore, mid-channel, fore-reef, and offshore patch reef habitats) to: (1) test the potential application of this methodology in documenting reef resilience and resistance to bleaching impacts; and (2) establish eight permanent plots (replicated by habitat type) to monitor future temporal, colony-based patterns of bleaching, mortality, and recovery.

As part of the Florida Reef Resilience Program's yearly bleaching surveys, we identified eight sites (n = 2 per habitat type) where permanent plots (5 m x 5 m) were established by hammering and cementing sections of rebar into the reef substrate. The center of each plot was marked with a buoy and a GPS location was established from the surface (Figure A59). At each site, digital video and still images were collected at 1.5 – 2 m from the bottom.

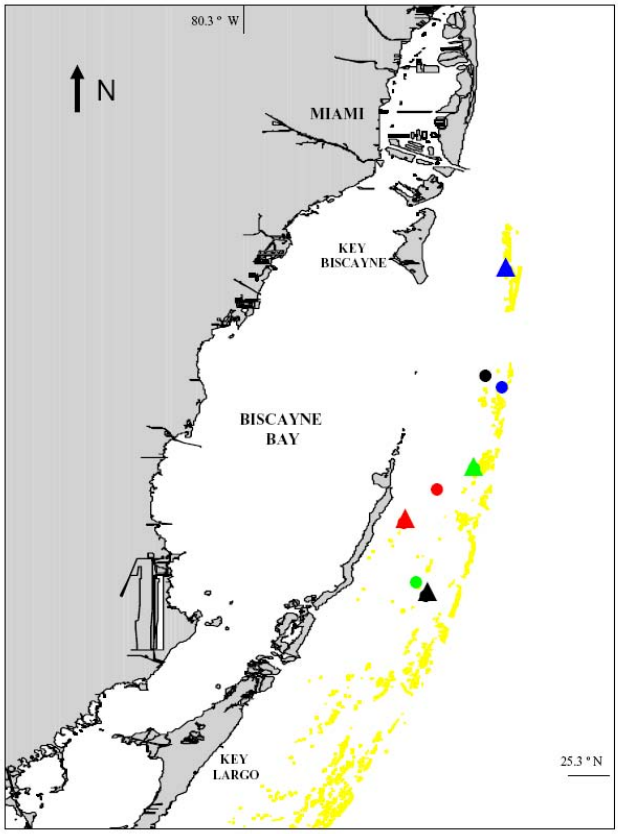


Figure A59. Location of the permanent sites established as part of the bleaching-mosaic assessment of the Biscayne Subregion of the Florida Reef Tract in the summer of 2008.Reef habitats appear in yellow. Red = Inshore sites, green = mid-channel sites, blue = fore-reef sites, black = offshore patch reef sites. Triangles mark the locations of the permanent sites for which video mosaics were constructed (Figs. A60-A63).

For four of the eight permanent plots, video mosaics were created using the algorithm described in detail by Lirman et al. (2007). The four mosaics constructed for this study have a ground

resolution of 1-2 mm.pixel^{-1} (Figs. A60-A63). These video mosaics cover areas of roughly 100-125 m^2 and allow for the tracking of hundreds of coral colonies without the need to tag individual colonies. The spatial accuracy of the mosaics also provide a way to measure coral sizes and patterns of tissue mortality that would be important indicators of individual and population responses to stress. Future surveys require only that divers relocate the permanent markers and video surveys can be easily completed in < 30 min of bottom time.

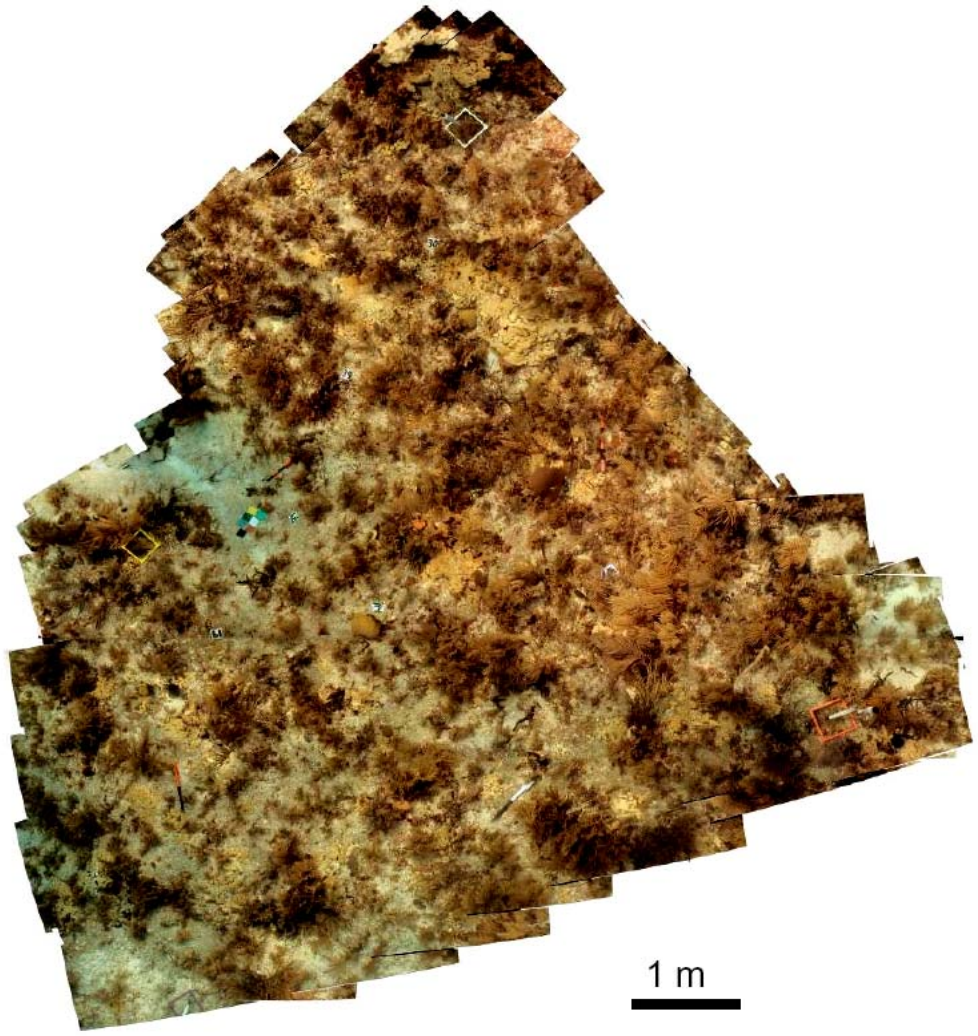


Figure A60. Landscape video mosaic of a permanent plot established within an Offshore Patch Reef habitat as part of the Florida Reef Resilience Program in the summer of 2008. Site number = 1188, Site location = 25° 24.088' N, 80° 9.208' W, depth = 12 m.

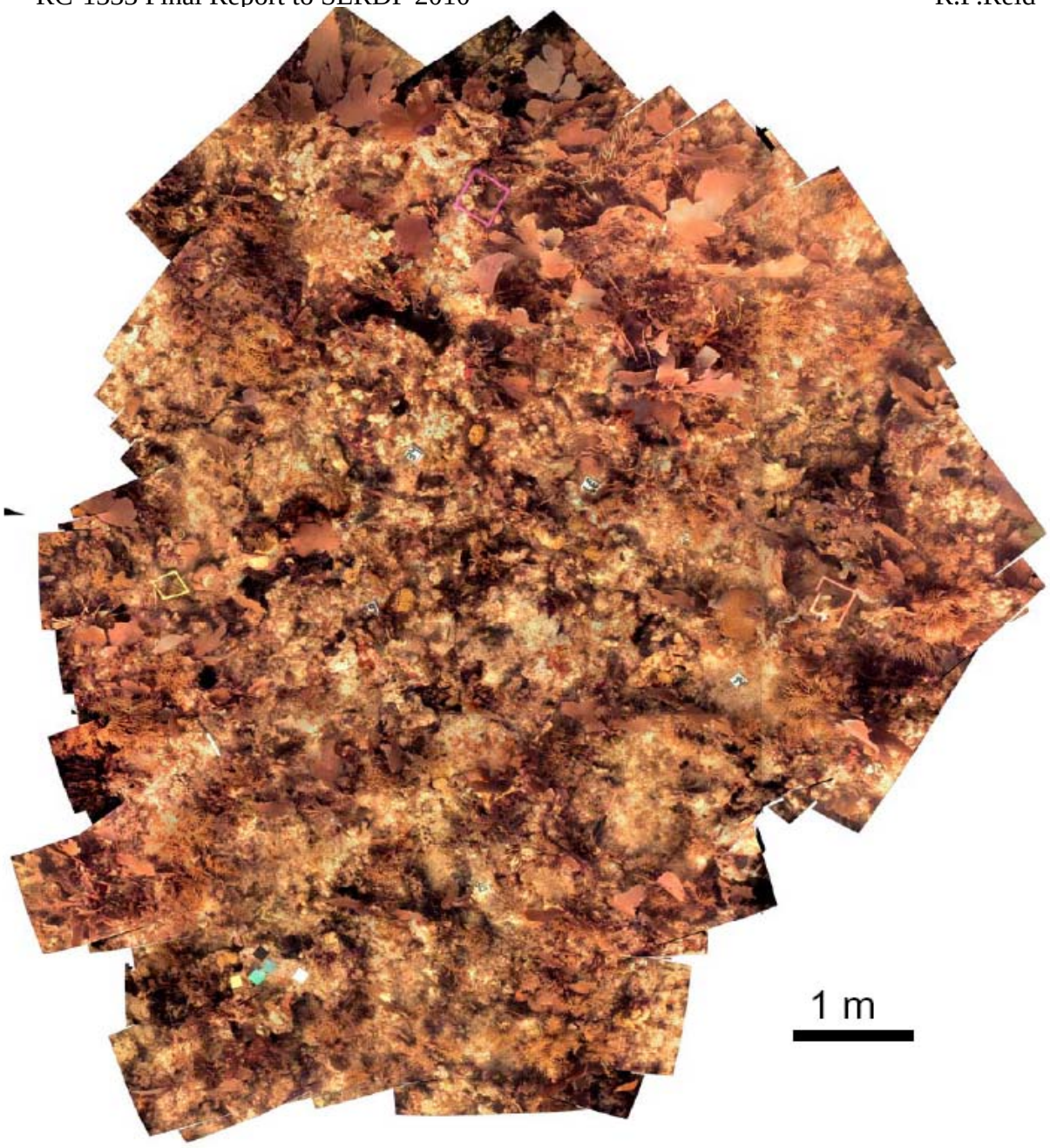


Figure A61. Landscape video mosaic of a permanent plot established within a Mid-Channel Patch Reef habitat as part of the Florida Reef Resilience Program in the summer of 2008. Site number = 2197, Site location = 25° 30.525' N, 80° 7.232' W, depth = 4 m.

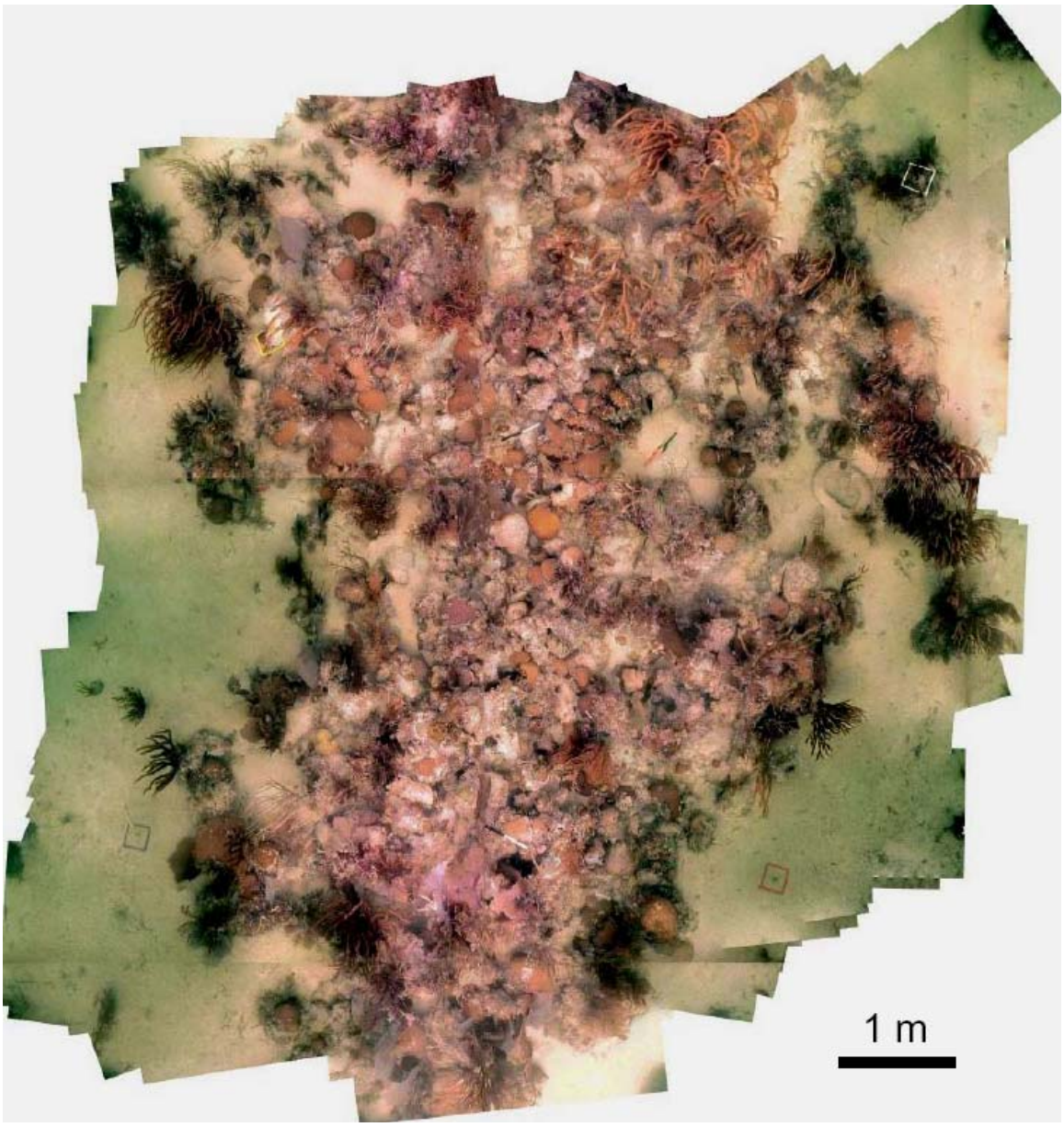


Figure A62. Landscape video mosaic of a permanent plot established within an Inshore Patch Reef habitat as part of the Florida Reef Resilience Program in the summer of 2008. Site number = 3161, Site location = 25° 27. 819' N, 80° 10.085' W, depth = 3 m.

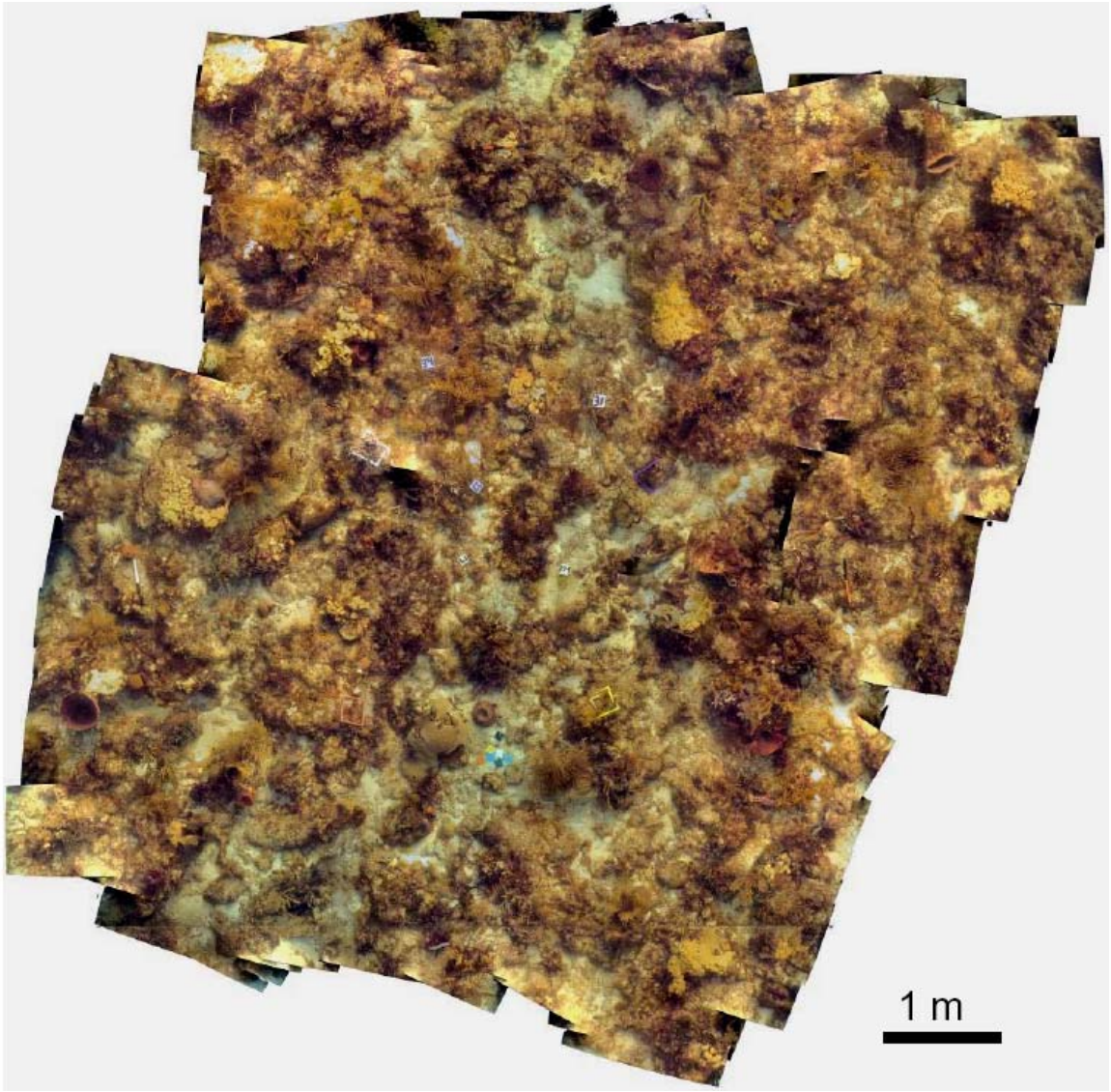


Figure A63. Landscape video mosaic of a permanent plot established within a Fore-Reef habitat as part of the Florida Reef Resilience Program in the summer of 2008. Site number = 3202, Site location = 25° 40.508' N, 80° 5.908' W, depth = 11 m.

While the principal objective of this project was to exploit the benefits of mosaic images to track spatial patterns of coral bleaching response and recovery, no significant coral bleaching was observed in 2008 (only a few colonies showed signs of bleaching within the plots established; Figs. A60-A63). Nevertheless, the eight permanent sites established, the video and stills collected, and the four mosaics created provide the tools and resources needed to, in the event of a future bleaching event, document bleaching impacts rapidly and accurately and establish a baseline against which patterns of mortality and recovery (i.e., resilience) can be accurately assessed over time.

The four mosaic sites surveyed in 2008 were re-visited in the summer of 2009. Bleaching prevalence in 2009 (as was the case in 2008) was limited. Nevertheless, a small number of

colonies within the survey plots exhibited signs of bleaching. The coral colonies showing signs of paling or bleaching were identified and marked with numbered tiles that appear in the mosaics, tagged with numbered aluminum tags, and measured. These tiles were deployed within the area appearing in the mosaic and thus provide a way of finding and identifying these colonies for future assessments (Figure A64). Subsequent mosaic surveys will enable us to assess the patterns of growth, survivorship, and mortality of these bleached colonies, thus providing a good tool to evaluate bleaching impacts and reef resilience for the different reef habitats of the Florida Reef Tract.

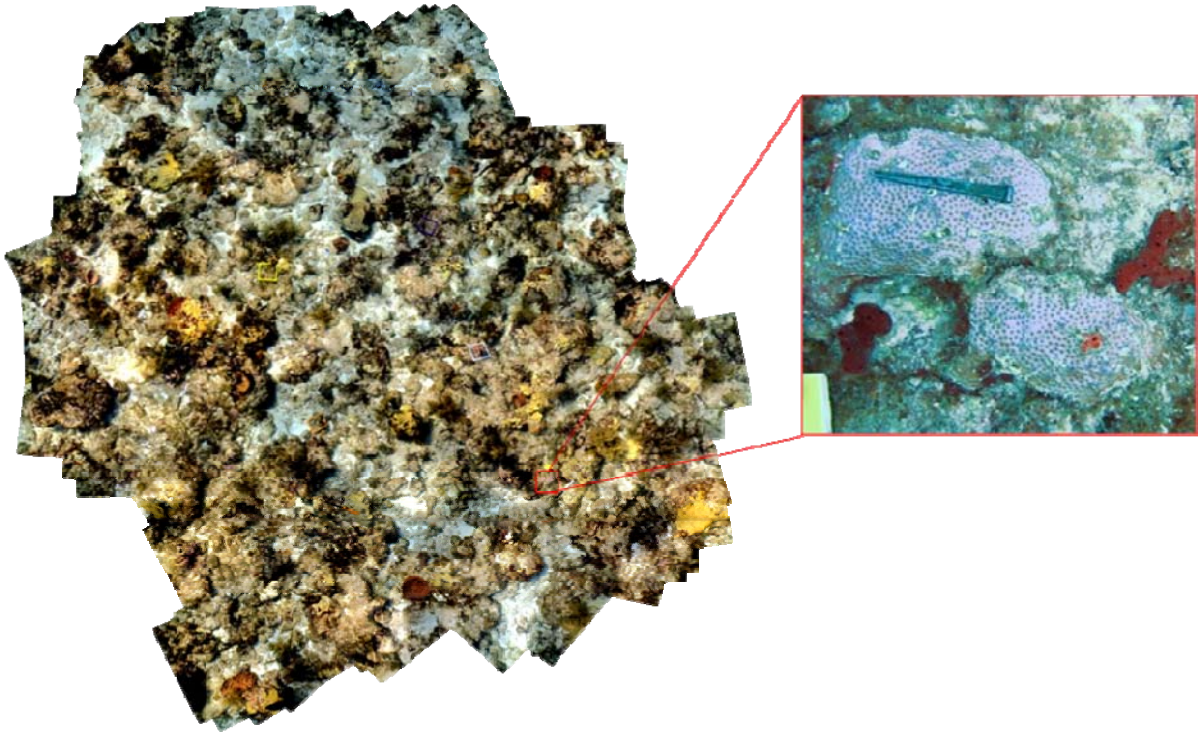


Figure A64. Landscape mosaic of a Fore-Reef habitat showing the location of bleached colonies of *Siderastrea siderea*. Bleached colonies within mosaics were identified with a numbered or colored tile.

A2.5.6 Rutgers University

As part of the project extension, we were asked to collaborate with Rutgers University to evaluate the potential for integrating landscape mosaic technology with another methodology developed under SERDP: Fluorescence Induction and Relaxation technique, or FIRe, developed by Drs. Maxim Gorbunov and Paul Falkowski at Rutgers.

On June 16-18, 2008, researchers from the University of Miami and Rutgers University conducted a joint sampling effort in the northern section of the Florida Reef Tract to evaluate the potential for integrating these two distinct coral monitoring methodologies into an integrated sampling strategy. As an initial evaluation of this potential integrated approach, two coral reefs sites were selected and surveyed jointly. At each reef, high-resolution video and still images were collected from a reef area roughly 10 x 10 m. The data collected will be used to construct a

spatially accurate, high-resolution video mosaic using the methods described by Lirman et al., 2007. In addition, 20-30 benthic organisms dominant in the area (including hard corals, soft corals, sponges, macroalgae) were identified within the imaged plot and FIRe fluorescence measurements were taken for each organism using the diver-operated FIRe instrument as described in (Gorbunov et al, 2001; Gorbunov and Falkowski, 2005).

The first reef surveyed, Brooke's Reef, is located at 25 40.508^{o}N, 80 5.908^{o}W. This reef is found at 10 m of depth and it has been surveyed annually since 2004 by University of Miami researchers using the video mosaic technology. The plot surveyed within Brooke's Reef is demarcated by four pipe sections permanently attached to the bottom. These markers are easily identified within the video mosaic, which allows for multiple mosaics to be referenced against each other for change-detection analyses. Prior to the collection of the video imagery for constructing the video mosaics, 30 benthic organisms were identified within the plot by deploying numbered tiles. These tiles are commonly used to identify organisms or features within the completed video mosaics. In this case, the tiles will be used to link the organisms within the video mosaic with the physiological measurements obtained for each one. After the completion of the image acquisition (~30 min), researchers from Rutgers University collected fluorescence measurements for each of the organisms identified by the numbered tiles. The time required to collect the fluorescence information from 30 objects (with 3-4 replicates on each target) was approximately 40-60 min.

The same procedure was repeated at a second, shallower reef (5 m) (25 35.255^{o}N 80 6.778^{o}W). In this case, a permanent plot, roughly 5 m x 5 m, was established by cementing rebar stakes onto the reef bottom. Within this plot, 20 benthic organisms were identified with numbered tiles as described, and video images were collected. As described, fluorescence measurements of all of the tagged benthic organisms were collected after the collection of the video. The two research groups worked well as a team and permanent sites were established and surveyed within two hours of bottom time.

The results of the field experiment resulted in a combined mosaic-FIRe product as shown in Figure A65.

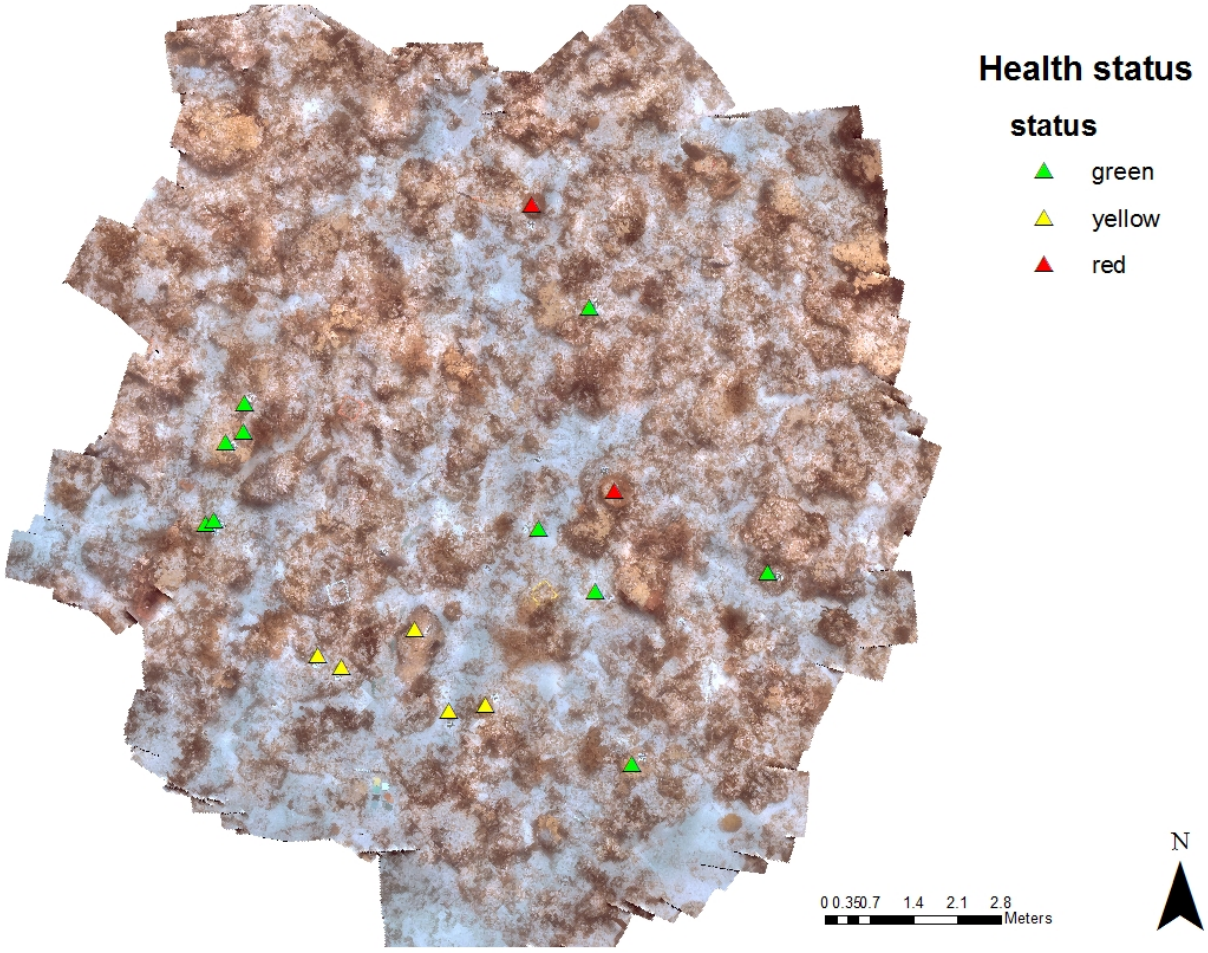


Figure A65. Combined mosaic/FIRe product. Locations of individual organisms examined with the underwater FIRe instrument are demarcated by the triangles (above). The color of the triangles indicates the relative photosynthetic stress on the organism as determined by Dr. Gorbunov (green= healthy; yellow= potential stress; red= photosynthetic stress).

Individual FIRe measurements of corals, sponges, and gorgonians were spatially mapped by matching numbers from tiles placed near the test organism at the time of mosaic acquisition to those indicated by diver notes. Measurements were evaluated by Dr. Gorbunov and given a relative health index based on the 5 measurements obtained from individual FIRe measurements (F_o, F_m, F_v/F_m, sigma, and Tau1). Health indices were separated into three groups; green, yellow and red based on their FIRe values. Green indicated limited stress on the target organism, yellow indicated possible stress, and red indicated significant stress on the target organism.

Analysis of the combined products was difficult due to the limited number of sample points at each site. Despite this limitation a vision of a future integrated product was developed as part of the collaboration (shown below in Figure A66).

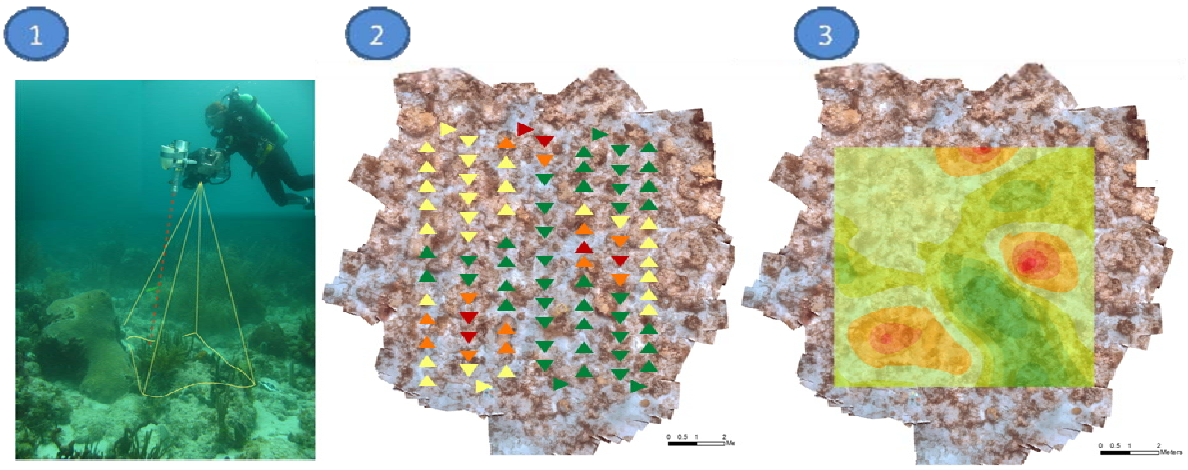


Figure A66. Future of integrated mosaic/FIRe survey technology. 1) Vision of integrated platform with second-generation mosaic system combined with new distance FIRe instrument. Both will be acquired simultaneously at a distance of 2m from the bottom. 2). Results of integrated instrumentation. High resolution mosaic products will be combined with 100's to thousands of FIRe measurements taken during a single survey. 3). Using information from the combined product we can produce dense benthic health maps to locate hot spots of stress in coral environments.

The possible combination of the two survey techniques provides a significant enhancement to current reef monitoring technology by providing three levels of reef health information: landscape level (mosaic products), colony level (integrated stills) and physiological (FIRe) from a single survey platform. Our vision of the future technology allows for a diver to swim a single platform with FIRe and video imaging hardware enabling the capture of both video mosaic and FIRe data simultaneously. This acquisition of 100's to 1000's of FIRe measurements during a single dive survey will provide much greater health information about the reef as a whole than is capable using the single colony approach (Figure A66.2). The dense FIRe measurements and the spatial reference data available from the high resolution mosaics will also allow users to create dense probability maps of reef health which could lead to the identification of local hotspots of stress along affected reefs (Figure A66.3). Over time, these maps could be used to track both visible and physiological changes in reefs at a landscape level and help determine the impacts of reef stressors in a way that is currently inaccessible to modern reef scientists.

A2.5.7 NOAA Restoration Group

In May of 2006 two species of coral, *Acropora palmata* and *Acropora cervicornis*, were listed as "threatened" on the endangered species list due to their widespread declines throughout the Caribbean. Under the Endangered Species Act (ESA), 16 USC §§1531-1544 Federal agencies must "insure that any action authorized, funded, or carried out by such agency is not likely to jeopardize the continued existence of any endangered species or threatened species or result in the destruction or adverse modification of habitat of such species." In accordance with this Federal protection, governmental stakeholders are responsible for the documentation and monitoring of these threatened species with respect to any DoD or NOAA actions. To ensure this protection, the NOAA restoration group in association with the

University of Miami/RSMAS has begun to monitor two local populations of *Acropora palmata* in the Florida Keys using landscape video technology.

The two monitoring sites in the Upper Florida Keys were chosen to represent different stages of *A. palmata* population health. Both sites were marked and surveyed in June 2009. Site one at South Carysfort Reef is a shallow site (~2m deep) that experienced significant declines over recent decades but is now showing moderate recovery (Figure A67). Colonies are sparsely distributed and smaller in overall size than Site two. Numerous small colonies are distributed throughout the site representing recent cementation and growth events.



Figure A67. South Carysfort Reef, Florida Keys. Large dead skeletons and mostly sparse small colonies distributed throughout the site characterize this population of threatened coral species *Acropora palmata*.

Site two at Horseshoe Reef is perhaps the largest grouping of live *Acropora palmata* left in the Florida Keys (Figure A68). This stand is deeper (~3m) than the Carysfort site and consists of very densely packed *Acropora palmata* colonies. Colonies at this site appear healthy with some evidence of fish predation. This stand is believed to have survived much of the catastrophic damage to their population as seen elsewhere in the Florida Keys during the last few decades. Colonies are densely packed with several layers of healthy *A. palmata* understory. The site was surveyed as two overlapping sections (both ~400m2) and will be used along with mosaics at site one to inventory, map, and follow these stands of threatened Acropora palmata through time.

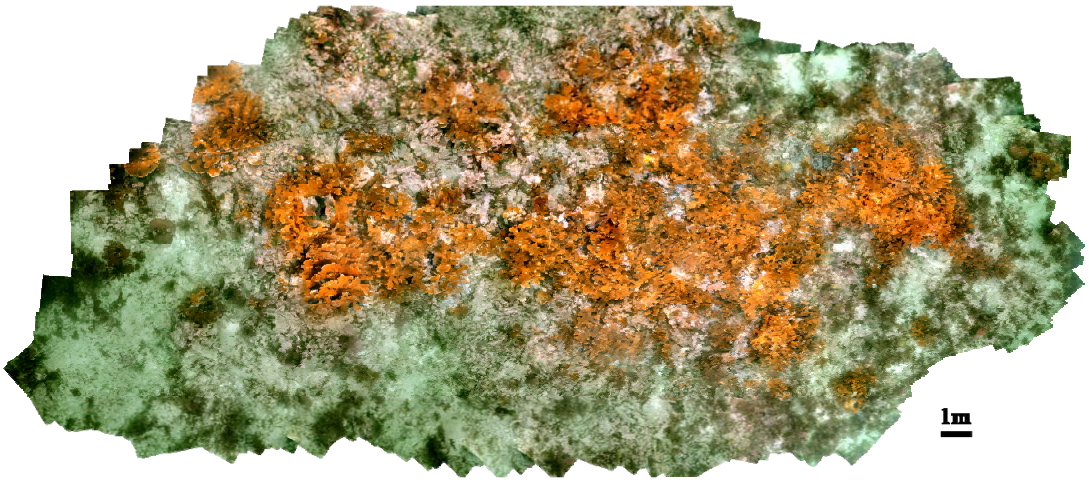


Figure A68. Horseshoe Reef, Florida Keys. This population of *Acropora palmata* is one of the largest and healthiest stands remaining in the Florida Keys National Marine Sanctuary. The image above represents 650m^2 and is only half of the entire mosaic study site.

The branching growth form and life-history characteristics of *A. palmata* pose a considerable challenge to traditional reef monitoring methods. *Acroporids* often grow in shallow, high-energy reef areas as thickets of interlaced colonies. This often limits our ability to distinguish individual colonies and makes the deployment of lines and quadrats cumbersome and damaging to the resources that can be fragmented easily. Furthermore, the main mode of reproduction of *Acroporid* species is through branch detachment and fragmentation (Lirman, 2000), which can produce very quick and dynamic changes in colony size and abundance that are not easily tracked through conventional diver-based methods.

Due to these difficulties, mapping methodologies that cover areas larger than single colonies will be beneficial for assessing the status of populations of these threatened species and their recovery through time. The use of video mosaic monitoring technology in areas of threatened *A. palmata* and *A. cervicornis* species provides a non-invasive and large area method of recording the current status of these species in a given area. Individual colonies and thickets can be monitored through time without the need for tagging of individual colonies (Gleason et al., 2007). A landscape mosaic will permanently acquire an overall detailed view/image of a given reef habitat and its benthic components including ESA-listed corals *Acropora cervicornis* and *A. palmata* and their designated critical habitat. These mosaics will yield information on the presence/absence of ESA-listed corals *A. cervicornis* and *A. palmata*, as well as accurate estimates of *A. cervicornis* and *A. palmata* cover or density per sampled area, and colony size. A succession of mosaics over time will enable the accurate monitoring of the dynamics of *A. cervicornis* and *A. palmata* at a given site.

A2.5.8 NOAA Marine Heritage

The National Oceanic and Atmospheric Administration Office of National Marine Sanctuaries (NMS) coordinates efforts to document national maritime heritage resources. Landscape mosaics may help documentation and communication efforts for many of the underwater archaeological sites they survey.

Trained underwater archaeologists have intensively surveyed only a relative handful of high-priority sites, such as the USS Monitor. For such high-priority sites, landscape mosaics can complement traditional methods of underwater archaeology by helping document large-scale changes to the site over time and facilitate effective communication, for example in educational displays or web sites describing the site. NOAA NMS does not have the resources to conduct intensive excavations or create base maps for the vast majority of underwater heritage sites, however. For these numerous lower-priority sites, at which imagery is likely to be the only source of data, landscape mosaics can provide crucial documentation of the artifacts and site condition.

We conducted a pilot effort to evaluate whether the landscape mosaic software could contribute to the NMS mosaic efforts. The schooner *Kyle Spangler* was chosen as a test site because NMS archaeologists had previously created both a detailed archaeological base map and a hand-made landscape mosaic (http://thunderbay.noaa.gov/shipwrecks/spangler.html). The resulting mosaic produced from our software (Figure A69.A) resembles the hand-made mosaic made by NMS archaeologists (Figure A69.B). The two primary differences between the mosaics were, first, that the main (aft) mast has been cropped out of the automated mosaic, and, second, that the scale is not constant in the automated mosaic. Differences in data acquisition between the method normally employed by the RSMAS team for coral reef surveys and the method used for the Spangler survey explain the differences in the resulting mosaics.

The cropped mast is due to an extreme violation of one of the assumptions used in the automated mosaic algorithm, namely that the maximum relief in the scene is small relative to the altitude of the camera above the seabed. Although there is no hard-and-fast rule about what constitutes “small” relief, the normal rule of thumb used by the RSMAS team when acquiring imagery for coral reef surveys is to place the camera about 1.5 to 2 times as high as the highest relief object in the scene. For example, if there were a 1 m high coral head in the area surveyed we would normally acquire data 1.5 to 2 m above the bottom. The Spangler images containing the masts obviously violate this “small relief” assumption as the camera was actually *below* the tops of the masts. Fortunately, most of the images in the dataset did not have such extreme relief. The blending scheme used by the automated mosaic method has cropped out the mast because it was designed to reduce the deleterious effects of parallax on the presentation of the final mosaic. The reason that it removed only the main mast and not the forward mast is probably due to the number of images available. Near the ends of the ship there were probably fewer potential images that could have been placed in the mosaic, so cutting out the forward mast might have left a hole in the mosaic.

The scale variation in the automated mosaic, visible as the front portion of the ship appearing wider than the rear, was caused by a different approach to data acquisition. The automated algorithm relies on substantial overlap in both along-track and across-track directions and performs best when “tie-lines” (i.e. multiple passes over the same portion of the scene) are available. NMS acquired the data, however, as just a single pass down one side of the vessel and a second pass up the other side. This approach minimizes time in the water and gave sufficient images for a manual match, but was sub-optimal for the automated algorithm. The automated

mosaic of the Spangler was created from only 24 frames, whereas the coral reef mosaics typically use between 800 - 5000 frames to ensure sufficient overlap.

The experience with the Spangler mosaic suggests that automated landscape mosaics have the potential to assist NMS marine heritage resource inventory personnel. Results indicate two avenues to pursue to improve future results. First, we should coordinate with the divers acquiring data to make some small adjustments to the survey methodology to increase overlap and add tie-lines. Second, modifications to the algorithm might be possible to detect and *retain* areas of high parallax, as opposed to the current method of detecting and *discarding* areas of high parallax. Modifying the algorithm in this way would require additional research effort and would probably degrade results over reefs, which could be overcome by reverting to the current version of the algorithm for reef work and using the modified version only when necessary.

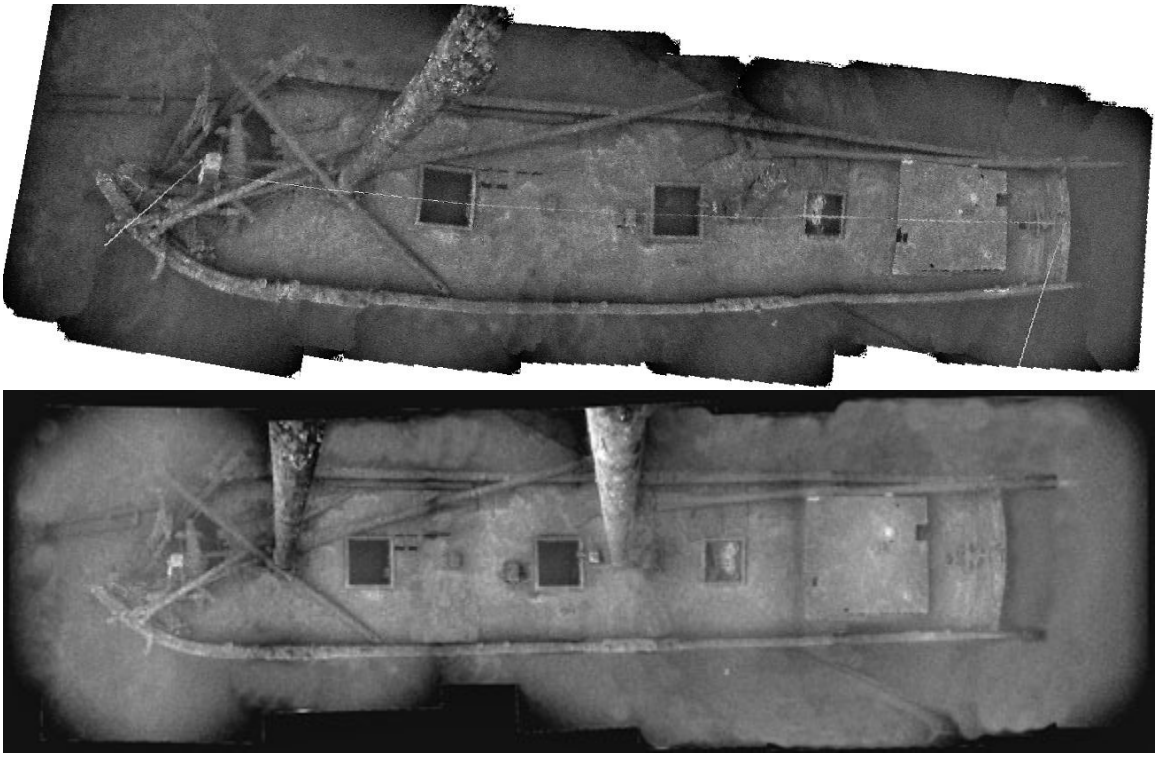


Figure A69. Landscape mosaics of the Kyle Spangler. Mosaic created using the automated procedures developed in this project (Top). Mosaic created by NMS by hand-matching each image (Bottom).

A2.5.9 Florida Fish and Wildlife Conservation Commission

The Coral Reef Evaluation and Monitoring Project (CREMP, funded by EPA, NOAA, and the State of Florida) is an annual survey of over 40 permanent monitoring sites throughout the Florida Reef Tract. As part of their coral survey methodology, their team uses underwater video transects that are subsequently subsampled by extracting individual video frames. These video frames are analyzed using point-count methods to determine percent cover of corals. This monitoring program

represents one of the longest running programs in the Florida Keys and was one of the original programs to implement video-based reef monitoring into their survey methodologies.

In November 2009, a pilot collaboration effort was conducted between the University of Miami and CREMP to co-survey two sites (consisting of two stations each) using CREMP standard methods as well as UM's Video Mosaic method. Both data sets, collected at the same time, will be analyzed and the metrics of coral condition obtained will be compared between programs to determine whether video mosaics can: 1) provide comparable estimates of coral cover, and 2) expand the number of indicators of coral condition that can be extracted from each site using video-based survey methodologies. In addition the collaboration hopes to utilize historical video data to create a 10+ year comparison of video mosaic sites in the Florida Keys.

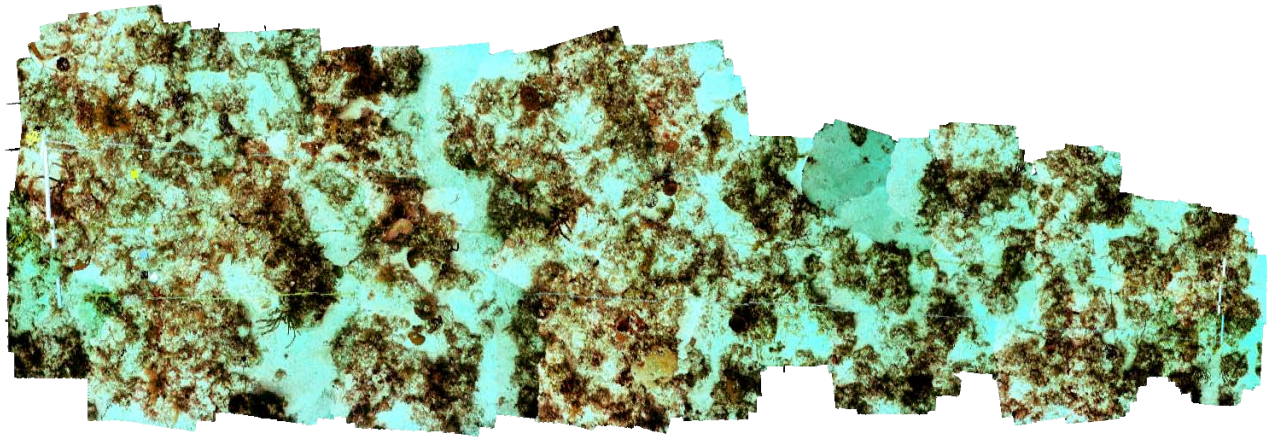


Figure A70. Video mosaic of 2mx20mtransect at Sombrero Reef, Florida Keys.

A2.5.10 Potential Department of Defense Collaborations/Users

The following report was compiled by Lorri Schwartz and colleagues, NAVFACHQ.

DEPARTMENT OF DEFENSE NEEDS FOR MAPPING, INVENTORY, AND ASSESSMENT OF BENTHIC MARINE COMMUNITIES

The Department of Defense (DoD) needs to inventory, identify, document and assess benthic reef communities and other benthic habitats in order to have baseline information to comply with regulations and resource management requirements in proximity to installations and operational areas. DoD utilizes tools such as Habitat Equivalency Analysis for performing analysis of potential impacts for construction activities. Additionally, DoD needs to conduct monitoring of

benthic habitats in order to fulfill NEPA or permit mitigation, Trustee obligations or other conservation commitments. The benthic reef community includes corals, algae, and other sessile and mobile invertebrates and associated substrates.

Technologies fulfilling these needs will provide operators and natural resources personnel with comprehensive knowledge of benthic habitats and coral reef communities under DoD purview. This information is necessary for operational and environmental planning and provides decision-makers with crucial information needed to maintain compliance with statutes, regulations, and executive orders directly related to operations conducted in benthic areas, including:

- Clean Water Act (33 USC §1251 et seq.)
- Coastal Zone Management Act of 1972(16 USC §§1451-1465)
- Comprehensive Environmental Response, Compensation, and Liability Act (42 USC Chapter 103)
- Coral Reef Conservation Act of 2000 (16 USC §6401 *et seq*.)
- Magnuson-Stevens Fisheries Conservation and Management Act (16 USC §§1801-1882)
- Marine Protection, Research and Sanctuaries Act (16 USC §§1431-1445a)
- National Environmental Policy Act as amended (42 USC §§4321-4347)
- Oil Pollution Act of 1990, 33 USC §2701
- Rivers and Harbors Act (33 USC §403)
- Sikes Act Improvement Act of 1997 (16 USC §670a-o)
- Executive Order 13089, Coral Reef Protection
- Executive Order 12114, Environmental Effect Abroad
- Executive Order 12777, Oil Pollution Act Implementation
- Executive Order 13158, Marine Protected Areas

Obtaining baseline data is an important element not only for Federal coastal management of protected resources but to provide a foundation for environmental documentation necessary to conduct operations. Such documentation requires the assessment of environmental conditions prior to any incidents possibly resulting in damage to or loss of habitat. Successful and legally defensibly documentation requires the assessment of environmental conditions prior to conducting operations and implementation of mitigation measures. Assessment information is also necessary in resolving Federal trustee matters related to damage assessments. Legally defensible data is necessary to communicate and negotiate all regulatory actions in the marine environment.

- Efficient assessment of benthic habitats to support routine activity planning
    - Reduced time and expense for data collection
    - Reasonable operator experience and dive time requirements
    - Experts spend more time in lab analyzing data than in field collecting data
    - Applicable in a wide range of locations (see military facility table below)
    - Support day or night data collection as required
- Data quality to support compliance requirements
    - Quantitatively and qualitatively characterize the diversity, abundance, temporal variation and spatial distribution of corals, algae and other invertebrates
    - Support Habitat Equivalency Analysis tool and NEPA analyses, as well as permit and mitigation compliance

- Provide a common monitoring protocol for the benthic community was formulated with regards to location and frequency of surveys
- Robust, reliable and legally defensible
- Locate survey start and end points located using Global Position System (GPS) sensors
- Provide data/image archival capability and data compatibility with existing software including military GIS applications (EIMS and PMAP)

- Facilitate interoperability between DoD components and cooperation with other Federal and State agencies for compliance and stewardship efforts.
  - Mutual benefit to use same tools
  - Cost savings to share the same data for regulatory needs.
  - Low cost, high benefit, ease of deployment will allow expanded benthic habitat assessment and monitoring
  - Potential to leverage research needs

Table A13. Military Facilities with Adjacent Coral Reef Resources

Branch	Facility Name	Location
Air Force	Anderson Air Force Base	Guam
Air Force	Cape Canaveral Air Force Station	Florida
Air Force	Eglin Gulf Test and Training Range (EGTTR)	Florida
Air Force	Hickam Air Force Base	Hawaii
Air Force	Tyndall AFB	Florida
Air Force	Bellows Air Force Station	Hawaii
Air Force	Patrick Air Force Base	Florida
Air Force	Wake Atoll (Wake Island)	US Territory
Air Force/ Navy	Eglin AFB	Florida
Army	Fort Buchanan	Puerto Rico
Army	Fort Shafter	Hawaii
Army	Johnston Atoll Chemical Agent Disposal System Facility (JACAD)	US Territory
Army	Kwajelein Atoll, Reagan Test Site, Marshall Islands	US Territory
Army	Pohakuloa Training Area	Hawaii
Army	Schofield Barracks	Hawaii
Army	Tripler Army Medical Center	Hawaii
Marine Corps	Marine Corps Base Hawaii	Hawaii
Marine Corps	Marine Corps Base Hawaii Ranges	Hawaii
Navy	Andros Island, AUTEC	Bahamas
Navy	Awase Transmitter Site, Okinawa	Japan
Navy	Barbers Point Family Housing and Support	Hawaii
Navy	Diego Garcia Navy Support Facility	BIOT
Navy	Diego Garcia Range Complex	BIOT

Branch	Facility Name	Location
Navy	Farallon De Madinilla (FDR)	CNMI
Navy	Ford Island Naval Station Annex	Hawaii
Navy	Guam Naval Activities	Guam
Navy	Guantanamo Bay Naval Station	Cuba
Navy	Guantanamo Complex	Cuba
Navy	Gulf of Mexico Training Area	Florida
Navy	Hawaiian Range Complex	Hawaii
Navy	Japan Range Complex	Japan
Navy	Key West Range Complex	Hawaii
Navy	Key West Naval Air Station	Florida
Navy	Marianas Range Complex	CNMI
Navy	NAMFI Complex	Mediterranean
Navy	NASD, EMA & AFWTF	Puerto Rico
Navy	Naval Supply Center Red Hill	Hawaii
Navy	Okinawa Naval Activities	Japan
Navy	Okinawa Complex	Japan
Navy	Pachino Complex	Mediterranean
Navy	Pacific Missile Range Facility (PMRF) Barking Sands, Kauai	Hawaii
Navy	Panama City Coastal Systems Center	Florida
Navy	Pearl Harbor Naval Station	Hawaii
Navy	Pensacola, Naval Air Station	Florida
Navy	Tinian Island, Military Leased Areas	CNMI
Navy	White Beach Naval Facility, Okinawa	Japan

A2.5.11 Landscape Mosaics website

In 2008 a website detailing information on underwater landscape mosaics was constructed and put on-line for users to have free access to basic information on mosaic creation, current coral monitoring projects using this technology, and contact information for any interested parties. The website is continually being updated to include more information and better imagery as they become available. Lists of our publications and PDF's of many of our posters are also available here. The web address is:
www.rsmas.miami.edu/groups/reidlab



Figure A71. Screen-capture of landscape mosaic website homepage www.rsmas.miami.edu/groups/reidlab**.**

A2.6 Software deliverables

A2.6.1 Landscape (2D) Mosaic Software

A significant portion of our efforts in the final two years of the project focused on the development of user-friendly software for use by external users for the creation of 2D video mosaics. As such, a set of 2D mosaicing programs has been written to run under the commercially available Matlab computation platform. Additionally a detailed user manual was produced to cover the use of all 2D mosaic creation programs and is provided in Appendix 3. A brief introduction to these programs is given below.

The Mosaic Creation program allows a user to create a 2D video mosaic from an "AVI" media file. The program and interface consists of six main modules: 1) Frame Extraction, 2) Sun Flicker Correction, 3) Global Matching, 4) Video and Still Registration, 5) Global Match

Inspection and 6) Mosaic Rendering. When the Mosaic Creation toolbox is executed, a toolbox menu will appear showing the main steps of mosaic creation as the user's options (Figure A72).

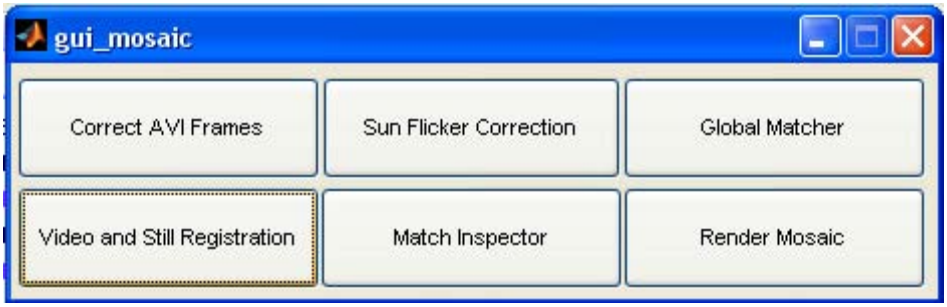


Figure A72. Main Mosiacing Program GUI

A2.6.1.1 Frame Extraction

As a first step, users extract individual video frames from an input "AVI" media file, compensate for camera lens distortion and remove interlaced scan lines. This is accomplished by clicking on the "Correct AVI Frames" option in the toolbox menu (shown above). This then opens a new "Frame Extractor" interface (Figure A73).

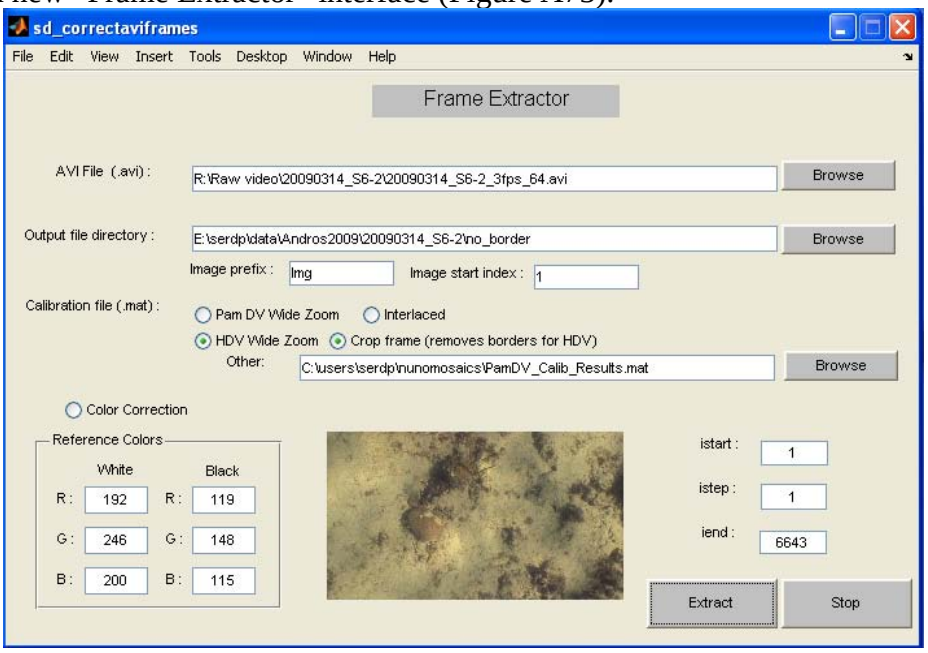


Figure A73. A screen capture of the video frame extraction GUI.

The user can correct the color balancing and enhance the contrast, by providing black and white references. The output is a set of undistorted individual video frames that are the basis for the next steps in the mosaic creation process.

A2.6.1.2 Sunflickering Removal

The second module is targeted at removing sunflickering and is optional. The processing is done in two steps: (1) Sequential matching and (2) sunflicker filtering. The first step of sequential matching finds the registration parameters among time-consecutive images. In this step, normalized cross correlation is used as a similarity measure between images, since it outperforms the Scale Invariant Feature Transform (SIFT) method for images heavily affected by refracted sunlight. The SIFT method is used in our mosaicing software for matching images under normal illumination conditions. The second step of sunflicker filtering step uses the registration parameters to estimate and remove the instantaneous illumination field caused by the sunlight.

The user interface is shown in Figure A74. The separation of the processing in two steps allows, if needed, for re-running filtering step with different parameters without having to re-run the matching, which is the most time consuming part of the method.

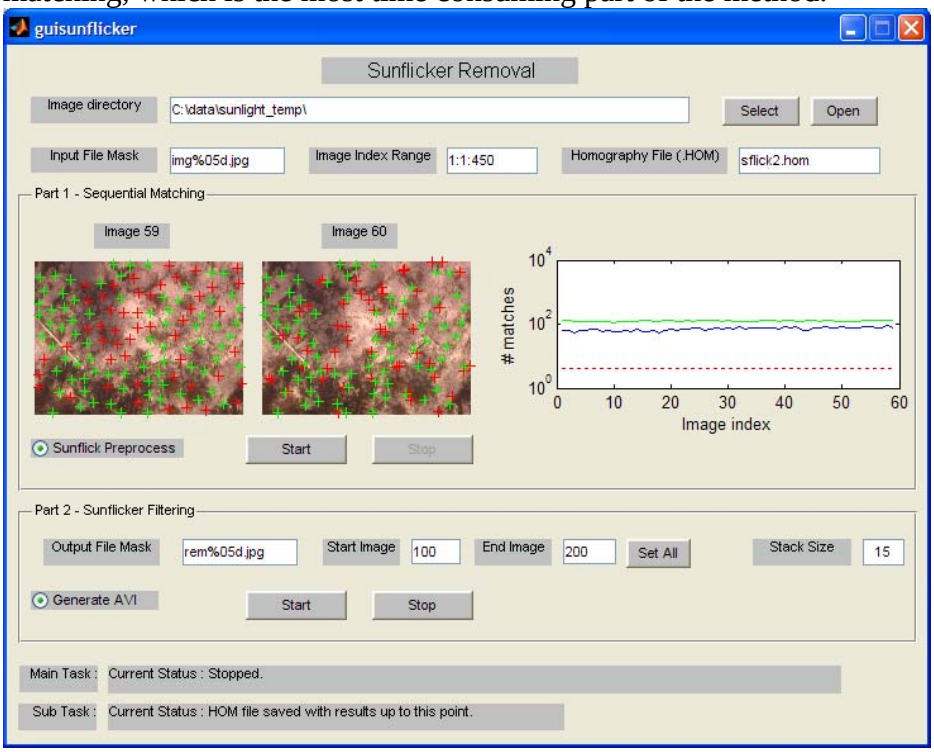


Figure A74. Graphic user interface for the sunflicker removal module.

A2.6.1.3 Global Matching

The third module, called Global Matcher performs three main tasks:

- Image selection: computes image features, performs sequential matching and removes frames that are found to have very large overlap
- Global matching: computes the fast similarity measure among all images and performs matching for all pairs of high similarity

- Global optimization: finds the best displacement for all images, using the result of the global matching.

The Global Matcher interface (Figure A75) allows for setting all the relevant mosaicing parameters, such as the range of image to be matched, and the thresholds for image selection and matching. These thresholds can be adjusted to improve the matching performance for particularly difficult image sets (for example containing strong topography). Upon finishing, data files are created with all the information needed to blend the mosaic.

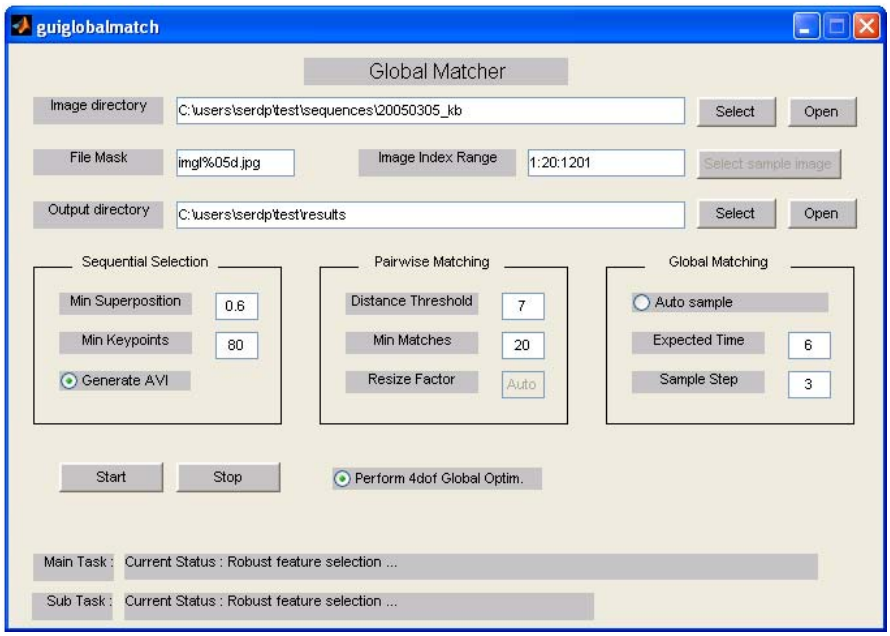


Figure A75. The global matching interface.

A2.6.1.4 Video and Still Registration

The forth module allows for registering high definition stills against the video frames that were used in a run of the Global Matching module, using the user interface shown in Figure A76.

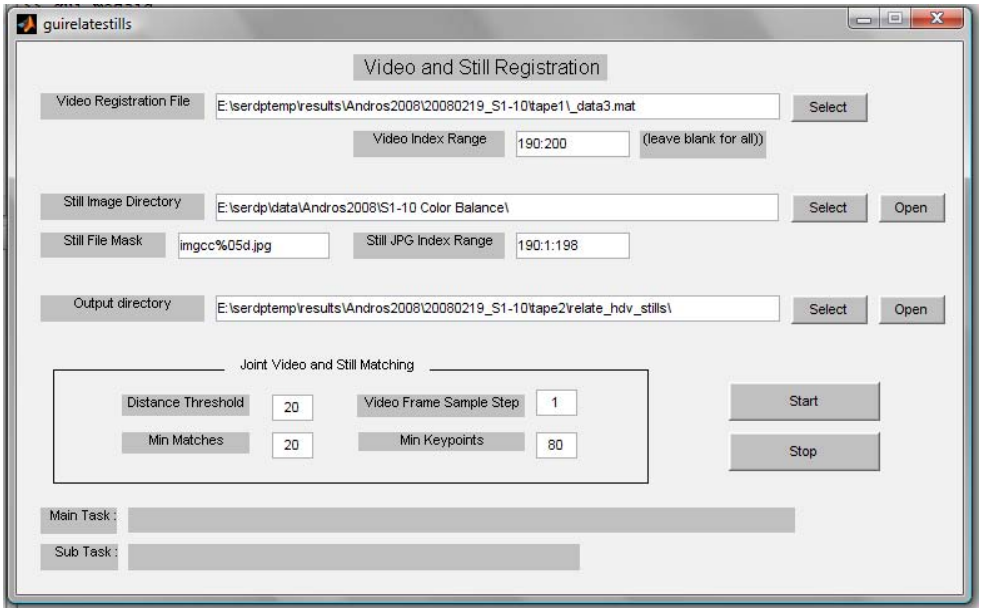


Figure A76. The video frame and still image registration interface.

A2.6.1.5 Global Match Inspection

The fifth module is the Global Match Inspector (Figure A77). This optional module allows the user to inspect the results of the global matching. More specifically, the user will be able to view individual pairs of matched images (with the corresponding feature points overlaid), manually add or clear global matches to correct optimization, as well as create new optimization files for the rendering process.

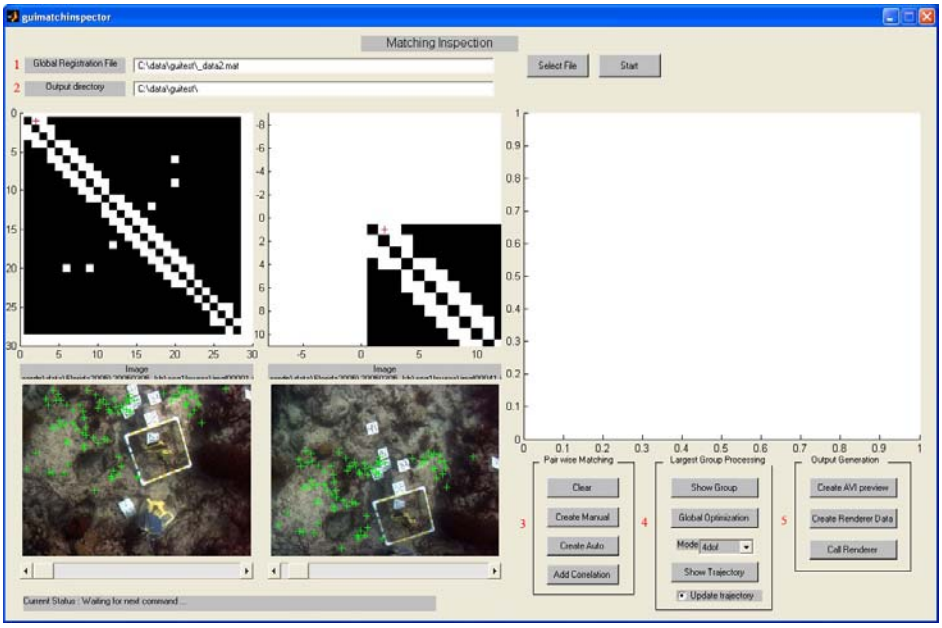


Figure A77. The match inspector GUI.

A2.6.1.6 Mosaic Rendering with Improved Blending

The sixth module is the Mosaic Rendering (Figure A78). It renders a complete mosaic using the results of the global matching and optimization.

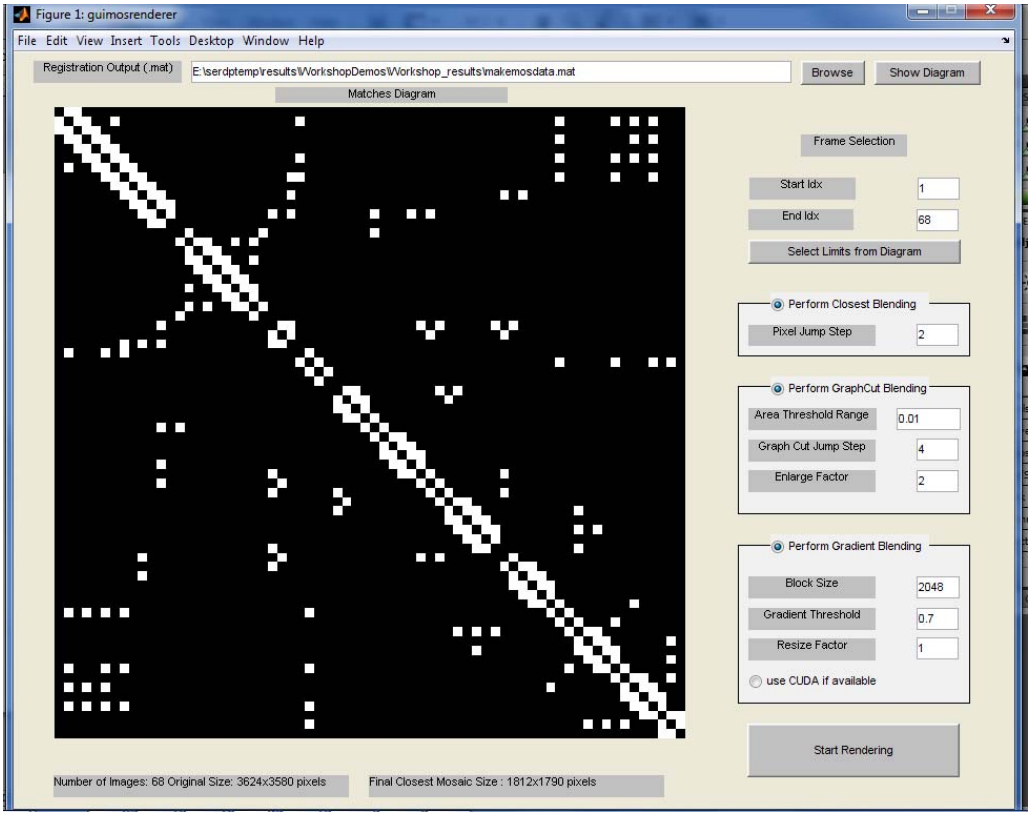


Figure A78. Mosaic Rendering GUI.

The user may select an image subset to render by clicking on a section of the global matching table. This table is useful to check the parts of the sequence that contain loops, which typically correspond to the intended survey area. The user may also perform a variety of image blending techniques: Closest, Graph-Cut and/or Gradient Blending. The final outcome is a “PNG” format picture file created at a desired resolution.

A2.6.1.7 Heading Integration Module

The heading integration module is intended to be used with the hardware developed for the second-generation mosaics. This module processes the audio file that contains the raw heading information (recorded in the video camera audio channel) and converts the information into heading angles (GUI shown in Figure A79).

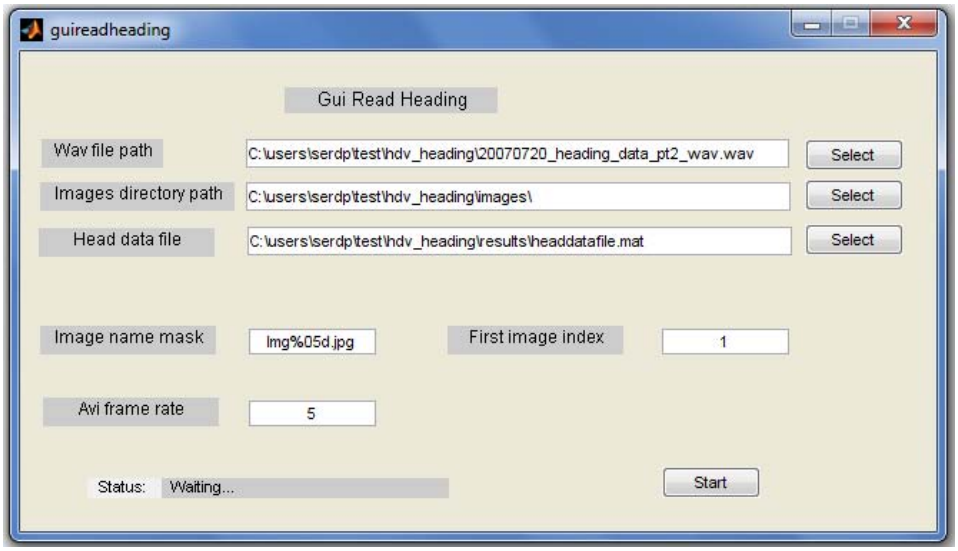


Figure A79: Heading integration module.

A2.6.1.8 Additional Features

A few extra features have been added to complement the mosaic creation deliverable and allow some ecological analysis of the final mosaic. The first is the "Point and Click" feature, allowing the user to select a desired point/area on the mosaic and view the corresponding full resolution video frames. Calling the "point_click" function in the Matlab command line will display the following interface (Figure A80).

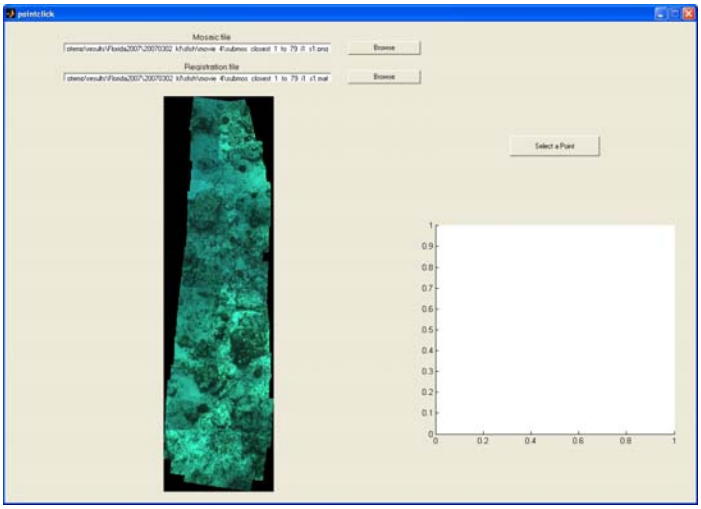


Figure A80: Basic point click GUI.

With the pathname of the mosaic and the corresponding registration file, the user would simply click the "Select a Point" button and select a point/area in the mosaic of interest. The closest

frame to the desired area will be displayed next to the mosaic as well as a feature box showing the frame's place in the mosaic, as seen below. This provides users with an un-manipulated view of the area or point of interest. Often this provides a clearer image than the 2D mosaic and can provide additional health information (Figure A81).

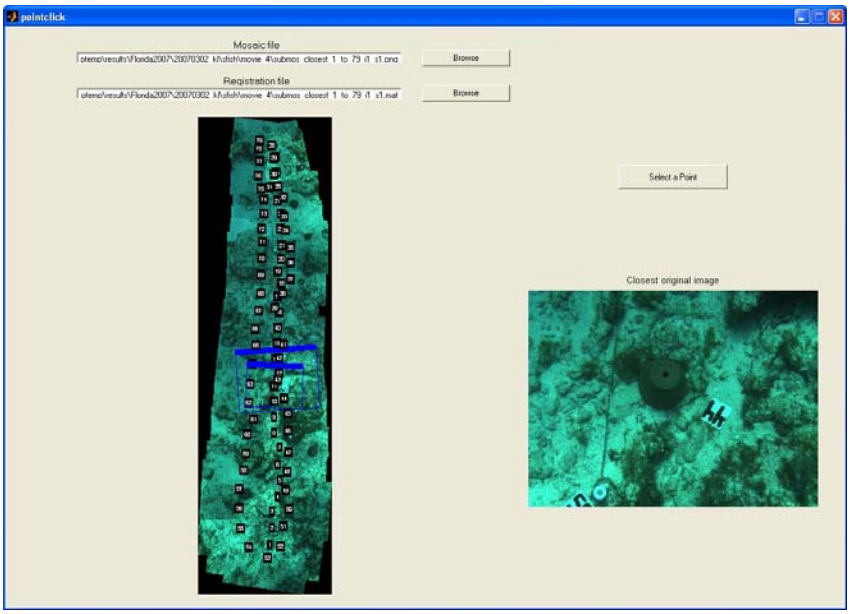


Figure A81. Basic Point Click GUI showing a selected video frame.

The second ecological analysis feature is the "Mosaic Info" function. Calling "mosaic_info" in the Matlab command line will call the following interface to the user (Figure A82)

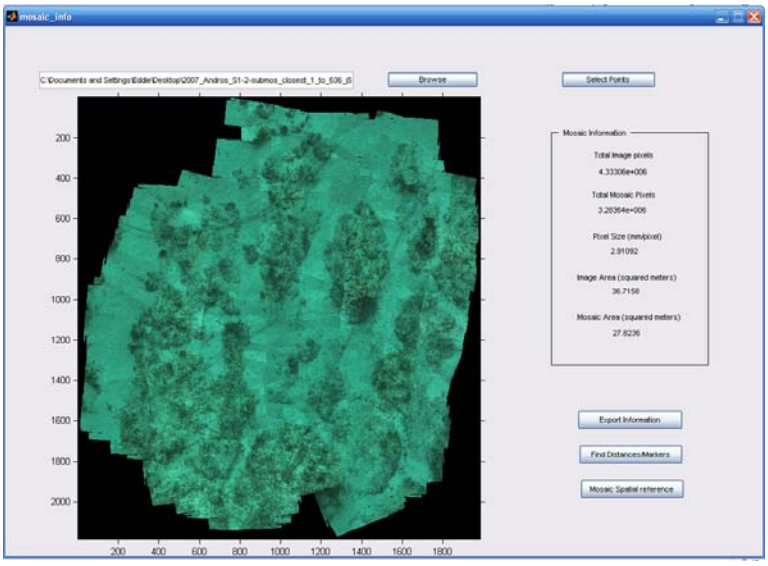


Figure A82. Mosaic Info GUI.

A total description of the mosaic is displayed to the right, including information of the size of the mosaic (in Pixels) and the area covered during the mosaic survey (in meters). The user can determine the distance (in meters) between two points within the mosaic by clicking the "Find Distance/Marker" button. This has been used to assess the size of coral colonies within a video mosaic as well as spatial patterns of coral distributions. After selecting desired points of interest in the area, the user is given the option to save a copy of the mosaic with the points marked on it for reference, as well as an excel/csv output file that contains the distances of the markers to each boundary corner (Figure A83).

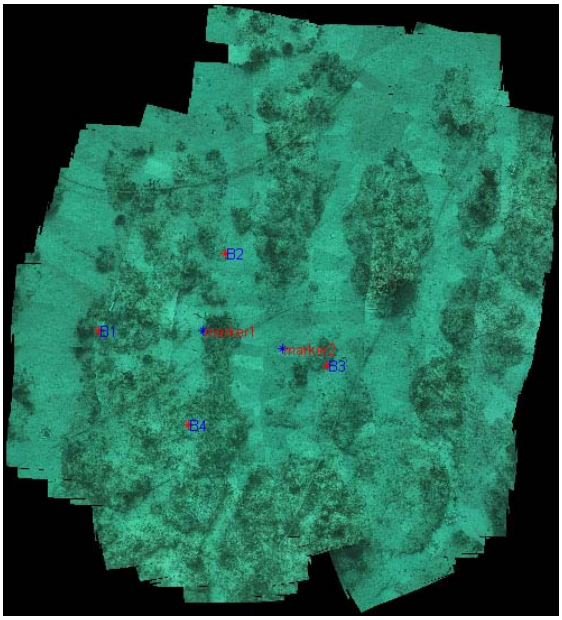


Figure A83. A mosaic with distance markers created by the mosaic_info GUI.

For further information on the Mosaic Creation steps and processes, please see Appendix 3, "Mosaic Creation Manual".

A2.6.2 Ecological Analysis Module

An objective of the landscape mosaicing system is to provide end users with improved monitoring products that provide important information on reef health. One index of reef health commonly used by monitoring and scientific purposes is that of percent cover. When using benthic imagery to extract this index, users typically upload images to point count software (e.g. CPCe, Kohler and Gill, 2006) that displays a number of random points within the image that are then assessed for benthic composition. Landscape mosaics have been used with pre-existing software (namely CPCe) to extract indices of percent cover directly from mosaics or from portions of mosaic images. However, due to the limited resolution of first-generation mosaic products percent cover indices were often limited to major benthic categories such as sand,

macroalgae, coral, soft coral and zoanthids. Thus information on species-level cover or different macroalgal groups was not available using first-generation products.

The creation of the second-generation of landscape mosaics provides a product with thousands of incorporated still images. These high resolution still images provide sub-millimeter resolution for end-users, species level identification capabilities for most corals, and genera level for most macroalgae. Because these improvements in resolution are substantial, it is important to be able to utilize the information within the georeferenced images in point counting analyses. Up until this point the only way to use the georeferenced still images within common point count analysis software was to identify the area in which analysis is needed and using Matlab attempt to click on the area where the point was for identification purposes. To make this process easier, and to better incorporate second-generation mosaic products with existing image analysis software, we have created an automated extraction program that uses CPCe point count information to not only identify benthic points within a mosaic image but also within the closest corresponding still image.

CPCe Points Extraction module

The Coral Point Count program is a Windows-based program that provides a tool for the determination of coral cover using transect photographs (in this case a rendered mosaic). *Note: CPCe program developed by Kevin E. Kohler (http://www.nova.edu/ocean/cpce/)*

To use the CPCe points extraction module the user will first open a mosaic in the CPCe program, select an area of interest and establish the number of random points that will be created (Figure A84). Each point is given a unique name (usually letters A, B, C etc) that is used to identify the substrate under each set of crosshairs.

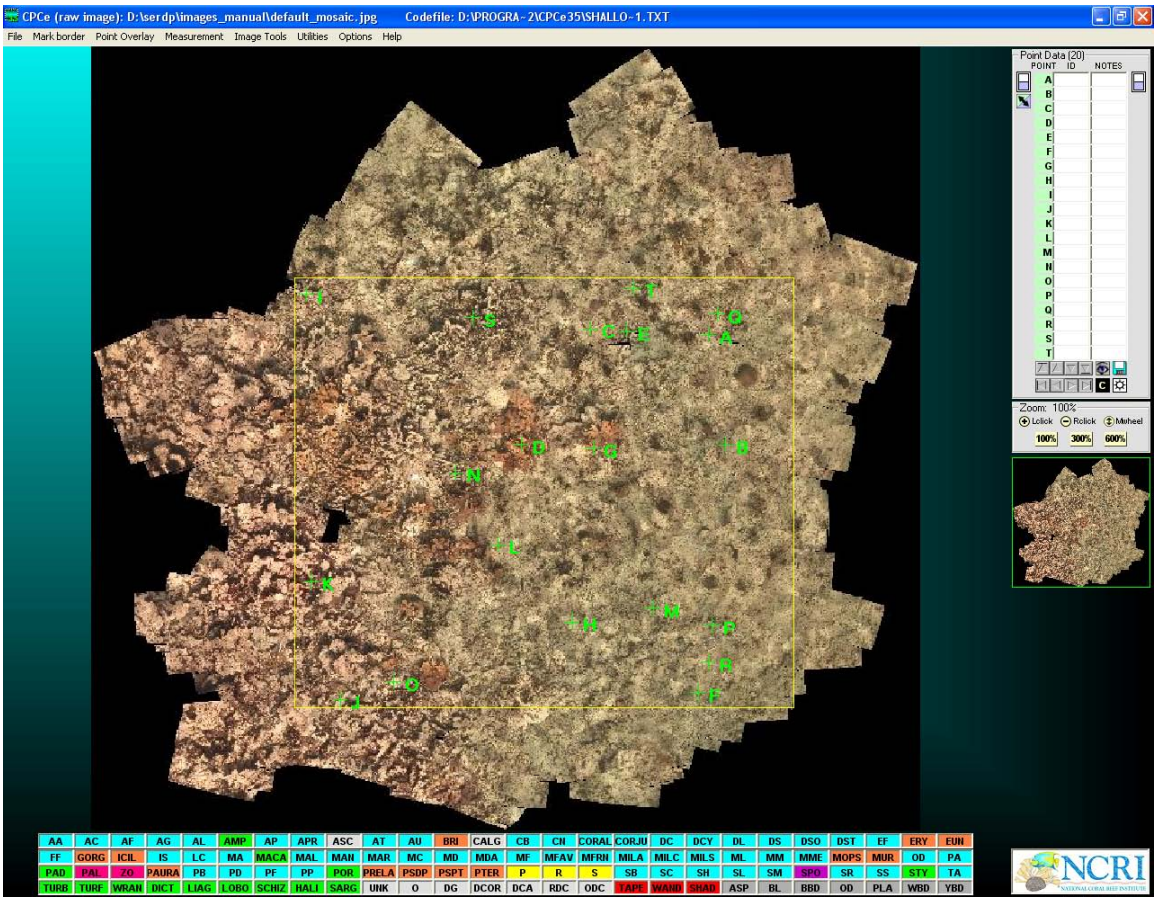


Figure A84. Screen-capture of a mosaic image being used with CPCe point count program. The user has selected an area of interest (yellow box) and 20 random points within the image (points shown in green). The user can then save a .cpc file with the locations of each point within the image that is then used to extract the corresponding still images.

Once the points have been established on the mosaic file, the user will save the set of points as a *.cpc file. This creates a location file for each of the points created by the program.

After the CPC file has been created for the desired mosaic, users can click the 'Extract Frames from CPC file' button on the "Point and Click Video and Stills" GUI. Matlab will prompt the user to find and select the appropriate *.cpc file and choose an output folder in which the extracted images will be saved to. This feature will proceed to read all the random points from the selected .cpc file and extract the closest video/still frame for each point. The exact location of the random point will be computed for the still frame and a cross-hair corresponding to the random point will be placed on the designated still image (Figure A85). All still images needed for this analysis will be extracted to their own folder and renamed with the name of the random point designated by CPCe. These images can then be analyzed in CPCe or any other image viewer. The result of this process is the ability to incorporate second-generation mosaic products into commonly used image analysis software without extensive user intervention.

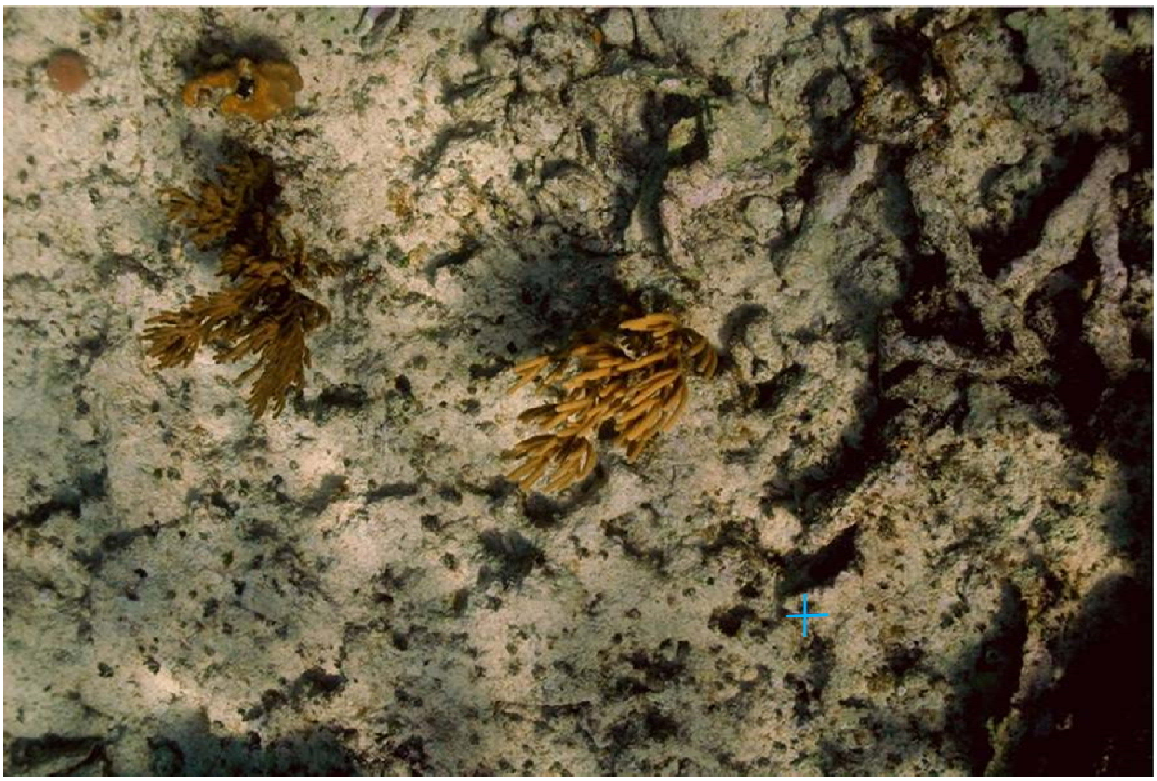


Figure A85. Extracted still image of point I. The location of the random point is computed on the extracted frame and displayed with the blue crosshairs shown in the bottom right of the image. Images can be analyzed using CPCe or any other image viewing program.

A2.6.3 External viewer

The external viewer allows the user to view a specific area in a mosaic and retrieve the closest original frame and high-resolution stills. This viewer runs outside of the Matlab environment, and can be easily distributed as a standalone windows applications.

The input required by the external viewer is generated using a simple interface shown below.

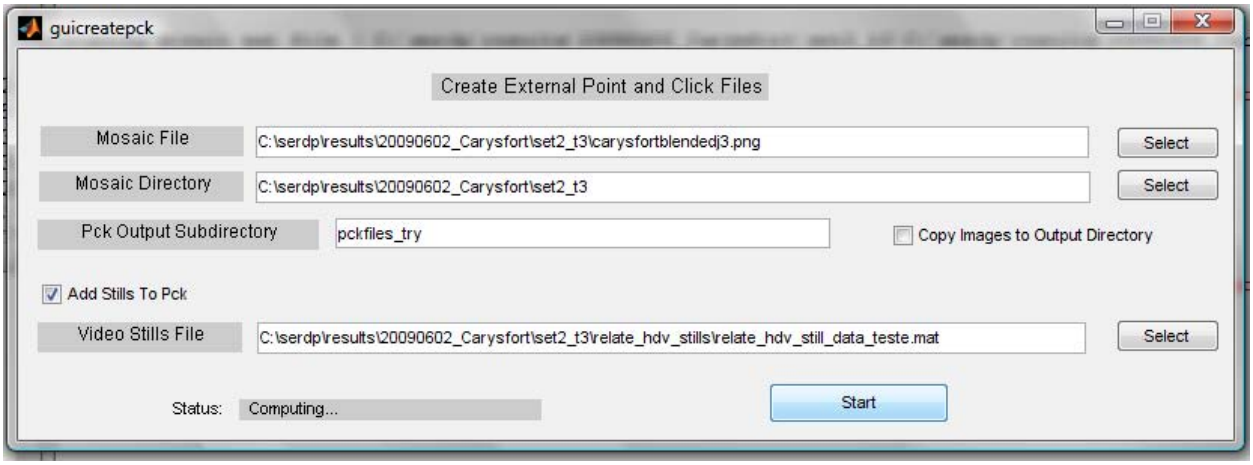


Figure A86. Screenshot of GUI that creates the file used for the external point and click viewer.

When open, the external mosaic viewer allows the user to click on the mosaic to retrieve individual video frame and high resolution still.

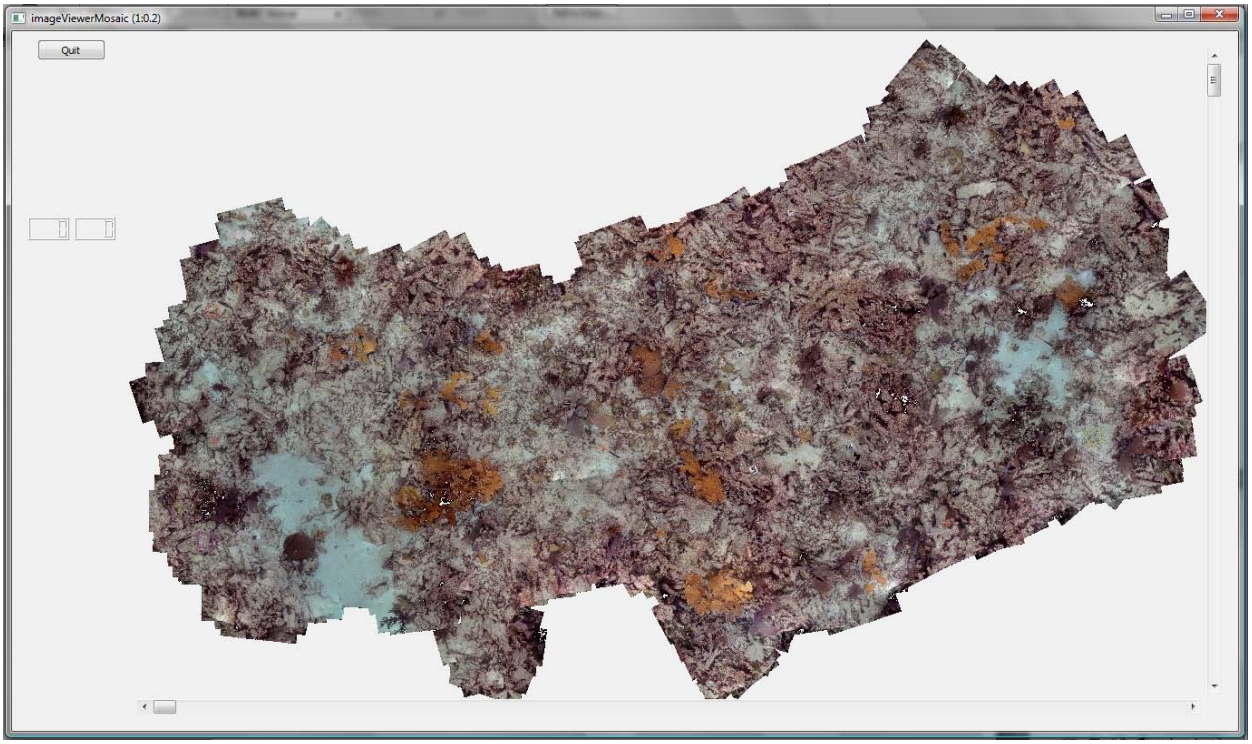


Figure A87. External point click viewer interface.

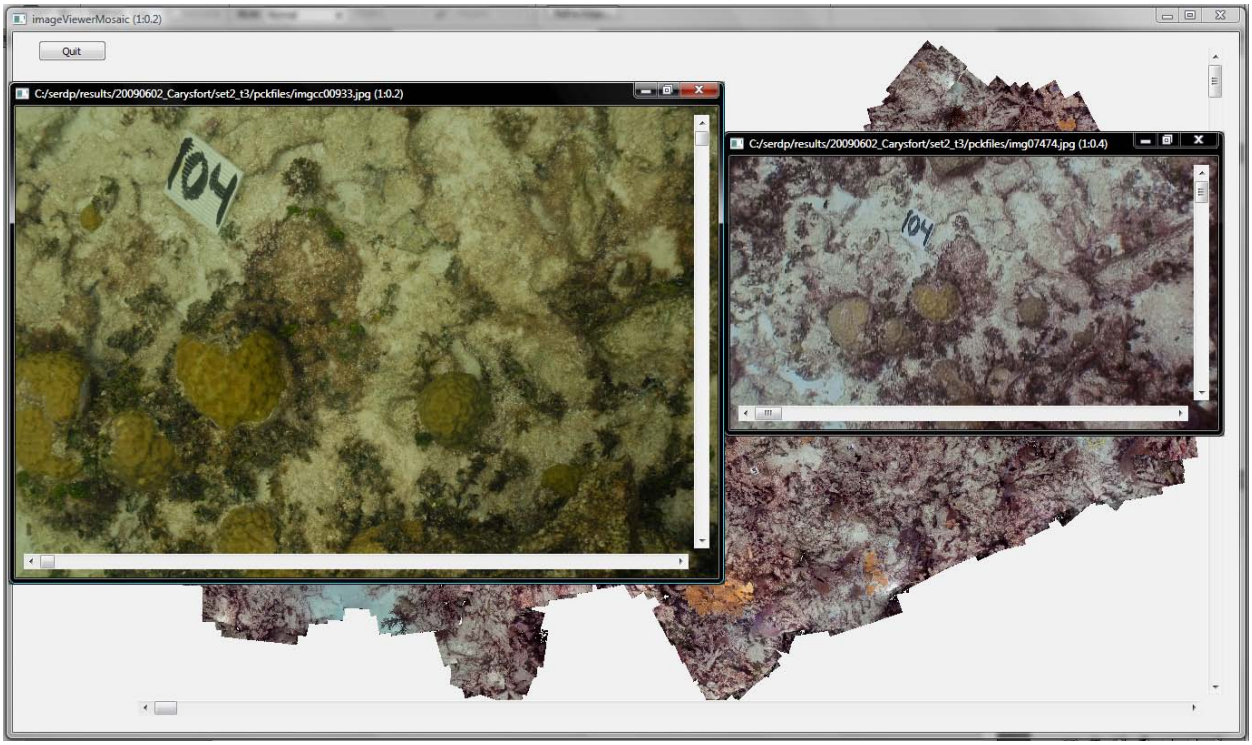


Figure A88. Result of clicking on mosaic on interface. The two screens brought up are the still image (on the left) and the video frame (on the right).

A3. Conclusions and Implications for Future Research/Implementation:

SERDP project SI 1333 has developed and assessed the use of a novel technology-underwater, landscape (2D) image mosaics- for use in coral reef mapping and monitoring. A major goal in this project was to determine whether landscape mosaics address critical limitations of traditional, diver-based assessment (considered to be the 'gold standard' in reef monitoring), while simultaneously retaining the strengths of the diver-based approach (Table A14). Our overall assessment is that mosaic technology accomplishes this role, thereby advancing state-of-the-art capabilities for reef mapping and monitoring in a variety of important ways.

Landscape mosaics are automatically created from numerous, overlapping, nadir-view, underwater images acquired within a few meters of the seabed. The algorithms used to create the mosaics evolved over the duration of the project (Section A2.1). Initial mosaicing capability used algorithms developed by Neghadaripour and Gracias prior to the start of the project to stitch together frames grabbed from a video camera. Refinements and enhancements to the Gracias algorithm as part of SI 1333 during 2003-2007 created what we refer to as our 'first-generation' mosaicing algorithm. The first-generation algorithm improved mosaicing capability to the point where the hardware used for data acquisition became the limiting factor for mosaic quality. During 2007-2009, improvements were made to address these limitations and create 'second generation' mosaics. These improvements involved integration of a high resolution still camera and a heading sensor with the video acquisition system. The integration provided increased

spatial resolution and improved performance in areas with high topographic relief. In addition, the mosaicing algorithm was upgraded to accommodate the additional data. Underwater landscape mosaics created using our 'second generation' system cover areas of up to 400 m^2 with sub-millimeter pixel resolution.

Technology		Historical "Gold Standard"	Technology Commonly Employed Today		2-D Landscape Mosaic Technology		
Technique		Diver Transect	Photo-quadrat	1-D "Strip" Mosaic	Initial Capability	First-Generation Mosaics	Second-Generation Mosaics
Platform		Scientific Diver	Diver or unmanned vehicle	Diver or unmanned vehicle	Diver or unmanned vehicle	Diver or unmanned vehicle	Diver or unmanned vehicle
Strengths of the Diver-transect (aim to retain using technological approaches)							
Analysis of Benthic Indicators	Percent cover of main benthic organisms	Excellent: Species level	Excellent: Genus to Species level	Excellent: Genus to Species level	Poor	Adequate: Major cover types	Excellent: Genus to Species level
	Diversity indices	Excellent: Species level	Excellent: Genus to Species level	Excellent: Genus to Species level	Poor	Adequate: Major cover types	Excellent: Genus to Species level
	Juvenile coral density	Excellent: Can ID recruits	Adequate: > 5 cm	Adequate: > 10 cm	Poor	Adequate: > 10 cm	Adequate: > 5 cm
	Disease / Bleaching / Parital Mortality	Excellent	Adequate	Adequate	Poor	Adequate: Major cover type	Excellent: Genus to Species level
	Coral Colony Size	Excellent	Poor: limited footprint	Poor: limited footprint	Adequate	Excellent	Excellent
Limitations of the Diver-transect (aim to improve using technological approaches)							
Required operator experience		Poor: Scientific training required	Excellent: diver or unmanned vehicle	Excellent: diver or unmanned vehicle	Excellent: diver or unmanned vehicle	Excellent: diver or unmanned vehicle	Excellent: diver or unmanned vehicle
Required time at each site		Poor: Long dives required	Excellent: rapid survey capability	Excellent: rapid survey capability	Excellent: rapid survey capability	Excellent: rapid survey capability	Excellent: rapid survey capability
Archive	Statistical re-analysis	Poor: hand-written notes only	Adequate: limited footprint	Adequate: limited footprint	xcellent	Excellent	Excellent
	Repeatability (track changes over time)	Poor: requires many markers	Poor: requires many markers	Poor: requires many markers	ent	Excellent	Excellent
Able to survey all depths		Poor: Only < 20m practical	Adequate: very deep and very shallow not possible	Adequate: very deep and very shallow not possible	equate: very shallow not possible	Adequate: very shallow not possible	Excellent: with heading / GPS input at surface
Landscape view (map large features)		Poor: very time consuming	Poor: limited footprint	Poor: limited footprint	Excellent	Excellent	Excellent
Spatial accuracy		Poor: very time consuming	Adequate: only for small objects within frame	Poor: large distoritions likely	Excellent	Excellent	Excellent

Table A14: Summary of advancements to the state-of-the-art in coral reef monitoring techniques. Capabilities and characteristics of various techniques are rated as 'excellent' (green), indicating a desired level of performance; 'adequate' (yellow) for an acceptable level of performance; and 'poor' (purple), indicating unsatisfactory performance. See text for details.

Performance of the mosaicing algorithms improved dramatically throughout the course of SI 1333 as the algorithm was refined and upgraded (Section A2.1.2). Landscape mosaics created at the start of the project (i.e. 'initial capability' or arrow A Table A14) addressed the limitations of diver-based surveys and resulted in improved capabilities relative to other reef-monitoring image-based techniques, but performed poorly in terms of analysis of benthic indicators. 'First generation' mosaics, produced with our initial upgraded algorithm, resulted in improvements in analysis capability, such that traditional benthic indicators could be extracted from the mosaics with a degree of detail that was adequate for many applications (arrow B, Table A14). Despite improvement relative to the initial capability, resolution was insufficient for detailed benthic analysis. Incorporation of a still camera in the data acquisition system, to generate 'second-generation landscape mosaics', resulted in performance that was comparable to the 'gold standard' of diver-based transects (arrow C, Table A14). The increases in capabilities shown in Table A14 are summarized in the following paragraphs (for further details, see Section A2.3.3).

An important component of project SI 1333 was to assess whether landscape mosaics retained the strengths of diver-based coral reef assessment. Five classic indicators of reef condition were considered in addressing this question (Table A14): percent benthic cover, diversity index, juvenile coral density, disease/bleaching/partial mortality, and coral colony size. Benthic indicators extracted from our initial mosaics compared poorly with diver-based measurements (see 'initial capability', Table A14). Refinements and enhancements performed under SI 1333 to create the 'first-generation mosaic algorithm' (Sections A5.1.1, 5.1.2) improved the ability to extract benthic indicators of reef condition (see 'first generation mosaics' Table A14). The percent cover of corals and major reef taxa, diversity indices, and bleaching/disease/mortality metrics analyzed from first-generation mosaics were not significantly different from those analyzed by divers as long as analysis was restricted to major groups of biotic taxa (e.g. corals, macroalgae, sand, sponges; Lirman et al. 2007). As coarse levels of classification are acceptable for many reef monitoring purposes, first-generation performance was deemed 'adequate' (Table A14). With the higher resolution available from the second-generation mosaics, analysis was further improved such that species-level identification was possible (see 'second generation mosaics', Table A14). As a result, second-generation performance was considered 'excellent' (i.e. on a par with divers; Table A14). Sizes of coral colonies measured from both first and second-generation mosaics did not significantly differ from diver-based measurements, and thus mosaic measurements were assessed as 'excellent' (Table A14; Lirman et al. 2007).

One category where ecologic analysis of even 'second generation mosaics' was deemed 'adequate', rather than 'excellent', was documenting juvenile coral density. Documenting the abundance and fate of juvenile corals is a key monitoring need, as the ability of reef communities to persist over time and recover from disturbances is dependent on the continuous influx of coral recruits. Image-based approaches in general are, however, not as good at documenting recruits as divers because recruits and juvenile corals are very small (order of mm to cm) and can be easily obscured from view by larger corals, or occur on bottom surfaces not imaged with downward looking cameras. Nevertheless, identification and monitoring of larger juvenile corals (> 10cm) can be accomplished using 2D mosaics and other image-based approaches (Lirman et al. 2007). Identification of juveniles as small as 5 cm is better on second-generation than first-generation mosaics, but in neither case is as good as diver identification. We cannot envision development of a technology in the near future that could replace divers for monitoring very small or cryptic recruits. Mosaics are, however, useful for monitoring juveniles on the order of 5-10 cm, which could be adequate for many coral monitoring needs.

SI 1333 also assessed whether landscape mosaics were useful in overcoming limitations of a diver-based approach to coral reef assessment. Six metrics were evaluated (required experience; data collection time; archive potential; depth limitations; mapping large scale features; and spatial resolution; Table A14). As indicated on Table A14, even the initial mosaics excelled in most categories. Advantages of mosaics compared to the diver based approach and other imaging techniques (i.e. photo quadrats and 1D strip mosaics) are summarized below.

Field personnel lacking the scientific expertise required for diver-based measurements can conduct Mosaic surveys. Imagery can be acquired using regular divers or with unmanned platforms, such as a remotely operated vehicle (ROV). This may be an advantage at DoD

facilities, where trained ROV operators may be more available than divers trained as coral reef biologists!

Data acquisition with image-based approaches to reef monitoring is rapid relative to data acquisition by trained divers. Relative speeds of the photo-quadrat, strip mosaics, and full 2-D mosaics are difficult to compare because times will be dependent on survey sampling design. As an indication of speed, however, it takes about 30 minutes to acquire the video for a 10 m x 10 m 2-D mosaic. Diver surveys of a similar site could take hours to days.

Image-based techniques for reef monitoring have excellent archive potential, providing a capability that is vastly superior to that offered by written notes made by divers. Image-based techniques excel because variables can be extracted at any time by different people. In addition, mosaics are superior tools to track patterns of change over time. Mosaics collected in repeat surveys can be easily referenced to one another with only four permanent markers and large numbers of coral colonies can be easily monitored over time without the need for extensive tagging (Lirman et al. 2007). This way, individual colonies can be followed to document changes, such as burial, or removal from plots (Lirman et al. 2006). In contrast, tracking changes over time with photo-quadrats requires that several permanent markers be deployed per image, which is tedious to set up and easily disturbed. Strip mosaics can be re-run with permanent markers, but it is not possible to ensure that exactly the same area is covered every time. The field of view is very narrow with strip mosaiced imagery (~0.5 m), and consequently even small drifts can result in large portions of the strips not being covered in a repeat survey.

Mosaics are also ideal for documenting reefs at or beyond the depth limit for scientific SCUBA diving. These deep reefs are increasingly being recognized as essential reef habitats. We processed mosaics from the "Sherwood Forest" in the Dry Tortugas National Park, Florida at a depth of 30 m and the Marine Conservation District of the U.S. Virgin Islands at depths up to 45 m (Gleason et al. 2009). Since image data may be acquired from platforms such as ROVs or AUVs, there are no theoretical depth limits to data collection, thereby adding considerable flexibility to a reef monitoring program.

As a further benefit, mosaics provide a landscape view of coral reefs that has previously been unobtainable. In this sense, mosaics bridge a gap between macro-scale coral reef mapping from airborne imagery and detailed underwater monitoring by trained divers. Strip mosaics over coral reefs cover typically < 10m2 (Jaap et al., 2002). In contrast, 2-D mosaics can cover in excess of 400m2 of reef habitat at mm scale pixel size (ground resolution). This landscape view of the reef makes new measures of reef health practical, such as documenting spatial relationships of disease patterns, or the effects of hurricane damage (Gleason et al. 2007) and ship groundings (Lirman et al. in press).

Finally, mosaics have a spatial accuracy on the order of a few centimeters (Lirman et al. 2007). This high level of performance, which greatly improves upon the accuracy of strip mosaics, combined with the large footprint, enables accurate measurements of large features, such as grounding scars, as well as small features such as the size of individual coral colonies. In corals, key life-history processes such as growth, mortality, and reproduction are directly related with colony size. Moreover, the age-structure of coral populations is increasingly being used as an

indicator of disturbance levels on reef communities (Bak and Meesters 1999). Lirman et al. (2007) showed that coral colony sizes measured from mosaics were as accurate as those measured by divers. Lirman et al. (in press) showed that two mosaics of a grounding scar in Biscayne National Park, FL, could be accurately georeferenced and could be used to measure the size of the damaged area with no significant difference from diver-based measurements.

The results above indicate that the landscape mosaics developed within project SI 1333 address the limitations of diver-based coral reef assessment, while simultaneously retaining most of the strengths of a diver-based approach. These strengths were further demonstrated through practical applications to a variety of coral reef monitoring efforts (Section A2.4). The spatial accuracy and archive potential of landscape mosaics, for example, allows individual coral colonies to be monitored without extensive tagging; this characteristic was exploited to monitor damage due to hurricanes (Gleason et al. 2007; Section A2.4.4) and mass bleaching events (Section A2.4.5). In addition, the landscape view of mosaics enables visualization and measurement of large features; this characteristic was exploited to map a scar from a ship grounding (Lirman et al. in press; Section A2.4.1) and to measure the size of a large slumping feature (Gleason et al. 2007; Section A2.4.4). The short dive times and utility of mosaics for monitoring deep sites was also explored in the imaging of mesophotic reefs (Gleason et al. 2009; Section A2.4.3).

The practical applications of the landscape mosaic technology, as outlined above, allowed us to test the system, and also served as an outreach tool to coral reef science community (Section A2.5). Each of the applications was conducted in partnership with scientists from different organizations. Over the course of the project we conducted field operations with personnel from eight agencies (or groups within agencies). The SERDP Coral Reef Monitoring and Assessment Workshop and the project web site were sources for further interactions with other agencies.

Additional examples illustrate the near-term future implications of the mosaic technology. NAVFAC Engineering and Support Center Scientific Diving Services (SDS) would like to transition the landscape mosaicing technology to an operational product to use in routine monitoring of coral reefs near Naval bases. As a first step in making this transition, SDS, along with partners from SPAWAR, the University of Miami, and the University of Girona, Spain, have submitted a proposal to the Environmental Security Technology Certification Program (ESTCP) to evaluate the operational costs and performance of the mosaics. In addition, NOAA Assessment & Restoration Division is planning to evaluate the use of landscape mosaics for documenting the December 2009 grounding of a 920’ tanker on a reef off the south coast of Puerto Rico. Finally, future use of landscape mosaics may extend to applications beyond coral reef mapping and monitoring. For example, NOAA’s Ocean Service and Office of National Marine Sanctuaries are considering the use of mosaics to assist mapping and monitoring of discarded military munitions off Oahu Hawaii.

In summary, landscape mosaics developed under SI 1333 provide scientists and resource managers with novel, powerful survey tools. Project deliverables include software to generate mosaics, tools to facilitate viewing the mosaics and assist in the extraction of ecological information, and user manuals. Landscape mosaics can now be used to routinely map large underwater areas at high spatial resolution (on the order of 400 m^2 at sub-mm resolution), resulting in spatially accurate, landscape views of the bottom that were previously unobtainable.

These landscape mosaics will be useful for DoD reef monitoring requirements and open doors for new applications in reef mapping and change detection.

A4. Action Item

In your final Report provide an operational cost analysis between the ROV/mosaic/3D technique and the current industry standard using divers and 2D data.

Response:
As an action item from a previous IPR, we were asked to provide an operational cost analysis of the landscape mosaic technique developed in the present project (SI 1333) in comparison to current industry standard reef-survey methodologies that utilize divers to conduct assessments of reef condition.

At present there is not a single industry standard for reef surveys – the method for any reef monitoring protocol necessarily depends on the particular questions being asked. We have chosen to compare the cost of conducting reef surveys using landscape video mosaics with traditional diver-based methods, such as those that were used to document reef status at AUTEC in the 70s and 80s, and a more recent rapid reef survey methodology (AGRRA), used currently at AUTEC.

A direct comparison of the cost of each survey methodology is hindered by the fact that while some of the indicators collected are common to all three methods (see Table A15 for a list of indicators), there are unique, method-specific indicators that need to be considered in the cost comparison. The cost of each survey needs to be weighed according to the diversity, accuracy, and precision of the indicators being collected as well as the potential application of the data collected. In this report, we provide a list of the indicators collected by each method as well as a description of the applications and advantages and disadvantages of each methodology that help qualify the cost estimates shown in Table A16.

Diver-Based Mapping Methodology

The goal of the diver-based mapping methodology, used by NAVO at AUTEC during the 70s and 80s to monitor status and trends of coral reefs, is to map the abundance and distribution of corals and other organisms within marked, permanent plots. These plots are re-visited periodically to evaluate changes over time. The emphasis of this methodology is on within-site precision and accuracy as well as repeatability. The final product of this methodology is a hand-drawn map of the reef bottom. The location and size of individual coral colonies or other features is determined by divers in the field using flexible underwater tapes. The metrics collected during these surveys include coral abundance, diversity, and colony sizes. Other organisms such as sponges and soft corals are also included in the maps. Once developed, these maps can be used to measure the benthic coverage of the main reef organisms.

The positive aspects of the diver-based mapping methodology are: (1) the maps collected using this methodology provide a landscape sketch of the reef bottom that can be archived for

reference and change detection over time; and (2) the identification of individual coral colonies within plots provides a high accuracy and precision to detect changes over time.

The negative aspects of this methodology are: (1) the time required to complete an assessment of a typical permanent site (2 days for a plot roughly 20 m x 20 m) limits the number of sites that can be practically surveyed within a region during a monitoring mission, (2) the divers conducting the surveys need to be trained in species identification; (3) the spatial accuracy of the maps is limited because they are hand-drawn by divers in the field; (4) the field maps need to be transferred into digital format for analysis using digitizing software; and (5) the lack of replication due to the long time required to survey each site influences the representative-ness of the observed patterns, which can not be easily extrapolated to the regional level.

	SURVEY METHODS		
	NAVO	AGRRA	MOSAICS
Indicators			
Coral Cover	Y	Y	Y
Coral Diversity	Y	Y	Y
Coral Colony Diameter	Y	Y	Y
Recent Mortality	N	Y	Y
Old Mortality	N	Y	Y
Juvenile Coral Density	Y	Y	Y
Macroalgal Cover	N	Y	Y
Sponge Cover	Y	N	Y
Soft Coral Cover	Y	N	Y
Topography	N	Y	N
Macroalgal Canopy Height	N	Y	N
Spatial Patterns	Y	N	Y
Disease Prevalence	N	Y	Y
Bleaching Prevalence	N	Y	Y
Uchin abundance	N	Y	N
Data Collection			
Field	2 days	2 hrs	30-40 min
Lab	2 days	4 hrs	2 days
Number of Divers	4-5	4	2
Training Level			
Field Personnel	HIGH	HIGH	LOW
Lab Personnel	LOW	LOW	HIGH
Other			
Spatial Accuracy	LOW	N/A	HIGH
Permanent Record	Y	N	Y
Landscape Image	hand-drawnmap	N	digital image
Products	Data Maps	Data	Data Digital, spatially accurate high-resolution landscape images

Table A15. Methods comparison. Overview of the characteristics of each survey method, including the reef condition indicators extracted, the effort required for data collection, the training required for personnel, and other survey characteristics.

AGRRA (Atlantic and Gulf Rapid Reef Assessment)

The main goal of the AGRRA methodology is to document large-scale patterns of reef condition using rapid in-water surveys to collect indicators of coral reef condition. The information gathered during AGRRA surveys, which is focused on stony corals, includes coral diversity, abundance, condition (recent and old partial mortality), and colony sizes. Other metrics include percent cover of corals, macroalgae, and other organisms, as well as macroalgal cover canopy height and reef topography. The prevalence of coral diseases, bleaching, and the abundance of sea urchins (*Diadema*) are also noted. Finally, the potential causes of coral mortality (e.g., sponge overgrowth, macroalgal overgrowth, sediments) are documented.

The positive aspects of this methodology are: (1) the bottom time at a given site is commonly short (< 2 hrs) allowing for multiple sites to be surveyed in one day; (2) to date, > 700 sites have been surveyed with this methodology, providing a regional baseline against which new surveys can be compared; and (3) during AGRRA surveys, all of the reef condition indicators are collected in situ. Data transcription and analyses are conducted at a later time in the lab, but no lab time is required for extracting indicators (e.g. coral cover) from raw data (e.g. video).

The negative aspects of this methodology are: (1) within-site accuracy and precision are de-emphasized in lieu of spatial coverage and number of sites sampled; (2) the ability of this methodology to detect changes over time has not been tested, as the number of repeat surveys of the same areas has been limited to date; (3) corals < 10 or 20 cm in diameter are often excluded to expedite the surveys; and (4) the divers conducting AGRRA surveys need to be trained in species identification and go through a rigorous calibration training exercise.

Landscape Video Mosaics

Landscape video mosaics are used to obtain a high resolution (mm-scale pixels) composite image of a large area (hundreds of m^2) of the seabed that allows for the direct extraction of coral indicators such as coral cover and colony sizes. This methodology provides a bridge between rapid and comprehensive reef survey methodologies by requiring only a short time of data collection in the field and shifting the assessment load from the field to the lab. Moreover, video mosaics can be analyzed to extract the same general suite of indicators of reef condition that are collected with the AGRRA and diver-based mapping methods, but they also provide a unique set of metrics and products that can't be collected using the former methods (Table A15). The final product of a video mosaic survey is a spatially accurate landscape digital image of the reef bottom that can be analyzed to extract indicators of reef condition.

The positive aspects of this methodology are: (1) digital video mosaics offer all of the advantages of diver-drawn maps such as high precision and accuracy to detect within-site changes over time; (2) mosaics provide the added capability to extract accurate size and distance measurements directly from the images, a unique tool to document and assess the impacts of disturbances such a ship groundings or anchor damage that are hard to assess in the field; (3) reef plots can be surveyed very quickly (< 40 min by a single camera operator), thus allowing for multiple sites to be surveyed in a given mission; (4) camera operators do not need any prior ecological training; (5) this methodology shifts the analysis time form the field to the lab where operations are generally cheaper and less time-constrained; and (6) the end product provides a powerful visual tool that can be easily archived for future reference.

The negative aspects of this methodology are: (1) the construction of mosaics can take up to 48 hrs in the lab and requires qualified technicians; (2) because only the top surface of the reef is captured in the video, cryptic habitats can't be surveyed; and (3) video surveys can't be conducted in conditions of limited visibility.

Cost Comparison Among Survey Methodologies

The relative costs of each survey method were estimated from four components of the survey process: boat time, diver time, data processing time, and analysis time. Boat cost was computed as the price of boat rental for one day (assumed to be $1000) divided by the number of sites that could be surveyed in one day. The number of sites possible in one day was based on field experience and assumed favorable conditions (e.g. short distances between sites, no problems anchoring, good weather and so forth). Diver cost was computed as the number of divers required times the cost per day per diver (assumed to be $500) divided by the number of sites per day. Data processing time includes data transcription from field sheets to electronic format (for NAVO and AGRRA methods) and mosaic creation (Mosaic method only). For the mosaics, computer time required to create the mosaic is not included, only the time required for interactive input from the technician. Extracting indicators from the NAVO and AGRRA data is rapid, once the data are in digital form. Extracting indicators from the mosaics involves point counting so takes longer than the other methods. Technician costs for data processing and indicator extraction were estimated at $500/day. Costs for consumable supplies such as waterproof paper, video tapes, PVC quadrats and so on are small when calculated on a per-site basis ($10 or so), so were not included in these calculations.

The depth of survey sites is an important variable to consider for planning diving operations. Depth will dictate the required surface intervals between dives and therefore impact the number of sites that can be visited in a single day. In order to capture this element of cost we have made estimates of the number of sites possible per day in three depth ranges: 0-30 feet, 30-50 feet, and 50-90 feet. The cutoff at 30' was chosen because shallower than 30' bottom time is not a limiting factor. The cutoff at 50' was chosen because virtually no AGRRA surveys have been conducted below that depth. The cutoff at 90' was chosen as the maximum depth at which a diver on air would have enough time to realistically complete acquisition of a 10 m x 10 m mosaic in one dive.

As shown on Table A16, the most expensive method is diver-based maps, at an estimated cost of $7700 per site. Below 30 feet it is not practical to complete diver-based maps. In shallow water, the AGGRA method is the least expensive, at an estimated cost of $1100 per site. The mosaicing method is slightly more expensive than AGGRA, at a cost of approximately $1350 per site in shallow water. In the middle depth range, 30-50', the mosaics become slightly less expensive than AGRRA. Below 50 feet, the mosaics are the most cost effective method.

Survey Components	SURVEY METHODS		
	NAVO	AGRRA	MOSAICS
Boat			
N sites per day (< 30')	0.5	4	6
N sites per day (30' - 50')	N/A	2	6
N sites per day (50' - 90')	N/A	N/A	4
Cost per site (< 30')	2000	250	167
Cost per site (30' - 50')	N/A	500	167
Cost per site (50' - 90')	N/A	N/A	250
Divers			
N divers (< 30')	4	4	2
N divers (30' - 50')	N/A	4	4
N divers (50' - 90')	N/A	N/A	4
Cost per site (< 30')	4000	500	167
Cost per site (30' - 50')	N/A	1000	333
Cost per site (50' - 90')	N/A	N/A	500
Data Processing			
Technician-Days of processing per site	4	0.5	1
Cost	2000	250	500
Extracting Indicators			
Technician-Days of analysis per site	0.2	0.2	1
Cost	100	100	500
Total per Site (< 30')	**8100**	**1100**	**1333**
Total per Site (30' - 50')	**N/A**	**1850**	**1500**
Total per Site (50' - 90')	**N/A**	**N/A**	**1750**

Table A16: Estimates costs per site of three reef survey methodologies. The costs assumed were: Boat = $1000/day, Diver = $500/day, Data processing and indicator extraction = $500/day.

Conclusion

The products of the mosaicing method are comparable to the diver-based maps, but are much cheaper to produce. AGRRA surveys are less expensive than mosaics in shallow water but become more expensive than mosaics in deeper water. Additionally, mosaics overcome some limitations of the AGGRA method, providing within-site accuracy, ability to detect changes over time through repeat surveys, detection of small corals and no need for scientifically trained divers.

Section B: Single Object 3D Reconstruction

To assist the classification of landscape mosaics, a secondary goal of project SI 1333 was to investigate 3D reconstruction of single objects within the landscape mosaics. 3D metrics such as height and rugosity can provide users with information on the topographical complexity created by corals, which can be used to identify key habitat features for a variety of organisms. Additionally, the 3D structure of coral colonies is important in many physiological processes such as coral calcification, growth, mortality, and fecundity. Despite importance of topography, 3D coral colony structure is not commonly incorporated in monitoring programs because it is extremely difficult to measure.

Research conducted within SI 1333 developed a 3D reconstruction tool that allows a user to visualize and measure topographic structure and heights of single objects, such as coral colonies, from landscape mosaics created from stereo imagery. With a user-friendly interface, the software relies on the camera trajectory and indexed images used for mosaic construction. Starting with the identification of an object of interest in the mosaic, the user follows a number of steps that lead to the construction of a 3D map of the coral colony or specific area of interest. The results obtained using the 3D reconstruction software compare favorably with diver measurements. Overall our research has demonstrated that the 3D system is a useful tool that can automatically determine object sizes and small scale rugosity measurements from stereo views.

B1. Materials and Methods

In order to make 3D measurements, a 3D map of an object or region of interest must be constructed. As part of SI 1333, we investigated two approaches: 1) an optical flow-based method applied to monocular video sequence for the dense estimation of a 3D map, and 2) a feature-based technique allowing 3D reconstruction of single objects. We determined that the second approach was more suitable for developing a tool for non-expert use in coral reef applications.

Simple geometric triangulation provides the foundation for feature based 3D reconstruction of stereo video imagery. Consider a pair of overlapping images taken from slightly different points. If the baseline between the focal points of the two images and the transformation from pixel row and column to angle from the camera optical axis are known, then the distances from each camera to a single point visible in both images can be computed geometrically.

Given stereo images acquired in a down-looking configuration from above an object, the differences between the z-coordinates of a point near the top of the object and one near the base of the object give the approximate height of the object. When only a few points are matched between a pair of images, the result is a "sparse depth map". On the other hand, when nearly every pixel in one image can be matched with a pixel in the other image the result is a "dense depth map", which is essentially an elevation model or terrain model of the surface in the images. Even a dense depth map, however, is not a full three dimensional reconstruction like those computed by Bythell et al. (2001) and Cocito et al. (2003) because in a single overhead stereo pair, there will generally be occluded areas that are not imaged and can therefore not be triangulated (reconstructed).

Our methodology for feature-based 3D reconstruction of single objects is as follows: First, construct and calibrate an underwater stereo camera. Second, acquire overhead stereo images of the survey area. Third, process the stereo pairs to form dense depth maps and then select points near the top and bottom of each object of interest to get the heights of the objects. Further details are given below.

The stereo imaging system used for this work was custom-built using commercially available components as much as possible. The imaging device was a Videre Designs MDCS2 variable baseline digital stereo head set to an approximate baseline of 20 cm. A VIA EPIA Mini ITX computer running RedHat Linux 9.0 performed all control functions. The stereo head was driven over an IEEE-1394 connection by the Small Vision Systems (SVS) version 4.1 software library that was provided with the cameras to perform data acquisition. The standard interface to this library had to be modified to accept control from a touch pad rather than the default mouse-driven interface. During acquisition, images were written in raw format to an 80 GB hard disk. Image acquisition averaged about 5 frames per second. When downloaded at the end of the day the images were converted to color at 1280x960 resolution.

The stereo video system was calibrated using the Camera Calibration Toolbox for Matlab (Bouguet 2002). The calibration routine solved for the intrinsic parameters for each camera (focal length, lens distortion, pixel aspect ratio, center pixel coordinates) as well as the extrinsic parameters (rotation and translation) relating the coordinate systems of the two cameras.

Image processing consists of six steps for each stereo pair: image selection, image pre-processing, feature matching, match propagation, interpolation, and height extraction. The first three steps create a "sparse depth map" as defined above. The fourth and fifth steps fill in the areas between the matched features to create a "dense depth map".

Image selection involves reviewing the captured images and extracting only the stereo pairs to be processed: namely, those containing the objects marked by the divers. We have built a graphical interface for image selection, within which the images are first stitched together into a mosaic using the methods described in Lirman et al. (2007) and then a user clicks on objects of interest (numbered tiles in this case) to bring up all stereo pairs that overlapped that point.

The second step is image pre-processing, in which the camera calibration parameters are applied to each stereo pair to a) remove lens distortion effects, and b) rectify the images such that matching features would appear on the same row in each image (Bouguet 2002).

The third step is feature matching, in which specific features visible in both images are identified as belonging to the same physical point on the seabed. The Shift-Invariant Feature Transform (SIFT) algorithm is used to automatically match features in each pair of images (Lowe 2004). The SIFT-generated matches are reviewed to discard any incorrect matches and flag any areas of the image where SIFT failed to find matches.

Match propagation, the fourth step, uses each of the SIFT-generated matches as a seed point to look for additional matches within a small window around that point. The idea is to search for

additional matching points near points known to be good matches. The algorithm implemented for match propagation is guided local disparity computation (Chen and Medioni 1999). Theoretically, if the distances to the cameras vary slowly, and if there is adequate texture across the image, then match propagation could fill in matches across the entire image from a single seed point. In practice, depth map discontinuities due to occlusions or illumination artifacts violate these constraints and match propagation can fill in only a local region around each seed point. Therefore, having many SIFT-generated seed points to start with helps this process succeed.

The fifth step interpolates between matched points to fill in gaps following match propagation. The result after the fifth step is a dense depth map computed for the area of overlap between the two images. The final step is to identify the top and bottom of the object(s) of interest and compute the depth difference between those points. A graphical interface was designed to facilitate this process. The analyst clicks with a mouse on the pixels at the top of the object of interest and on the benthos surrounding the object to calculate and record the vertical height of the object.

B2. Results and Discussion

As a culmination of our work in 3D mosaicing we developed a *"point and click"* system that allows users to select features of interest from a 2D video mosaic (created from stereo imagery) and create a small-scale 3D interpolation of that object. The steps involved in using the *"point and click"* system are described in methods.

Sample results are given in Figures B1-B7. In Figure B1, elevation has been encoded by color (red highlights low elevation, and purple is the highest elevation); the elevation display is generated using the GeoZui system (University of New Hampshire website). The representations allow users to click on map features and examine their elevations, or click on pairs of points on the map to determine the elevation difference. This feature allows us to determine the 3D height of corals or other benthic objects directly from mosaic products.

Figure B2 depicts an example of various steps of the point-click system. In (b), we have shown both features detected and matched by the algorithm, as well as those added manually over the coral (within rectangular region). The disparity map in (c) has been shown by gray-level coding, with the gray bar code given to the right of the map. The horizontal and vertical distances between various points in (d) are determined by clicking on pairs of points on the image. Using this technology we can select two points within an image and view the regional rugosity between the points of interest. Figure B3 shows the selection of various lines of interest (for examining regional rugosity) in four different reef scenes. Figure B4 shows the results of the rugosity computations of these scenes from the 3D map.

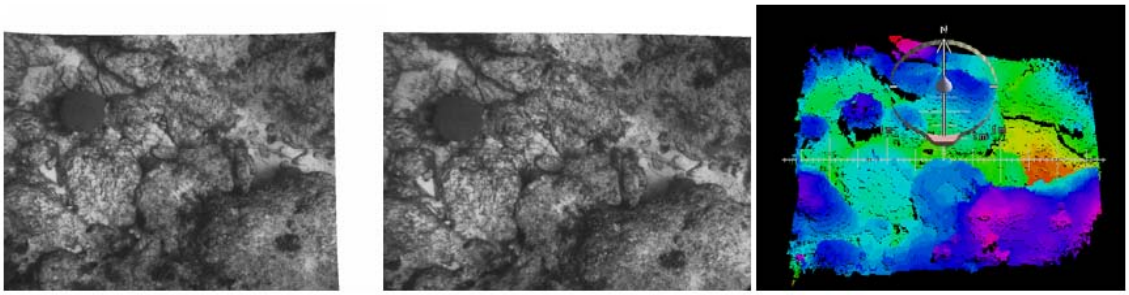


Figure B1. A sample stereo pair, shown in (a) and (b), are processed by our method to generate the 3D map in (c). Here, colors encode height, with red the low points and purple the highest elevation.

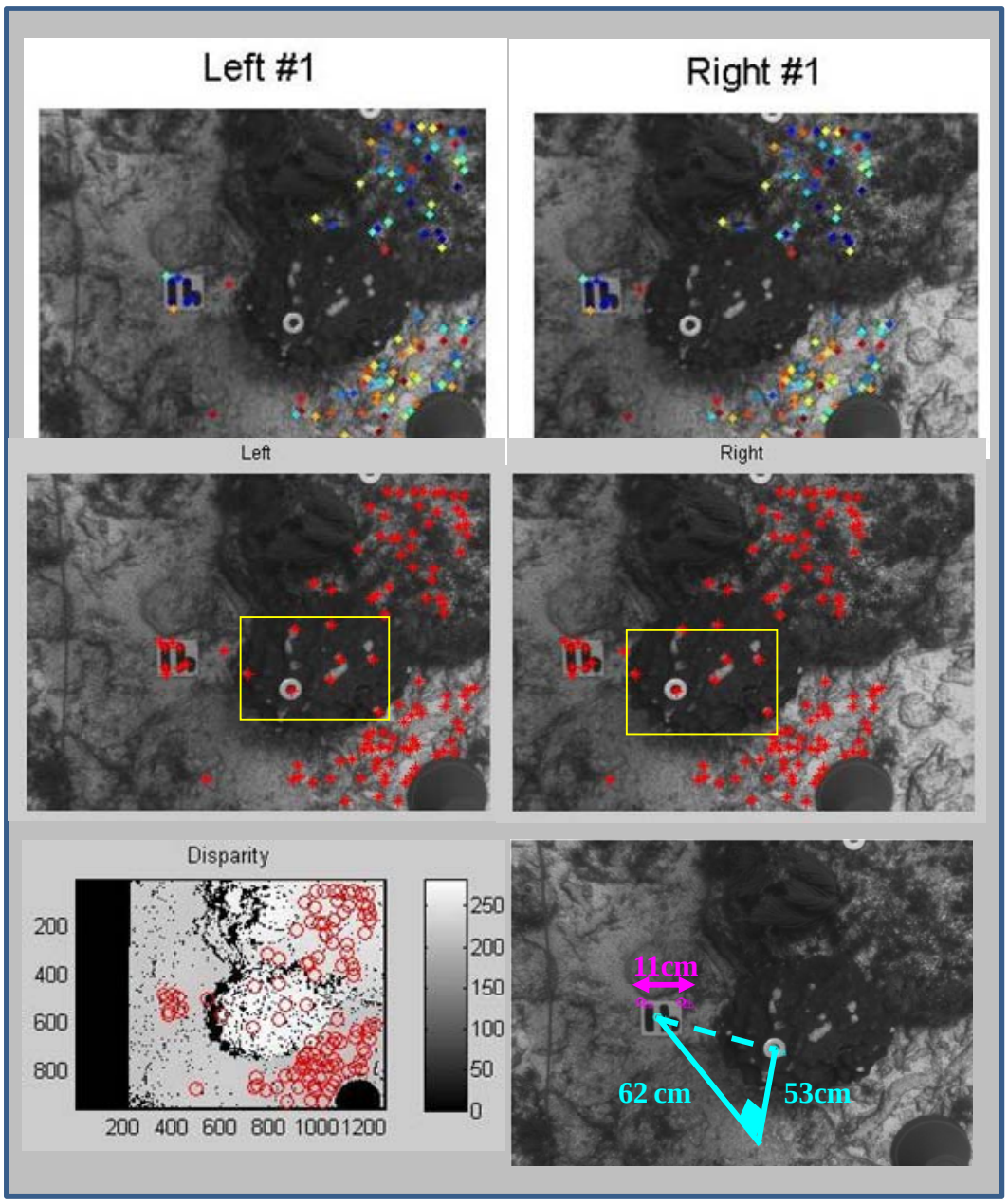


Figure B2. Sample stereo pair with matching features (a). Features over the coral reef, within yellow rectangle have been added manually (b). Computed disparity map in (c) allows the reconstruction of 3D map, and measurement of D distances (d).

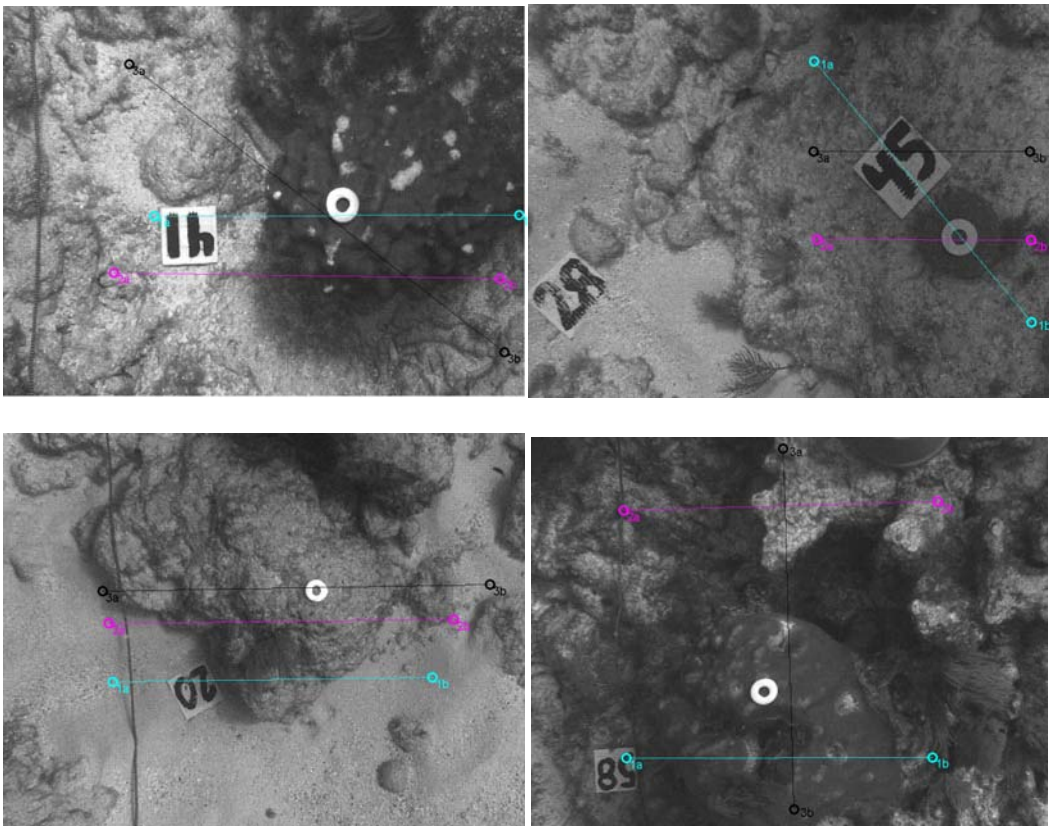


Figure B3. Sample left view of a stereo pair, showing the corals that have been processed for 3D reconstruction.

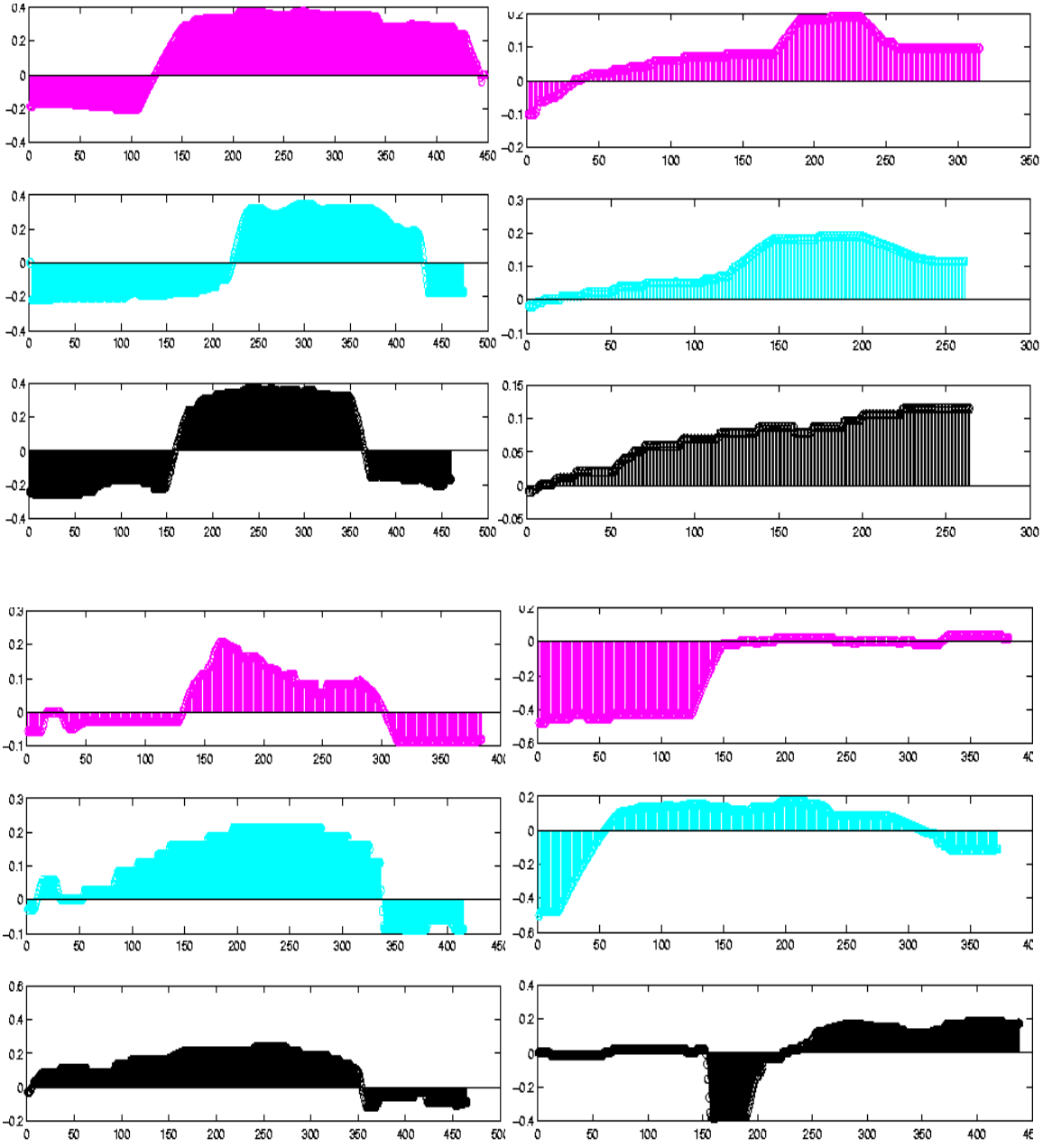


Figure B4. Scan lines from the 3D reconstruction of corals in figure B3.

Accuracy of the 3D system has been assessed by comparing measurements with those made by two divers, as well as known sizes (14.5” and 19”) of a number of flower pots placed on the sea floor. The height has been determined from the top of the object to a nearby point on the sea floor. For the corals, these two locations were marked by a 2’’ round metallic washer and a 4.3’’x 4.3’’ tile, respectively. Height estimates using the point and click system for coral and reef rubble are compared to two independent diver measurements in Figure B5. Comparison of the point and click system to objects of known size are shown in Figure B6.

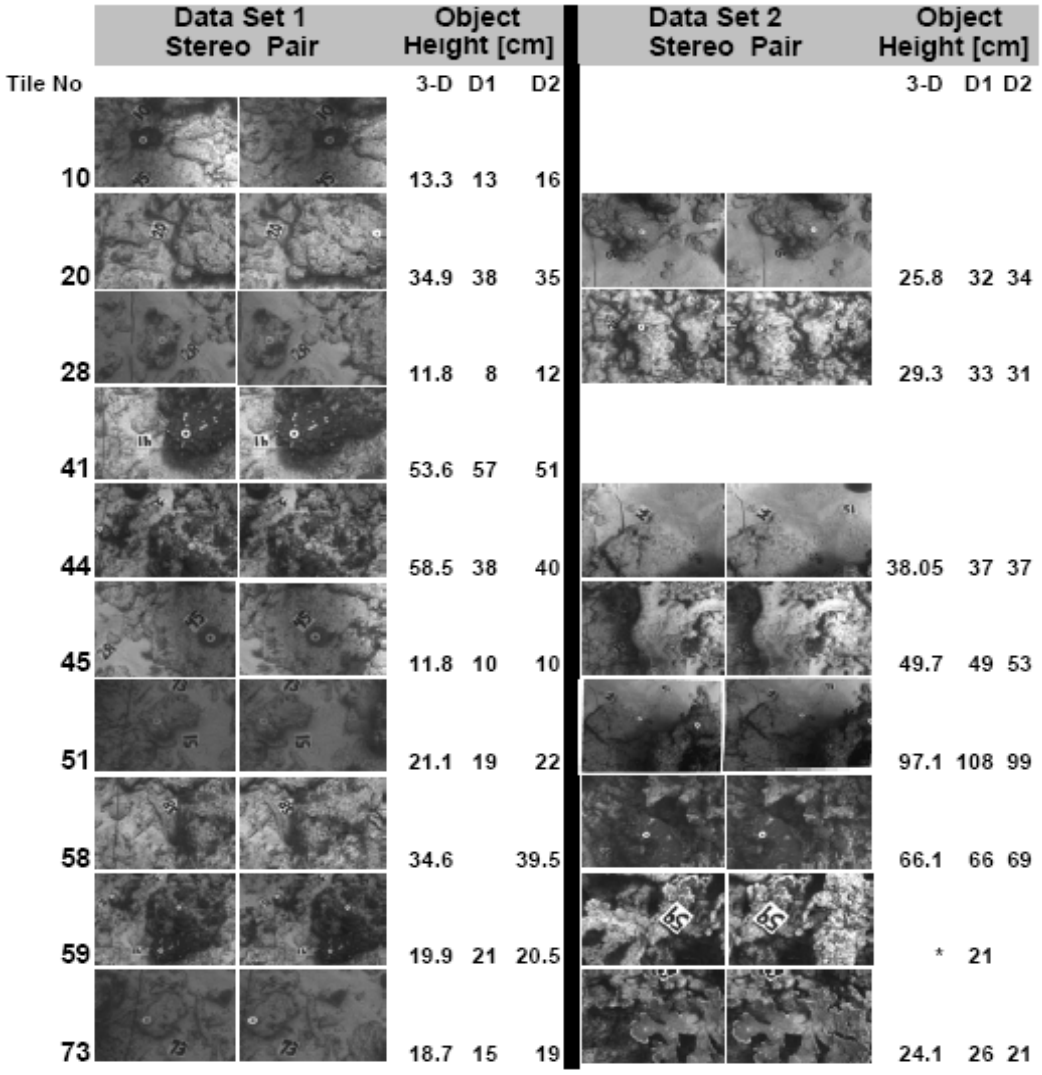


Figure B5. Height measurements for various corals or reef rubble imaged by the stereo camera system. Heights are given for measurements calculated by the point and click (3D column) as well as 2 independent diver measurements (D1 and D2).

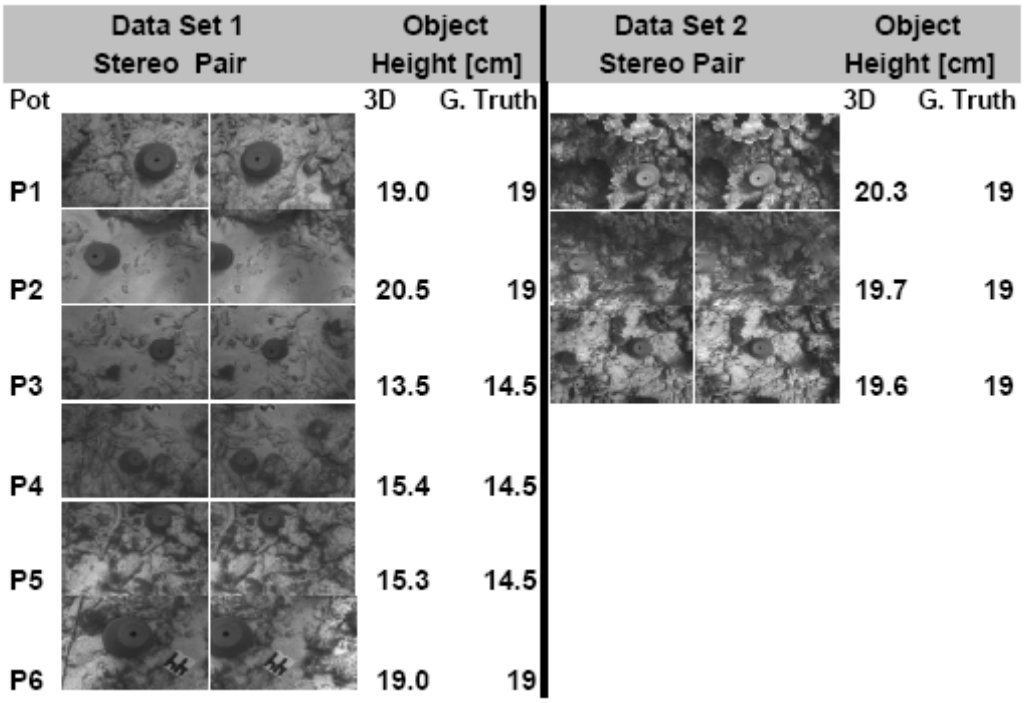
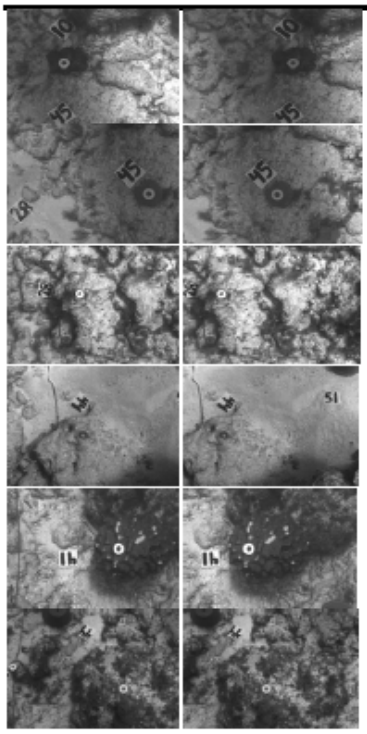


Figure B6. Control points for 3D point and click calibration. Flower pots of known dimension were placed on the seafloor and measured in the same way as coral colonies or rubble. Height estimates from the point and click system (3D column) are compared to that of laboratory measurements of the pots (G-truth column).

In all but three cases, the results show that the estimates from the 3D system are in close agreement with the two diver measurements, as well as the pot sizes. In one case, tile 51 in the 2nd data set, one diver measurement agrees well with the estimate from the 3D system (97.1 [cm] –vs- 99 [cm]), but varies by roughly 10% from the 2nd diver measurement (108 [cm]). In another case, tile 20 of 2nd data set, the discrepancy is roughly 25% (25.8 [cm] –vs- average diver measurement of 33 [cm]). Only in one case, tile 44 in data set 1, the 3D system and diver measurements disagree significantly (58.5 [cm] –vs- average diver measurement of 39 [cm]). Given that 3 independent estimates by the 3D system have produced consistent results (see next paragraph) and the two diver measurements are within 2 [cm], such a large discrepancy can only be attributed to some unknown factor that we have not been able to identify (such as recording error).

The consistency and (or) repeatability of the 3D system was investigated by determining the height for selected corals from different stereo pairs. More precisely, we have applied our method to 3 different stereo pairs of the same object recorded from nearby positions of the stereo platform. Figure B7 shows these results. The standard deviation of the three measurements for each object is equal or less than 2.5% of the average estimate in all but one case, where it is 5.8%. From these results, one can conclude that the 3D system is a useful tool to determine the missing height dimension automatically from a pair of stereo views.



Stereo Pair	Object Height [cm]										
	3 Indep. 3D Measurements						2 Indep. Diver Measurements				
	3D	3D	3D	avg	std	std/avg	D1	D2	avg	std	std/avg
	13.5	13.5	13	13.3	0.3	2.3%	13	16	14.5	2.1	14.5%
	11.5	12.1	11.7	11.8	0.3	2.5%	10	10	10	0	0.0%
	27.7	31	29.3	29.3	1.7	5.8%	33	31	32	1.4	4.4%
	37.6	38.5	38.1	38.1	0.4	1.1%	37	37	37	0	0.0%
	52.7	53.8	54.5	53.6	0.9	1.7%	57	51	54	4.2	7.8%
	58.6	58.9	57.9	58.5	0.50	0.9%	38	40	39	1.4	3.6%

Figure B7. Independent measurements of the same coral colony or reef rubble by the 3D point and click system (3 different stereo pairs) and 2 diver measurements.

B3. Conclusions and Implications for Future Research/Implementation

Our overall mosaicing research has targeted the development of image-based technologies, to increase the speed and repeatability with which reef plots can be mapped and inventoried. Because of habitat complexity, monitoring tools that document the 3D topography can provide valuable information on reef structure and function which are not commonly obtained by standard monitoring methodologies for measuring coral cover as the proportion of the bottom occupied by corals in a planar view. More precisely, utilizing our tool for the 3D size measurements, the user can more readily acquire the minimum technical knowledge for assessing the performance of the underlying methods comprising the entire system.

The 3D tool, which has a user-friendly GUI, is applied to a 2D mosaic of a reef area. It relies on the camera trajectory and the indexed images that are utilized in the construction of the mosaic. Starting with the identification of an object of interest in the mosaic, the user can follow a number of simple consecutive steps leading to the construction of the final 3D map. These steps allow the user to examine each intermediate result, which as a product can be readily assessed by a non-expert. For example, choosing between two different methods for establishing the

correspondences in the two stereo images, he/she can verify if the stereo matches have been identified correctly. The user can readily remove outliers if they exist. Alternatively, in regions where our system fails to identify correspondences, the user can manually add matched features.

The results obtained from our 3D system have been compared to the heights measured by two divers using flexible tapes, as well as the flower pots of know sizes laid on the sea floor. The 3D estimates are in good agreement with independent diver measurements and the true pot sizes (see Appendix 5). Furthermore, repeatability of the estimates from the 3D system has been demonstrated by applying our method to three different stereo pairs for each of several objects (Appendix 5). Our investigation has demonstrated that the 3D system is a useful tool to determine object sizes automatically from stereo views.

Section C: Multispectral Imaging

A method for automated classification of reef benthos would improve coral reef monitoring by reducing the cost of data analysis. Spectral classification of standard (three-band) color underwater imagery, however, does not work well for distinguishing major bottom types. Recent publications of hyperspectral reflectance of corals, algae, and sediment, on the other hand, suggest that careful choice of narrow (~10 nm) spectral bands might improve classification accuracy relative to the three wide bands available on commercial cameras. We built an underwater multispectral camera to test whether narrow spectral bands were actually superior to standard RGB cameras for automated classification of underwater images. A filter wheel was used to acquire imagery in six 10 nm spectral bands, which were chosen from suggestions in the literature.

Results indicate that the algorithms for classifying underwater imagery suggested in the literature require careful compensation for variable illumination and water column attenuation for even marginal success. On the other hand, research in project SI 1333 suggests that a new algorithm, based on the normalized difference ratio of images at 568 nm and 546 nm can reliably segment photosynthetic organisms (corals and algae) from non-photosynthetic background. Moreover, when this new algorithm is combined with very simple texture segmentation, the general cover classes of coral and algae can be discriminated from the image background with accuracies on the order of 80%.

These results suggest that a combination of high spectral resolution and texture-based image segmentation may be an optimal methodology for automated classification of underwater coral reef imagery.

C1. Materials and Methods

C1.1 System Development, Data Acquisition, and Preliminary Processing

An underwater, six band, multispectral camera (MSCAM) was constructed for image acquisition. The main components of the system included an Apogee Instruments Inc. AP47p CCD camera, However motorized filter wheel with space for six 25.4 mm interference filters, a Tamron 24mm, f/2.5 lens, and a single board computer for controlling the camera and filter wheel as well as storing images during acquisition. All of these components were housed in a watertight canister that was tethered to the surface via a cable supplying power and communication. The MSCAM design is almost identical to the NURADS camera (Voss and Chapin 2005) except the latter used a fish-eye lens and dome port to acquire hemispherical images. In contrast, the MSCAM full field of view was only about 45 degrees.

Recent literature on the hyperspectral reflectance of biotic organisms and substrates associated with coral reefs (Holden and LeDrew 1998; Holden and LeDrew 1999; Clark et al. 2000; Hochberg and Atkinson 2000; Holden and LeDrew 2001; Holden and LeDrew 2002; Hochberg and Atkinson 2003; Hochberg et al. 2003) was consulted for guidance the spectral bands considered most useful for optical seabed classification. In Figure C1 each row of points

corresponds to the bands used by a particular study. Solid points mark band centers, while squares and diamonds mark the locations of derivatives (see legend for details). Only six filters fit in the MSCAM at once, so two sets of six filters were used; these are marked by the vertical blue and red rectangles. Bands centered at 546, 568, and 589 nm were used in both filter sets.

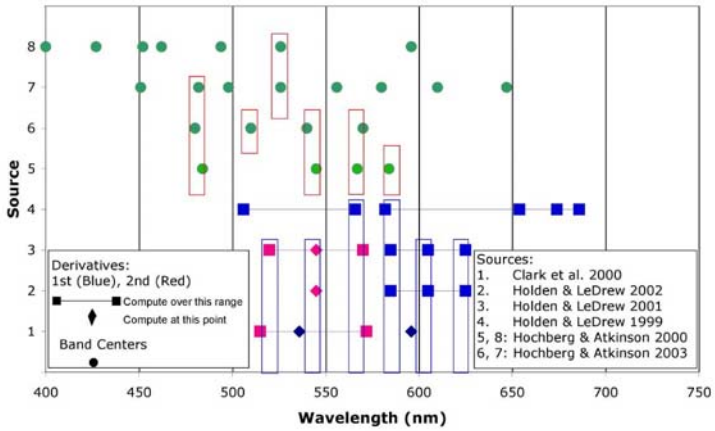


Figure C1. Proposed spectral bands for coral reef mapping. See text for description.

A full system calibration was performed (see Voss and Chapin 2005), but the only correction used in these experiments was for the camera lens rolloff, defined as the relative response of the imaging system as a function of location within the field of view.
During data acquisition, the camera rested on a tripod in a downward looking configuration and acquired multiple sets of images with each of the six filters. A panel of spectralon (LabSphere, Inc.) with 20 % Lambertian reflectance was placed in the camera field of view during data acquisition. For each scene imaged, several complete sets of light (shutter open) and dark (shutter closed) images were acquired for each filter. The AP47p has 1024 x 1024 pixel resolution, but a bin factor of two was used in some cases, so the resulting images are either 1024 x 1024 or 512 x 512 pixels.

After data acquisition with the MSCAM, images of each scene were acquired with a Sony P-93 in order to have traditional three-band (RGB) underwater images for comparison. Images with the Sony camera were also taken from the tripod in order to maintain the same distance to the seabed.

Initial data processing steps were common to all experiments. The first step in data processing was to correct the raw image digital numbers (DNs) for the CCD dark current and system rolloff factor (1).

$$DN_c = (DN_L - DN_D) / R_{off}. \quad (1)$$

DN_L and DN_D are the digital numbers in the light and dark current images, respectively. R_{off} is the correction for system rolloff (Figure C3). DN_c are the corrected digital numbers. The corrected DN_c were then converted to reflectance (R) by dividing all pixels in the image by DN_{cs}, (the average corrected digital numbers observed over the spectralon panel)(2). All calculations in (1) and (2) are performed on a pixel-by-pixel basis for each band, so all terms except for DN_{cs} are functions of row, column, and wavelength.

$$R = DN_c / DN_{cs} . \quad (2)$$

Finally, the average reflectance image (R_A) for each band was then computed as the mean of all (N) images acquired in each dataset.

C1.2 Experiments with Filter Set 1

Experiments with filter set 1 were designed to test algorithms proposed by Clark et al. (2000) and Holden and LeDrew (2001; 2002). Four datasets were acquired, two in the field and two in saltwater tanks at the University of Miami (Table C1). Four rules-based classification algorithms were tested, two from Clark et al. (2000), and one each from Holden and LeDrew (2001; 2002).
Clark et al. (2000) algorithm A:

- If the first derivative at 596 nm > -0.1 then live coral
- Else if the first derivative at 596 nm > -0.19 and < -0.1 then recently dead coral
- Else old dead coral

Clark et al. (2000) algorithm B:

- If the second derivative over 515-572 nm > 0.00253 then live coral
- Else if the first derivative at 536 nm > 0.07 then recently dead coral
- Else old dead coral

Holden and LeDrew (2001) algorithm:

- If the first derivative between 605-625 nm > 0.0 then sand
- Else if the second derivative at 545 nm > 0.0 then live coral
- Else if the first derivative between 585-605 nm > 0.0 then dead coral

Holden and LeDrew (2002) algorithm:

- If the first derivative between 605-625 nm > 0.0 then sand
- Else if the first derivative between 585-605 nm > 0.0 then bleached coral
- Else if the second derivative at 545 nm > 0.0 then live coral
- Else dead coral or algae

A fifth algorithm was tested with decision steps identical to Clark et al. (2000) algorithm B but with thresholds for each decision tuned to the particular scene.

Table C1. Images for Experiments with Filter Set 1

Shorthand	Location	Lighting	N
Tank 1	UM Tank	Ambient	1
Pickles	24°59.07' N / 80°24.97' W	Ambient	6
Tank 2	UM Tank	Ambient	5

Shorthand is the name used to refer to the dataset within the text. Location is the decimal latitude / longitude of the dataset in degrees or "UM Tank" for a saltwater flow though tank on the University of Miami / RSMAS campus. The sun provided "Ambient" lighting; N is the number of image sets (all six filters) that were averaged to create the single image used for analysis.

C1.3 Experiments with Filter Set 2

Hochberg and Atkinson (2000; 2003) used stepwise band selection and linear discriminant function analysis to demonstrate that spectral separation of coral, algae, and sand reflectance spectra is possible with as few as four non-contiguous narrow wavebands. Experiments with Filter Set 2 were designed to see if their suggested bands could be used to classify underwater images.

The actual discriminant functions used by Hochberg and Atkinson (2000; 2003) were not reported, so step one was to assemble hyperspectral reflectance measurements of live coral, algae, and calcareous sediment that we had made with underwater point spectrometers (both the DiveSpec Mazel 1997 and the GER1500 were used) and to extract the portions of those measurements corresponding to the six spectral bands in our camera. Step two was to calculate the multivariate discriminant functions that best separated the spectra belonging to the three groups (manova1 function in MATLAB 2006b, Mathworks, Natick, MA). Finally, the discriminant functions were applied to four MSCAM datasets from the field (Table C2) to create the classified images.

Table C2: Images for Experiments with Filter Set 2

Shorthand	Location	Lighting	N
Grecian 1	25.10603 N / 80.31810 W	Ambient	31
Grecian 2	25.10603 N / 80.31810 W	Ambient	11
Andros 1	24.71900 N / 77.77012 W	Ambient	16
Andros 2	24.71260 N / 77.74770 W	Ambient	14

Shorthand is the name used to refer to the dataset within the text. Location is the decimal latitude / longitude of the dataset in degrees or "UM Tank" for a saltwater flow though tank on the University of Miami / RSMAS campus. The sun provided “Ambient” lighting; N is the number of image sets (all six filters) that were averaged to create the single image used for analysis.

C1.4 Experiments with Combined Spectral / Texture Classification

The method used for combined spectral / texture classification had three steps. First, a spectral band ratio was used to separate coral and algae from other, "background" portions of the image. Second, texture metrics were used to separate coral from algae only for the part of the image that has not been masked as background. Finally, the output was smoothed to combine multiple texture measures and to reduce blocky artifacts introduced when small subsections of the image are passed to the texture computation. These steps are described in detail in Gleason et al. (2007), and will be outlined below.

The normalized difference ratio of bands centered at 568 and 546 nm ($ND_{568\text{-}546}$) was computed from the averaged reflectance values, R_A (3).

$$ND_{568\text{-}546} = (R_{A,568} - R_{A,546})/(R_{A,568} + R_{A,546}). \quad (3)$$

A threshold for $ND_{568\text{-}546}$ was chosen interactively to segment pixels containing coral and algae from "background" pixels containing anything else (Table C3). Photosynthetic organisms such as

corals and algae tend to have higher values of $ND_{568-546}$ than other organisms, sediments, and bare rock. All pixels below the threshold were set to zero.
The grey level co-occurrence matrix (GLCM) algorithm provided with MATLAB (R2006b; The MathWorks, Inc. Natick, MA) was used to compute three texture metrics from the thresholded $ND_{568-546}$ image. The MATLAB image processing toolbox documentation[2] contains details on the calculations and provides two references (Haralick et al. 1973; Haralick and Shapiro 1992). In addition, descriptions of the algorithm are available in many image processing textbooks (e.g. Jain et al. 1995). Thresholds were visually established for the other three texture metrics at a level that maximized the discrimination between coral and algae (Table C3).

Table C3. Thresholds Used For Each Algorithm and Dataset

	Thresholds			
	Spectral	Grey Level Co-occurrence Metrics		
Dataset	$ND_{568-546}$	Correlation	Energy	Homogeneity
Tank 1	0.10	0.37 +	0.12 *	0.64 *
Grecian 2	0.05	0.75 +	0.05 *	0.63 +
Andros 1	0.08	0.35 +	0.20 *	0.50 +
Tank 3	0.05	0.35 +	0.20 *	0.68 *

Thresholds are all unitless. Pixels with values less than the spectral threshold were masked to a zero value (background). Pixels with values greater than the spectral threshold were then assigned to coral or algae classes based on their value relative to each of the GLCM thresholds. Values less than the GLCM thresholds marked with an asterisk (*) were assigned to the coral class and values greater than the GLCM thresholds marked with an asterisk (*) were assigned to the algae class. The reverse is true for GLCM thresholds marked with a cross (+).

Output of the three GLCM computations was smoothed using a sliding window and majority filter in order to produce a single output image.
The accuracy of the classified images was assessed by point counting the original input images. For each of the datasets, an analyst used CPCe software (Kohler and Gill 2006) to place 400 random points over a false color image created from three of the six MSCAM bands. The analyst then classified each of the points as coral, algae or background.

Results from point counting were compared with the classified images in two ways. First, for an image-wide comparison, the percentage of points identified by the analyst as coral, algae and background was compared to the percentage of pixels classified by the spectral / texture algorithm in those classes. For each of the three classes ($_C$), accuracy (A_C) for that class was then computed following (4), where $P_{I,C}$ is the percentage of pixels in the image classified in class C, and $P_{A,C}$ is the percentage of points identified by the analyst as class C.

$$A_C = 1 - (P_{I,C} - P_{A,C}) / P_{A,C} . \quad (4)$$

Second, for a point-based comparison, the class for each of the 400 points identified by the analyst was extracted from the corresponding pixel in the classified image. An error matrix was then constructed for each dataset (Congalton and Green 1999) and the overall accuracy was

[2]http://www.mathworks.com/access/helpdesk/help/pdf_doc/images/images_tb.pdf

computed following (5), where A_O is the total overall accuracy, N_C is the number of points that were correctly classified in class (C), and N_T is the total number of points counted (400). The analysis was repeated both on the final classified image, which had coral, algae, and background classes, as well as on the thresholded $ND_{568-546}$ image, which is also a simple classification with just two classes: coral and algae combined, and background.

$$A_O = \Sigma N_C / N_T . \quad (5)$$

Four datasets were used for testing the spectral / texture approach (Table IV).

Table C4: Images for Experiments with Spectral / Texture Classification

Shorthand	Location	Lighting	N
Tank 1	UM Tank	Ambient	1
Grecian 2	25.10603 N / 80.31810 W	Ambient	11
Andros 1	24.71900 N / 77.77012 W	Ambient	16
Tank 3	UM Tank	Artificial	5

Shorthand is the name used to refer to the dataset within the text. Location is the decimal latitude / longitude of the dataset in degrees or "UM Tank" for a saltwater flow though tank on the University of Miami / RSMAS campus. The sun provided "Ambient" lighting; Two Deep Sea Power and Light 500 W MultiSeaLite halogen lamps provided the “Artificial” lighting. Images with artificial lighting were acquired at night. N is the number of image sets (all six filters) that were averaged to create the single image used for analysis.

C2. Results and Discussion

C2.1 System Development

System integration was accomplished during 2004 (Figure C2). Most cameras have maximum response at the principal point and decreased response towards the edges of the field of view; the MSCAM rolloff was typical in this regard (Figure C3).

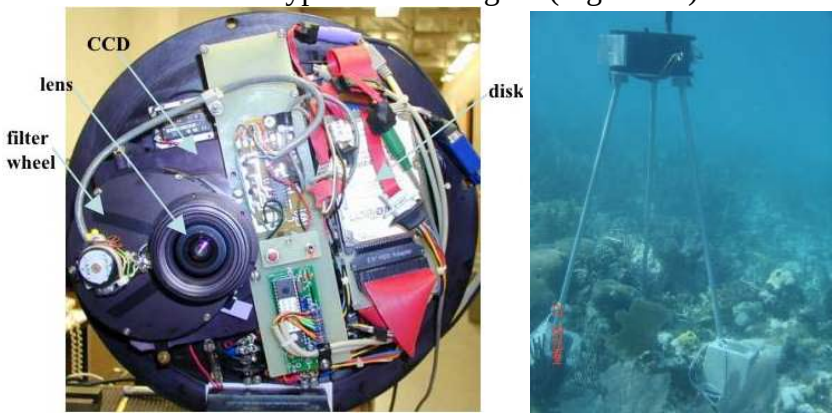


Figure C2. (Left) Interior of multi-spectral camera. (Right) Camera in operation.

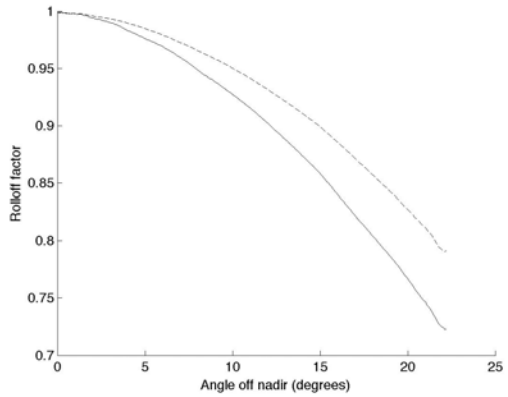


Figure C3. System rolloff factor as a function of angle from the center pixel. For clarity, only two of the six bands are shown: 487.1 nm (sold) and 589.0 nm (dashed). The response of the other bands falls between these extremes.

C2.2 Experiments with Filter Set 1

Efforts to classify imagery from the multi-spectral camera based on the schemes tested with filter set 1 were not successful. Negative results were probably due to two factors. First, the spectra used by Holden and LeDrew (2001; 2002), and Clark et al. (2000) were not corrected for water column attenuation, which is significant even at very short distances. Second, the classes investigated by Holden and LeDrew (2001; 2002), and Clark et al. (2000) include only live, bleached, and dead coral, and sand. Real images include additional classes (algae, silt substrate, reflectance standard etc..) that are not accommodated in the Holden and LeDrew (2001; 2002), and Clark et al. (2000) schemes.
Results from only the "Tank 1" dataset are presented here (Figures C4, C5), but they were similar for the other three images.

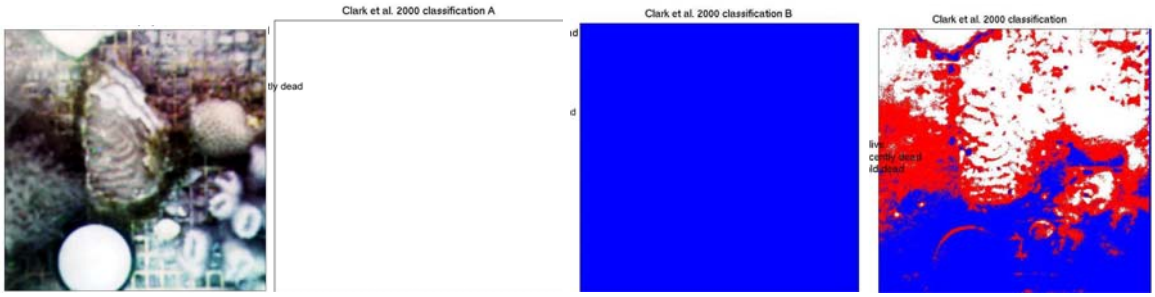


Figure C4. False color 600, 589, 568 nm RGB image of the "Tank 1" dataset (Far left). Clark 2000 A, B, and tuned classifications for this dataset (Center left, center right, far right, respectively). In the classified images white = live coral; red = recently dead coral; blue = old dead coral.

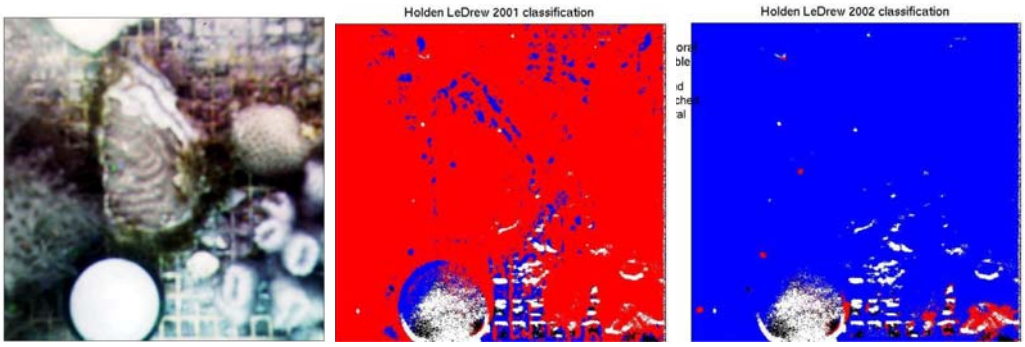


Figure C5. False color 600, 589, 568 nm RGB image of the "Tank 1" dataset (Far left). Holden LeDrew (2001) classification for this dataset (Center; white = sand; red = live coral; blue = old dead coral; black = unclassified). Holden LeDrew (2002) classification for this dataset (Right; white = sand; red = live coral; blue = bleached coral; black = algae/rubble).

C2.3 Experiments with Filter Set 2

The discriminant functions (DFs) computed from our spectra appeared similar to those calculated by Hochberg et al. (2000) when applied to the training data (the point spectrometer data; Figure C6). The overall variance along each DF axis was similar, as was the ability of the DFs to discriminate coral, algae, and sand.

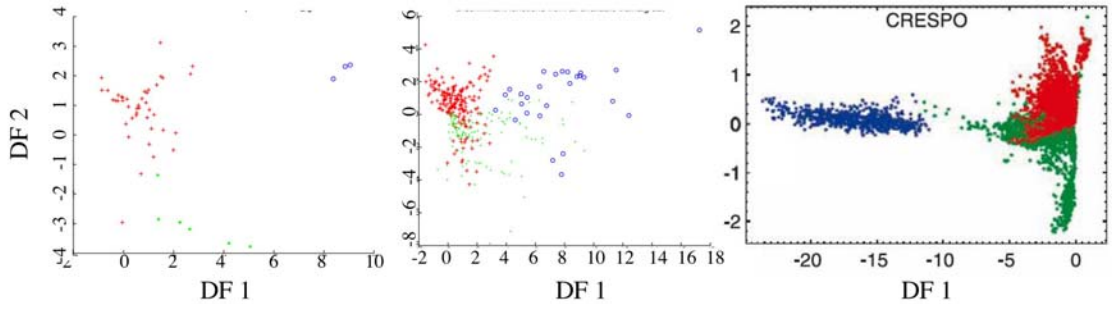


Figure C6. Discriminant functions one (DF1) and two (DF2) computed from our full-spectrum data base (left), from our partial-spectrum data base (center), and from Hochberg and Atkinson's (2003) database for their hypothetical CRESPO sensor. In all cases red points are for spectra of live corals, green points for spectra of algae, and blue points for spectra of sediment. Note that the sign of DF1 is flipped between our data and Hochberg and Atkinson (2003), but the ranges of both DF1 and DF2 are approximately the same.

When the discriminant functions were applied to the multispectral images (Figure C7), in all cases the ranges (max-min values) of both DF1 and DF2 were much larger in the MSCAM data than they had been in the spectrometer data (top row of Figure C7). This suggests that there is additional variance in the images not accounted for by the model. Displaying the projected data as images, with DF1 in red and DF2 in green (bottom row of Figure C7), reveals that there are structured patterns related to the geometry of the scene, not the benthic cover. The conclusion is that geometry is contributing at least as much to the variance of the scene as variations in the bottom reflectance.

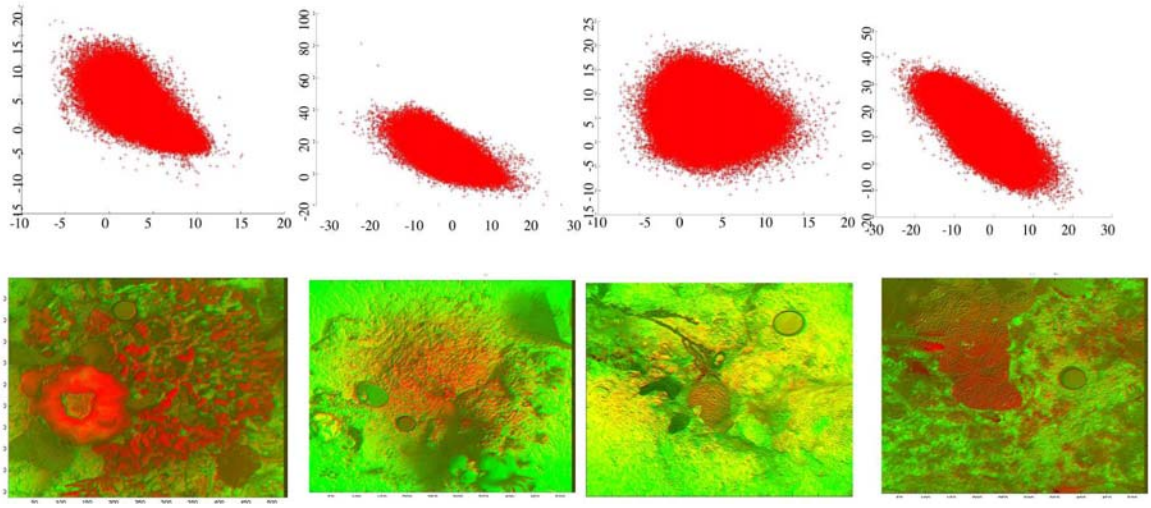


Figure C7. Four MSCAM scenes acquired with filter set two. Top row: results of applying the discriminant functions to the image data for each scene. Note the range of the DF1 and DF2 axes are much larger than in Fig. 6. Bottom row: DF1 displayed in red and DF2 displayed in green. Note variations in color related to the structure of the scene and not just the benthic cover; this is particularly noticeable in the middle two images.

C2.4 Experiments with Combined Spectral / Texture Classification

False color RGB images of the MSCAM datasets as well as the resulting classified images are shown for all four datasets in Figure C8.

The classified images agree well with the point count data when considering image-wide accuracy, which assesses estimates of the total percentage of each class present in the scene. The image-wide accuracy, defined by (4), was greater than 70% for 11 of 12 classes and greater than 75% for 9 of 12 classes (Table C5).

The classified images also agree well with the point count data when considered on a point-by-point basis. The overall accuracies, as computed from error matrices using (5), were greater than 80% for three of the four datasets (Table C5).

Table C5: Image-Wide Accuracy

Dataset	Coral	Algae	Background
Tank 1	74 %	71 %	98 %
Grecian	77 %	96 %	77 %
Andros	78 %	11 %	81 %
Tank 2	94 %	93 %	98 %

Image-wide accuracy was computed using (4) for each dataset.

Table C6: Point-Based Overall Accuracy

Dataset	Overall Accuracy
Tank 1	86 %
Grecian	67 %

Andros	84 %
Tank 2	87 %

Overall accuracy was computed using (5) for each dataset.

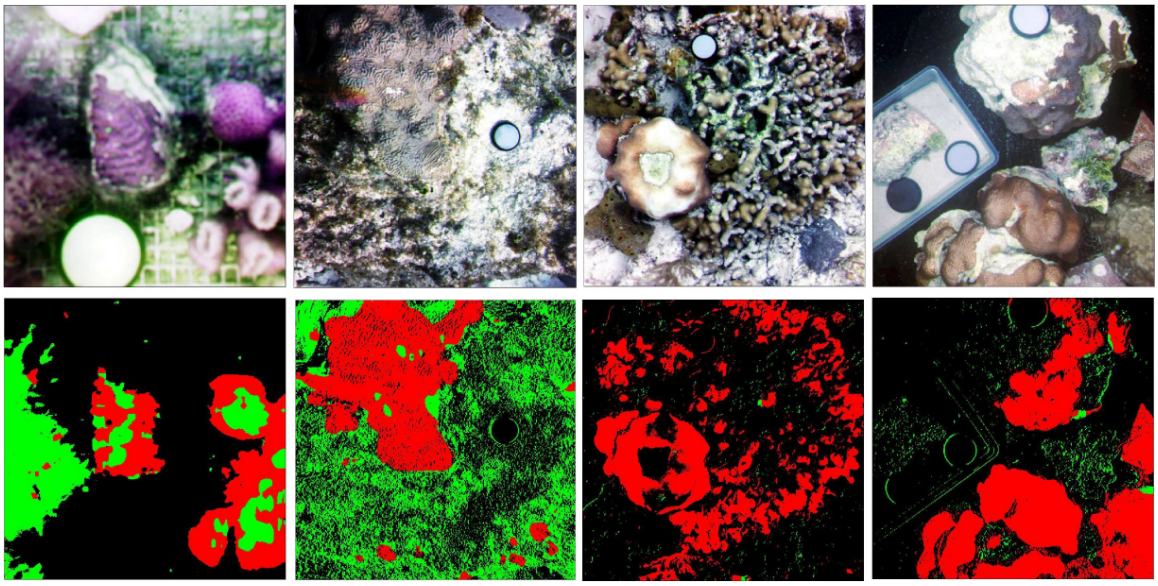


Figure C8. Summary of results for combined spectral / texture classification. Top row: False color images composed of three multispectral camera bands (589, 548, 487 nm) displayed in RGB. Bottom row: Final smoothed classified images with three classes: coral (red), algae (green), background (black). The datasets are placed in columns in the same order as Table C5: Tank 1, Grecian, Andros, Tank 2, from left to right.

C3. Conclusions and Implications for Future Research/Implementation

As mentioned in Section C3, initial experiments testing whether the spectral bands suggested in (Holden and LeDrew 1998; Holden and LeDrew 1999; Clark et al. 2000; Hochberg and Atkinson 2000; Holden and LeDrew 2001; Holden and LeDrew 2002; Hochberg and Atkinson 2003; Hochberg et al. 2003) could be used for automated classification of underwater imagery were not successful. The results presented above, indicate, however, that high spectral resolution may nevertheless be useful for underwater image classification because such data can greatly simplify subsequent processing by a texture classification algorithm.

High spectral resolution is an improvement over coarse spectral bands for classifying underwater imagery; the evidence for this is the ability of $ND_{568-546}$ to more accurately segment out coral + algae than color matching with standard underwater photography.
Narrow spectral bands alone are not a complete solution for automated underwater classification of reef images, however. Segmenting coral *and* algae, together as one class, from the background is not a useful end in itself. On the other hand, segmenting coral and algae with a narrow spectral band ratio was useful in this study when combined with image texture measures. The evidence for this was that thresholds of texture images computed with the GLCM algorithm were able to separate coral and algae after the background had been identified with the narrow band ratio, but they could not do so without the prior application of the narrow band ratio.

The approach followed here was semi-automated in the sense that some user intervention was required to select the four thresholds that need tuning for each dataset. Although a fully automated system would be ideal, the semi-automated approach was still faster than point counting, and there are at least three reasons to expect additional progress could be made toward a fully automated system, as follows:

First, the range of thresholds to search was fairly small. The thresholds for $ND_{568-546}$, GLCM Correlation, and GLCM Homogeneity varied by about a factor of two. It would be easy to create an interface to facilitate threshold picking so that many images could be analyzed quickly.

Second, no theoretical work has been performed on the texture properties of reef benthos that is particularly relevant for guiding the choice of GLCM parameters. This differs significantly from the situation for spectral parameters, for which a number of previous studies have suggested that wavelength regions around 546 and 568 nm were good for discriminating corals, algae, and substrate. Upon investigation, it may be possible to find better values for the GLCM block size, offset, and smoothing parameters than the nominal values used above.

Third, the GLCM algorithm was chosen simply for convenience due to its existing implementation in MATLAB. Better results may be expected with more sophisticated texture algorithms, such as those being pursued by (Konotchick et al. 2006; Pizarro et al. 2006; Mehta et al. 2007), but the point is that regardless of the texture algorithm used, acquiring data in narrow spectral bands is likely to improve the results.

High spectral resolution was an improvement over coarse spectral bands for classifying underwater imagery, but narrow spectral bands alone were not a complete solution for automated classification of reef images. The important result was that acquiring underwater imagery in narrow spectral bands and pre-processing the data with a band ratio greatly simplified texture classification. Texture classification became easy enough, in fact, that the GLCM approach, which on its own was not useful for segmenting these images, was found to produce reasonable results when combined with $ND_{568-546}$.

The potential for full automation of underwater high spectral resolution imagery is promising and will benefit from three future areas of research: 1) careful correction for scene geometry, 2) combination of spectral and more sophisticated texture algorithms, 3) additional research on the texture properties of corals, algae, other organisms and the substrate associated with coral reef environments.

Literature Cited

Bernhardt, S. P. and L. R. Griffing (2001). An Evaluation of Image Analysis at Benthic Sites Based on Color Segmentation. *Bulletin of Marine Science* **69**(2): 639-653.

Bouguet, J.Y. (2002). Matlab camera calibration toolbox. (http://www.vision.caltech.edu/bouguetj/calib.doc).

Brown, M., and D. Lowe. (2003) Recognizing panoramas. Proc Int Conf Comp Vision, Washington, DC, USA, 1218 p

Bythell, J., P. Pan, and J. Lee. (2001) Three-dimensional morphometric measurements of reef corals using underwater photogrammetry techniques. *Coral Reefs* **20(3):** 193-199.

Chen, Q. and G. Medioni (1999). A volumetric stereo matching method: Application to image-based modeling. *Proc. IEEE Conference on Computer Vision and Pattern Recognition Colorado* **1**: 29-34.

Clark, C. D., P. J. Mumby, J. R. M. Chisholm, J. Jaubert and S. Andrefouet (2000). Spectral discrimination of coral mortality states following a severe bleaching event. *International Journal of Remote Sensing* **21**(11): 2321-2327.

Cocito, S., S. Sgorbini, A. Peirano and M. Valle. (2003) 3-D reconstruction of biological objects using underwater video technique and image processing. *Journal of experimental Marine Biology and Ecology* **297(1):** 57-70.

Congalton, R. G. and K. Green (1999). Assessing the Accuracy of Remotely Sensed Data: Principles and Practices, Boca Raton, Lewis Publishers, 137 pp.

Courtney, L.A., W.P. Davis, and W.S. Fisher. Estimating 3-dimensional surface area of field corals. *Submitted to Coral Reefs*, 2006.

Delaunoy, O., N. Gracias and R. Garcia (2008) Towards detecting changes in underwater image sequences. Proceedings of MTS/IEEE Oceans08 Conference. Kobe, Japan, April 2008.

Elibol, A., N. Gracias and R. Garcia. (2009) Match Selection in Batch Mosaicing using Mutual Information. Proc. of the 4th Iberian Conference on Pattern Recognition and Image Analysis (IbPRIA2009). Povoa do Varzim, Portugal, June 2009.

Fisher, W.S., W.P. Davis, R.L. Quarles, J. Patrick, J.G. Campbell, P. S. Harris, B. L. Hemmer, and M. Parsons (2007). Characterizing coral condition using estimates of three-dimensional colony surface area. *Environ Monit Assess* **125**: 347-360.

Foley, B. P. and D. A. Mindell. Precision Survey and Archaeological Methodology in Deep Water. *ENALIA The Journal of the Hellenic Institute of Marine Archaeology*. Volume VI: 49-56, 2002.

Gardner, T.A., I.M. Cote, J.A. Gill, A .Grant, and A.R. Watkinson. (2003) Long-Term Region-Wide Declines in Caribbean Corals. Science 301:958-960

Gifford, J. A. Mapping Shipwreck Sites by Digital Stereovideogrammetry. *Underwater Archaeology*, 9-16, 1997.

Gintert, B., Gracias, N., Gleason, A.C.R., Lirman, D., Dick, M., Kramer, P., Reid, R.P. (2008) Second-Generation Landscape Mosaics of Coral Reefs. Proceedings of the 11th International Coral Reef Symposium. Fort Lauderdale, FL, July 7-11, 2008. (In-press)

Gleason, A. C. R., N. Gracias, D. Lirman, B. E. Gintert, T. B. Smith, M. C. Dick, R. P. Reid (2009). Landscape video mosaic from a mesophotic coral reef, Coral Reefs, doi: 10.1007/s00338-009-0544-2.

Gleason A., D. Lirman, D. Williams, N. Gracias, B. Gintert, H. Madjidi, R. Reid, G. Boynton, S. Negahdaripour, M. Miller and P. Kramer. (2007) Documenting hurricane impacts on coral reefs using two-dimensional video-mosaic technology. Mar Ecol 28:254-258

Glynn P.W. (1988) El Niño warming, coral mortality and reef framework destruction by echinoid bioerosion in the eastern Pacific. Galaxea, 7, 129–160.

Gorbunov, M.Y., Z.S. Kolber, M.P. Lesser and P. Falkowski. (2001) Photosynthesis and Photoprotection in Symbiotic Corals. Limnology and Oceanography. 46(1) 75-85

Gorbunov MY, and Falkowski PG. (2005) Fluorescence Induction and Relaxation (FIRe) Technique and Instrumentation for Monitoring Photosynthetic Processes and Primary Production in Aquatic Ecosystems. In: "Photosynthesis: Fundamental Aspects to Global Perspectives" - Proc. 13th International Congress of Photosynthesis, Montreal, Aug.29 – Sept. 3, 2004., V.2, pp. 1029-1031

Gracias, N. and J. Santos-Victor. (2000) Underwater video mosaics as visual navigation maps. Computer Vision and Understanding 79: 66-91.

Gracias, N. and J. Santos-Victor. (2001) Trajectory reconstruction with uncertainty estimation using mosaic registration. Robotics and Autonomous Systems 35(3-4): 163-177.

Gracias, N. and S. Negahdaripour. (2005) Underwater Mosaic Creation Using Video Sequences from Different Altitudes. Proc. IEEE/MTS Oceans'05, Washington, DC.

Gracias, N., S. Negahdaripour, L. Neumann, R. Prados and R. Garcia (2008a) A motion compensated filtering approach to remove sunlight flicker in shallow water images. Proc. of the MTS/IEEE Oceans 2008 Conference, Quebec City, Canada, September 2008.

Gracias, N., M. Mahoor, S. Negahdaripour, and A. Gleason. (2009) Fast Image Blending using Watersheds and Graph Cuts, Image and Vision Computing, 27(5): 597-607.

Gracias, N., A. Gleason, S. Negahdaripour and M. Mahoor. (2006) Fast Image Blending using Watersheds and Graph Cuts. Proceedings of the British Machine Vision Conference '06, Edinburgh, U.K., 4-7 September 2006: pp. paper #259.

Gracias, N., van der Zwaan, S., Bernardino, A., and Santos-Victor, J. (2003). Mosaic Based Navigation for Autonomous Underwater Vehicles. IEEE Journal of Ocean Engineering, 28(4):609-634

Haralick, R. M., K. Shanmuga and I. Dinstein (1973). Textural Features for Image Classification. *IEEE Transactions on Systems, Man, and Cybernetics* **3**(6): 610-621.

Haralick, R. M. and L. G. Shapiro (1992). Computer and Robot Vision: Vol. 1, Addison-Wesley, 459 pp.

Harmelin-Vivien M.L. (1994) The effects of storms and cyclones on coral reefs: a review. Journal of Coastal Research Special Issue, 12: 211–231.

Harris, C. and M. Stephens. (1988) A combined corner and edge detector. In: Proc. Alvey Conf., pp. 189–192.

Harvey, E., Fletcher, D., & Shortis, M. (2001). A comparison of the precision and accuracy of estimates of reef-fish lengths determined visually by divers with estimates produced by a stereo-video system. *Fisheries Bulletin, 99*: 63–71.

Hochberg, E. J. and M. J. Atkinson (2000). Spectral discrimination of coral reef benthic communities. *Coral Reefs* **19**(2): 164-171.

Hochberg, E. J. and M. J. Atkinson (2003). Capabilities of remote sensors to classify coral, algae, and sand as pure and mixed spectra. *Remote Sensing of Environment* **85**: 174-189.

Hochberg, E. J., M. J. Atkinson and S. Andrefouet (2003). Spectral reflectance of coral reef bottom-types worldwide and implications for coral reef remote sensing. *Remote Sensing of Environment* **85**(2): 159-173.

Holden, H. and E. LeDrew (1998). Spectral Discrimination of Healthy and Non-Healthy Corals Based on Cluster Analysis, Principal Components Analysis, and Derivative Spectroscopy. *Remote Sensing of Environment* **65**: 217-224.

Holden, H. and E. LeDrew (1999). Hyperspectral identification of coral reef features. *International Journal of Remote Sensing* **20**(13): 2545-2563.

Holden, H. and E. LeDrew (2001). Hyperspectral discrimination of healthy versus stressed corals using in situ reflectance. *Journal of Coastal Research* **17**(4): 850-858.

Holden, H. and E. LeDrew (2002). Measuring and modeling water column effects on hyperspectral reflectance in a coral reef environment. *Remote Sensing of Environment* **81**(2-3): 300-308.

Holt, P. (2000). The site surveyor guide to surveying underwater. *Technical Report*, 3H Consulting Ltd.

Hudson JH, Diaz R (1988) Damage survey and restoration of M/V Wellwood grounding site, Molasses Reef, Key Largo National Marine Sanctuary. Proc 6th Int Coral Reef Symp 2:231–236

Nicosevici, T. and Garcia, R. (2008) Online Robust 3D Mapping Using Structure from Motion Cues. Proc. IEEE/MTS Oceans Conf. '08, Kobe, Japan, April 2008.

Jaap, W.C., 2000. Coral reef restoration. Ecol. Eng.

Jaap, W. C., J. W. Porter, J. Wheaton, C. R. Beaver, K. Hackett, M. Lybolt, M.K. Callahan, J. Kidney, S. Kupfner, C. Torres, and K. Sutherland. EPA/NOAA Coral Reef Evaluation and Monitoring Project, Florida Fish and Wildlife Conservation Commission Report, 28 pp., 2002

Jain, R., R. Kasturi and B. G. Schunck (1995). Machine Vision, Boston, McGraw Hill, 549 pp.

Kohler, K. E. and S. M. Gill (2006). Coral Point Count with Excel extensions (CPCe): A Visual Basic program for the determination of coral and substrate coverage using random point count methodology. Computers and Geosciences 32(9): 1259-1269.

Konotchick, T. H., D. I. Kline, D. B. Allison, N. Knowlton, S. J. Belongie, D. J. Kriegman, G. W. Cottrell, A. D. Bickett, N. Butko, C. Taylor and B. G. Mitchell (2006). Computer Vision Technology Applications for Assessing Coral Reef Health. *EOS Trans. AGU Ocean Sci. Meet. Suppl., Abstract OS15I-06* **87**(36).

Kramer, P.R. and J.C. Lang. (2003) The Atlantic and Gulf Rapid Reef Assessment Protocols: Former Version 2.2. In: Lang JC (ed) Status of Coral Reefs in the Western Atlantic: Results of Initial Surveys, Atlantic and Gulf Rapid Reef Assessment (AGRRA) Program: Atoll Research Bulletin 496. Smithsonian Institution, Washington, D.C., pp. 611-624

Lirman D. (2000) Fragmentation in the branching coral Acropora palmata (Lamarck): Growth, survivorship, and reproduction of colonies and fragments. Journal of Experimental Marine Biology and Ecology, 251 (1), pp. 41-57.

Lirman D., G. Deangelo, J.E. Serafy, A. Hazra, D.A. Hazra, and A. Brown. (2008). Geospatial Video Monitoring of Nearshore Benthic Habitats of Western Biscayne Bay

(Florida) Using the Shallow-Water Positioning System (SWaPS). Journal of Coastal Research 24(1): 135-145

Lirman, D. and P. Fong. (1995) The effects of Hurricane Andrew and Tropical Storm Gordon on Florida reefs. *Coral Reefs* **14**, p. 172.

Lirman D., N. Gracias, B.E. Gintert, A.C.R. Gleason, S. Negahdaripour, P. Kramer, and R.P. Reid. (2007) Development and application of a video-mosaic survey technology to document the status of coral reef communities. Environmental Monitoring and Assessment 125:59-73

Lirman, D., N. Gracias, B. Gintert, A. C. R. Gleason, G. Deangelo, M. Gonzalez, E. Martinez, R. P. Reid (in press):Damage and Recovery Assessment of Vessel Grounding Injuries on Coral Reef Habitats Using Georeferenced Landscape Video Mosaics, Limnology and Oceanography: Methods.

Louchard, E. M., R. P. Reid, F. C. Stephens, C. O. Davis, R. A. Leathers and T. V. Downes (2003). Optical remote sensing of benthic habitats and bathymetry in coastal environments at Lee Stocking Island, Bahamas: A comparative spectral classification approach. *Limnology and Oceanography* **48**(1, part 2): 511-521.

Lowe, D. G. (2004). Distinctive Image Features from Scale-Invariant Keypoints. Int. Journal of Computer Vision 60(2): 99-110.

Mader, G.L. (1996) Kinematic and Rapid static (KARS) GPS positioning: Techniques and recent experiences. In: Beutler, G.; Hein, G.W. Melbourne., and Seeber, G. (eds.) IAG Symposia No. 115, Springer-Verlag, Berlin, pages 170-174, 1996.

Manzello, D., M. Brandt, T. Smith, D. Lirman, J Hendee, and R. Nemeth. (2007) Hurricanes benefit bleached corals. Proceedings of the National Academy of Sciences, U.S.A. 104: 12035-12039.

Mazel, C. H. (1997). Diver-operated instrument for in situ measurement of spectral fluorescence and reflectance in benthic marine organisms and substrates. *Optical Engineering* **36**: 2612-2617.

Mazel, C. H., M. P. Strand, M. P. Lesser, M. P. Crosby, B. Coles and A. J. Nevis (2003). High-resolution determination of coral reef bottom cover from multispectral fluorescence laser line scan imagery. *Limnology and Oceanography* **48**(1, part 2): 522-534.

Mehta, A., E. Ribeiro, J. Gilner and R. van Woesik. (2007) Coral Reef Texture Classification Using Support Vector Machines. International Conference of Computer Vision Theory and Applications - VISAPP, Barcelona, Spain: pp. 302-305.

Miller, S.L., M. Chiappone, D. Swanson, J. Ault, S. Smith, G. Meester, J. Luo, E. Franklin, J. Bohnsack, D. Harper and D. McClellan. (2001) An extensive deep reef terrace on the Tortugas Bank, Florida Keys National Marine Sanctuary. Coral Reefs 20(3): 299-300

Mobley, C. D., L. K. Sundman, C. O. Davis, T. V. Downes, R. A. Leathers, M. Montes, J. H. Bowles, W. P. Bissett, D. D. R. Kohler, R. P. Reid, E. M. Louchard and A. C. R. Gleason. (2004) A Spectrum-Matching and Look-up-table Approach to Interpretation of Hyperspectral Remote-sensing Data. *Applied Optics* **44**(17): 3576-3592.

Mumby, P. J., E. P. Green, C. D. Clark and A. J. Edwards. (1998) Digital analysis of multispectral airborne imagery of coral reefs. Coral Reefs 17(1): 59-69.

Negahdaripour, S., & Madjidi, H. (2003). Stereovision imaging on submersible platforms for 3-D mapping of benthic habitats and sea floor structures. *IEEE Journal Ocean Engineering, 28*, 625–650.

Negahdaripour S., R. Prados and R. García. (2005) Planar homography: accuracy analysis and applications. ICIP (1) 2005: 1089-1092

Negahdaripour, S., X. Xu and A. Khamene. (1998) A vision system for real-time positioning, navigation, and video mosaicing of sea floor imagery in the application of ROVs/AUVs. *Applications of Computer Vision, 1998. WACV '98. Proceedings., Fourth IEEE Workshop on* pp.248-249, 19-21 Oct 1998

Nicosevici, T., N. Gracias, S. Negahdaripour and R. Garcia. (2009) Efficient 3D Scene Modeling and Mosaicing, Journal of Field Robotics, (26)10**:** 759 – 788.

Pizarro, O., S. Williams, I. Mahon, P. Rigby, M. Johnson-Roberson and C. Roux (2006). Advances in Underwater Surveying and Modelling from Robotic Vehicles on the Great Barrier Reef. *EOS Trans. AGU Ocean Sci. Meet. Suppl., Abstract OS15I-08* **87**(36).

Precht W.F. and M. Robbart. (2006) Coral reef restoration: the rehabilitation of an ecosystem under siege. In: W.F. Precht, Editor, *Coral Reef Restoration Handbook*, Taylor & Francis, Boca Raton, FL (USA), pp. 1–24.

Reid, R.P., S. Negahdaripour, D. Lirman, and P. Kramer. (2007) SI-1333 Application of ROV-based Video Technology to Complement Coral Reef Resource Mapping and Monitoring. Annual Report to The Strategic Environmental Research and Development Program. December 2006-December 2007.

Riegl, B., and W.E. Piller. (2003) Possible refugia for reefs in times of environmental stress. International Journal of Earth Science 92:520-531

Ryan, D.A.J., and Heyward, A. (2003) Improving the precision of longitudinal ecological surveys using precisely defined observational units. *Environmetrics, 14*, 283–293

Schechner, Y. and N. Karpel. (2004) Attenuating natural flicker patterns. In Proceedings of OCEANS '04. MTS/IEEE TECHNO-OCEAN '04, volume 3, pages 1262–1268 Vol.3, Nov. 2004

Shutler, S.K., S. Gittings, T. Penn, and J. Schittone. (2006) Compensatory restoration: how much is enough? Legal, economic, and ecological considerations. p. 77-94. *In* W.E. Precht [ed.], Coral Reef Restoration Handbook. CRC Press. Boca Raton, Florida.

Smith, T.B., R.S. Nemeth, J. Blondeau, J.M. Calnan, E. Kadison and S. Herzlieb. (2008) Assessing coral reef health across onshore to offshore stress gradients in the US Virgin Islands. Marine Pollution Bulletin 56:1983-1991

Smith T.B., J. Blondeau, R.S. Nemeth, S.J. Pittman, J.M. Calnan, E. Kadison and J. Gass. (2009) Benthic structure and cryptic mortality in a Caribbean mesophotic coral reef bank system, the Hind Bank Marine Conservation District, U.S. Virgin Islands. Coral Reefs this volume (in review)

Somerfield, P.J., W.C. Jaap K.R. Clarke, M. Callahan, K. Hackett, J. Porter, M. Lybolt, C. Tsokos and G. Yanev. (2008) Changes in coral reef communities among the Florida Keys, 1996 – 2003. Coral Reefs 27:951–965

SPAWARSYSCEN PAC. 2008. Proceedings from the Coral Reef Monitoring and Assessment Workshop, 18-19 November 2008, Miami, Florida. Prepared for the Strategic Environmental Research and Development Program and Rosenstiel School of Marine and Atmospheric Sciences by SPAWARSYSCEN PAC, San Diego, California.

Symons, L.C., Stratton A., and Goodwin W. (2006). Streamlined Injury Assessment and Restoration Planning in the U.S. National Marine Sanctuaries. Coral Reef Restoration Handbook by William P.F. Taylor & Francis Group

Van der Meer J., (1997) Sampling design of monitoring programmes for marine benthos: A comparison between the use of fixed versus randomly selected stations *Journal of Sea Research*, 37 (1-2), pp. 167-179.

Voss, K. J. and A. L. Chapin (2005). Upwelling radiance distribution camera system, NURADS. *Optics Express* **13**(11): 4250-4262.

Weiss, Y. (2001) Deriving intrinsic images from image sequences, Proceedings of the Eighth IEEE Int. Conf. on Computer Vision ICCV 2001, 2:68–75 vol.2, 2001.

Xu, X. (2000) Vision-based ROV system, PhD thesis. University of Miami

Appendix 1. Publications and Presentations Acknowledging SERDP Support

2003

[1] Barafauldi, C., Firoozfam, P. and Negahdaripour, S. (2003) An Integrated Vision-Based Positioning System for Video Stabilization and Accurate Local Navigation and Terrain Mapping. Proc. IEEE/MTS Oceans Conf. '03, San Diego, CA.

2004

[2] Madjidi, H. and Negahdaripour, S. (2004) On Robustness and Localization Accuracy of Optical Flow Computation from Color Imagery. Proc. IEEE Int. Conf. 3D Visualization, Processing and Transm. '04, Thessaloniki, Greece.

[3] Kramer, P., Reid, R.P., Negahdaripour, S., Gleason, A., Doolittle, D., Gintert, B. (2004) Application of ROV-based Video Technology to Complement Coral Reef Resource Mapping and Monitoring. 10th International Coral Reef Symposium, 28 June – 2 July 2004, Okinawa, Japan.

[4] Reid, R.P., Gracias, N., Negahdaripour, S., Lirman, D., Kramer, P.A., and Voss, K. (2004) Application of ROV-based Video Technology to Complement Coral Reef Resource Mapping and Monitoring. SERDP Partners in Environmental Technology Symposium. 30 November – 2 December 2004, Washington D.C. USA. (Oral presentation).

[5] Reid, R.P., Gracias, N., Negahdaripour, S., Lirman, D., Kramer, P.A., Voss, K., Doolittle, D.F., Gleason, A. and Gintert, B. (2004) Application of ROV-based Video Technology to Complement Coral Reef Resource Mapping and Monitoring. SERDP Partners in Environmental Technology Symposium. 30 November – 2 December 2004, Washington D.C. USA. (poster presentation).

2005

[6] Gleason, A. (2005) New Technologies for Addressing Depth and Scale Limitations of Coral Reef Remote Sensing., First NCORE Coral Reef Research Forum, National Center for Coral Reef Research, Miami, FL USA, 19 February 2005. (oral presentation).

[7] Madjidi, H. and Negahdaripour, S. (2005) Global Alignment of Sensor Positions with Noisy Motion Measurements. IEEE Trans. Robotics, 21(6): 1092-1104.

[8] Gracias, N. and Negahdaripour, S. (2005) Underwater Mosaic Creation Using Video Sequences from Different Altitudes. Proc. IEEE/MTS Oceans'05, Washington, DC.

[9] Nicosevici, T., Negahdaripour, S., and Garcia, R. (2005) Monocular-Based 3-D Seafloor Reconstruction and Ortho-Mosaicing by Piecewise Planar Representation. Proc. IEEE/MTS Oceans'05, Washington, DC.

2006

[10] Gracias, N. R., Gleason, A. C., Lirman, D., Gintert, B., Doolittle, D., Reid, R. P., and Negahdaripour, S. (2006) Two-Dimensional Video Mosaics for Mapping and Monitoring Coral Reef Resources, AGU Ocean Sciences meeting, Honolulu, HI, February 20-24, 2006, Abstract OS15I-05.

[11] Madjidi, H. and Negahdaripour, S. (2006) On robustness and localization accuracy of optical flow computation for underwater color images. Computer Vision and Image Understanding 104(1): 61-76.

[12] Gracias, N., Gleason, A., Negahdaripour, S. and Mahoor, M. (2006) Fast Image Blending Using Watersheds and Graph Cuts. British Machine Vision Conference (BMVC06), Edinburgh, Scotland, September 2006.

[13] S. Negahdaripour. (2006) Challenges in Underwater Vision: Prelude to Session's Technical Talks. Oceans'06, Boston, MA USA, 18 September, 2006.

[14] Reid, R.P. and Lirman, D. (2006) Landscape video mosaics: New tools for coral reef monitoring. Invited seminar, NOAA Coral Reef Conservation Program, 19 May, 2006.

[15] Negahdaripour, S., Barufaldi, C., and Khamene, A. (2006) Integrated Systems for Robust 6 DOF Positioning Utilizing New Closed-Form Visual Motion Estimation Methods for Planar Scenes. IEEE J. Oceanic Engineering 31(3): 533-550.

2007

[16] Gleason, A.C., Lirman, D., Williams, D., Gracias, N.R., Gintert, B.E., Madjidi, H., Reid, R.P., Boynton, G.C., Negahdaripour, S., Miller, M. and Kramer, P. (2007) Documenting hurricane impacts on coral reefs using two-dimensional video-mosaic technology. Marine Ecology 28:1-5.

[17] Gleason, A., Reid, R. and Voss, K. (2007) Automated classification of underwater multispectral imagery for coral reef monitoring. Proceedings of MTS/IEEE Oceans '07, Vancouver, BC, Canada. (Poster presentation)

[18] Gleason, A., Gracias, N., Lirman, D., Gintert, B., Reid, R. and Negahdaripour, S. (2007) Two-Dimensional Video Mosaics for Mapping and Monitoring Coral Reef Resources. 2007 AAUS Symposium, Miami, FL. (Poster presentation)

[19] Reid, R., Gracias, N., Negahdaripour, S., Lirman, D., Gleason, A., Gintert, B., and P. Kramer. (2007) Application of ROV-Based video technology to complement coral reef resource mapping and monitoring. SERDP Partners in Environmental Technology Symposium. December 4-6, 2007, Washington D.C. USA. (Poster presentation).

[20] Gleason, A. (2007) Two-Dimensional Video Mosaics for Mapping and Monitoring Coral

Reef Resources. Invited presentation at the Center for Imaging Science Rochester Institute of Technology, May 18, 2007.

[21] Gracias, N. (2007) Visual Navigation and Efficient Blending. Invited presentation at MacDonald, Dettwiler and Associates Ltd. (MDA), Vancouver, October 2007.

[22] Lirman, D., Gracias, N., Gintert, B., Gleason, A., Reid, R., Negahdaripour, S., and Kramer, P. (2007) Development and Application of a Video-Mosaic Survey Technology to Document the Status of Coral Reef Communities. Environmental Monitoring and Assessment, Vol. 125, pp:59-73

2008

[23] Reid, P. and Lirman, D. (2008) High Resolution Landscape Mosaics for Coral Reef Monitoring. Invited Seminar NOAA Coral Reef Conservation Program, Silver Springs, Maryland, 8 February, 2008.

[24] Delaunoy, O, N. Gracias, R. Garcia, (2008) Towards detecting changes in underwater image sequences, Proceedings of the IEEE / MTS Oceans 2008 conference. Kobe, Japan, April 2008.

[25] Gintert, B., Gracias, N., Lirman, D., Gleason, A., Reid, P., and Kramer, P. (2008) Landscape Mosaics of Coral Reefs: A new Survey Technology for Mapping and Monitoring Reef Condition. International Coral Reef Symposium, July 9, 2008. (Presentation)

[26] Reid, P., Negahdaripour, S., Gracias, N., Lirman, D. A. Gleason, B. Gintert, P. Kramer, T. Szlyk, M. Ciminello, (2008). Landscape video mosaics: New tools to Complement Coral Reef Resource Mapping and Monitoring. International Coral Reef Symposium, July 9, 2008. (Poster)

[27] Gintert, B., Gracias, N., Reid, R., Szlyk, T., Ciminello, M. (2008) Long-term Spatiotemporal Dynamics of Benthic Organisms at Andros Island Reefs. International Coral Reef Symposium, July 9, 2008. (Poster)

[28] Reid, P., Gracias, N., Lirman, D., Gleason, A., Gintert, B., Kramer, P., Szlyk, T., Ciminello, M. (2008) High Resolution Video Mosaics for Monitoring Andros Island Reefs. International Coral Reef Symposium, July 9, 2008 (Presentation)

[29] Gracias, N., Negahdaripour, S., Neumann, L., Prados, R. and Garcia, R. (2008) A motion compensated filtering approach to remove sunlight flicker in shallow water images. Proc. of the MTS/IEEE Oceans 2008 Conference, Quebec City, Canada, September 2008.

[30] Reid, P., Gracias, N., Lirman, D., Gleason, A., Gintert, B., Kramer, P. (2008) A new survey technology for mapping and monitoring reef condition. SERDP Coral Reef Monitoring and Assessment Workshop, November 18-19, 2008. (Presentation)

[31] Gracias, N., Martinez, E., Dick, M., Gintert, B., Reid, R.P., Lirman, D., Gleason, A., Kramer, P. (2008) Creating 2D Mosaics for Mapping and Monitoring Reef Condition. SERDP Coral Reef Monitoring and Assessment Workshop, November 18-19, 2008. (Presentation)

[32] Lirman, D., Reid, R.P., Gorbunov, M., Falkowski, P. (2008) Landscape Video Mosaic and Florescence Induction and Relaxation System Integration. SERDP Coral Reef Monitoring and Assessment Workshop, November 18-19, 2008. (Presentation)

[33] Gintert, B., Gracias, N., Gleason, A.C.R., Lirman, D., Dick, M., Kramer, P., Reid, R.P. (2008) Second-Generation Landscape Mosaics of Coral Reefs. Proceedings of the 11th International Coral Reef Symposium. Fort Lauderdale, FL, July 7-11, 2008. (In-press)

[34] Reid, P., Negahdaripour, S., Gracias, N., Lirman, D., Gleason, A., Gintert, B., Kramer, P., Szlyk, T., Ciminello, M. (2008). Landscape video mosaics: New tools to Complement Coral Reef Resource Mapping and Monitoring. SERDP Partners in Environmental Technology Technical Symposium and Workshop, December 2-4, 2008. (Poster)

[35] Nicosevici, T., Garcia, R. (2008) On-line robust 3D Mapping using structure from motion cues. Proc. MTS/IEEE Techno-Ocean Conference (Oceans'08), Kobe, Apr. 2008.

2009

[36] Gleason, A.C.R., Lirman, D., Gintert, B.E., Dick, M.C., Reid, R.P. (2009) Landscape video mosaic from a mesophotic coral reef. Coral Reefs(Published Online Sept 18, 2009)

[37] Lirman, D., Gracias, N., Gintert, B., Gleason, A., Deangelo, G., Gonzalez, M., Martinez, E., Reid, R.P. (2009) Damage and Recovery Assessment of Vessel Grounding Injuries on Coral Reef Habitats Using Georeferenced Landscape Video Mosaics. Limnology and Oceanography: Methods (In Press)

[38] Gintert, B., Gracias, N., Lirman, D., Gleason, A., Dick, M., Kramer, P., Reid, R.P. (2009) Reef Imaging Technology: A new tool for coral community assessment and monitoring. NCORE Forum 2009. August 24-25, 2009. (Presentation)

[39] Gintert, B., Gracias, N., Lirman, D., Szlyk, T., Ciminello, M., Reid, R.P. (2009) Underwater video mosaics: a new spatial dynamics tool for coral communities. CERF Conference 2009, November 1-5, 2009. (Presentation)

[40] Ncosevici, T., Gracias, N., Negahdaripour, S., Garcia, R. (2009) Efficient 3D Scene Modeling and Mosaicing, Journal of Field Robotics, (26)10: 759 – 788.

[41] Gracias, N., M. Mahoor, S. Negahdaripour, and A. Gleason. (2009) Fast Image Blending using Watersheds and Graph Cuts, Image and Vision Computing, 27(5): 597-607.

[42] Reid, P., Gracias, N., Lirman, D., Gleason, A., Gintert, B., Dick, M. (2009). Landscape Mosaics of Coral Reefs: Powerful Tools for Community Assessment and Monitoring. SERDP Partners in Environmental Technology Technical Symposium and Workshop, December 1-3, 2009 Washington, DC. (Poster)

[43] Elibol, A., N. Gracias and R. Garcia (2009) Match Selection in Batch Mosaicing using Mutual Information. *Proc. of the 4th Iberian Conference on Pattern Recognition and Image Analysis* (IbPRIA2009), Povoa do Varzim, Portugal, June 2009

2010

[44] Gintert, B., Gleason, A.C.R., Gracias, N., Lirman, D., Gonzalez, M., Szlyk, T., Ciminello, M., Reid, R.P. (2010) Underwater Landscape mosaics: A unique tool for linking reef ecology and reef mapping. Ocean Sciences Meeting. February 24th, 2010, Portland, OR. (Poster)

[45] Gintert, B., Gracias, N., Lirman, D., Gonzalez, M., Szlyk, T., Ciminello, M., Reid, R. (2010) Novel Imaging Technology Provides a Unique View of Long-term Reef Decline. 39th Annual Benthic Ecology Meeting. March 10-13 2010, Wilmington, NC. (Presentation)

Appendix 2. Supporting Data: Landscape Mosaics

A copy of each final landscape mosaic created during this project will be included in the DVD of supporting data.

Appendix 3. Supporting Data: Landscape Mosaic Creation Manual

The complete Landscape Creation Manual will be provided in the DVD of supporting data.

Appendix 4. Supporting Data: Landscape Mosaic Creation Software

The Landscape Mosaic Creation Software Package including the external viewer application and demonstration images will be included as a separate DVD of supporting data.

Appendix 5. Supporting Data: 3D mosaicing

The 3D point and click software, instructions and sample images are all included in a DVD of supporting data.

Appendix 6. Supporting Data: Multispectral Data

Supporting data and software are provided on a DVD with this report. Top level directories are divided in four categories: data, calibration, software, and analysis (Table C7). Matlab software (the MathWorks, Natick MA) will be required to access many of these data files.

"Data" directories correspond to the "shorthand" columns of Tables C1, C2, C3, C4. All of the data directories have subdirectories named "ccdimages" and "digital_camera". Some of the data directories also contain additional subdirectories "ac9" or "divespec". The "ccdimages" directories contain a matlab data file ("*.mat") that has the averaged reflectance image for that dataset in a variable named "Irefmean" or "Irefavg" and the variance of the reflectance image in a variable named "Irefvar". Irefmean is an average of the N replicate images acquired for that dataset, where N is listed in Tables C1, C2, C3, C4. The "digital_camera" subdirectory contains hand-held underwater photographs of the scene for comparison with the MSCAM images. Usually there are additional photographs in the "digital_camera" subdirectory providing close-ups of various organisms in the scene or images documenting the experimental set up. The "divespec" directories, when present, contain reflectance measurements made with underwater spectroradiometers for that dataset. The divespec files are named MDDHHMMS.AYY where M = month(A-L), DD = day(00-31), HH = hour(00-23), MM = minute(00-59), S = 1/10 of second (0-9), A is the instrument ID (always A for our instrument), and YY is the two digit year. The format of the divepsec files is ASCII text with a short header followed by two columns: wavelength (nm) and reflectance factor (0-1). The AC-9 directories contain AC-9 raw data files (*.dat), processed data files (*.mat) and plots (*.jpg), as well as the matlab scripts used for processing (*.m). The AC-9 raw data format is described in the file "ac9usersguide.pdf", contained on the DVD. The processed ac-9 files contain structures at various levels of processing. The one of interest is named "wmedcorscat" (the highest level of processing). It contains water column absorption (a) and attenuation (c) values in the field "medianpluswater".

The "calibration" directories contain rolloff correction images computed on two dates. On 28 September 2004 we performed a calibration averaging all six filters (filter set 1). The result is contained in the matlab data file "rolloff_040928.mat". It is a matrix the same size as the images that were multipled by the raw data to generate the reflectance images. On 7 April 2007 a second calibration was performed (filter set 2). In this set, a different rolloff image was generated for each filter (they are slightly different). The calibration images should not be needed for further processing, but are provided as a reference.
The "software" directory contains Matlab functions used for processing. The files in "ac9" were used to calibrate the raw ac-9 data. The file "loaddivespec.m" was used to read the divespec data files. The scripts in the "msc" directory were used to process and display the MSCAM images themselves. There are descriptions in the comment section at the beginning of each of these files describing their functionality.

The "analysis" directory contains output from the three experiments described in the report. Files under "exp_filterset1_clark_holden_ledrew" were used to test the filter set one algorithms. Files under "exp_filterset2_discriminant_analysis" were used to test the filter set two algorithms. Files under " exp_spec_texture" were used to test the combined spectral threshold and texture processing algorithm. Generally, these files contain a matlab script ("*.m") that controlled the processing, output images ("*.jpg") and, in some cases, intermediate data files ("*.mat").

Appendix 7. Supporting Data: Landscape Mosaic Surveying Technology Requirements

Software Requirements

The mosaic creation requires the following software

- SERDP Mosaic software deliverable disk
- Microsoft(R) Windows XP (64 bit) professional SP2
- MathWorks(R) Matlab version R2009A (later versions are not recommended and may have compatibility problems) with the following toolboxes: Optimization, statistics, image processing
- Camera calibration toolbox for Matlab (freely available at http://www.vision.caltech.edu/bouguetj/calib_doc/)

The following software is highly recommended. It may be replaced with other packages that provide the same functionality. However, this manual provides detailed examples using these packages.

2. Adobe(R) Premiere 6.0 (if using Standard Definition Video)
3. Sony(R) Vegas Movie Studio HD (if using High Definition Video)
4. JASC(R) Paint Shop Pro (any version)
5. Videolan(R) VLC media player (freely available at http://www.videolan.org/vlc/)

Software Installation

1. Install Microsoft(R) Windows XP, MathWorks(R) Matlab, Adobe(R) Premiere 6.0, Sony(R) Vegas Movie Studio HD, JASC(R) Paint Shop Pro and Videolan(R) VLC according to product instructions.
2. Install the camera calibration toolbox.
3. Copy the contents of the SERDP Mosaic software deliverable disk into directory *c:\users\serdp* . After copying, there should be a subdirectory *c:\users\serdp\ nunomosaics* with several subdirectories, that contains the mosaicing code. There will be also a directory *c:\users\serdp\test* that contains test data.
4. Inside MATLAB, open menu *File->Set Path*, and click on '*add with subfolders*'.
5. Select the *c:\users\serdp\nunomosaics* directory and press '*save*'.

Acquisition Hardware

The following acquisition hardware was used to produce the examples shown in this manual, and for the results in the project report.

- Sony TRV900 digital video camera (standard definition)
- Sony HVR - A1U digital video camera (high definition)
- Nikon D200 10MPixel digital still camera with AF-S Nikkor 18-70mm ED lens
- KVH Industries C100 Compass Engine
- Precision Voltage to Frequency Converter LM231 manufactured by National Semiconductor and we implemented the circuit in figure 1 "Simple Stand-Alone Voltage-To-Frecuency Converter with +-0.03% Typical Linearity (f=10Hz to 11 KHz) to convert compass output voltage into a frequency modulated audio signal, recorded by one of the HDV camera audio channels. Datasheet for Precision Voltage to Frequency Converter LM231, 2006, National Semiconductor, www.national.com/ds/LM/*LM231*.pdf

There is no requirement for specific camera model, image resolution or type of lenses to use the mosaic creation and analysis tools covered by this manual. However, the camera needs to be calibrated (detailed in the next section) in order to eliminate the effect of lens and housing distortions.

The heading sensor is composed of a fluxgate compass with a precision voltage frequency converter. The compass interface electronic circuit was designed, tested and calibrated for this particular project. The heading information is provided by a KVH fluxgate electronic compass that measures the Earth's magnetic field and produces an analog voltage output proportional to the compass heading. This voltage is converted to a frequency in the audio range and stored in the audio channel #1 of the high definition video camera. The heading sensor and converter produce an audio signal with the following relevant characteristics:

- Frequency at 0 degree heading : 236Hz
- Frequency at 360 degree heading: 4411Hz
- Linear frequency response
- The heading to frequency transfer function is freq(Hz) = 11.5989 x heading(deg) + 236

The software can use any other heading sensor that has been adjusted to have a similar frequency transfer function.

Computing hardware and typical disk and CPU usage

The minimum hardware configuration is

- Pentium4 2GHz
- 3 GB RAM
- 30 GB free disk space per survey

The recommended configuration is

- Pentium Core2 Quad 2.8GHz or higher
- 8 GB RAM
- NVIDIA CUDA(tm) enabled graphics card
- 30 GB free disk space per survey

The following tables show disk usage and execution times for a typical mosaic creation job. The survey covered 250 sq meters and was recorded in 30 min High Definition Video. The mosaic was created on a 2.8GHz Pentium IV with 3GB RAM. The *CPU Processing* table refers to the computation time. The *Required User Intervention* table refers to the actual intervention time spend by the user (human attention).

DISK USAGE

Raw Video Download	Extracted Video to be processed	Extracted and corrected images	Intermediate processing files	Final Mosaic Image
5GB	1.5GB	2.1 GB	200MB	20MB

CPU PROCESSING TIME

Video download from camera	AVI creation	Image extraction and correction	Matching and global optimization	Mosaic rendering	Job Total Time
0.5h	5h	11h	36h	3h	55.5h

REQUIRED USER INTERVENTION TIME

Video download from camera	AVI creation	Image extraction and correction	Matching and global optimization	Mosaic rendering	Total User Time
10min	40min	10min	15min	15min	90min

Guidelines for handheld image acquisition

This text contains some guidelines to assist divers during handheld image acquisition.

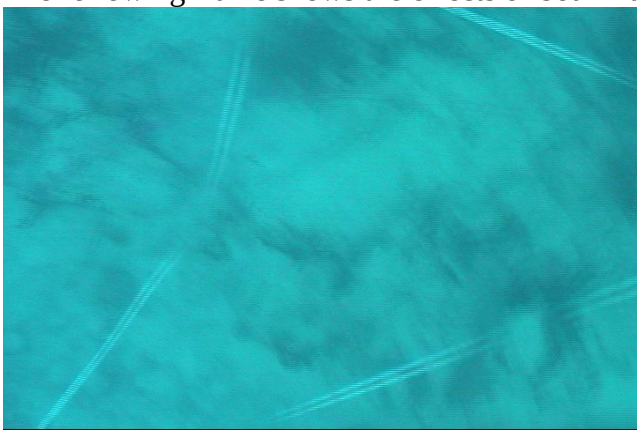
Generic guidelines

- Camera should be facing the floor
- Avoid pan (i.e. sideways) and tilt (i.e. up and down) rotation.
- Avoid fast rotation motion (at the end of each swath).

Handheld video cameras

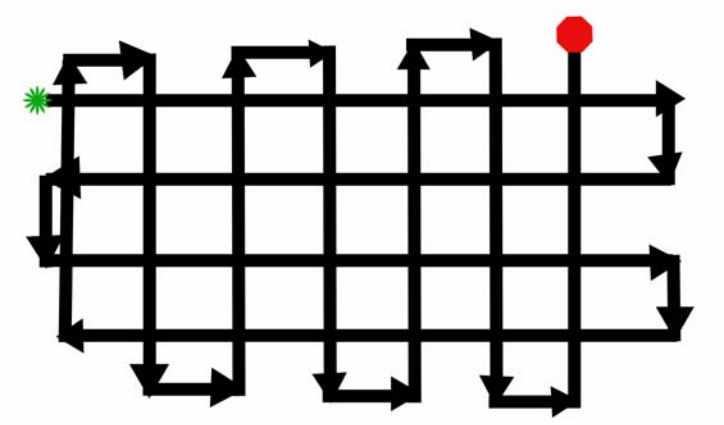
- ***DV video camera should be set to non-interlaced video mode.*** Commonly video cameras operate in interlaced mode, where each recorded image contains two independent half-resolution frames acquired at different times (typically 60 Hz). This creates smoother motion to the human eye during playback. However it ruins the performance of the mosaic creation algorithms which assume each frame is captured at a single instant.
- ***Cameras should be set to high shutter speed.*** Some cameras allow for manually defining the shutter speed, while the aperture (camera iris) is automatically controlled to adjust to the light conditions. In such case, this mode should be used at a high shutter speed (1/200 or higher), as long as there is enough light. By using high shutter speed, the motion blur on each frame is reduced, resulting in more precise motion estimation.
- ***Camera motion should be slow.*** This way, the effects of motion blur are reduced. As a rule of thumb use such speed that an object entering the top of the image takes at least 5 seconds to disappear at the bottom of the image.
- ***Zoom settings should not be changed during acquisition.*** The motion estimation algorithms usually assume that the camera's focal length is constant throughout the sequence. Also, in order to allow angular measurements over the images, it is extremely helpful to have images of the calibration grid acquired with the *same zoom setting*. A typical good zoom setting is having the cameras at the widest angle (i.e. largest field of view).

The following frame shows the effects of both interlacing and motion blur:



During Acquisition

Cover the area using a double "lawn mower" pattern



First forward and backwards, and then sideways.

Make sure you have noticeable overlap between strips. Do not forget to do the sideways pattern; otherwise the sequence is unusable for mosaicing. If possible, keep the relative camera orientation the same. Rotate the diver around the camera when changing directions rather than rotating the camera.

Still Photography Camera

Still cameras can provide very high resolution, but cannot acquire sequences in a continuous and smooth way. Not all mosaicing algorithms can take advantage of still images. However the high resolution can be valuable in providing texture details. The main guidelines are the following

- Ensure high superposition from image to image. Superposition should be at least 60% between every pair of consecutive images.
- Stand still when taking the photo, especially if there is low light intensity.
- Whenever possible, keep camera facing down at constant distance.

Camera Setup Guidelines for High Definition Video and 10MP Still Cameras

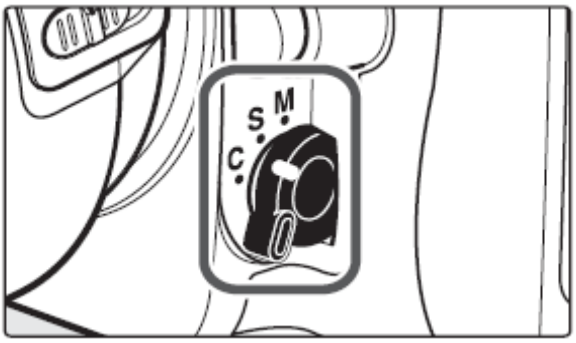
HDV setup:

- Wide Angle Zoom:
  - Use the ZOOM radial button on the exterior of the camera to the widest possible angle zoom.

Slide the power switch down to CAMERA-TAPE mode. Touch P-MENU →[MENU]. Select the CAMERA SET menu.

- Turn off automatic camera stabilization:
  - Move down in the CAMERA SET menu and select STEADYSHOT.
  - Set STEADYSHOT to OFF.
  - Then press [OK].
- Set shutter speed to 1/250:
  - Move down in the CAMERA SET menu and select the SHUTTR SPEED.
  - Select the MANUAL setting and use the -/+ buttons to scroll through the different options and select the shutter speed of 250.
  - Then press [OK].
- Set the exposure to AUTO:
  - Move down in the CAMERA SET menu and select the EXPOSURE.
  - Select the AUTO setting.
  - Then press [OK].
- Set white balance to highest color temperature:
  - Move down in the CAMERA SET menu and select the WHITE BAL.
  - Frame a blue paper/object in front of the camera, the paper/object should take up the entire view of the camera.
  - Select the ONE PUSH option which looks like a rectangle over two symmetrical triangles.
  - Touch the ONE PUSH symbol once again.
  - The ONE PUSH symbol will begin to flash quickly. When the white balance has been adjusted and stored in the memory, the indicator stops flashing.
  - After the white balanced has been stored, push [OK]
- Set white balance to highest color temperature:

Still Camera setup:

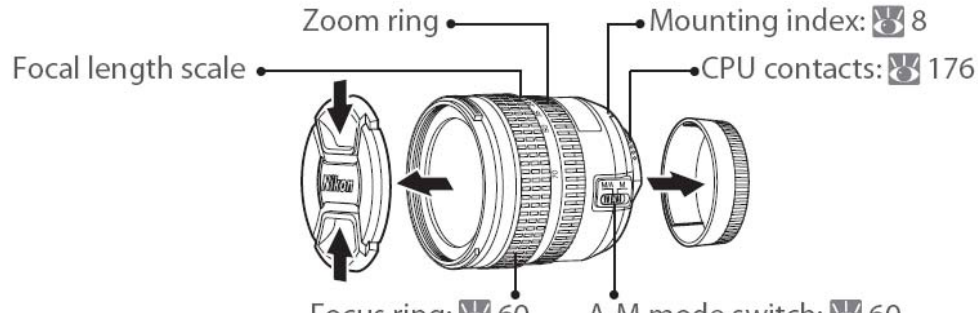


- Verify the camera is in auto focus:
  - The Focus mode should be set at S mode on the exterior button of the camera.

- Set camera to highest zoom:
  - Use the ZOOM RING to adjust for the highest zoom (24 mm)

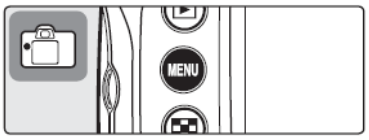
Lens

An AF-S DX 18–70 mm f/3.5–4.5G ED lens is used in this manual for illustrative purposes. The parts of the lens are shown below.

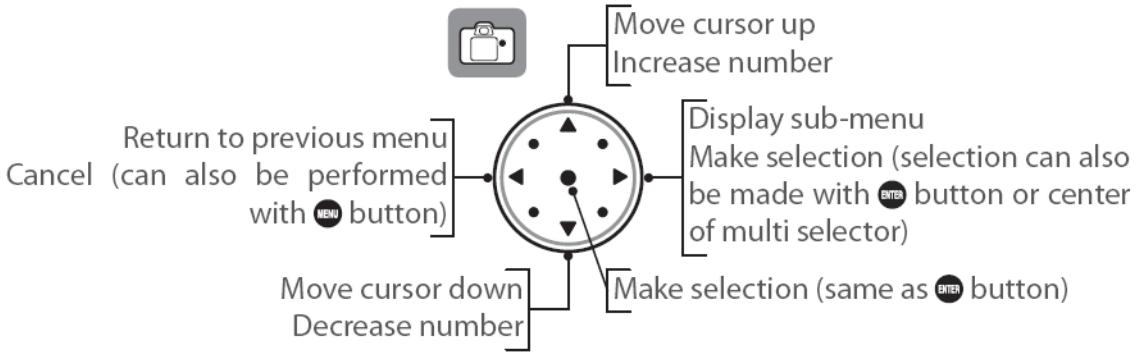


The following settings will require entering the cameras menu:

Most shooting, playback, and setup options can be accessed from the camera menus. To view the menus, press the MENU button.



The multi selector is used to navigate through the camera menus.



- Program camera for 1 frame every 2 seconds:
  - In the MENU select the SHOOTING MENU highlighted as a small camera icon.



3 Press the multi selector left or right to highlight the following options and press the multi selector up or down to change interval timer set-



3 Press the multi selector left or right to highlight the following options and press the multi selector up or down to change interval timer settings.



Option	Description
Start time	Enter start time for interval timer photography when **Start time** is selected for **Start**. Press multi selector left or right to highlight starting hour or minute, press up or down to change. Not available when **Now** is selected for **Start**.
Interval	Enter time between shots. Press multi selector left or right to highlight hour, minute, or second, press up or down to change. Note that camera will not be able to take photographs at specified interval if interval is shorter than shutter speed or time required to record images.
Select Intvl*Shots	Choose number of intervals and number of shots taken at each interval. Press multi selector left or right to highlight number of intervals or number of shots, press up or down to change. Total number of shots that will be taken appears to right.
Remaining (intvl*shots)	Shows number of intervals and total shots remaining in current interval program. This item can not be edited.
Start	Choose **Off** to adjust settings without starting interval timer. To start interval timer, select **On** and press OK. Shooting will start at selected start time and will continue for specified number of intervals.

series of shots will be taken at the specified starting time. Shooting will continue at the selected interval until all shots have been taken. If shooting can not proceed at current settings (for example, if a shutter speed of **bulb** is currently selected in manual exposure mode, or the starting time is less than one minute from the current time), a warning will appear and the interval timer menu will be displayed again.

Use of a tripod is recommended.

- Set ISO to 800 (for very bright day and depth of < 4 meters, use ISO at 400)
  - In the SHOOTING MENU select the ISO SENSITIVITY menu.
  - Use the multi selector to set the ISO to 800 (400 for bright days and small depths).
- Set image quality setting (Large; High Quality; JPEG):
  - In the SHOOTING MENU select the IMAGE QUALITY menu.
  - Highlight the 'JPEG FINE' option of the image quality list and press the multi selector to the right.

- Set the white balance to 10000K color temperature:

- In the SHOOTING MENU select the WHITE BALANCE menu.
- Select the CHOOSE COLOR TEMP menu.
- Select the 10000K option and right click [OK].

- Set Exposure program to shutter priority with shutter speed 1/320:
  - Press the exterior button MODE and use the main command dial until the M (Manual) option shows up.

Rotate the main command dial to choose a shutter speed of 320.

Appendix 8. Supporting Data: Action Items

On the disk of supporting data will be two additional reports submitted to SERDP: 1) an analysis of advances in mosaicing and benthic survey technology accomplished during the course of SI1333 and 2) a cost benefit analysis of survey methodologies.

Appendix9. Other Materials (Awards)

Gleason, A. C. R., R. P. Reid, K. J. Voss. (2007) Automated classification of underwater multispectral imagery for coral reef monitoring, Awarded "Best Student Poster" and the IEEE/MTS OCEANS 2007 Conference and Exhibition, Vancouver, BC, Canada, 1-4 October 2007.

Reid, R.P., Gracias, N., Lirman, D., Gleason, A., Gintert, B., Dick, M. (2009). Landscape Mosaics of Coral Reefs: Powerful Tools for Community Assessment and Monitoring. Awarded “Project of the Year 2009.” At the SERDP Partners in Environmental Technology Technical Symposium and Workshop, December 1-3, 2009 Washington, DC. (Poster)

Gintert, B., Gracias, N., Lirman, D., Gonzalez, M., Szlyk, T., Ciminello, M., Reid, R. (2010) Novel Imaging Technology Provides a Unique View of Long-term Reef Decline. Winner of “Student Presentation Award, Graduate Student Oral Presentation” 39th Annual Benthic Ecology Meeting. March 10-13 2010, Wilmington, NC.